THE MOVING WATER TABLE IN TILE DRAIN SYSTEMS

by

NAZAR MOHAMMAD AWAN, B.E., M.Sc.

Thesis presented to the Faculty of Engineering in the University of London for the degree of Doctor of Philosophy

Department of Civil Engineering
Imperial College of Science & Technology
London, S.W.7.

September, 1969.

ABSTRACT

A Hele-Shaw model is used to study unsteady flow in two drainage systems. The first system is concerned with unsteady tile drainage over a horizontal impermeable bed. Both rising and falling stages of the unsteady state have been investigated in the system. The drainage factors whose effects on the rate of the mid-point water table recession and rise have been examined are: the initial steady state water table height above the drain axis; the depth of the impermeable bed below the drain axis; the drain size; the submergence of the drain outlet below the outlet channel water level and the steady rate of recharge.

The experimental results are used for checking the validity of the existing unsteady state drainage solutions for the above mentioned factors. The experimental and analytical studies show good agreement over certain ranges of the drainage factors and thus delineate the limitations of these analytical studies.

The second drainage system covers steady and unsteady drainage over a moderately sloping impermeable bed. The specific system that is investigated relates to a case when the downslope flow due to vertical recharge is dammed by an underground clay barrier. The system is finite with vertical impermeable boundaries at the upper and lower ends and consists of three tile drains situated 22.9 cms above the impermeable bed

and 100 cms apart.

An analytical solution based on the Boussinesq equation is developed for the steady and unsteady drainage. The solution, although only an approximate representation of the experimental set up, shows a remarkable agreement when compared with the experimental results for the steady and unsteady state conditions.

PREFACE

The experimental study of the moving water table in tile drain systems described in this thesis was carried out in the Hydraulics Laboratory of the Department of Civil Engineering, Imperial College of Science and Technology, London. The study was carried out with two objectives in view, both of which are implied in the title of the thesis.

The term 'systems' in the title covers, in fact, two systems. The first system deals with the moving water table (rising and falling) over a horizontal impermeable bed and the second with the steady and unsteady (falling water table only) flow over a moderately sloping impermeable bed. The latter system, although of great practical significance, does not seem to have been studied in great depth.

It is hoped that the study of the first system would improve the knowledge of some of the existing unsteady state solutions by delineating their range of validity of which little is known to-date. The study of the second system advances the present knowledge of the system by considering the initial steady state water table profile. All the existing studies of such a system assumed an initial water table profile parallel to the sloping impermeable bed.

Although there is a vast amount of material covering different

aspects of tile drainage problem, only the relevant and more important references have been reviewed in the thesis. Where specific information is cited, the reference is indicated by subscripts.

The presentation of the research work in the thesis follows a systematic pattern. In Chapter 1 is given a description of drainage problems in general, followed by the introduction of the present research problem. Chapter 2 describes the nature and properties of porous media and gives derivation of the basic flow equations.

The review of the existing steady and unsteady state solutions is given in Chapters 3 and 4. The emphasis in the review has been placed on outlining the assumptions underlying the analytical solutions.

Chapter 5 gives a detailed description of the present experimental set up and experimental accuracy, which is followed by the discussion of the experimental results for the symmetrical drainage system.

The experimental and analytical studies of flow over a moderately sloping impermeable bed are described in Chapter 6. The Summary of the conclusions is presented in Chapter 7.

Finally, there are many people to thank for the assistance

and encouragement in this research work.

Firstly, I should like to express my gratitude to my research Supervisor, Mr. T. O'Donnell, for his continued help, guidance and encouragement.

I must also thank Professor J. R. D. Francis for the interest he has taken in this work.

I am indebted to Professor Bickley and Mr. Selvalingam who assisted me in solving the differential equation for flow over a moderately sloping impermeable bed.

I have to express my grateful appreciation of the work done by Mr. Tait and his laboratory staff, without whose technical skill this research would have been greatly hindered.

I gratefully acknowledge the award of a scholarship by the West Pakistan University of Engineering and Technology, Lahore, Pakistan, to enable me to carry out this research.

Nazar Mohammad Awan

NOTATIONS

Symbols		Description
A	=	Cross-sectional area
a	=	slope factor $= \alpha C/D$
b	=	width of interspace
C	=	KD/f
d	=	depth of drains above the impermeable bed
D	=	weighted mean depth of the ground water stream $= \frac{Y_m}{2} + d$
f	=	drainable porosity
g	=	acceleration due to gravity
h	=	height of water table measured above the impermeable bed
h_m	=	steady state mid-point water table height measured from the impermeable bed.
Δh_o	=	fall of water table in the upper drain of a Zone in a certain time t.
Δh_L	=	fall of water table in the lower drain of a Zone in a certain time t.
H_o	=	steady state height of water table at the upper drain measured from the sloping impermeable bed.
H_L	=	steady state height of water table at the lower drain measured from the sloping impermeable bed.
H_2	=	free surface height of the outlet channel, measured from the impermeable bed.
i	=	unit of imaginary numbers $= \sqrt{-1}$
K	=	hydraulic conductivity of the soil

Symbols		Description
k	=	intrinsic permeability
l	=	half drain spacing
L	=	drain spacing = $2l$
n	=	integers 0, 1, 2, 3 ....
p	=	intensity of pressure
P	=	$2R/K$
Q	=	drain discharge/length
r	=	drain radius
R	=	rate of recharge/area
R_e	=	Reynolds number
s	=	independent variable of Laplace transforms
t	=	time since water table recession or rise begins.
v	=	seepage velocity
v^*	=	pore velocity
x,y,z	=	cartesian coordinates
Y	=	height of water table, at time t, measured from the drain centre.
Y_m	=	steady state water table height, midway between drains, measured from the drains centre.
Y_o	=	steady state height of water table, over the drains, measured from the drains centre.
α	=	slope of the impermeable bed
μ	=	absolute viscosity

Symbols		Description
ν	=	kinematic viscosity
ρ	=	density of the liquid
ϕ	=	potential function
ψ	=	stream function
θ	=	angle which the steady state water table makes with the horizontal at the point of inflexion.
δ	=	K_s eg
ΔY	=	vertical displacement

CONTENTS

CHAPTER 1

INTRODUCTION

1.1	Causes of drainage problems	1
1.2	Water table depth in relation to plant growth and soil	3
1.3	Tile drainage	6
1.4	General solution of drainage problems	9
1.5	Objects of the present research	
	1.5.1 Research needs	13
	1.5.2. Research objects	16

CHAPTER 2

GROUNDWATER FLOW

2.1	Porous media	18
2.2	Mechanism of groundwater flow	20
2.3	Darcy's law	22
2.4	Equation of motion	26
2.5	Dupuit assumptions	30
2.6	Unsteady Unconfined flow over a horizontal and sloping impermeable bed.	32

CHAPTER 3

REVIEW OF STEADY STATE PROBLEMS

3.1 The Dupuit-Forchheimer method 36

3.1.1 Ellipse equation 39

3.2 Radial flow assumption 41

3.3 Exact Solutions 44

3.3.1 Childs' analogue experiments 44

3.3.2 Solutions based on hodograph method 45

3.3.3 Kirkham's Potential Function method 50

3.3.4 Hammad's method 54

3.3.5 Dagan's method 57

3.4 Comparison between experimental studies and rational methods. 59

CHAPTER 4

REVIEW OF UNSTEADY STATE PROBLEMS

4.1 General 65

4.2 Glover's Solution 67

4.3 Improvement of Glover's Solution

4.3.1 Brooks' approach 71

4.3.2 Van Schilfgaarde's approach 72

4.4 Isherwood's relaxation method 75

4.5 Moody's iteration method 77

4.6 Solutions based on extension of Steady State to Unsteady State.

4.6.1 General theory 78

4.6.2 Kirkham's analysis 81

4.6.3 Hammad's Solution 82

4.7 Intermittent recharge 83

CHAPTER 5

DRAINAGE OVER A HORIZONTAL IMPERMEABLE BED

5.1 Introduction 85

5.2 Viscous flow analogy

5.2.1 Theory of simulation 88

5.2.2 Scaling laws 90

5.3 Viscous flow model

5.3.1 General 92

5.3.2 Description of the model 94

5.4 Objectives of the experiments 104

5.4 Experimental Procedure 104

5.5 Flow conditions in the drains 107

5.6 Experimental accuracy 107

5.6.1 Observational errors 107

5.6.2 Measurement of viscosity 108

5.6.3 Uniformity of interspace 111

5.6.4 Rainfall distribution 111

5.6.5 Boundary effect 112

5.6.6 Effect of temperature on water table height 114

5.6.7 Capillary effect 115

5.7 Experimental results for the symmetrical drainage system

5.7.1 The falling water table 117

5.7.1.1 Normalised parameters 117

5.7.1.2 Effect of initial steady state water table height, Y_m. 118

5.7.1.3 Comparison of experimental results with analytical solutions 124

5.7.1.4 Effect of depth of impermeable bed 129

5.7.1.5 Effect of drain size 136

5.7.1.6 The water table profile 144

5.7.2 Falling water table between submerged drains 146

5.7.3 Rising water table 149

5.7.3.1 Effect of rate of rainfall 149

5.7.3.2 Effect of depth of impermeable bed 156

5.8 Effect of misalignment of tile drains on falling water table

5.8.1 Introduction 156

5.8.2 The problem 159

5.8.3 Experimental procedure 160

5.8.4 Analysis of results: drain running under some back pressure due to resistance to flow in the drain 162

CHAPTER 6

DRAINAGE OVER A SLOPING IMPERMEABLE BED

6.1 Introduction 168

6.2 Review 171

6.3 Statement of the present problem 174

6.4 Mathematical analysis

6.4.1 General 176

6.4.2 Steady state 181

6.4.3 Unsteady state 183

6.5 Description of the model 191

6.6 Experimental procedure 195

6.7 Results for the steady state

6.7.1 Submerged flow due to resistance to flow in the drain

6.7.1.1 Experimental results 198

6.7.1.2 Theoretical water table profile 204

6.7.2 Free flow 206

6.8 Results for the unsteady state 208

6.8.1 Submerged flow due to resistance to flow in the drain 208

6.8.1.1 Experimental results 208

6.8.1.2 Theoretical water table profile 211

6.8.2 Free flow 212

6.9 Conclusions 215

CHAPTER 7

SUMMARY OF CONCLUSIONS

7.1 Symmetrical drainage system 216

7.1.2 Falling water table between submerged drains 219

7.1.3 Rising water table 219

7.2 Misaligned drainage system 220

7.3 Drainage over a moderately sloping impermeable bed 221

References 224

Tables 234

Appendix I 266

Appendix II 270

Appendix III 284

CHAPTER 1

INTRODUCTION

The objectives of this chapter are first to outline, very briefly, the natural causes that give rise to drainage problems; secondly, to discuss the salient features of crop growth in relation to fluctuations in the groundwater table; thirdly, to discuss qualitatively the physical and ecological principles that determine the water table depth; and lastly, to introduce the present research problem. This sequence of description aims at providing the background against which the research problem can be viewed prior to a systematic presentation of its experimental and theoretical solution in the later chapters.

1.1 CAUSES OF DRAINAGE PROBLEMS

Fluctuation of the groundwater table in response to intermittent percolation is a common phenomenon. The occurrence of this phenomenon and its importance in the evaluation of ground-water resources as well as in the study of irrigation and drainage problems has occupied the attention of many investigators in recent decades.

The main sources of percolation giving rise to drainage problems are: precipitation, surface irrigation and seepage from open waters such as lakes, streams and canals. The effect of these sources may not necessarily be confined to the areas of their occurrence. The

water may seep laterally through the subsoil from lands at higher elevations to lower lands. Childs (1) has applied the term 'foreign water' to this latter situation, implying that the water comes from a source not in the area to be drained. In such cases, it is always the lowlands which suffer most from a rising water table situation.

Artificial drainage may not be necessary in areas having natural subsurface drainage, such as areas underlain by coarse material like sand and gravel which have lateral drainage routes. Excessive water in these areas can percolate vertically and then move laterally through the permeable soil to the natural outlets. However, in the absence of any such natural outflow or if there is no artificial abstraction, the groundwater table will continue to rise when there is percolation. The rise will depend on the duration and rate of percolation, on the size and shape of the area over which percolation takes place and on the hydraulic and geometric parameters of the underlying water table aquifer.

A rising water table situation creates problems to crops when it reaches a shallow depth. The water table must be controlled by artificial drainage to a certain optimum depth depending on the type of crop and the soil and climatic conditions. In a drainage design, the optimum depth is governed not only by the length of time that the plants will be exposed to high water table or even waterlogging conditions (Section 1.2) but also by

the salinity of the groundwater. The highest water table must be kept deeper in the latter case so that harmful salts are not drawn to the ground surface by capillary flow and deposited there as the water evaporates.

1.2 WATER TABLE DEPTH IN RELATION TO PLANT GROWTH AND SOIL

It is well recognised that plants need air as well as moisture in their root zones. The availability of air and moisture to plants depends on the position of the water table and the moisture holding capacity of the soil, the latter depending on the soil type and structure.

Every soil has two distinctive amounts of moisture content in the course of alternate wetting and drying phases. These two amounts, the so called moisture constants, are the field capacity and the wilting coefficient. The field capacity is, in broad terms, the lowest moisture content to which the soil may be brought by gravity drainage alone in any reasonable time (i.e. in a matter of days). For example, if an initially high water table, sufficient to maintain the surface layers nearly at saturation (see curve 1 in Fig. 1.1), is much lowered by drainage, water will drain down to the new water table thus resulting in a reduction of the moisture content in the upper soil layers. This causes an increased resistance to water movement so that in fact, after a reasonable time, the moisture profile takes a steady form shown by curve 2 in Fig. 1.1,

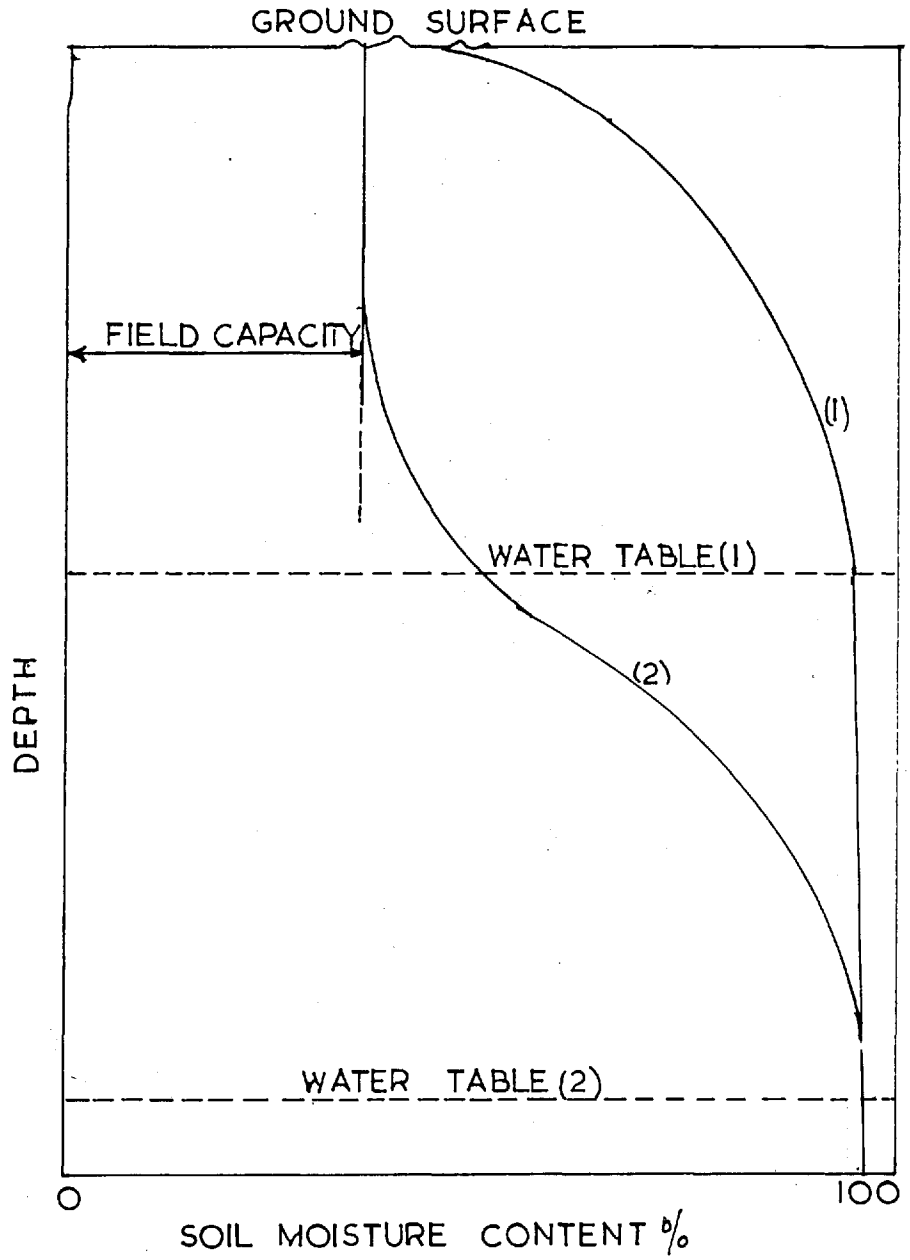


FIG: 1.1

SOIL MOISTURE PROFILE ABOVE A FALLING WATER TABLE

in which the moisture content is nowhere less than an amount which is characteristic of the soil. This minimum amount is the field capacity.

In the absence of any transpiration by plants or vegetation and if there is no diffusion of water vapour to the ground surface, the soil well above the water table will end up at field capacity and will stay at this state for an indefinite time until a new recharge occurs. This state would, however, be disturbed by plants. The soil moisture would be reduced below the field capacity by transpiration. As soil moisture decreases it becomes harder and harder to extract the soil moisture in attempting to meet the leaf transpiration. Eventually the wilting point is reached and plant growth ceases. The soil moisture content characteristic of the soil at this stage is called the wilting coefficient.

The direct aim of a drainage operation is to control the moisture content of the root zone of plants between the field capacity and the wilting level. This is achieved by controlling the water table depth. In deciding upon the depth at which the water table should be kept for a specific drainage problem, one should bear in mind that the water table should not be lowered so far below the root zone that water deficiency may be likely to occur. At the same time, it should not be so shallow that the moisture content in the root zone is much above the field

capacity (i.e. almost saturated). This would prevent air penetrating into the root zone. Thus, two limiting depths of the water table need be considered: an upper limit dictated by the demand that air should have sufficient access to the roots, and a lower limit set by the water requirements of the crops.

The reaction of crops to fluctuations of the water table within the above limits at different stages of their growth has been the subject of much research. It may, however, be pointed out that despite a great number of experiments on the plant growth-water table depth relationship, our knowledge of the required optimum water table depth is still incomplete. It is very difficult to arrive at a definite conclusion of a general validity about the water table depths which would guarantee optimum crop growth.

Wesseling (2) has reported optimum water table depths obtained from field investigations on different crops. Although this information may serve as a general guide, variation in climatic conditions from place to place may cause considerable variation in the optimum water table depth for a particular crop.

1.3 TILE DRAINAGE

Once the optimum depth has been decided upon, the control of the water table within the root zone of crops may be accomplished by one of three methods: (a) pumping of ground water,

(b) open ditches and (c) covered tile drains. The suitability of any of these methods depends on the topography of the ground surface and on the characteristics of the aquifer. Discussion in this thesis will centre on the tile drainage technique.

Before describing the specific tile drainage problems, it might be appropriate to discuss the classical steady state tile drainage problem as illustrated in Fig. 1.1A. It consists of cylindrical porous drains of diameter 2r placed in a permeable soil layer of hydraulic conductivity K overlying a horizontal impermeable bed. There is a recharge rate R per unit area of the soil surface. The drains are spaced L apart and their centres are at a height d above the impermeable bed. The water table (the surface over which the soil moisture pressure is atmospheric) generally lies above the drains but may cusp downwards into the drains. In the classical delineation of the tile drainage problem, the drains repeat indefinitely at the spacing L. Due to the resulting symmetry, attention can be confined to that part of the system lying between two vertical sections: one through a drain and the other through the midpoint between that drain and a neighbouring drain (Fig. 1.2).

The drains may run part-full at atmospheric pressure or may run full either at atmospheric pressure or at a higher pressure (back pressure). The latter may be caused either due to resistance to flow along the drains (Fig. 1.2) or because the drain

outlets are submerged below the free water surface in a collector ditch (Fig. 1.4). Both causes may also act together. If the drains run at atmospheric pressure, whether full or part-full, the water table may intersect the drain periphery at low values of R/K (Fig. 1.3) or it may stand at the height Y_o above the drain centres at higher values of R/K. If the drains run under back pressure, the water table immediately over the drains will stand at a height Y_o greater than the back pressure head because of the resistance to flow between the water table and the drain. The difference between Y_o and the back pressure head decreases with R/K. It may be mentioned here that while the two types of back pressure, whether due to the resistance to flow in the drain or due to submergence of the drain outlets below the free water surface in the collector ditch, give virtually the same steady state problem, there is a difference in the ultimate water table position during the falling water table. The water table ultimately falls to the centre of the drain in the former and to the ditch water level in the latter.

The present study was based on three flow conditions:

(i) the drains ran full under pressure due to resistance to flow in the drain. The water table was standing at a height Y_o above the drain centre (Fig. 1.2);

(ii) the drains ran part-full at atmospheric pressure at low values of R/K, the water table height Y_o being

zero. This flow condition will hereafter be called 'free flow condition' (Fig. 1.3);

(iii) the drains ran full under pressure because their outlets were submerged below the free water surface in a collector ditch (Fig. 1.4). There was, however, no effect of drain resistance because a large drain was considered and the value of R/K was small. Under these conditions, the water table in Fig. 1.4, to all intents and purposes, touched the water surface in the collector ditch, i.e. $Y_o = Y_1$. In this case, the amount of submergence of the drain is defined by the 'submergence ratio', which is the ratio of the depth of the drain centres (Y_1) to the depth of the impermeable bed (H_2) below the free water surface in the collector ditch.

1.4 GENERAL SOLUTION OF DRAINAGE PROBLEMS

The object of the general solution of a drainage problem is to determine the effect of the geometric parameters of a drainage system on the shape, location and the rate of movement of the water table and on the flow of water to the drains, for given conditions of percolation and soil hydraulic conductivity. The solution of this problem is faced with formidable mathematical difficulties. This is because in the first place the problem is non-linear, but

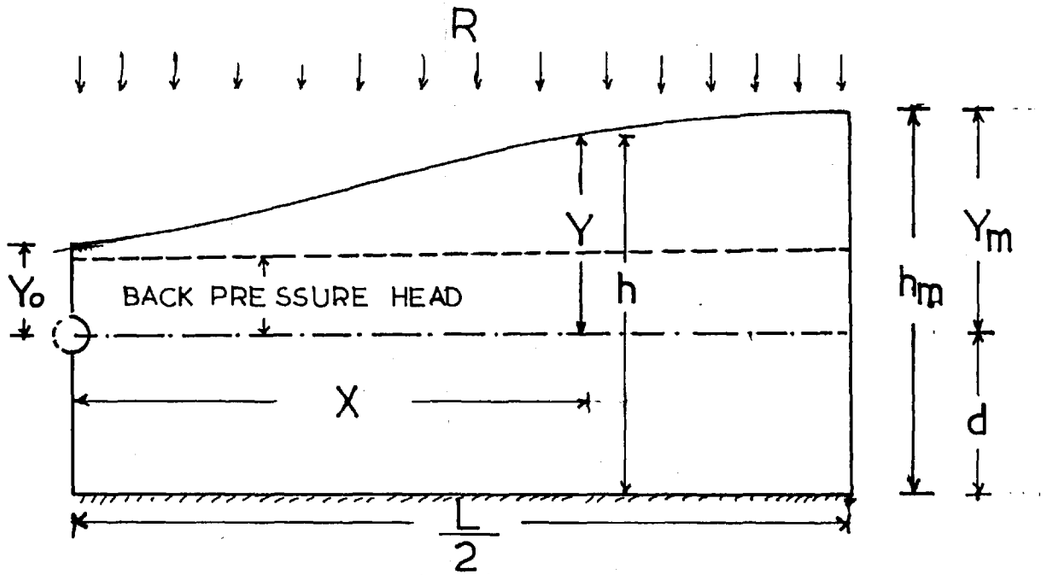


FIG: 1.2

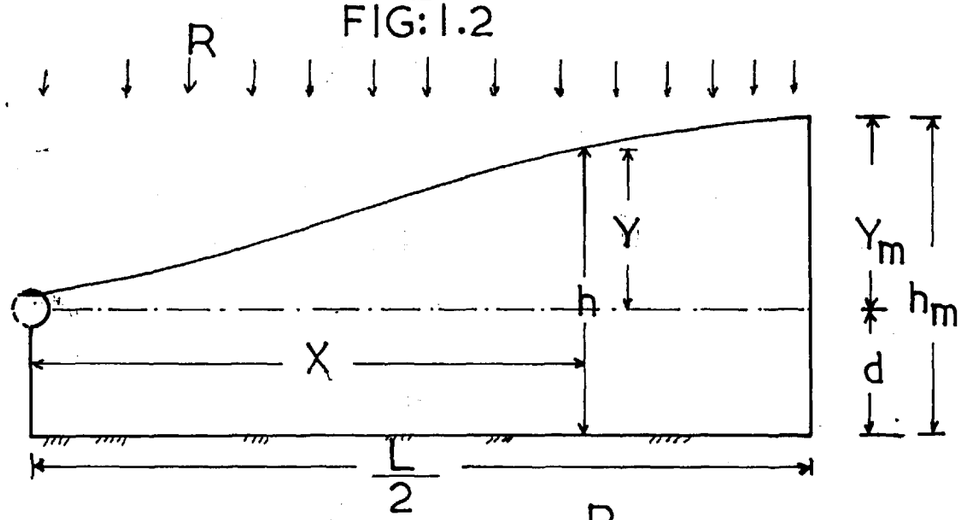


FIG: 1.3

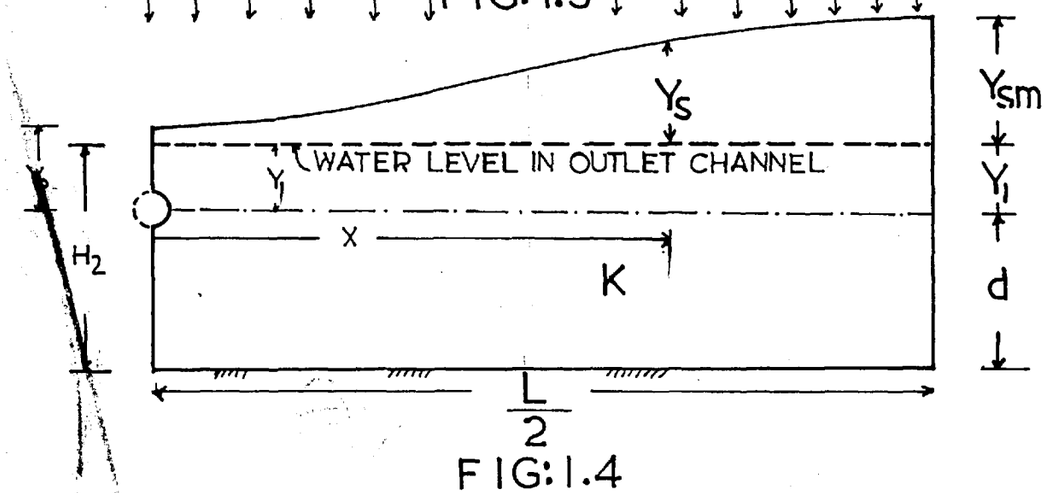


FIG: 1.4

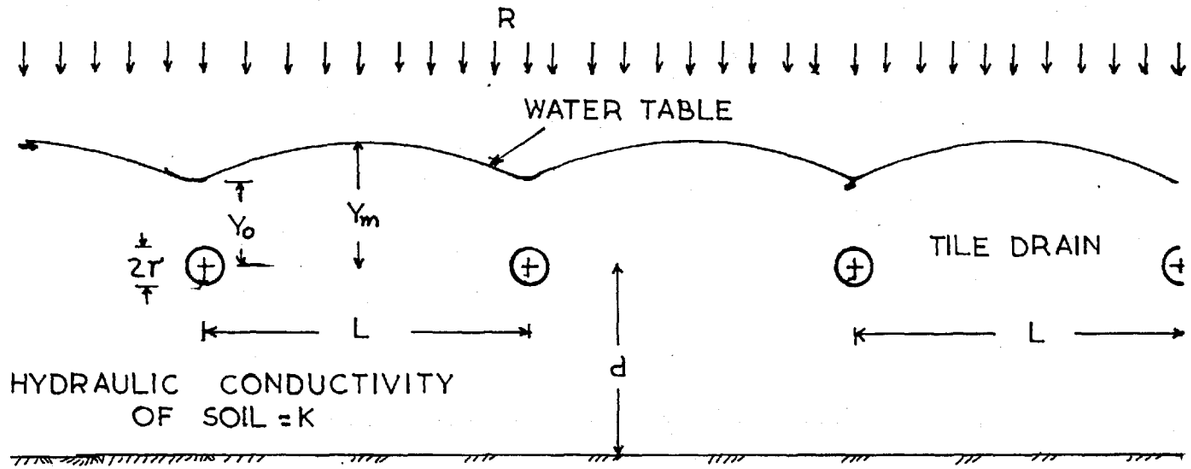


FIG: 1.1A

what makes it even more difficult is the fact that the shape of the water table is not known a priori and hence the domain in which the solution is to be determined is not known in advance. In addition, the free surface boundary in the unsteady state varies with time as the water table fluctuates above the tile drains.

In order to make progress in the development of methods for the design of tile drainage systems, it has in general been necessary to simplify the theoretical approach by making special assumptions of one kind or another. These assumptions differ in the different methods that are now available. However, the most common assumptions inherent in these methods are: the percolation moves vertically downward in the unsaturated zone until it joins the water table; there is uniform flux across all parts of the water table; the mid point water table depth above the drains is smaller than the depth of the impermeable bed below the drain; and the flow takes place in a homogeneous, isotropic unconfined aquifer.

Drainage design, in the early 1930's, was based on the simplified conditions of assuming drainage to be a steady state process and ignoring any cyclic behaviour of the recharge and hence of the ground-water table. This led to the development of steady state flow methods which allowed the designer to obtain answers to the problems of the design of proper spacing of drains

if the rate of steady recharge was known.

The steady state approach, although a great step forward in achieving a design criterion, could not be considered to provide an adequate answer to the actual unsteady state drainage. This state is generally observed both in arid and humid areas. In arid areas, the ground-water table rises during the irrigation season and reaches its highest elevation at the end of the season. The water table then recedes during the non-irrigation period and rises again during the irrigation season in the following year. The s me phenomenon occurs in humid areas due to deep percolation from rainfall.

In spite of its widespread practical importance, the unsteady state drainage problem has been given less attention than the steady state problem. This is because the unsteady state is intractable analytically with present mathematical knowledge. However, since the late 1940's, many research workers have developed approximate methods for studying unsteady subsurface drainage. A detailed review of these methods will be given in Chapter 3. It will suffice here to mention that the Fourier Series method, the electrical analogue technique, the viscous flow analogue technique, finite difference methods and perturbation methods are five distinct methods of attack for the solution of unsteady state drainage problems.

1.5 OBJECTS OF THE PRESENT RESEARCH

1.5.1 Research needs.

The moving water table problem can be considered under two conditions, viz. the rising water table and the falling water table. After a thorough study of the available literature on tile drainage, it is clear that the rising phase has been given very little attention when compared with the falling phase. Except for Childs and O'Donnell's study (3), there does not appear to be any experimental or analytical study relating to the rate of rise of water table with drainage parameters (Section 1.5.2). Drainage design is generally based on the unrealistic assumption that the water table rises instantaneously to the steady state. For a more reliable design, therefore, it is essential that the rising phase should be properly understood.

Contrary to the rising water table, the falling water table has been the subject of considerable analytical research in the last two decades. In the development of analytical methods several research workers have made certain simplifying assumptions to obtain workable solutions of the problem. It seems that, after Childs' analogue study (4), no experimental investigation was carried out to test the validity of these assumptions until recently (1967) Maasland (5) used a viscous flow analogue (Hele-Shaw model) to demonstrate the limitations of Glover's original equation (6). Moreover, no general solution that is

entirely acceptable for design purposes has so far been found for problems involving a falllng water table. Therefore, to develop a practicable and useful method of designing a drainage system, it is essential that the various analytical methods should be evaluated critically and compared both mutually and with experimental data. This data can be easily obtained from a Hele-Shaw model, which may be considered as one of the most versatile tools to give solutions of unsteady drainage problems.

Apart from the symmetrical drainage problems mentioned above and illustrated in Fig. 1.1A, there are problems of unsymmetrical drainage systems of which little is known as yet. For example, a symmetrical drainage system may not be feasible in rough terrains. It may be necessary to misalign some drains (Section 5.8) vertically in sections of relatively low elevation. No research work on the moving water table between misaligned drains appears to have been reported in the literature and this problem therefore needs to be examined.

Another interesting unsymmetrical drainage problem occurs when a drainage system lies over a sloping impermeable bed. It may happen that the normal downslope flow of the seepage water is stopped by an underground "dam" consisting of a barrier of impermeable clay adjacent to the drainage area (Fig. 1.5). The water, if not drained, may soon approach the ground surface above the barrier and cause water-logging of the area. This problem,

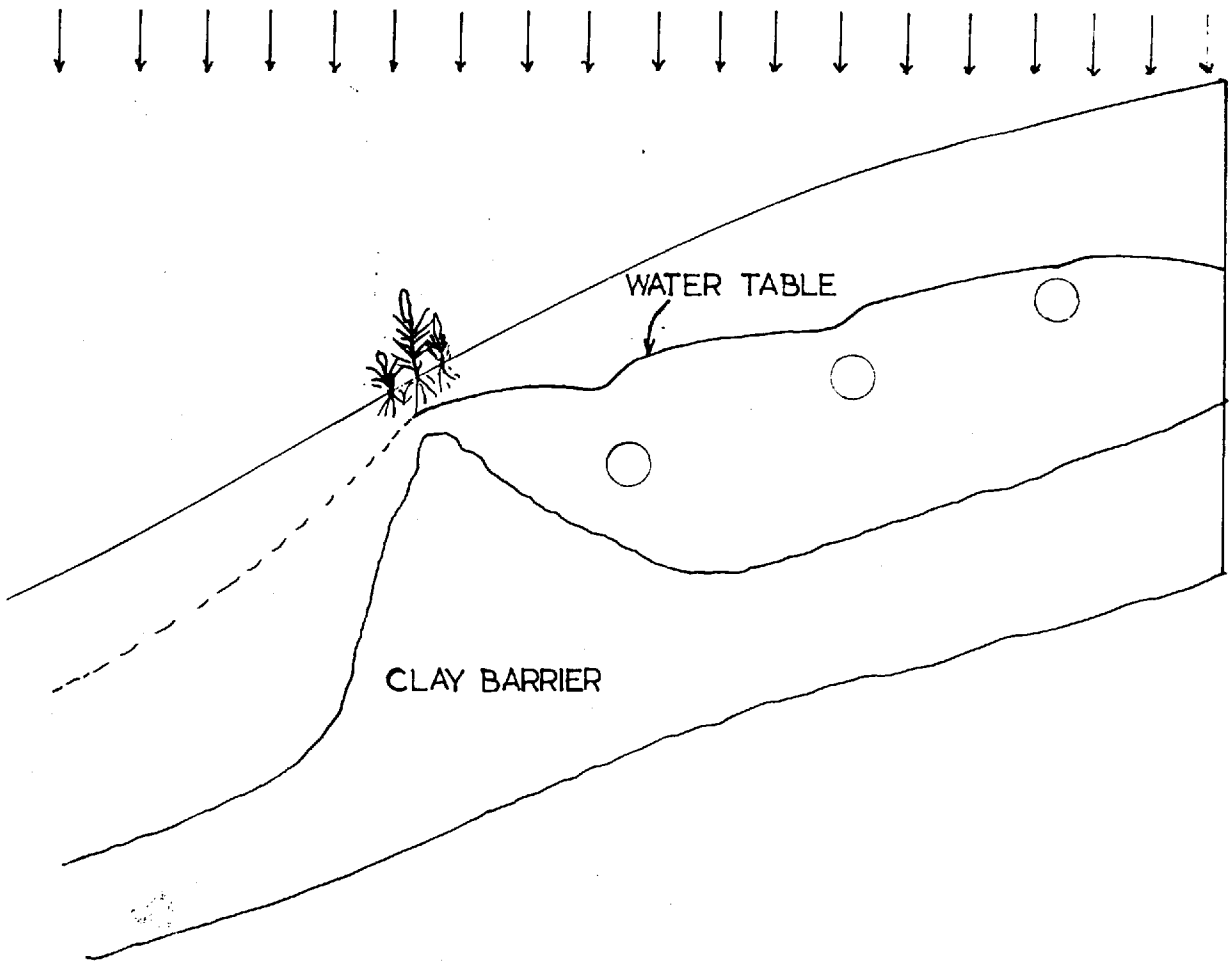


FIG:1.5 DRAINAGE OF SLOPING LAND

(LUTHIN, 1957, PAGE 360)

although of great practical importance, has not yet received much attention either analytically or experimentally.

1.5.2 Research objects:

The object of the present research is to provide solutions to the type of problems discussed in Section 1.5.1. For the symmetrical drainage system, the assumptions underlying a number of analytical methods for steady and unsteady state problems will be discussed in detail in Chapters 3 & 4. Hele-Shaw model results will then be compared with the analytical solutions in Chapter 5. It is believed that this evaluation will be useful in determining the extent to which the symmetrical drainage system solutions predict actual drainage conditions.

In symmetrical drainage systems, soil water drains most slowly at the midpoint between drains. Adequate drainage should remove the water at this point at a sufficiently high rate to keep the midpoint water table low enough to prevent crop damage. It is thus necessary for a rational design to determine the relationship between the rate of movement of the midpoint water table and other drainage parameters. Those considered in this investigation are: depth of impermeable bed below the drains; midpoint water table depth at the steady state condition; rate of percolation; hydraulic conductivity and drainable pore space of soil. Since almost all unsteady

state theories have been simplified to give the water table recession at the midpoint, therefore the rate of fall of water table only at this point is recorded in the experiments. The shape of water table with respect to time from the beginning of recession has been obtained from photographs. The rate of rise of the water table midway between the drains has also been investigated (Section 5.7.3).

Water table recession between drains submerged below the outlet ditch water level has been studied and the experimental results compared with analytical solutions wherever possible (Section 5.7.2).

The above procedure was also adopted for the unsymmetrical drainage systems(Section 1.5.1). In these systems, however, emphasis has been given to the highest point on the water table. This point may not necessarily be the midpoint as in the symmetrical drainage system.

The experimental results are presented in dimensionless form, the analysis of which is discussed in Chapter 5. The sloping drainage system is analysed mathematically and the solution is compared with experimental results in Chapter 6. A summary of the experimental results is presented in Chapter 7.

CHAPTER 2

GROUNDWATER FLOW

This chapter first describes the nature and properties of porous media. The mechanism of flow in such media, both on the macroscopic and microscopic scale, are then described in detail. The equations of motion for anisotropic and isotropic porous media are derived. A linear partial differential equation for flow over a sloping impermeable bed is also derived. This equation will later be solved in Chapter 6 for various boundary conditions.

2.1 POROUS MEDIA

A porous medium may be considered typically as a body of loose material containing innumerable irregularly shaped voids comprising "pore spaces" or interstices. The particles in the material may have a wide range of assorted shapes and sizes which, in turn, determine the geometry of the pore spaces. Each pore is connected by constricted channels to other pores, the whole forming a complex interconnected network of openings which form the channels through which a fluid may flow.

The term "porous material" encompasses a wide variety of materials. Within the context of ground water, for example, it includes the relatively fine grained soils and unconsolidated

sands, consolidated sands such as the common sandstones, lime stones and other porous rocks.

The most important properties affecting the flow of fluids in porous media are "porosity" and "hydraulic conductivity". Porosity is a measure of the pore space of a medium and is defined as the fraction of pore space in the medium relative to its total volume. Hydraulic conductivity is a measure of the ease with which a fluid passes through porous media. (A quantitative definition is given in Section 2.3).

The fluid capacity of a medium may not necessarily be the same as the total volume of pore space between the particles. A considerable amount of capillary and pellicular water may remain in the pores after drainage by gravity or applied suction. There may even be isolated pores that can never receive or yield water. The whole pore space may not be replenished during the rising water table phase because of a certain amount of entrapped air which remains in the pores. These effects are taken into account by re-defining porosity as "effective porosity" by which is meant the ratio of volume of water drained off under gravity to the total volume of the medium. In this thesis, the term 'porosity' refers to 'effective porosity".

The factors which influence the effective porosity and the hydraulic conductivity of a medium are: (a) the mean particle size, (b) the packing of particles, (c) the shape of the individual

particles, (d) the size distribution of the individual particles in the material and (e) the orientation of the particles. However, the actual shape and size of the individual particles and the way they are distributed are in reality so irregular that, when inquiring into the nature of a porous medium, its porosity and hydraulic conductivity are only meaningful if determined by average quantities over a volume of the medium that is much larger than any one pore. Such average quantities are used in the study of flow of fluids in porous media in the later sections.

Finally, it should be noted that all the mathematical developments in this thesis are based on the assumption that the porous medium is undeformable, i.e. there is no change in the flow geometry of the medium owing either to deformation in the medium itself or to foreign matter brought in by the fluid, which grows as the time of flow continues.

2.2 MECHANISM OF GROUNDWATER FLOW

The flow of groundwater in a porous medium occurs through its interconnected pore spaces. The path of individual fluid particles through the multiplicity of these pore spaces is excessively complex due to the tortuousity of the capillary channels formed by the interconnected pores, rapid changes in their cross-sectional area and possible changes in the flow conditions from laminar to turbulent flow. This complex pattern of fluid flow at the microscopic scale

would be describable by the continuum model normally used in Fluid Mechanics. However, the motion in the microscopic scale is complicated even in the simplest regular cases such as the flow through a set of regularly packed spheres. Moreover, even if such a solution were possible, it would be of little value in the study of actual groundwater flow.

In view of these difficulties, the flow pattern of groundwater is best considered on a macroscopic scale, i.e. we determine some average values of velocity, pressure, rate of discharge etc. over a large number of pores and disregard the effect of shape and size of the individual pores. Thus, at a porosity f, the average 'pore velocity' v* due to a discharge Q over a small area A (one considerably larger than a pore cross-section) is

$$v^* = \frac{Q}{fA} \qquad \text{..... (2.1)}$$

In the study of groundwater flow, the real flow of the fluid through the pores is generally replaced by an imaginary seepage flow which is assumed to fill the volume of both the pores and the soil skeleton. The velocity of flow due to the imaginary flow is termed the "seepage velocity" v. This velocity due to a discharge Q over an area A is given by

$$v = \frac{Q}{A} \qquad \text{..... (2.2)}$$

Equations (2.1) and (2.2) yield the relationship between the pore velocity and seepage velocity

$$v = fv^* \quad \ldots\ldots\ldots\ldots\ldots\ldots\ldots\ldots \quad (2.3)$$

Since $f < 1$, it follows that $v < v^*$ for a given situation. In this thesis, unless stated otherwise, the velocity will hereafter refer to the seepage velocity.

2.3 DARCY'S LAW

The first rational analysis of groundwater flow was the work of Henri Darcy. His report published in 1856 contained a text on infiltration through sand. From this study, he proposed a formula for the discharge through a cross-sectional area A:

$$Q = KIA$$

in which K is the Darcy coefficient and I is the hydraulic gradient. From the above equation it follows that

$$\therefore \quad v = \frac{Q}{A} = KI \quad \ldots\ldots\ldots\ldots\ldots\ldots\ldots\ldots \quad (2.4)$$

This equation formed the basis of all subsequent studies of flow through porous media.

Darcy's investigation was restricted to the empirical formulation of equation (2.4). He did not explicitly state whether the equation holds for laminar or turbulent flow, nor did he state specifically the properties of the medium/of the water in his empirical coefficient K. However,

subsequent to Darcy's publication, much research has been directed to an interpretation of the individual parameters that determine K. This coefficient, in fact, involves two sets of characteristics: one related to the pore geometry of the medium and the other to the physical properties of the fluid. Historically, the analytical evaluation of the first characteristic was based on the assumption that a relationship exists between the size of the individual particles comprising the porous medium and the dimensions of the pore channels available for flow.

The characteristics of K were first analysed by Hazen (7) by the method of dimensional analysis. According to Hazen, Darcy's coefficient K for laminar flow through porous media is given by

$$K = \frac{Cd^2}{\nu} g \qquad \text{..... (2.5)}$$

where d is the mean diameter of particles in a homogeneous porous medium; C is a dimensionless quantity which takes into account the effect of porosity, shape of grains and degree of cementation and ν is the kinematic viscosity of the fluid. Basically, therefore, Cd^2 is the geometrical characteristic of the porous medium and ν refers to the physical properties of the fluid.

An analytical justification of Darcy's Law can also be obtained from classical hydrodynamics. The simplest approach to this justification applies only to the extremely idealised case of laminar flow between a network of parallel circular tubes containing a porous medium consisting of small spheres of equal diameter. Such an idealised

sphere-type model was used by Rumer and Ralph (8) who deduced analytical results that were compatable with equation (2.5).

The product Cd^2 in equation (2.5) is defined as the intrinsic permeability k. The Darcy coefficient K is defined as the hydraulic conductivity. The Darcy law can thus be written in the differential form

$$v = -\frac{g}{\nu} k \frac{\partial h}{\partial s}$$

$$= - K \frac{\partial h}{\partial s} \qquad \text{..... (2.6)}$$

where $h = z + \frac{p}{\gamma}$

in which z is the elevation measured as positive above an arbitrary datum plane and p is the pressure in the fluid. The minus sign in equations (2.6) indicates that h decreases as the distance s increases. For a homogeneous anisotropic porous medium, the velocities in the three coordinate directions are given by

$$v_x = - K_x \frac{\partial h}{\partial x}$$

$$v_y = - K_y \frac{\partial h}{\partial y}$$

$$v_z = - K_z \frac{\partial h}{\partial z} \qquad \text{..... (2.7)}$$

Much research has been carried out on the significance of the individual parameters of a porous medium and the flow therein to find the range of validity of the Darcy law. Experiments showed that at large hydraulic gradient (and velocity), Darcy's law no

longer applied. It was to be expected that by analogy with the laminar and turbulent flow in pipes at low and high hydraulic gradients, the Darcy flow range might be confined to laminar flow conditions. This lead naturally to a consideration of a Reynolds number (R_e) for groundwater flow for use as a criterion for Darcy and non-Darcy flow regimes. A convenient R_e for groundwater flow is defined in terms of the seepage velocity and the mean grain size of the porous medium viz $R_e = \frac{vd}{\nu}$. Many experiments have been performed to establish the critical R_e for groundwater flow, below which Darcy's law applies but above which it does not. The experimental results showed a wide divergence in the range of critical R_e which could not be explained on physical grounds. For example, Linguist (7) conducted some experiments on grains of uniform size in the range of 1 to 5 mm. and a porosity of 38%. He observed that the Darcy law holds for $R_e \leq 4$. He also noted that for this medium, the flow became turbulent at $R_e > 180$. In another experiment on uniform glass beads, he found the Darcy law to hold up to $R_e \leq 12$, whereas for an unconsolidated and heterogeneous medium the limit was $R_e < 1$. The low value in the latter was attributed to a large variation in the pore space.

In view of the uncertainties discussed above, Muskat (7) considered it reasonable to accept a Reynolds number equal to one as a safe limit above which deviation from the Darcy law would occur. Muskat (7) also indicated that in the majority of groundwater flow

systems laminar flow would occur, except possibly in some localised parts of the porous medium, as for example, in the immediate vicinity of wells and tile drains.

Darcy's law is generally expressed in terms of velocity potential ϕ for the convenience in analysis of the groundwater flow either analytically or experimentally with models and analogues. Therefore, if the medium is homogeneous and isotropic and if the fluid is of constant density and viscosity, equation (2.4) becomes

$$v = -\frac{\partial \phi}{\partial s}$$

in which $\phi = Kh$

Velocities in the three coordinate directions will then be

$$v_x = -\frac{\partial \phi}{\partial x} \quad ; \quad v_y = -\frac{\partial \phi}{\partial y} \quad ; \quad v_z = -\frac{\partial \phi}{\partial z} \quad \ldots\ldots\ldots \quad (2.8)$$

2.4 EQUATION OF MOTION

The Darcy law does not permit the solution of a problem by itself. It merely gives information about the local velocity and its relationship to the local potential gradient. An equation giving the distribution of potential (ϕ) or head h is needed. The object in this Section, therefore, is to derive the general form of such an equation and this is done by a consideration of the conservation of matter. The particular boundary conditions valid for any given drainage problem along with the general equation for ϕ

form the starting point for the solution of that problem. Boundary conditions will be discussed in Chapter 3.

Consider an isolated small element of volume dx, dy, dz of a porous medium in the form of a parallelepiped (Fig. 2.1). Let the centre of the element be at the point x, y, z and the velocities of flow in the coordinate direction at this point be v_x, v_y and v_z. Further, let the medium be homogeneous but anisotropic with the values of hydraulic conductivity in the three coordinate directions K_x, K_y and K_z. The fluid is assumed to be incompressible

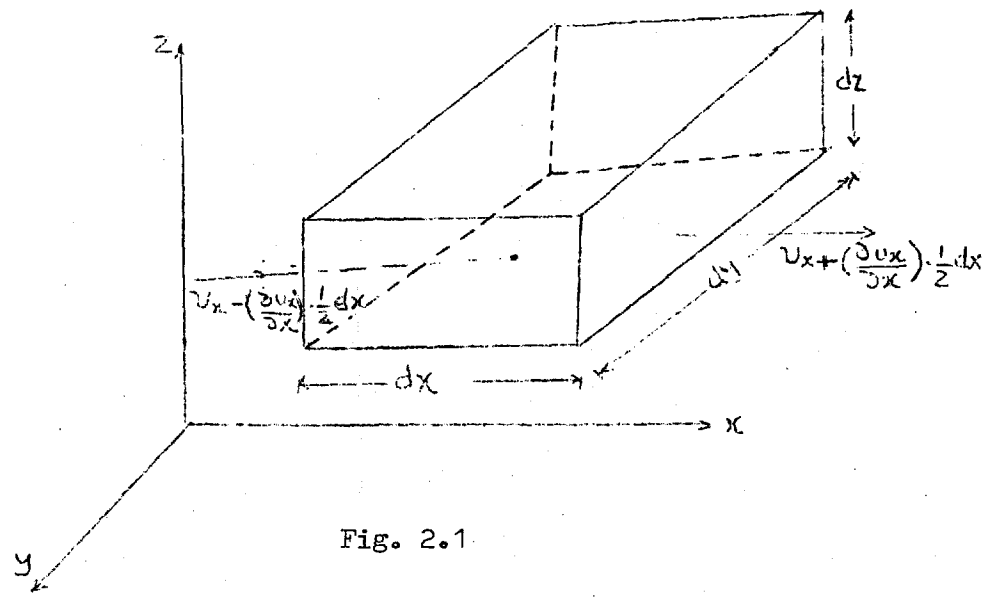


Fig. 2.1

In the x-direction, the rate of inflow is

$$\left[v_x - \left(\frac{\partial v_x}{\partial x}\right) \left(\tfrac{1}{2}dx\right) \right] \; dy \; dz$$

and the rate of outflow

$$\left[v_x + \left(\frac{\partial v_x}{\partial x}\right) \left(\tfrac{1}{2}dx\right) \right] \; dy \; dz$$

Therefore, the rate of storage on account of the inequality between inflow and outflow is

$$-\frac{\partial v_x}{\partial x}\, dx\, dy\, dz \qquad \ldots\ldots\ldots\ldots\ldots\ldots\ldots\ldots \quad (2.9)$$

A similar procedure in respect of the rates of storage in the volume element due to the flow components in the y and z directions gives

$$-\frac{\partial v_y}{\partial y}\, dx\, dy\, dz \qquad \ldots\ldots\ldots\ldots\ldots\ldots\ldots\ldots \quad (2.10)$$

and

$$-\frac{\partial v_z}{\partial z}\, dx\, dy\, dz \qquad \ldots\ldots\ldots\ldots\ldots\ldots\ldots\ldots \quad (2.11)$$

The total rate of storage of fluid in the volume element is therefore

$$-\left[\frac{v_x}{x} + \frac{\partial v_y}{\partial y} + \frac{\partial v_z}{\partial z}\right] dx\, dy\, dz \qquad \ldots\ldots\ldots\ldots\ldots\ldots \quad (2.12)$$

In the absence of sources and sinks in the element volume, conservation of matter requires that the sum given by equation (2.12) must be zero, i.e.

$$\frac{\partial v_x}{\partial x} + \frac{\partial v_y}{\partial y} + \frac{\partial v_z}{\partial z} = 0 \qquad \ldots\ldots\ldots\ldots\ldots\ldots\ldots\ldots \quad (2.13)$$

This equation is valid both in steady and unsteady saturated flow in a porous medium under the incompressibility condition.

In a homogeneous anisotropic medium, values of v_x, v_y and v_z are given by equations (2.7). Substituting these values in the above equation yields

$$K_x \frac{\partial^2 h}{\partial x^2} + K_y \frac{\partial^2 h}{\partial y^2} + K_z \frac{\partial^2 h}{\partial z^2} = 0 \qquad \ldots\ldots\ldots\ldots\ldots\ldots \quad (2.14)$$

This equation can be simplified by a change in the scales of the coordinate system. Let a new rectangular coordinate system X,Y,Z be related to x,y,z by the equations

$$X = x$$
$$Y = (K_x/K_y)^{\frac{1}{2}}\, y$$
$$Z = (K_x/K_z)^{\frac{1}{2}}\, z \qquad \text{.....} \qquad (2.15)$$

The substitution of equations (2.15) in equation (2.14) will result in

$$\frac{\partial^2 h}{\partial X^2} + \frac{\partial^2 h}{\partial Y^2} + \frac{\partial^2 h}{\partial Z^2} = 0 \qquad \text{.....} \qquad (2.16)$$

If, however, the medium is homogeneous and isotropic, i.e. $K_x = K_y = K_z$, equation (2.14) directly gives rise to

$$\frac{\partial^2 h}{\partial x^2} + \frac{\partial^2 h}{\partial y^2} + \frac{\partial^2 h}{\partial z^2} = 0 \qquad \text{.....} \qquad (2.17)$$

This is the well known Laplace equation for the three-dimensional flow in an isotropic homogeneous porous medium. For two-dimensional flow the above equation reduces to

$$\frac{\partial^2 h}{\partial x^2} + \frac{\partial^2 h}{\partial y^2} = 0 \qquad \text{.....} \qquad (2.18)$$

This equation has been used in the solution of the steady state and unsteady state drainage problems that will be reviewed in Chapters 3 and 4.

It may be seen that the effect of the transformation (2.15) on the anisotropic problem is to distort the linear dimensions in such

proportions as to render the problem isotropic in the transformed X,Y,Z space. The transformed Laplace equation is first solved and then the solution is transformed back into the x,y,z space by an inverse transformation (7).

2.5 DUPUIT'S ASSUMPTIONS

Dupuit's approach to groundwater flow problems was via equations for pipe and channel flow. He assumed the porous medium to be a collection of minute channels formed by interconnected pores in each of which the condition of flow was analogous to that in capillary tubes. He generalised the concept for the entire volume of the porous medium by assuming that all capillary tubes intersected in a vertical section were subject to identical condition of hydraulic gradient and that the velocity resulting therefrom was the same. The assumptions involved in this approximation were:

(i) the velocity across all points on a vertical section is independent of the depth;

(ii) the hydraulic gradient over a given vertical section is proportional to the slope of the water table at that section.

The limitations and inconsistencies of the Dupuit assumptions can best be explained by differentiating equations (2.7) for the isotropic case and thereby obtaining the identities

$$\frac{\partial v_x}{\partial z} = \frac{\partial v_z}{\partial x}, \quad \frac{\partial v_y}{\partial z} = \frac{\partial v_z}{\partial y}$$

Since the velocity across a vertical section is independent of the

depth

$$\frac{\partial v_x}{\partial z} = \frac{\partial v_y}{\partial z} = 0$$

so that $\frac{\partial v_z}{\partial x} = 0$ and $\frac{\partial v_z}{\partial y} = 0$. This means that v_z, the vertical velocity component, must be constant in the x,y plane of the flow system. Since v_z will be zero at those points where the flow is horizontal, such as at the inflow surface of a vertical well, v_z must be zero everywhere in such a system. Such a condition is obtained only if the slope of the water table is zero everywhere, and further, according to the Dupuit second assumption, all velocities must be zero. This suggests the absurd conclusion that there will be no flow in the system.

A rigorous examination of the Dupuit assumptions shows that they lead to an irreconcileable situation, but it does not invalidate the use of these assumptions. It is obvious that the flow, according to the second assumption, will essentially be horizontal so that the loss of head in the vertical direction will be negligible compared with the loss in the horizontal direction in many cases, especially those cases in which there is little convergence of the streamlines. An indiscriminate use of the assumptions to cases other than these would lead to inconsistancies due to their application in solving problems to which they do not apply.

The Dupuit assumptions have also been applied to a variety of drainage problems that will be discussed in detail in Chapter 3.

2.6 UNSTEADY UNCONFINED FLOW OVER A HORIZONTAL AND/SLOPING IMPERMEABLE BED

Consider a two-dimensional flow of an incompressible fluid in a small isolated element of a homogeneous isotropic porous medium (Fig. 2.2). Let the flow along the x-axis through the element be governed by the Dupuit assumptions, i.e. the water table is approximately flat and parallel to the impermeable bed (horizontal or moderately sloping). Let the equation of the water table be given by $h = f(x,t)$.

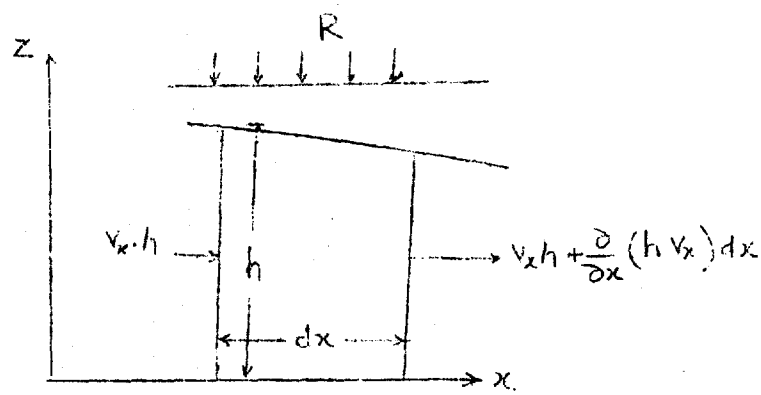


Fig. 2.2

Suppose the fluid flows through the left hand face of the element with a seepage velocity v_x. Then the rate of flow per unit width through the left hand face is $v_x h$. The rate of flow through the right hand face is

$$v_x h + \frac{\partial}{\partial x}(h\, v_x)\, dx$$

The rate of storage in the element is equal to the difference between the inflow and the outflow rates, viz.

$$-\frac{\partial}{\partial x}(v_x h)\, dx$$

In addition, suppose vertical percolation from the ground surface is occurring at a rate R per unit area of the horizontal surface. The rate of increase in storage in the element will be R dx.

Summing the above two expressions yields the total volume of the fluid stored in the element, i.e.

$$-\left[\frac{\partial}{\partial x}(v_x\, h) - R\right] dx \qquad \text{(18a)}$$

The rate of rise of water table is $\partial h/\partial t$. This increases the volume of the element at the rate

$$f\,\frac{\partial h}{\partial t}\,dx \qquad \text{(2.19)}$$

Equating (2.18a) and (2.19)

$$\frac{\partial}{\partial x}(v_x\, h) + f\,\frac{\partial h}{\partial t} - R = 0 \qquad \text{(2.20)}$$

Replacing v_x in the first term of this equation by

$$v_x = -K\,\frac{\partial h}{\partial x}$$

will transform equation (2.20) into the form

$$\frac{\partial}{\partial x}\left(h\,\frac{\partial h}{\partial x}\right) - \frac{f}{K}\,\frac{\partial h}{\partial t} + \frac{R}{K} = 0 \qquad \text{(2.21)}$$

For a moderately sloping impermeable bed, Darcy's law is

$$v_x = -K\left(\frac{\partial h}{\partial x} - \alpha\right)$$

where α is the slope of the impermeable bed with the horizontal

and h is the distance measured in the direction perpendicular to the horizontal. Substitution of the above equation in equation (2.20) will result in

$$\frac{\partial}{\partial x}\left[h \left(\frac{\partial h}{\partial x} - \alpha\right)\right] - \frac{f}{K}\frac{\partial h}{\partial t} + \frac{R}{K} = 0$$

or

$$\frac{1}{2}\frac{\partial^2(h^2)}{\partial x^2} - \alpha\frac{\partial h}{\partial x} - \frac{f}{K}\frac{\partial h}{\partial t} + \frac{R}{K} = 0 \quad \ldots\ldots\ldots\ldots \quad (2.22)$$

Equation (2.22) can be linearised by substituting

$$h^2 = y$$

$$\frac{\partial h}{\partial x} = \frac{1}{2\sqrt{y}}\frac{\partial y}{\partial x}$$

$$\frac{\partial h}{\partial t} = \frac{1}{2\sqrt{y}}\frac{\partial y}{\partial t}$$

with the result that

$$\frac{\partial^2 y}{\partial x^2} - \frac{\alpha}{\sqrt{y}}\frac{\partial y}{\partial x} = \frac{f}{K}\frac{1}{\sqrt{y}}\frac{\partial y}{\partial t} - \frac{2R}{K} \quad \ldots\ldots\ldots\ldots\ldots \quad (2.23)$$

If it is now assumed that 'h' deviates only a small amount from a weighted mean depth D of the groundwater stream, the [illegible] above equation is linearised in the form

$$\frac{\partial^2 y}{\partial x^2} - a\frac{\partial y}{\partial x} = \frac{1}{C}\frac{\partial y}{\partial t} - P \quad \ldots\ldots\ldots\ldots\ldots\ldots \quad (2.24)$$

in which $a = \alpha/D$

$P = 2R/K$

$C = KD/f$

By putting $\partial y/\partial t = 0$ in equation (2.24), the differential equation for the steady flow becomes

$$\frac{\partial^2 y}{\partial x^2} - a\frac{\partial y}{\partial x} = -Pr \qquad \text{.....} \qquad (2.25)$$

Equations (2.24) and (2.25) will be used in Chapter 6 for the analysis of flow between drains lying over a sloping impermeable bed.

CHAPTER 3

REVIEW OF STEADY STATE PROBLEMS

In the last three decades a number of solutions of steady state problems have been put forward. In this Chapter, some of these solutions (both for free flow and submerged flow conditions) are reviewed, the object being to outline the assumptions which have been made and, as such, to find out their limitations. The review of the steady state solutions is also important because some of the unsteady state solutions to be presented in Chapter 4 are considered as a series of successive momentarily steady states.

Of the many assumptions that are made to make a drainage problem amenable to analytical solution, the two most common are: (a) the Dupuit-Forchheimer assumptions for near-horizontal flow, and (b) the assumption of radial flow. The former is applicable to flat water tables where the spacing of drains is large compared to their depth. The radial flow assumption can best be visualised as being similar to the flow into a vertical well in a confined aquifer of uniform thickness and infinite in lateral extent. A tile drain can be considered as a horizontal well.

Some solutions are based on a combination of radial flow near the drain and horizontal flow at some distance away between drains (Fig. 3.1). Analytical methods based on these assumptions

are also reviewed in this Chapter.

3.1 THE DUPUIT -FORCHHEIMER METHOD

The Dupuit-Forchheimer method has been used extensively in the solution of drainage problems even though it is based on approximate assumptions (Section 2.5). Van Schilfgaarde (9) and Kirkham (10) critically evaluated the assumptions underlying the method and discussed its usefulness as a result of comparison with other methods based on physically more acceptable assumptions. They concluded that if the limitations underlying the method are well understood and not exceeded, it can, in some cases, lead to useful simpler solutions than are possible by the use of more rigorous methods based on the Laplace equation.

From a mathematical point of view, the main advantage of the D.F. assumptions (Section 2.5) of small water table gradient is that the average height of the water table ($D = \frac{y_m}{2} + d$) above the impermeable bed is used to represent the area available for ground-water flow. This simplification, as shown in Section 2.6, is essential to convert a non-linear partial differential equation to the simpler linear form of the equation of heat conduction. The latter can be solved easily by any of the conventional methods applied to the conduction of heat in solids.

Many investigators have carried out research to check the validity of the D.F. method. Guoyon (11) observed that the

method predicts a correct discharge, but not the correct water table profile, if the method is restricted to ditch drains penetrating to a shallow impermeable bed. A similar conclusion was arrived at by Hantush (12) for fully penetrating gravity wells. The method, however, may not be true for partially penetrating ditches and tile drains. In such cases, owing to the curvature of the streamlines, the majority of the flow may be confined to the upper strata of a system with the lower strata not contributing any appreciable flow. Therefore, if a system is already of sufficient depth for the full development of the active region of flow, any increase in the saturated depth below the drain will not result in an increase in the rate of flow or decrease in the depth of water table. This is in contrast to the D.F. method in which the flow is required to increase with depth according to the relation

$$Q = K\, D \frac{dh}{dx} \qquad \text{.....} \qquad (3.1)$$

in which Q is the drain discharge and D is the weighted mean depth of the saturated medium.

The validity of equation (3.1) can easily be checked with Hammad's analytical results (13). He showed that the drain discharge is some asymptotic function of the depth of the impermeable bed. The discharge was found to have essentially reached its maximum value when the depth from the drains to the bed was one quarter of the drain spacing, beyond which it remained constant. Equation (3.1), of

course, holds for small values of D, which indicates that the drain should lie near the impermeable bed. Therefore, the nature of the discharge-depth relationship, as given by Hammad's solution, may not be very surprising at higher values of depth-spacing ratios.

3.1.1 Ellipse Equation

One of the earliest attempts to find a mathematical solution of the ditch drainage problem was made by Hooghoudt (14). He equated equation (3.1) with the continuity equation of flow between ditch drains to obtain an ellipse equation for the shape of the water table

$$h^2 - h_o^2 = \frac{2Q}{LK}(Lx - x^2) \quad \ldots\ldots\ldots\ldots\ldots\ldots\ldots\ldots \quad (3.2)$$

where Q is the discharge through the ditch and other symbols are as shown in Figure 1.2. Equation (3.2) is useful, especially in a system in which the ditches are either at a small height above the impermeable bed or they penetrate completely to the impermeable bed. The validity of the equation near the vertical section midway between the ditch drains may be questioned because the flow is vertical here. However, this effect is offset because of the flow being approximately horizontal in the greater part of the flow region. Another feature of the ellipse equation is that it neglects the surface of seepage in the ditch drains. Consequently, its application is restricted to a low rate of percolation.

Several investigators have made various assumptions in applying the ellipse equation to partially penetrating ditches in the vicinity

of which the streamlines converge. Hooghoudt (14) considered the convergence effect by taking into account the longer path of the lower streamlines; Rothe and Kozeny (2, p. 84) suggested the hypothesis that the flow takes place only in the region above the horizontal line through the centre of the drains.

Schilfgaarde and Kirkham (2, p. 84) justified the application of the ellipse equation to tile drains on the grounds that the backfill over the drains retains higher permeability than the disturbed soil. This makes tile drains behave like partially penetrating ditches. A better approximation was thought to be obtained if the drains lie near the impermeable bed. In the cases of large depth below the drains to the impermeable bed, the flow is subject to considerable resistance due to the effect of convergence of the streamlines in the vicinity of the drains. Hooghoudt proposed a correction factor by substituting an equivalent depth d_e in place of the original depth of flow. He presented the solution of his complicated equation in a graphical form showing the depth of flow against the equivalent depth for various values of drain spacing. His graphs, however, were of limited use because they were applicable only to a specific size of drains. Moody (15) simplified Hooghoudt's formula to the form

$$\frac{d_e}{d} = \left\{1 + \frac{d}{L}\left[\frac{8}{\pi} \operatorname{Ln} \frac{d}{r} - \beta\right]\right\}^{-1} \qquad 0 \leq d/L \leq 0.3 \quad \ldots\ldots \quad (3.3)$$

in which

$$\beta = 3.55 - 1.6\,(d/L) + 2\,(d/L)^2 \quad \ldots\ldots\ldots\ldots \quad (3.4)$$

where the symbols are shown in Fig. 1.1A.

Moody showed that β varies very slowly in the range considered in equation (3.3). The variation was calculated to be less than 0.05 in that range. He therefore suggested that for all practical purposes β may be taken as a constant equal to 3.4. Thus, equation (3.3) can be re-written as

$$\frac{d_e}{d} = \left\{1 + \frac{d}{L}\left[\frac{8}{\pi} \operatorname{Ln} \frac{d}{r} - 3.40\right]\right\}^{-1} \qquad 0 \leq d/L \leq 0.3 \quad \ldots \quad (3.5)$$

For a case where the depth d is infinite, Maasland (16) gave a relation of the form

$$\frac{d_e}{L} = \left\{\frac{8}{\pi}\left[\operatorname{Ln}\left(\frac{L}{r}\right) - 1.15\right]\right\}^{-1} \quad \ldots\ldots\ldots\ldots\ldots\ldots \quad (3.6)$$

The original Hooghoudt equation is to be used for values of d/L beyond the range given by the above equations.

3.2 RADIAL FLOW ASSUMPTION

The radial flow assumption is necessary when the impermeable bed is either absent or exists only at a relatively great depth. In the earliest methods, radial flow was taken into account by using the similarity between the radial flow into a well and the flow into a tile drain. This technique became popular in solving drainage problems when the land was flooded to the surface. Hooghoudt (2, p. 85) used this technique to find an approximate solution for the steady flow towards a tile drain in a system having a very flat water

table. He postulated an infinite number of line sources on the horizontal line through the drain axes to identify a steady rate of rainfall. He then used the method of images to arrive at an approximate solution.

Hooghoudt's equation is expected to give satisfactory results if the curvature of the water table between drains is sufficiently small. This condition can only be obtained if the rate of rainfall is small compared to the soil permeability so that the height of the water table midway between drains is small compared to the depth of the saturated medium below the drains. This simplification, in fact, leads to the assumption that the head loss above the horizontal plane through the drains is negligible. A solution for such cases can then be obtained by taking an infinite number of images of the line sources as discussed previously. Hooghoudt, however, used a single row of images which cannot be considered sufficient to get an accurate solution.

The radial flow assumption breaks down as the impermeable bed approaches the drains. For intermediate depths of the impermeable bed, neither the horizontal flow nor the radial flow assumption alone gives a satisfactory solution. Hooghoudt solved this case by a judicious combination of the two assumptions as shown in Fig. 3.1. He assumed radial flow in the region near the drains and horizontal flow near the midpoint between drains.

The last equipotential in the horizontal flow region or the

first equipotential in the radial flow region was taken as a vertical line with the result that the potential drop ($\phi_A - \phi_B$ in Fig. 3.1) was zero. The horizontal distance X_1 was so chosen that ϕ_A approaches ϕ_B. Hooghoudt showed that

$$X_1 = (L - d/2)/2 \quad \text{for} \quad 0 < \frac{d}{L} \leq 0.25 \quad \ldots\ldots\ldots \quad (3.7)$$

Hooghoudt also found that the effect of the depth of the impermeable bed on the drain discharge is negligible for $\frac{d}{L} \geq 0.25$, so that d can be taken equal to 0.25 L for values greater than this ratio.

Although Hooghoudt's analysis was based on many approximations, it constituted one of the first comprehensive treatments of steady state tile drainage problems. So long as the assumptions are given full consideration, the method gives good results. Later studies based on more exact physical models showed close agreement with the appropriate Hooghoudt solution. Van Deemter (17) analysed the steady state drainage problem using the hodograph method which is based on the theory of conformal transformations. He assumed an infinite depth to the impermeable bed and found that his solution was in good agreement with the Hooghoudt analysis for the same boundary conditions. Wesseling (18) carried out extensive recomputations of Kirkham's method (Section 3.3.3) and compared the results with those from the Hooghoudt model. He showed that Hooghoudt's results (for the midpoint water table height) did not differ more than 5% from those of Kirkham's. Nevertheless, a drawback in Hooghoudt's solution is that it does

not give the shape of the water table. Also it does not take the size of the drain into account.

3.3 EXACT SOLUTIONS

Fairly exact solutions for the ground-water flow to equally spaced tile drains at uniform depth above the impermeable bed have been found by the hodograph method and the use of Fourier Series. Moreover, sufficiently accurate results have also been obtained by relaxation methods and electric analogues. Solutions of steady state problems by these methods have been obtained by assuming that a ditch or a tile drain conforms to a particular shape of equipotential. For tile drainage problems, the drain is assumed to ba a point sink of infinite negative potential at the drain centre. A zero equipotential surrounding the sink is identified with the tile circumference. This type of assumption is not true because none of the equipotentials conform exactly either to the shape of a fully penetrating ditch or to the tile drain, except, of course, when the impermeable bed is at a large depth.

3.3.1 Childs' Analogue experiments

Though many approximate analytical formulae were obtained prior to 1943, the effect of various parameters (Section 1.6) on tile drainage was still not well known. Childs (4a) carried out a series of experiments on a conductive sheet electric analogue to demonstrate the effect

of some fundamental drainage parameters which otherwise would have been difficult to examine analytically. He conducted experiments to study the effects of the size of a tile drain, the rate of percolation and the depth of the impermeable bed on the shape of the water table. He showed that flow to a tile drain is virtually unaffected by the depth of the impermeable bed for $d/L \geq 0.25$.

Childs also examined the effect of suction in the drain on the water table profile. He showed that the water table moves downward but that its shape does not change appreciably. Consequently, everywhere the water table is drawn down by much the same amount by the suction head in the drain.

Childs' experimental results could be applied only to the specific boundary conditions he used. These represented only a limited number of the several boundary conditions which really exist in steady state drainage problems. However, the results provided the means to verify the validity of mathematical solutions obtained by several subsequent research workers, for example, Engelund (19) and Van Deemter (17).

3.3.2 Solutions based on Hodograph method

Gustaffson (2, p. 127) gave the first analytically exact treatment of the tile drainage problem using the hodograph method. This, however, was a particular case of a more general solution later obtained by Van Deemter (17) and Engelund (19). A detailed account of the hodograph method was presented by Luthin, Kirkham

Van Deemter studied the seepage of steady rainfall through a saturated homogeneous soil of infinite thickness towards an array of equidistant parallel drains as shown in Fig. 3.2. He analysed the steady state problem by considering that state to have resulted from fluxes to or from two different regions. The first one was in the upper region and of magnitude N; the second one in the lower region was of magnitude M. With the origin of coordinates at the centre of a drain and the positive y-direction upwards, negative values of N and M indicated rainfall and deep seepage whereas positive values designated evaporation and artesian flow. Van Deemter divided his analysis into two sections depending on whether $M-N \gtrless 0$. If the difference M-N is +ve the drains will remove water. If it is -ve infiltration occurs from the tile line into the subsoil, i.e. sub-irrigation will result.

By using the hodograph method and conformal transformation, Van Deemter got a solution (for M-N +ve) in the form of two general equations giving the heights of the water table at the midpoint and over the drains. These equations are:

$$\frac{2\pi Y_m}{L} = \text{Ln}\,\frac{2+\beta}{\beta} + \frac{2}{\beta}\,\text{Ln}\,\frac{2+\beta}{2\beta} \qquad \ldots\ldots\ldots\ldots\ldots \quad (3.8)$$

$$\frac{2\pi Y_o}{L} = \text{Ln}\,\frac{2+\beta}{\beta} + \frac{2}{\beta}\,\text{Ln}\,\frac{2+\beta}{2+2\beta} \qquad \ldots\ldots\ldots\ldots\ldots \quad (3.9)$$

where

$$\beta = \frac{(1+\delta)\tan\theta + \left[1 + (1+\delta)^2 \tan^2\theta\right]^{\frac{1}{2}}}{\tan\theta + (1+\tan^2\theta)^{\frac{1}{2}}} - 1 \qquad \ldots \quad (3.10)$$

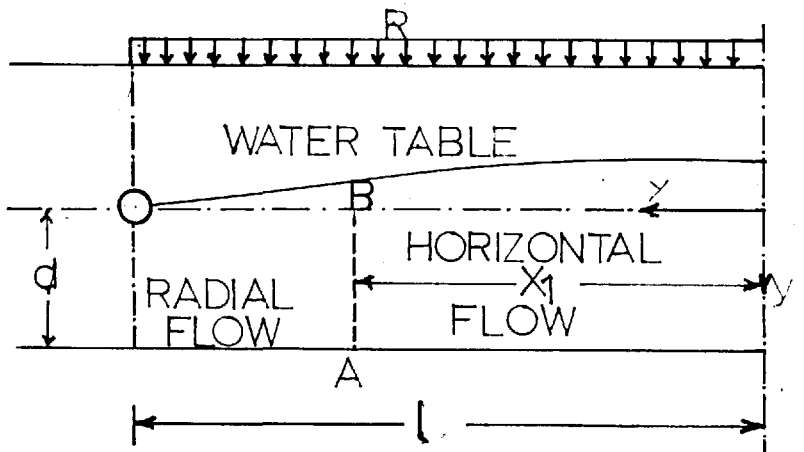


FIG: 3.1 HOOGHOUDT'S MODEL

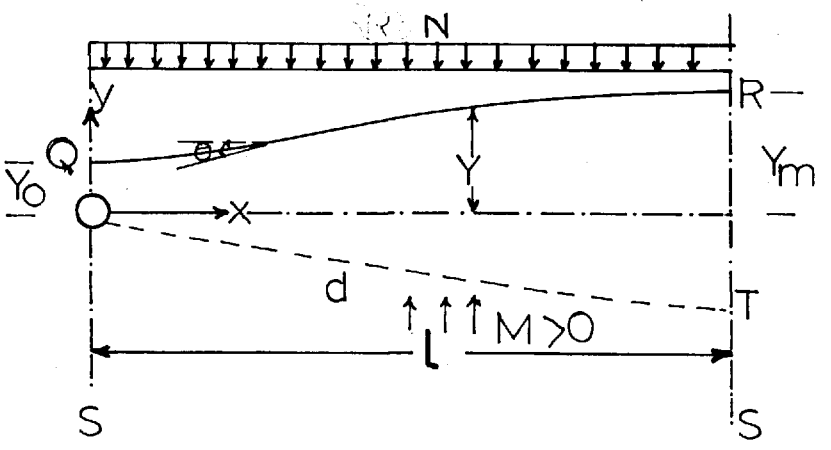


FIG:3.2 VAN DEEMTER'S MODEL

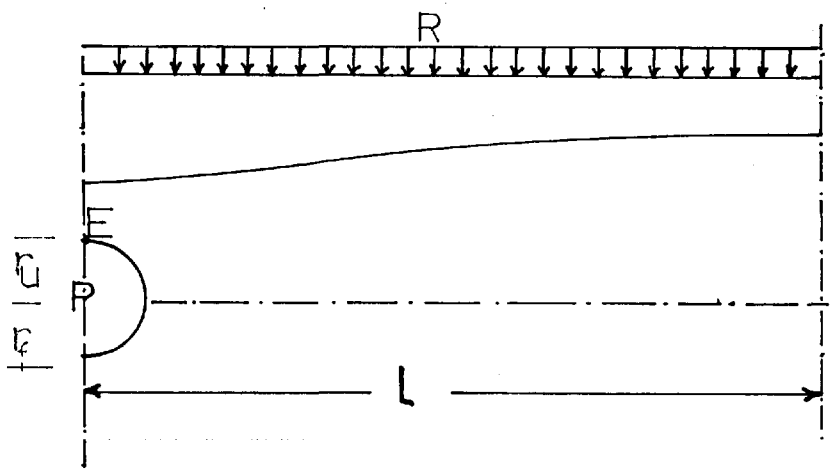


FIG:3.3 DRAIN RADIUS IN WATSON'S SOLUTION

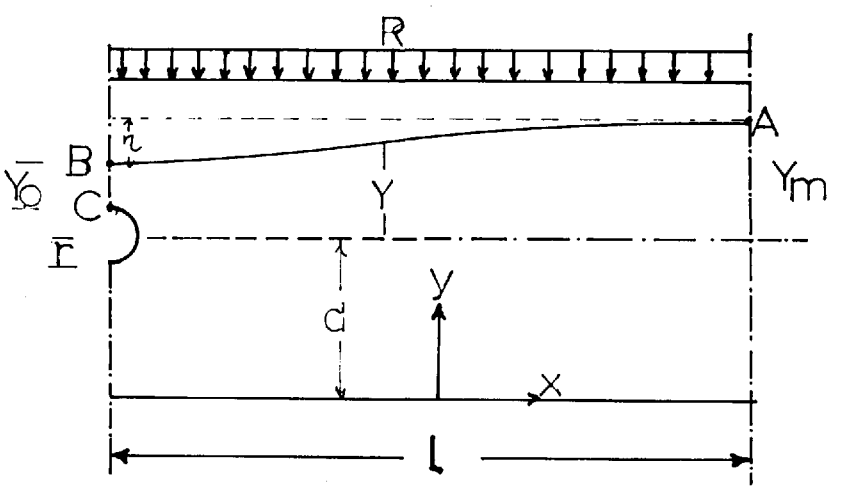


FIG:3.4 HAMMAD'S MODEL

and

$$\alpha = \frac{K + N}{M - N} \quad \ldots\ldots\ldots\ldots\ldots\ldots\ldots\ldots\ldots\ldots \quad (3.11)$$

β depends on the drain diameter and pressure in the drain. It decreases if the pressure in the drain increases or if the drain diameter decreases.

Van Deemter took the drain size into consideration by determining points around the sink P (Fig. 3.3) so that the potential at those points is of the same magnitude as at the point E. This assumption will hold if the drain runs full under back pressure.

The anomoly in Van Deemter's analysis lies in the assumption that the equipotential defining the boundary of a drain is circular, so that the distance r_u (Fig. 3.3) from the axis of the drain to the point where the equipotential line cuts the vertical through this axis above the drain is the radius of the drain. This is justifiable if the size of the drain is very small or the height of water table above the drain is very large.

Watson (20) made a more precise estimate of drain size by computing the distances r_u and r_f (Fig. 3.3) to the points of intersection of the equipotential line above and below the centre of the drain. He took the drain diameter as the sum of these distances. He determined the variation of $(r_u - r_f)/r_u$ with R/K for the optimum condition (θ = 90 deg. in Fig. 3.2) and showed that, in the range $0.001 \leqslant R/K \leqslant 0.03$, there was only a very small decrease in $(r_u - r_f)/r_u$

with increasing R/K. However, as R/K increased beyond 0.10, the difference increased rapidly until at R/K = 0.255, r_u equalled r_f; beyond this the rate of increase of r_f over r_u was found to be very large.

Theoretically the rapid increase in r_f indicates that the equipotential line (which is considered as the drain circumference in Van Deemter's solution) is assuming a shape greatly different from that of a circle because the distance r_f becomes greater than r_u as R/K increases beyond 0.255. This shows that Van Deemter's solution will be exact only for R/K = 0.255. Thus the general behaviour of the equipotential line with increasing R/K emphasises the care necessary in choosing the range over which the concept of the replacement of an equipotential line by a drain circumference is applicable.

Watson also studied the effect of the capillary fringe (a zone just above the water table throughout which the soil is saturated although under suction) over the difference in the lengths r_u and r_f. He concluded that for optimum condition $(r_u - r_f)/r_u$ increased with the thickness of the capillary fringe. The increase was observed to be more rapid for high values of R/K.

Engelund (19) analysed steady state drainage problems in a way similar to Van Deemter's. In fact, his solution can also be considered as a special case of a more general solution given

by Van Deemter. He related water table height and drain diameter to the corresponding parameters of an 'optimum drain'.

3.3.3 Kirkham's Potential Function method

Kirkham (21)refined Hooghoudt's analysis and derived equations for water table profiles over tile drains running either part-full at atmospheric pressure (Fig. 1.3) or submerged below the free water surface in a collector ditch (Fig. 1.4). He assumed that the curvature and the head loss in the water table arch were very small. In order to implement these approximations, he used a conceptual model in which he postulated closely spaced, infinitesimally thin, parallel strips extending vertically down the soil to the reference plane passing through the centre of the drains for the free discharging drains and through the free surface in the collector ditch for the submerged drains. Fig. 3.5 shows such a typical case for a submerged drain.

The frictionless strips made the flow vertical in the region of the water table arch. In this region, he imagined a highly permeable medium such as gravel to be placed so that the head loss in the water table arch could be ignored. In a subsequent work, Kirkham (22) improved this model by replacing the gravel with a less permeable soil. However, the assumption regarding the vertical flow in the frictionless strips was still retained.

Within the analytical limitations, Kirkham, like Van Deemter,

gave a general treatment of steady state drainage problems. The mathematical solution that Kirkham applied to his model was exact (i.e. granted the model assumptions) provided the shape of a drain or a ditch conformed to an equipotential about the line sink as discussed in Section 3.3.

Using Kirkham's (21) equation for the case of a free discharging drain and applying the correction factor developed by him for the head loss in the water table arch region, would give the water table height via

$$Y = \frac{LR}{\pi K(1-R/K)}\left[\operatorname{Ln}\frac{\sin(\pi x/L)}{\sin(\pi r/L)} + \sum_{m=1}^{\infty}\left[\frac{1}{m}\left\{(\cos 2m\pi r/L - \cos 2m\pi x/L)\right\}\right.\right.$$
$$\left.\left.\coth(2m\pi d/L) - 1\right]\right] \quad \ldots\ldots \quad (3.12)$$

in which the symbols are shown in Fig. 1.3. Equation (3.12) can be abbreviated to the form

$$Y = \frac{LR}{K(1-R/K)} F_1(x,0) \quad \ldots\ldots \quad (3.13)$$

where $F_1(x,0)$ is equal to $1/\pi$ multiplied by the bracketed portion of equation (3.12).

Wesseling (23) made an extensive recomputation of Kirkham's equations to study the relative advantage of submerged drains (Fig. 3.5) over free discharging drains (Fig. 1.3). He showed that the effect of submergence (Section 1.3(iii)) is to decrease the curvature of the streamlines and hence the length of the flow

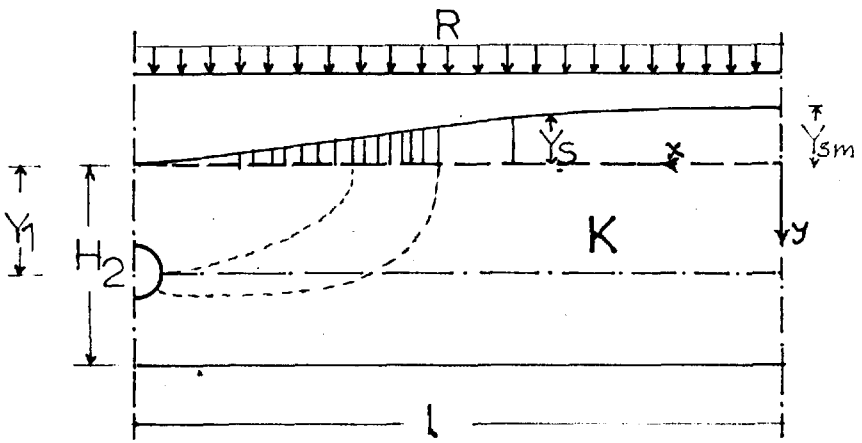


FIG:3.5 KIRKHAM'S MODEL FOR SUBMERGED FLOW

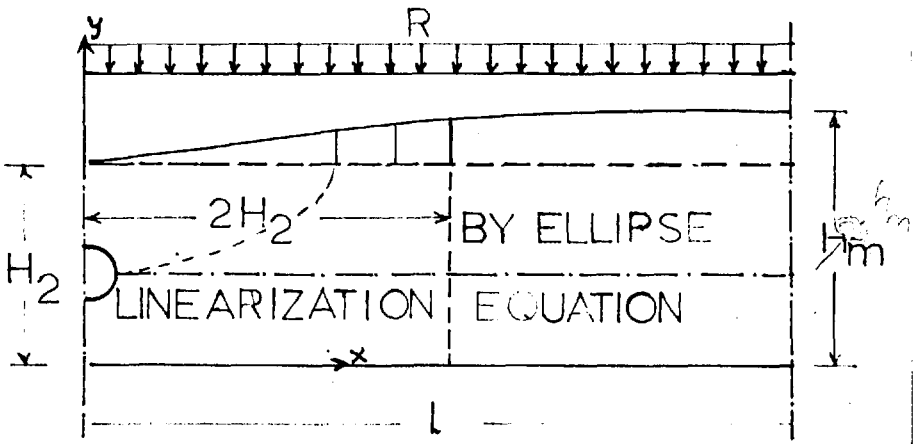


FIG:3.6 DAGAN'S MODEL

path. The decrease in the length of flow path results in a decrease of the loss of head. It means that for the same amount of flow, the midpoint water table height, relative to a particular datum plane, will be smaller over a submerged drain than over a free discharging drain. Wesseling also gave a simple numerical solution of Kirkham's equation for submerged drains.

A rearrangement and simplification of Kirkham's equations for submerged drains can be done to find the shape of the water table. This is necessary to compare experimental results with the computed water table profile (Section 5.7.2). The height of all points on an arched shaped water table is given by

$$Y_s = \frac{LR}{K(1 - R/K)} F_2(x,0) \quad \ldots\ldots\ldots\ldots\ldots\ldots\ldots\ldots \quad (3.14)$$

where the symbols are shown in Fig. 1.4, and

$$F_2(x,0) = \frac{1}{\pi}\left[\sum_{m=1}^{\infty}\left(\frac{1}{m}\right)\coth\left(2m\pi H_2/L\right)\left[1 - \cos\left(m\pi x/L\right)\right] - \sum_{m=1}^{\infty}\left(\frac{1}{m}\right)\left\{1 - \cos\left(m\pi Y_1/H_2\right)\right\}\right] \quad \ldots\ldots \quad (3.15)$$

Kirkham (21) showed that the algebraic summation of his equations (34) and (35) is zero for $x = 0$ and $y = 0$, but as x and y approach zero, the summation tends to a limiting value $\text{Ln } H_2/L$. Therefore, there will be a sudden finite jump of $\text{Ln } H_2/L$ in Y_s as x and y both become zero. Warrick (24) introduced this correction by subtracting $\frac{1}{\pi}\text{Ln } H_2/L$ from equation (3.15). Equation (3.15) is accordingly

modified as

$$F_2(x,0) = \text{Equation (3.15)} - \frac{1}{\pi} \ln H_2/L \quad \ldots\ldots\ldots\ldots\ldots\ldots \quad (3.16)$$

For given values of R and K, water table heights for submerged drains can be obtained by substituting function $F_2(x,0)$ in equation (3.14).

The major drawback in Kirkham's solution is that he assumed vertical flow in the layer above the drains. This is not always true, particularly in those cases where the hydraulic conductivity of the upper layer is larger than that of the lower layer. Wesseling showed how Kirkham's solution can be used in cases where the permeability in the water table arch is different from that of the rest of the medium. Childs (4a) observed experimentally that the assumption of vertical motion in the water table arch does not affect the results very much.

The assumption of vertical motion above the horizontal line passing through the drains centre also implies that no lateral flow occurs in this region. This may be true for low values of R/K when the water table is very flat. The horizontal component of the flow may be considerable when Y_m/d is very large due to high rate of R/K. Therefore, Kirkham's solution is restricted to low values of R/K or Y_m/d.

3.3.4 Hammad's method

Hammad's approach (13) to the steady state drainage problem

was obtained via the use of complex variables. The shape of the water table given by him greatly resembled the one given by Van Deemter because both assumed that the drains ran full under some over-drain water table height. By separating the real and imaginary parts of a complex velocity potential, Hammad got the potential at any point in the form

$$\phi = \frac{Q}{4\pi} \ln \left\{ \left[\sin(2\pi x/L) \cosh(2\pi y/L) + \cosh(2\pi d/L) \right]^2 + \cos^2(2\pi x/L) \sinh^2(2\pi y/L) \right\} + C \quad \ldots\ldots \quad (3.17)$$

in which Q is the drain discharge per unit length of the drain; and other notations are shown in Fig. 3.4.

Hammad obtained an equation for the water table by writing $\phi = \eta + d + Y_o$ and $y = d + Y_o$. He neglected η in the latter expression on the assumption that $2\pi\eta/L$ in the right hand side of equation (3.17) was very small. Thus

$$\eta = \frac{Q}{4\pi} \ln \left\{ \left[\sin(2\pi x/L) \cosh(2\pi(d + Y_o)/L) + \cosh(2\pi d/L) \right]^2 + \cos^2(2\pi x/L) \sinh^2 \frac{2\pi}{L}(d + Y_o) \right\} - (d + Y_o) + C \quad (3.18)$$

He solved equation (3.18) for the free surface by putting p = o at points A,B,C in Fig. 3.4.

Assuming that d/L, Y_o/L and Y_m/L were very small, Hammad found the following equations for the drain discharge and water table height

midway between drains:-

$$Q = \frac{2\pi K\, Y_m}{Ln\left[\frac{Y_m}{r} + \frac{L^2}{2\pi^2 d\, r}\right]} \text{ for } d/L \leq 0.25 \quad \ldots\ldots\ldots\ldots \quad (3.19)$$

$$Y_m = Y_o \frac{Ln\left[\frac{Y_m}{r} + \frac{L^2}{2\pi^2\, d\, r}\right]}{Ln\frac{Y_o}{r}} \text{ for } d/L \leq 0.25 \quad \ldots\ldots\ldots\ldots \quad (3.20)$$

Hammad observed that the greater part of the variation of Q takes place in the range $d/L \leq 0.25$ for which equations (3.19) and (3.20) were supposed to be better approximations. For values of $d/L > 0.25$, when the drain discharge is unaffected by the depth d, he obtained equations

$$Q = \frac{2\,\pi\, K\, Y_m}{Ln\left(\frac{Y_m}{r} + \frac{L}{\pi r}\right)} \quad \ldots\ldots\ldots\ldots \quad (3.21)$$

$$Y_m = Y_o \frac{Ln(Y_m/r + L/\pi r)}{Ln(Y_o/r)} \quad \ldots\ldots\ldots\ldots \quad (3.22)$$

List (25) made a numerical comparison between Hammad's method and those of Engelund and Van Deemter. He showed that Hammad's approximation of $2\pi d/L$ being small was not justified for low rates of rainfall. By appropriate adjustment of equation (3.21) and comparing it with Engelund's solution, he showed that Hammad's approximation was comparatively less accurate when the slope at the point of inflexion of the water table was very high. Similar

conclusions can be arrived at from the Van Deemter solution. Van Schilfgaard, Kirkham and Frevert (26) critically examined Van Deemter's solution to compare it with Hammad's. They showed that the difference in water table height between and over the drains is given by

$$\frac{\eta_c}{L} = \frac{Y_m - Y_o}{L} = \frac{2}{\pi\gamma} \ln(1 + \gamma) \quad \ldots\ldots\ldots\ldots \quad (3.23)$$

where $\gamma = \frac{K}{R} - 1$

Thus an increase in the rate of rainfall R will decrease γ and hence η_c/L in equation (3.23). Since η_c/L in Hammad's equation is supposed to be small, Hammad's solution is valid only for low rates of rainfall. On the other hand, a decrease in γ in Van Deemter's solution is associated with a decrease in β in equation (3.10) and hence the angle θ which the water table makes with the horizontal at the point of inflexion. Therefore, Van Deemter's solution applies for high rates of rainfall. This statement will be supported by comparing experimental data with Van Deemter's analytical results in Section 3.5. List also indicated that for $\theta = 20^{\circ}$ there was close agreement between Engelund's and Hammad's solutions.

3.3.5 Dagan's Approximation

Dagan's (27) method of approach was a combination of the methods of Hooghoudt and Kirkham. Like Hooghoudt, he divided the flow into two regions as shown in Fig. 3.6. One region was governed by Dupuit's elliptic equation (Section 3.1.1); in the second region

he used a linearised solution obtained by assuming that the vertical velocity of flow is equal to the steady rate of rainfall. Steady rainfall was arranged along a horizontal plane passing through the centre of the drains. This assumption implies that the water moves vertically through the water table arch. It is valid if the midpoint height of the water table is very small compared to the drain spacing (Section 3.1.1). Physically this assumption amounted to neglecting the flow in the water table arch as in Kirkham's model (Section 3.3.3) and thus to transforming the problem into one of a confined flow for a simple solution. It was also assumed that the drain is half-full and the drain radius is relatively small.

By combining the solutions based on the Dupuit assumptions and the linearization method, Dagan obtained equations for the maximum water table height midway between drains lying in isotropic and anisotropic soils. Equations (3.24) and (3.25) give the midpoint water table height for free and submerged drains in isotropic soil.

$$h_m^2 - d^2 = \frac{R}{K} \cdot \frac{L}{2}\left(\frac{L}{2} - 2\alpha_1 d\right) \quad \ldots\ldots\ldots\ldots \quad (3.24)$$

in which

$$\alpha_1 = \frac{1}{\pi} \operatorname{Ln}\left[2(\cosh \pi r/d - 1)\right]$$

$$h_m^2 - H_2^2 = \frac{R}{K} \frac{L}{2}\left(\frac{L}{2} - 2\alpha_2 H_2\right) \quad \ldots\ldots\ldots\ldots\ldots\ldots \quad (3.25)$$

where

$$\alpha_2 = \frac{1}{\pi} \operatorname{Ln}\left[2(1 + \cos \pi d/H_2)\right]$$

and other notations are shown in Fig. 3.6.

Since the analyses by Kirkham and Dagan are based on the same assumptions and both deal with free discharging and submerged drains, the two solutions are compared numerically to show the difference as might be expected due to Dagan's linearization approximation. Dagan's solution for submerged drains takes the size of the drain into account, whereas Kirkham assumed the drain to be a sink. Therefore, a comparison of results for submerged drains may not be expected to give fair agreement.

Using Wesseling's (23) data for drainage: R = 0.007 m/day, K = 0.2 m/day, d = 2.0 m, h_m = 2.5 m, r = 0.02 m and by applying the graphical solution given by Toksoz and Kirkham (28), Wesseling found that the spacing between the free dischargind drains was 9.4 metres.

From Dagan's Fig. 8, α_1 = -2.25 for r/d = 0.01 and R/K = 0.035. Substituting this value of α_1 in equation (3.24) gives a drain spacing equal to 9.0 metres. This result shows that the spacing calculated by Dagan's method is in close agreement with the Kirkham value.

3.4 COMPARISON BETWEEN EXPERIMENTAL STUDIES AND RATIONAL METHODS

Collis-George and Young (29) used a sand model to study the effect of the depth of the impermeable bed on water table height with various rainfall intensities. They observed that their sand model results agreed remarkably well with the Childs (4a) electric analogue results. They found that for a given R/K, the midpoint

water table height decreased as the depth of the impermeable bed below the drain level increased, but that it became constant for $d/L \geq 0.15$. Their experimental results with deep impermeable beds corresponding to this critical ratio agreed with Engelund's analytical solution.

Hammad's conclusion that for $d/L \geq 0.25$ the impermeable bed has no effect on Q/KY_m cannot be considered general, because the conclusions were drawn for a specific value of $L/\pi y_o = 100$ (for $y_o = r$) Q/KY_m will be different for different values of $L/\pi y_o$ in Hammad's equation.

$$\frac{Q}{KY_m} = \frac{2\pi}{\ln(1 + L/\pi y_o \coth 2\pi d/L)} \quad \text{for } Y_o > r \quad \ldots(3.26)$$

Dujaili (30) made an extensive study of the steady flow between equally spaced as well as misaligned tile drains. He compared his experimental data on the steady state midpoint water table height with the results obtained from equation (3.26) by using $L/\pi y_o = 100$ (for $y_o = r$) This comparison does not seem to be correct because the experimental value of $L/\pi y_o$ varies. Table 3.1 shows the correct values of Q/KY_m computed from equation (3.26). It will be observed that there is a close agreement between the observed and computed values of Q/KY_m at high values of d/L.

Dujaili's experimental results show that in most cases the water table height above the drain was greater than the drain radius i.e. $Y_o > r$. His experimental results, therefore, conform to the

TABLE 3.1

Prototype figures.

K = 28 cms/hr r = 5.0 cms

L = 3000 cm.

Experimental values*					Computed values	
Q cc/sec	Y_m cm.	Y_o cm.	d/L	Q/KY_m	Q/KY_m $Y_o = r$	$Q/Y_m K$ $Y_o = r$
0.828	134.00	24.10	0.0767	0.795	1.03	1.39
0.988	149.30	46.90	0.0933	0.850	1.07	1.70
1.066	149.00	51.40	0.1233	0.920	1.11	1.85
1.071	127.00	44.00	0.1933	1.085	1.16	1.90

* values taken from Dujaili's thesis (30, Table 17, page 121).

boundary conditions assumed in the solutions by Van Deemter and Hammad (Sections 3.3.3 & 3.3.4). This suggests that Dujail's experimental results should agree with the theoretical results obtained from those solutions.

For the sake of comparison, γ in Van Deemter's solution (equation 3.10) was determined by using Dujaili's experimental values of permeability and the steady rate of rainfall R. Knowing Y_o/L from the experimental results one can calculate β from equation (3.9) and finally Y_m is computed from equation (3.8). Y_m in Hammad's solution can be calculated from equation (3.21). The computed values for both cases are given in Table 3.2.

Comparison of the values shows that Hammad's and Van Deemter's solutions overestimate Y_m/L. The maximum difference between the Dujaili experimental data and Van Deemter's values is 82% and that between the experimental and Hammad's solution is of the order of 72%. Such a big difference may be caused by the fact that whereas the experimental drain is circular and of constant diameter, the size of the drain varies with the depth of water table above it in Hammad's and Van Deemter's solutions (Section 3.4.1). When the water table just touches the drain circumference, the drain may be horse-shoe shaped in the analytical solution rather than circular. It will also be observed that there is a large difference between the Hammad and Van Deemter analytical results. This may be attributed to Hammad's approximations discussed in Section 3.3.4.

TABLE 3.2

COMPARISON OF VAN DEEMTER AND HAMMAD'S SOLUTIONS

WITH EXPERIMENTAL RESULTS* FOR d/L = 0.30

r = 0.5 cm. L = 100 cm.

Experimental results				Analytical results			
				Van Deemter			Hammad
Q cc/sec.	K/R	Y_o/L	Y_m/L			Y_m/L	Y_m/L
6.03	2.765	0.083	0.160	1.765	1.350	0.238	0.275
5.10	3.270	0.054	0.132	2.270	1.975	0.206	0.230
3.75	4.430	0.037	0.100	3.750	3.100	0.166	0.164
2.34	7.130	0.023	0.070	6.130	5.275	0.118	0.0990
1.43	11.700	0.009	0.046	10.700	10.650	0.083	0.065
1.15	15.000	0.008	0.039	14.000	13.650	0.0680	0.0450

* taken from Dujaili's thesis (30, page 98).

Van Schilfgaarde and Kirkham (2, page 137) compared Childs' analogue results (4a) with Van Deemter's hodograph solution, because assumptions underlying both the solutions were identical. Difference of the order of 15% in Y_o/L and 4% in Y_m/L was found. This difference was attributed to the error in ascertaining the proper drain size in the analogue.

3.6 CONCLUSIONS

From the previous discussion it is clear that the steady state problem has been tackled in two ways. Whereas Kirkham and Dagan assumed that the water table over the drains does not rise above their centres, Hammad, Van Deemter and Engelund considered the drains to be running full with the water table a certain height above the drain (Fig. 1.2). Schilfgaarde and Kirkham(26) criticised Van Deemter's and Hammad's assumption of "above-drain" water table height. They argued that such a condition only develops when the soil is of very low permeability, or the recharge rate is high, conditions which they believed rarely exist in practice.

The discussion in this Chapter also explains why the available analytical methods are not expected to give a general solution incorporating all boundary conditions. Each deals with some specific aspect of the problem, and is based on different assumptions. Considerable experimental investigations are therefore needed to delineate the limitations of these assumptions.

CHAPTER 4

REVIEW OF UNSTEADY STATE PROBLEMS

In this chapter are reviewed several general solutions of the problem of the falling or rising water table between symmetrical tile drains following a sudden cessation or increase of surface recharge. The solutions can be generalised into three main categories. Those in the first category are based on simplifications such as the Dupuit assumptions. The second category of solutions has been obtained by solving a non-linear partial differential equation of unsteady drainage by iterative methods. The third category depends on the assumption that a time-independent relationship between a steady water table height Y and the corresponding steady drainage rate R (or rate of recharge) can be integrated with respect to time. With this assumption, some research workers have developed a simple technique that can be used to obtain a falling water table solution from an initial steady state relation between Y and R, whether this relation be given analytically, graphically or numerically. In Chapter 5 these solutions will be compared mutually as well as with the experimental data obtained during this research.

4.1 GENERAL

Problems involving moving water tables between equally spaced tile drains have long defied an exact mathematical analysis. Some investigators have attempted to find approximate solutions which

could give an estimate of the water table movement for design purposes. These solutions are based on various physical and mathematical assumptions, some of which are at variance with the known facts and hence they cannot be relied upon without an experimental verification.

The most common assumption in all problems of the moving water table is that the pore space is drained or filled abruptly as the water table falls or rises. In many solutions the porosity is also assumed constant, i.e. independent of the water table position and time. Childs (31), after evaluating the errors involved, considered these assumptions to be incorrect. Dumm (32) and Dumm and Wringer (33), when comparing field data with Glover's solution, considered drainable porosity as a variable and it was determined by evaluating the volume of water discharged from a field drain system, in a given time, in relation to the volume of soil drained. This technique is useful in comparing mathematical solutions with given field data. However, it may be difficult in predicting non-steady water table depths in drainage design, unless field data under similar soil conditions is available.

The general partial differential equation (2.21), derived in Chapter 2, can be used to study the flow between tile drains lying on a horizontal impermeable bed. For a falling water table following a sudden cessation of recharge, substitution of $R/K = 0$ in equation (2.21) yields

$$\frac{\partial}{\partial x}\left(h \frac{\partial h}{\partial x}\right) - \frac{f}{K} \frac{\partial h}{\partial t} = 0 \qquad \text{.....} \qquad (4.1)$$

in which f is the porosity and the other symbols are as in Fig. 1.2. If the coordinates are chosen with respect to the horizontal line passing through the centre of the drains instead of at the impermeable bed, then $h = Y + d$ and we can write

$$\frac{\partial}{\partial x}\left(h \frac{\partial Y}{\partial x}\right) - \frac{f}{K} \frac{\partial Y}{\partial t} = 0 \quad \ldots\ldots\ldots\ldots\ldots\ldots\ldots\ldots \quad (4.1a)$$

Equation (4.1a) is non-linear but, if the variation in h is small compared with its magnitude, the equation can be linearised by an approximation for h in the product term, viz. $h \simeq d + Y_m/2$. Thus,

$$\frac{\partial^2 Y}{\partial x^2} - \frac{f}{KD} \frac{\partial Y}{\partial t} = 0 \quad \ldots\ldots\ldots\ldots\ldots\ldots\ldots\ldots \quad (4.2)$$

The error due to the linearization approximation in equation (4.2) will be reduced if Y_m is very small compared to the depth of the impermeable bed. This assumption, therefore, implies that the water table should be approximately flat in accordance with the Dupuit assumptions.

The object of the discussion that follows is to present the essence of the several mathematical solutions of equations (4.1) and (4.2) that have been developed and improved by many research workers.

4.2 GLOVER'S SOLUTION

Glover (6) was the first to deal with the falling water table following the cessation of a uniform instantaneous recharge. He assumed that the water table was initially horizontal and that the

tile drain was of zero radius.

Starting from an initially horizontal water table (Fig: 4:1), i.e. $Y = Y_m$ for $0 \leq x \leq L$ and $t = 0$, and with an additional boundary condition $Y = 0$ at $x = 0$ and $x = L$ for $t > 0$, Glover obtained the following solution of equation (4.2).

$$Y = \frac{4Y_m}{\pi} \sum_{n = 1,3,\cdots}^{n = \infty} \frac{\sin (n\pi x/L)}{n} \exp(-n^2 \pi^2 KDt/fL^2) \quad \ldots (4.3)$$

Considering a point midway between two drains and neglecting all terms but the first, the above equation can be simplified to

$$\frac{Kt}{f} = \frac{L^2}{\pi^2 D} \operatorname{Ln} \frac{4Y_m}{\pi Y} \quad \ldots\ldots\ldots\ldots\ldots\ldots\ldots\ldots\ldots\ldots\ldots\ldots (4.4)$$

The error involved in the simplification of equation (4.3) into equation (4.4) becomes very small after a reasonable length of time. Schilfggarde and Kirkham (2, p.101) showed that when $KDt = 0.025\ L^2 f$, the error was of the order of 4%. Considering the approximations on which Glover's equation was based, this error is not of any great significance.

Glover also dealt with a limiting case, i.e. when the drain lies on the impermeable bed. In this case, the initial water table profile was assumed parabolic. The variation of the height of water table midway between drains with time for this case was given by

$$\frac{Kt}{f} = \frac{2}{9} L^2 \frac{Y_m - Y}{Y_m Y} \quad \ldots\ldots\ldots\ldots\ldots\ldots\ldots\ldots\ldots\ldots\ldots\ldots (4.5)$$

Dumm (6) reported that the difference in spacing calculated from equations (4.4) and (4.5), for equal values of the other parameters (d being zero in both cases), was always less than 10%. Subsequently, Schilfgaard (26) contradicted this conclusion by showing that, for a drop of the midpoint water table height by one foot below the steady state height, the ratio of drain spacings given by equations (4.4) and (4.5) varied from zero to infinity with increasing Y_m. Equation (4.4) was, therefore, found to be invalid when the depth of the impermeable bed is very small. This is to be expected since the linearization approximation ($Y_m << d$) of equation (4.1) does not hold in this case.

The major point of criticism of Glover's solution was that it was based on Dupuit's assumptions of horizontal flow. This assumption cannot be expected to give reliable results unless the depth of the impermeable bed is much less than the drain spacing. Besides this, equation (4.4) was originally developed for tile drains under the assumption that d is large compared with Y_m. These two conditions cannot be satisfied simultaneously. A reasonable compromise between these assumptions may give an approximate solution of the falling water table between tile drains.

The range of validity of either of Glover's spacing equations for intermediate depths of the saturated medium is still unknown. Different investigators have expressed different opinions, none of which is based on any laboratory verification. Bouwer (34)

analysed some field data and showed that for $d/Y_m \leq 0.1$, Glover's second spacing formula ($d = 0$) can be used. He also showed that for $0.1 \leq d/Y_m \leq 0.8$, the first equation would give satisfactory results in practice. This, however, seems to be only a speculation because Bouwer had no field data in this range.

Another rather unrealistic approximation in Glover's solution was his assumption that the water table over a drain suddenly drops from an initial height Y_m to its theoretical value zero. This condition can be satisfied only if the drain discharge at the beginning is infinite. In fact, it is some finite value with the result that it takes some time for the water table to drop to zero value as envisaged in the theory. Glover's theory, therefore, overestimates the initial rate of water table recession.

Tapp and Moody (35) developed a new spacing equation using a fourth degree polynomial to represent the initial water table condition for the case when the drains are above the impermeable bed, in contrast to Glover's assumption of a horizontal water table. The initial and boundary conditions were

$$Y = \frac{8Y_m}{L^4}(L^3x - 3L^2x^2 + 4Lx^3 - 2x^4) \text{ for } 0 \leq x \leq L \text{ at } t = 0$$

and $Y = 0$ at $x = o$ and $x = L$ for $t > 0$ ..... (4.6)

Equation (4.6) represents a function which initially passes through the points $x = 0$, $Y = 0$; $x = L/2$, $Y = Y_m$. Tapp and Moody solved Glover's problem by satisfying the above initial and boundary

conditions. Their solution was of the form

$$Y = \frac{192\ Y_m}{\pi^2} \sum_{m=0}^{\infty} \frac{(2m+1)^2\pi^2 - 8}{(2m+1)^5} \exp\left[-\frac{(2m+1)^2\pi^2\ t}{L^2}\right] \cdot \sin\frac{(2m+1)\ \pi x}{L} \quad \ldots\ldots (4.7)$$

They observed that the spacing obtained by using equation (4.7) was not greatly different from that obtained from equation (4.3).

4.3 IMPROVEMENT OF GLOVER'S SOLUTION

4.3.1. Brooks' approach:

It has already been mentioned that the assumptions of horizontal flow and linearization cannot hold at the same time in Glover's solution. Brooks (36), by using Emile Picard's method (37) of successive approximation, improved Glover's solution by solving the non-linear partial differential equation (4.1) and thus avoided Glover's assumption that $d >> Y_m$.

Brooks' original equation is very lengthy. However, he presented another approximate solution similar to that of Haushild and Kruse (38) and obtained ~~the~~ similar results in the range $0.1 < Y_m/d < 1.0$ to those given by his original equation. The simpler equation is of the form

$$Y_2 = -D + \sqrt{D^2 + 2DY + (Y_m/2)^2} \quad \ldots\ldots\ldots\ldots\ldots\ldots\ldots\ldots (4.8)$$

The symbols in equation (4.8) are shown in Fig. 4.2. In equation (4.8), Y was calculated from Glover's equation (4.3).

Brooks obtained good agreement between his results and those of Glover's solution for $Y_m/D \leq 0.1$. For higher values of Y_m/D, however, the rate of recession by Brooks' solution was comparatively smaller.

In spite of the improvement over Glover's solution, Brooks' analysis was still restricted to high values of L/D because it was based on the Dupuit-Forchheimer (D.F.) assumptions. Brooks compared his theoretical results with those of Isherwood's (39) computer solution and found close agreement between the two for $L/D \geq 25$. A comparative study of Isherwood's and Brooks' methods can be made for fixed values of Y_m/D and L/D. Curves presented by Brooks (36, Fig. 4) indicated that, with a fixed value of L/D, an increase in Y_m/D gives increasing deviation between the two solutions. This is justifiable, because Isherwood's solution was sufficiently accurate whereas that of Brooks' was based on the Dupuit assumptions, thereby restricting it to low values of Y_m. In both the methods, however, it was assumed that the water table is horizontal initially.

4.3.2. Van Schilfgaarde's Approach:

Van Schilfgaarde (40) solved the non-linear partial differential equation (4.1) by assuming that the initial profile of the

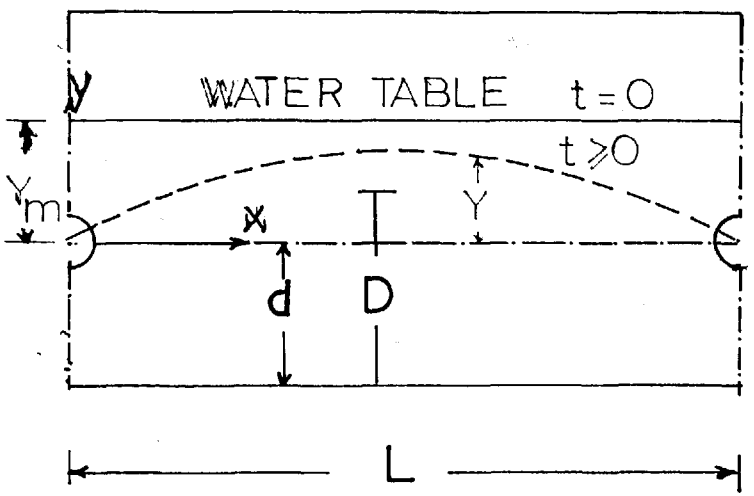


FIG:4.1
GLOVER'S MODEL

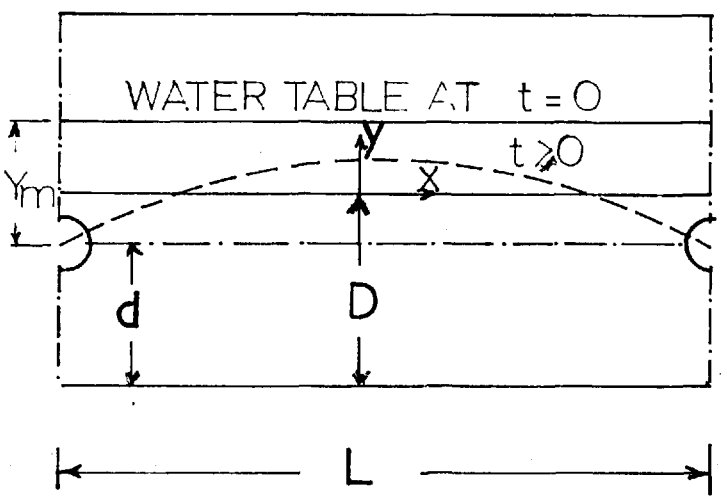


FIG:4.2
BROOK'S MODEL

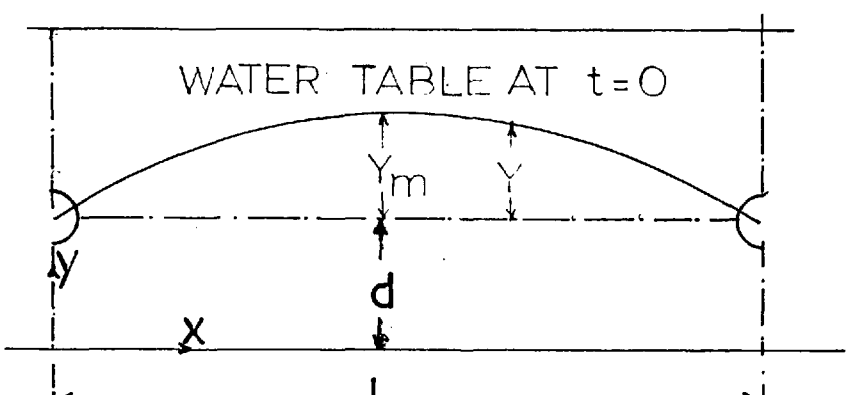


FIG:4.3,
SCHILFGAARDE'S MODEL

water table was parabolic. He analysed the falling water table for the same boundary conditions as were used by Glover for the case when d = 0. Unlike Glover, however, he avoided the assumption of constant thickness of the saturated medium. Schilfgaarde's equation (Fig. 4.3) for the water table recession is

$$\frac{Kt}{f} = \frac{4L^2}{9A^2} \frac{Y_m - Y}{(d + Y)(d + Y_m)} \quad \ldots\ldots\ldots\ldots\ldots\ldots \quad (4.9)$$

where A is the Incomplete Gamma function, the value of which can be found from tables. Schilfgaarde also showed that the value of A can be approximated by

$$A = \left[1 - (d/D)^2\right]^{\frac{1}{2}} \quad \ldots\ldots\ldots\ldots\ldots\ldots\ldots\ldots \quad (4.10)$$

with a maximum error of up to 3%. The convergence effect was taken into account by introducing Hooghoudt's correction, given by equation (3.4), into equation (4.9).

Schilfgaarde compared his theoretical results with the numerical values obtained from Glover's first equation (equation 4.4) and showed that, with a constant thickness of the water bearing stratum, a difference of the order of 40% resulted in spacings calculated from equations (4.4) and (4.9). Dumm (41) disagreed with this comparison due to the fact that the two equations were based on two different initial conditions. The difference was attributed to the use of Glover's formula for $d > 0$ instead of $d = 0$. Dumm showed that for $d = 0$, Schilfgaarde's equation is transformed into Glover's second equation (equation 4.5). For this case, the tK/f values given by the solutions by Glover and

Schilfgaarde were shown to be identical.

In the context of the conclusions of Tapp and Moody (35), the spacing obtained by using a parabolic profile of water table should not be different from that obtained by assuming a flat water table. The validity of this conclusion can well be understood by comparing Schilfgaarde's solution with that of Brooks. Both solutions are based on the same boundary conditions, except the difference in the initial conditions.

Brooks (42) made a comparative study of Schilfgaarde's results with those of his own. He showed that by assuming an initial horizontal water table, the computed spacings were generally smaller that those obtained by assuming an initially curved water table. Contrary to the conclusions of Tapp and Moody, therefore, there may be significant difference in the rate of water table recession due to the difference in the initial conditions. In order to find out the limitations of the methods of Brooks and Schilfgaarde, their results will later be compared with the experimental data obtained from the Hele-Shaw model.

4.4 ISHERWOOD'S RELAXATION METHOD

Isherwood used a finite difference method (39) after Kirkham and Gaskel (43) to solve the water table recession problem. He determined relationships between the rate of recession at the

midpoint and other variables, i.e. depth of the impermeable bed, drain spacing and soil permeability. He assumed that the medium was initially flooded to the ground surface. Isherwood's main conclusion was that the time required for the midpoint water table to fall unit distance below the surface was independent of the depth of impermeable bed for $L/d \geq .8$. He also observed that the higher the water table midway between drains the more rapidly is the water drained ~~from the surface~~ below the surface. This generalization was found to hold in all cases which he studied, regardless of drain spacing or the depth of the impermeable bed.

The relationships between various drainage parameters presented by Isherwood had the disadvantage that they were based on insufficient data, with the result that they could not be considered reliable for design purposes. Moreover, the assumption of flooded initial condition was also unrealistic. In spite of this, his conclusion that the impermeable layer deeper than L/8 below the tile drain axis had little influence on drainage characteristics was supported by Boumans (44) on the basis of practical experience, since he indicated that the hydraulic conductivity must be measured only to a depth below the tile lines equal to one-eighth the drain spacing.

4.5 MOODY'S ITERATION METHOD

Following Isherwood, Moody (15) presented a more comprehensive analytical treatment of the problem of water table recession. He also used a digital computer to get a numerical solution by an iterative method. His analysis was more comprehensive because he analysed almost all the important aspects of the drainage problem, including a graphical relationship between the drain discharge versus time. The only other theoretical equation expressing the latter is that of Kraijenhoff (45).

Moody used a parabolic profile for the initial water table as reported by Tapp and Moody(35). He compared his results with Boussinesq's solution (46) for d = 0, and found that for values of the dimensionless time parameter (KDt/fL^2) greater than 0.1, there was no significant difference between the two solutions. A small discrepancy occurring for values of the time parameter less than 0.1 was attributed to the difference in the shape of the initial water table profiles in the two solutions. Boussinessq assumed a horizontal initial water table profile compared to the parabolic one in the Moody solution.

Since Moody solved a non-linear partial differential equation based on the Dupuit assumptions, he accounted for the convergence effect by the introduction of the equivalent depth (equation 3.3), which together with his graphical results, gave the rate of recession of the water table.

Although both Isherwood and Moody have analysed the effect of the depth of the impermeable bed, their results cannot be compared because of the difference in the underlying assumptions. Isherwood's approach, even though based on unrealistic initial conditions, is possibly more accurate than that of Moody, because the latter used the ~~linearised differential equation~~ Dupuit assumptions. However, it may be worth pointing out here that the linear solutions, if inexact, are particularly useful in the study of the behaviour of the rising water table in response to intermittent recharge, because they permit superposition which the more exact non-linear solutions do not permit.

4.6 SOLUTIONS BASED ON EXTENSION OF STEADY STATE TO UNSTEADY STATE

4.6.1 General Theory

In the last few years, several investigators (Hammad, Luthin, Kirkham) solved falling water table problems by considering the unsteady state to consist of a series of successive momentary steady states. The solution of the problem by this approach was further simplified by introducing the following assumptions:

(i) the rate of fall of water table at all points between the drains is the same as that at the midpoint;

(ii) the porosity is constant;

(iii) the drainable porespace is emptied instantaneously.

Based on these assumptions, a general theory for the falling water table can be derived by the following procedure:

Let Q(t) denote the rate of discharge of a drain at time t after the initial steady state rate of rainfall R has ceased. Let dY be the fall of the midpoint water table occuring in a time interval dt. Then, according to assumption (i) above, f dY L units of water drain from dY in time dt, thus, giving

$$Q(t) = -fL\left(\frac{dY}{dt}\right)_{t=t} \qquad (4.11)$$

the negative sign is necessary because the water table depth decreases as time increases.

Now imagine that the midpoint water table which has fallen to a certain height Y in time t, should suddenly cease to fall, because of the onset, instantaneously, of another suitable steady state rate of rainfall R(t). This rate R(t), to maintain continuity of flow, would have to be given by

$$Q(t) = R(t).L \qquad (4.12)$$

Equating (4.11) and (4.12) would give

$$\frac{R(t)}{f} = -\left(\frac{dY}{dt}\right)_{t=t} \qquad (4.13)$$

It should be noted that since R(t) is the steady state rate of recharge to obtain a midpoint water table height Y at time t after the initial steady state rate of recharge has ceased, it can be determined from any steady state analytical solution.

The validity of equation (4.13) may be questioned on account of the assumption (i) above. Childs and O'Donnell (3) and later Kirkham

and Gaskel(43) observed that, following the ponded condition, the water table falls faster over the drain than in the middle. After having receded for some time in that manner, the water table falls fairly uniformly all over the spacing. In the last stages of the recession, the water table falls faster in the middle than over the drains. These studies, therefore, indicate that equation (4.13) is valid only in the middle range of the water table recession.

The validity of equation (4.13) was extended to the whole water table recession process by Schilfgaarde (34) by introducing a correction factor C_f to account for the non-uniformity in the beginning and the final stages of the water table recession discussed above. This factor can be considered as the ratio of the actual volume drained when the water table falls from one position to another (in a given time interval) to the volume drained when the distance of fall of the entire water table is equal to the fall at the midpoint. There are many examples in the drainage literature suggesting various values of C_f in relation to other parameters, such as Y_m/L and d. Bouwer (36) has shown that the average value of this ratio is about 0.8 for Y_m/L values from 0.02 to 0.08, and low d values. A C_f value of approximately 1.0 is indicated by Childs' work (4) for higher water tables with Y_m/L exceeding 0.15. Schilfgaarde(34), however, has indicated that a constant value of C_f equal to unity can

be taken for all practical purposes.

If the correction is applied in equation (4.13) then,

$$\frac{R(t)}{f} = - C_f\left(\frac{dY}{dt}\right)_{t=t} \quad \ldots\ldots\ldots\ldots\ldots\ldots\ldots\ldots \quad (4.14)$$

Bouwer and Schilfgaarde (34) solved equation (4.14) by using Hooghoudt's analytical equation,

$$R = \frac{4KY(d_e + Y)}{L^2} \quad \ldots\ldots\ldots\ldots\ldots\ldots\ldots\ldots \quad (4.15)$$

in which d_e is the equivalent depth of the impermeable bed and other symbols are as shown in Fig. 1.2. Substituting equation (4.15) into equation (4.14) and solving for $Y = Y_m$ at $t = 0$ with C_f as a constant, we get a solution (34),

$$\frac{Kt}{f} = \frac{4C_f L^2}{8d_e} \ln \frac{Y_m(Y + 2d_e)}{Y(Y_m + 2d_e)} \quad \ldots\ldots\ldots\ldots\ldots\ldots \quad (4.16)$$

The depth d_e in this equation is calculated from equation (3.5).

Equation (4.16) can be used to calculate Kt/f for a selected water table drop with fixed values of L and d_e. Multiplication of Kt/f with f/K will give the time required for the water table to drop to a selected height.

4.6.2. Kirkham's Analysis

Kirkham (47) used his steady state solution to show how the steady state water table can be extended to an unsteady state to solve a particular problem of flow between parallel ditches. He

compared his results with the experimental data obtained from a glass bead Glycerol model (47a) and found satisfactory agreement, except for a short time after the water table started falling.

Kirkham solved equation (4.13) by using his steady state solution for the ditch drains. The same procedure can be used here for Kirkham's solution for tile drainage (equations 3.13 and 3.16) to find the height of the falling water table above any fixed point. A general expression for the steady rate of rainfall R, applicable to both equations (3.13) and (3.16), was given by

$$R(t) = \frac{K\,Y}{L\,F(x,0) + Y} \qquad \ldots\ldots\ldots\ldots\ldots\ldots\ldots\ldots \quad (4.17)$$

where F(x,0) is given either by equation (3.12) or (3.16). He then combined equation (4.17) with equation (4.14) with $C_f = 1.0$ and integrated the resulting equation to get

$$L\,F(x,0)\,\mathrm{Ln}\,Y + Y = \frac{Kt}{f} + D \qquad \ldots\ldots\ldots\ldots\ldots\ldots\ldots \quad (4.18)$$

Using the initial condition $Y = Y_m$ at $t = 0$ he obtained

$$Y.\mathrm{Exp}\left[Y/L.f(x,0)\right] = Y_m\,\mathrm{Exp}\left[(Y_m - Kt/f/L.F(x,0)\right] \qquad \ldots\ldots \quad (4.19)$$

The results obtained from this equation will later be compared with the experimental results obtained from the Hele-Shaw model.

4.6.3 Hammad's Solution

Hammad (48) combined equation (3.21) with equation (4.14) and took C_f equal to unity. He then integrated the resulting equation

to obtain the following relationship for the falling water table for thin soil layers ($d/L \leq 0.25$)

$$Y = Y_m \, \mathrm{Exp}(-\xi t) \quad \ldots\ldots\ldots\ldots\ldots\ldots\ldots\ldots\ldots \quad (4.20)$$

in which

$$\xi = \frac{2\pi K}{f \, L \, \mathrm{Ln} \dfrac{L^2}{2 \pi^2 d r}}$$

The discharge per unit length of the drain was similarly obtained as

$$q = Q e^{-\xi t} \quad \ldots\ldots\ldots\ldots\ldots\ldots\ldots\ldots\ldots\ldots\ldots \quad (4.22)$$

in which q is the drain discharge at any time t.

4.7 INTERMITTENT RECHARGE:

The methods that have been discussed so far assumed isolated instantaneous recharge and the water table was assumed to attain a steady state before the occurrence of the next recharge. In practice, the water table may be in a continuous transient state due to frequent intermittent blocks of rainfall. In operational mathematics this is the case of a sequence of square step inputs, whereas the previous discussion was concerned with a single pulse input.

Werner (49) first gave a mathematical treatment of the intermittent recharge problem. He used equation (2.22) and linearised it in the manner discussed in Section (2.6). He used the linearised

equation to find a series of solutions for different boundary conditions using the Laplace transform method. By the principle of superposition, he could apply his solution to any sequence of square rainfall inputs.

Maasland (50) extended Werner's solution to study recharge patterns in detail. He analysed the problem of water table movement in response to repeated recharges and presented his results in the form of a combination of periodic and transient functions. The method was based on the assumption that the drains lie on the impermeable bed so that the flow is horizontal. For tile or ditch drains which do not completely reach the impermeable bed, he suggested Hooghoudt's correction for convergence.

Kraijenhoff (45) made a similar analysis to study the effect of an arbitrary rainfall pattern on the water table. He approximated the rainfall pattern as a summation of a series of square pulses.

Schilfgaarde (51) used the Kraijenhoff method to establish design criteria in terms of a probability distribution. The study was to find the probability of the rise of the water table above a certain permissible limit. He presented a method for the determination of the frequency distribution of water table heights as a function of soil and system parameters and of meteorological records.

CHAPTER 5

DRAINAGE OVER A HORIZONTAL IMPERMEABLE BED

This chapter describes the experimental apparatus and presents an analysis of the experimental results for the present investigation. Various model and analogue techniques generally used in the solution of drainage problems are first reviewed with special emphasis on the Hele-Shaw model. Scaling factors for this model are then derived to relate model quantities to those of a prototype. Some salient features of the present model are described and the experimental accuracy that can be obtained from the model is assessed. Experimental results both for the symmetrical and for the misaligned drainage systems are discussed and compared with the appropriate analytical solutions. The summary of these results is given in Chapter 7.

5.1 INTRODUCTION

The review of some of the existing steady and unsteady state solutions given in the previous chapters indicates that in view of the complicated nature of tile drainage problems, solutions of most of them are based on two general assumptions. The first assumption is that the height of the water table relative to the drains midway between drains should be small compared with the depth of the

impermeable bed below the drains; the second implies that the spacing between drains should be greater than the depth of the impermeable bed. The range of validity of these assumptions can be accurately determined experimentally. Experimental methods are also of considerable importance in those problems which cannot be solved analytically because of complex boundary conditions.

Two experimental techniques that are extensively used in the study of drainage problems are field experiments and laboratory models. For example, Kirkham, Schilfgaarde and Frevert (26), and Kirkham (2) and Dumm(32), checked Glover's solution with field data and obtained good agreement. Such an agreement is somewhat surprising because the Glover solution does not allow for intermittent recharge and the resulting rise and fall of the water table as it usually occurs in practice. A better check of unsteady state solutions can be made by comparing the results derived therefreom with the experimental data obtained from laboratory models. The models are useful because the boundary conditions assumed in the solutions can be easily simulated on a reduced scale.

Groundwater models are of three main types: sand models, electrical analogues and viscous flow analogues. Among these, the sand model is essentially a reproduction of the prototype conditions on a reduced scale. The other models are analogies

of groundwater flow in that the equations describing conditions both in the models and in the prototype are of identical form.

In a sand model, the water table is located by using the condition that the pressure over the water table is atmospheric. Also the potential everywhere on the water table is given by $\phi = Kz$ where z is measured relative to a particular datum plane. The equipotential lines are drawn by noting the piezometric head, h, at different points within the medium and joining up points of equal values of h. Donnan(52) and Childs (53) used sand models to study steady flow between tile and ditch drains. Youngs and Collis George (29) extended its application to study moving water tables.

Experimental difficulties are associated with sand models and arise from non-uniform distribution of rainfall over the sand surface, the effect of entrapped air on the permeability of the sand and the clogging of the screens of drain tubes. Also difficulty may arise in getting the sand packed isotropically and homogeneously, and thereafter maintaining these properties. Despite such difficulties, however, the sand model has the advantage over other types of models of taking into account the effect of the capillary fringe.

The conductive sheet electrical analogue was first used in the study of unsteady state problems by Childs (4) to study the problem of the falling water table. Subsequently, Childs and O'Donnell (3) used the same technique to study the rising water

table. The latter study concluded with the remark: "the technical difficulties of this particular experiment were such that the work described appears to have reached the limit of usefulness of the analogue method". Luthin (54) used a resistance network analogue for the solution of steady state drainage problems. In unsteady state problems, the use of this analogue is associated with similar limitations as those for the conductive sheet analogue. It is difficult as well as uneconomical to make small enough grids to account for small changes in the water table position.

The viscous flow analogue is free from the difficulties mentioned above. It gives an accurate representation of unsteady two-dimensional groundwater flow. The model is easy to handle because water table and seepage surfaces form by themselves and can be conveniently recorded photographically.

5.2 VISCOUS FLOW ANALOGY

5.2.1. Theory of simulation

The viscous flow analogy is based on the fact that laminar liquid flow between vertical parallel plates and two-dimensional groundwater flow in porous media are governed by the same differential equation, viz. the Laplace equation.

This analogy can be easily proved by using Poiseuille's law. According to this law, the velocity profile in the cross-section between parallel plates is found to be parabolic for a laminar flow and the mean velocity is given by

$$v = - \frac{gb^2}{12\nu} \frac{\partial h}{\partial s} \qquad \text{.....} \qquad (5.1)$$

where

$h = \frac{p}{\gamma} + z$, b is the interspace and ν is the kinematic viscosity of the fluid.

It is possible to re-write the above equation in the form:

$$v = - K_m \frac{\partial h}{\partial s}$$

or

$$v = - \frac{\partial \phi}{\partial s} \qquad \text{.....} \qquad (5.2)$$

where

$$\phi = K_m h$$

and

$$K_m = \frac{gb^2}{12\nu} \qquad \text{.....} \qquad (5.3)$$

The velocity components in the x and z directions will be:

$$v_x = - \frac{\partial \phi}{\partial x} \quad , \qquad v_z = - \frac{\partial \phi}{\partial z} \qquad \text{.....} \qquad (5.4)$$

If equations (5.4) are substituted into the continuity equation for two-dimensional flow, we obtain the Laplace equation in two dimensions:

$$\frac{\partial^2 \phi}{\partial x^2} + \frac{\partial^2 \phi}{\partial z^2} = 0 \qquad \text{.....} \qquad (5.5)$$

Equation (5.5) is of precisely the same form as equation (2.18). Thus the flow in a viscous flow model simulates groundwater flow. By proper simulation of prototype boundaries, such a model may be used to study prototype behaviour.

It must be observed that the above analogy presumes that the flow in the model must be laminar. This can be achieved with small b and/or large ν. However, the interspace width b cannot be made too small due to constructional difficulties. The smaller the interspace the more difficult it is to make the model.

An aquifer consisting of several layers of different hydraulic conductivities can be simulated in a viscous flow model by varying the interspace width. This is done by inserting thin strips into the interspace having the shape of the simulated layers, thereby having a narrower interspace for layers of lower hydraulic conductivity.

5.2.2. Scaling laws

(a) Time scale:

Since the flow of a viscous fluid in a Hele-Shaw model and the groundwater flow in porous media show a mathematical and physical similarity, the scaling laws for such models can be obtained by considering any appropriate differential equation governing the flow in the prototype and the model. For example, consider the unsteady flow of an incompressible fluid in a

homogeneous isotropic aquifer. The continuity equation (equation 2.2Φ) describing the flow is:

$$\frac{\partial}{\partial x}(v_x h) + f\frac{\partial h}{\partial t} - R = 0 \quad \text{.....} \quad 2.21b$$

Using the relationship

$$v_x = -K\frac{\partial h}{\partial x} \quad \text{.....} \quad (5.7)$$

the continuity equation (2.21b) can be put into the non-dimensional form:-

$$h\frac{\partial^2 h}{\partial x^2} + \left(\frac{\partial h}{\partial x}\right)^2 + \frac{f}{K}\frac{\partial h}{\partial t} - \frac{R}{K} = 0 \quad \text{.....} \quad (5.8)$$

For complete similarity each term in this equation must have the same value both in the model and in the prototype. Thus

$$\left(\frac{f}{K}\frac{\partial h}{\partial t}\right)_m = \left(\frac{f}{K}\frac{\partial h}{\partial t}\right)_p \quad \text{.....} \quad (5.9)$$

in which the subscript m and p refer to the model and the prototype. From equation (5.9), the time scale ratio, t_r, is given by

$$t_r = \frac{t_m}{t_p} = \frac{f_m}{f_p} \cdot \frac{h_m}{h_p} \cdot \frac{K_p}{K_m} \quad \text{.....} \quad (5.10)$$

writing $L_r = \frac{h_m}{h_p}$, noting that $f_m = 1$ for the model, and substituting $K_m = gb^2/12\nu$ (equation 5.3), yields

$$t_r = \frac{L_r}{f_p}\,\frac{12\nu K_p}{gb^2} = \frac{L_r}{K_r f_p} \quad \text{.....} \quad (5.11)$$

or

$$K_m = \frac{K_p L_r}{t_r f_p} \quad \text{.....} \quad (5.12)$$

The interspace can be computed from equation (5.11) after L_r and t_r have been selected.

(b) Drain discharge scale:

The similarity criterion mentioned in the previous Section, (Section 5.2.2e) requires that in equation (5.8),

$$\left(\frac{R}{K}\right)_m = \left(\frac{R}{K}\right)_p$$

i.e.

$$R_r = K_r$$

But

$$R_r = \frac{R_m}{R_p} = \frac{Q_m/b.L_m}{Q_p/1.L_p} \qquad \ldots\ldots\ldots\ldots\ldots\ldots\ldots\ldots \qquad (5.13)$$

where Q refers to steady state drain discharge. Equation (5.13) yields

$$R_r = \frac{Q_r}{b\ L_r}$$

or

$$Q_r = b.L_r.R_r = b.L_r.K_r \qquad \ldots\ldots\ldots\ldots\ldots\ldots\ldots \qquad (5.14)$$

5.3 VISCOUS FLOW MODEL

5.3.1 General

The viscous flow model was first developed by Hele-Shaw in 1897 to demonstrate the potential flow pattern around variously shaped boundaries and consequently is known as the Hele-Shaw model.

There are two types of the Hele-Shaw model: horizontal and

vertical. The basic principle of simulation in both types is the same. Santing (55) used horizontal flow models to study the effect of artificial replenishment of ground water on well fields.

The vertical flow model was first used by Dachler (56) to study steady state ground-water flow problems. This was followed by Gunther (57) who made extensive use of the model to investigate seepage flow under different boundary conditions. Krul and Liefrink (58) used the model to simulate precipitation, irrigation and evaporation effects on the ground water table. Santing (59) discussed its adaptability to sea water intrusion problems in coastal aquifers.

Todd (60) used a vertical flow model in the study of unsteady seepage flow due to a sudden rise of water level in a canal. He recorded water table profiles at various times by cine photography and obtained water table depths by scaling directly from projections of the individual frames of the films. Marino (61) used a similar model to study the problem of the growth and decay of a ground water ridge.

In tile and ditch drainage, Luthin (62) used a vertical flow model to study unsteady flow between ditch drains lying over a sloping impermeable bed. Dujaili (30) investigated steady flow between misaligned drains. Maasland (5) investigated the effect of d/L on the water table recession midway between

symmetrical drains.

The present model was designed to investigate the behaviour of unsteady ground-water flow between tile drains lying in a homogeneous and isotropic unconfined aquifer. A detailed description of the model follows in the next Section.

5.3.2 Description of the model

(a) The Model:

Fig. 5.1 (Plate I) shows a general layout of the Hele-Shaw model used in the present investigation. The model consisted of two Perspex plates 300 x 90 x 0.6 cm. thick. The plates were bevelled at the top to eliminate any possibility of losing a part of the incoming rainfall. To facilitate recording of water table profiles, graph paper ruled in millimetres was pasted on to the back plate.

Uniformity of the interspace between the plates was maintained by 2 mm steel spacers (Fig.5.2) at each of the clamping bolts holding the plates together and spaced at 10 cm centres. The 10 cm spacing was a compromise between too small and too large a spacing; the first might interfere too much with the flow and the second could allow bowing of the Perspex plates.

To prevent leakage from the bolt holes, rubber and brass washers were mounted on the bolts at the outer sides of the Perspex plates (Fig. 5.3). The bottom and both sides of the model were sealed

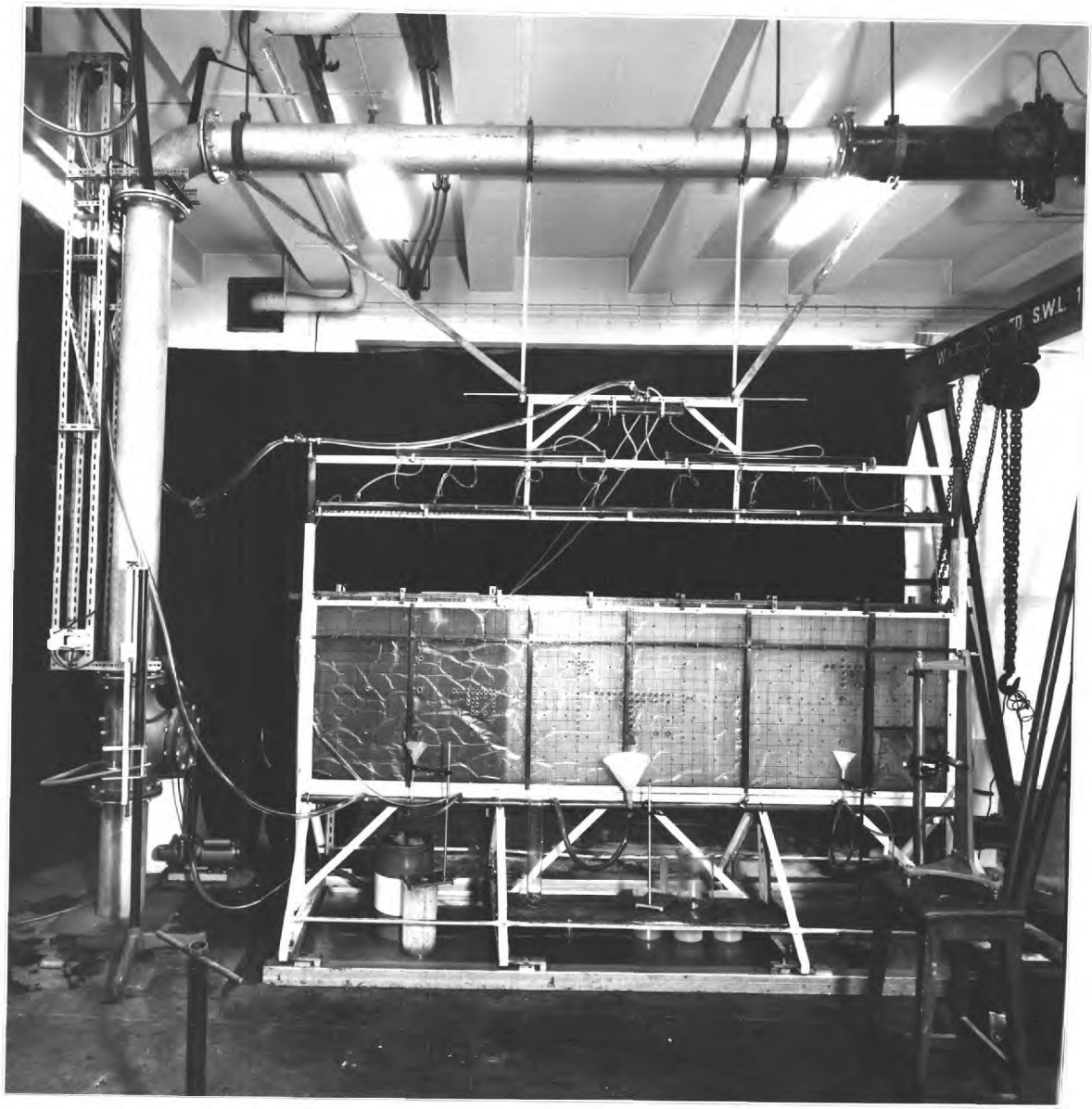


PLATE I

GENERAL LAYOUT OF

MODEL IN HORIZONTAL POSITION

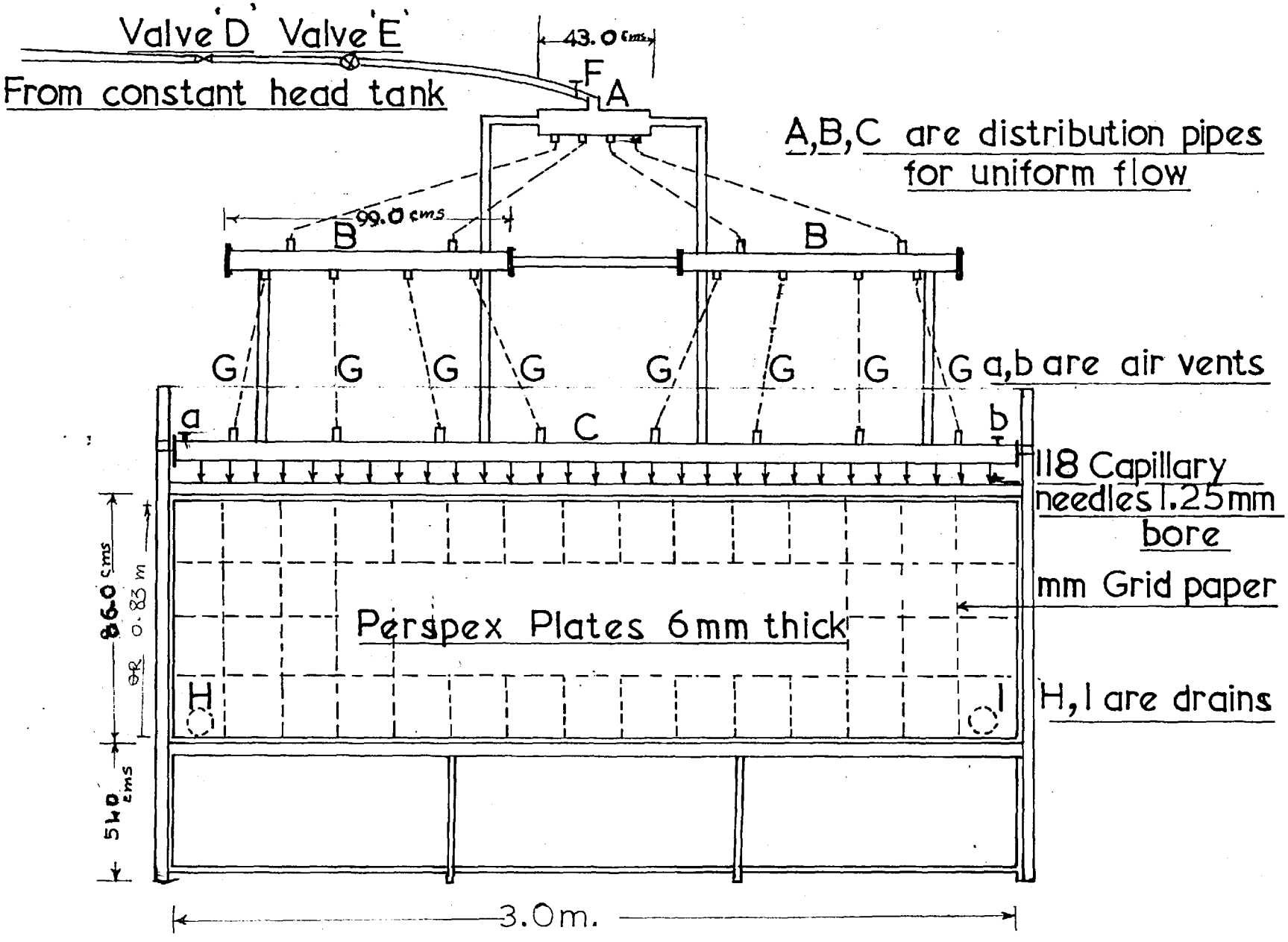


FIG:5.1 GENERAL VIEW OF VISCOUS FLOW MODEL

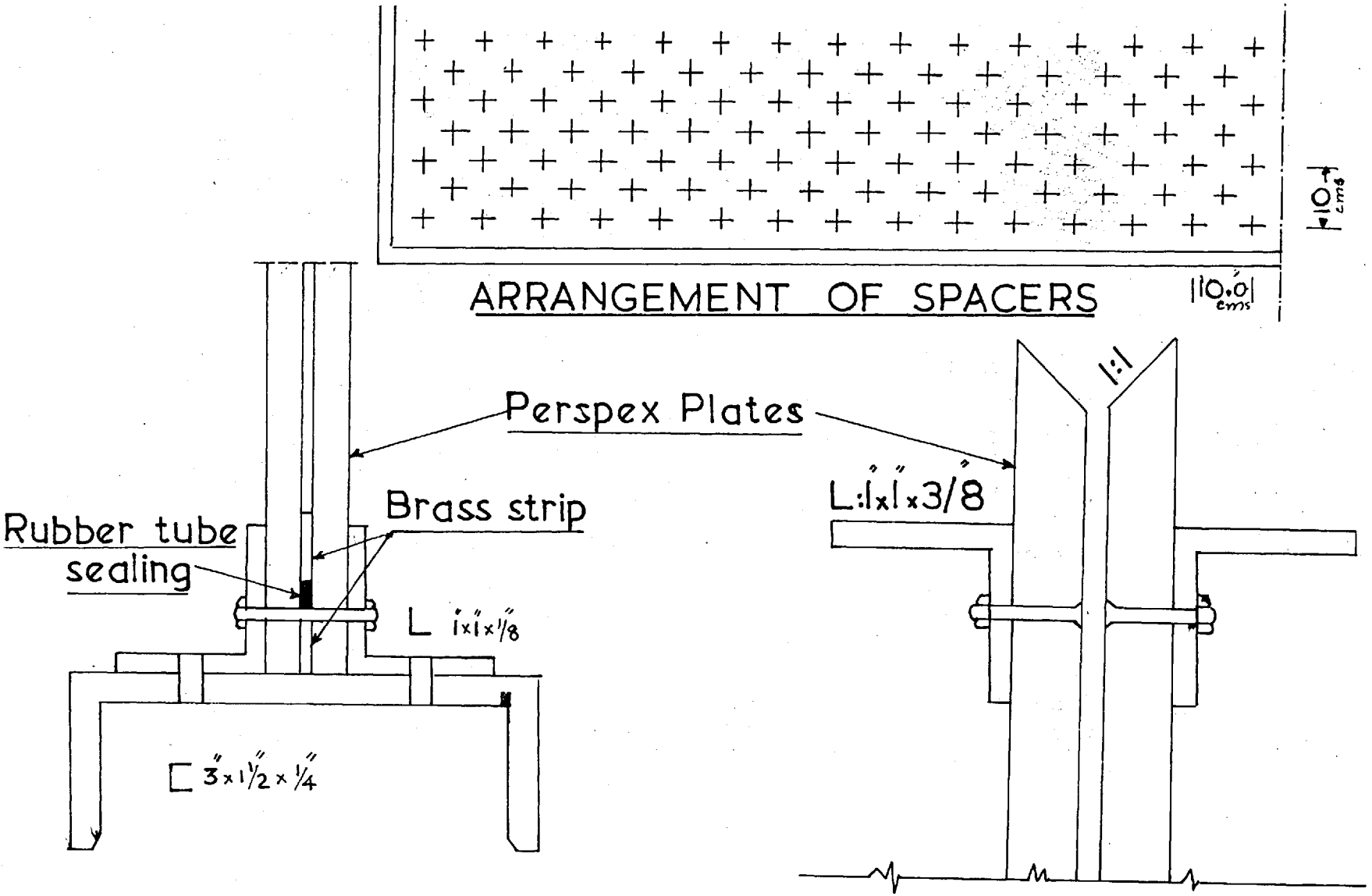


FIG: 5.2 CONSTRUCTIONAL DETAILS OF THE MODEL

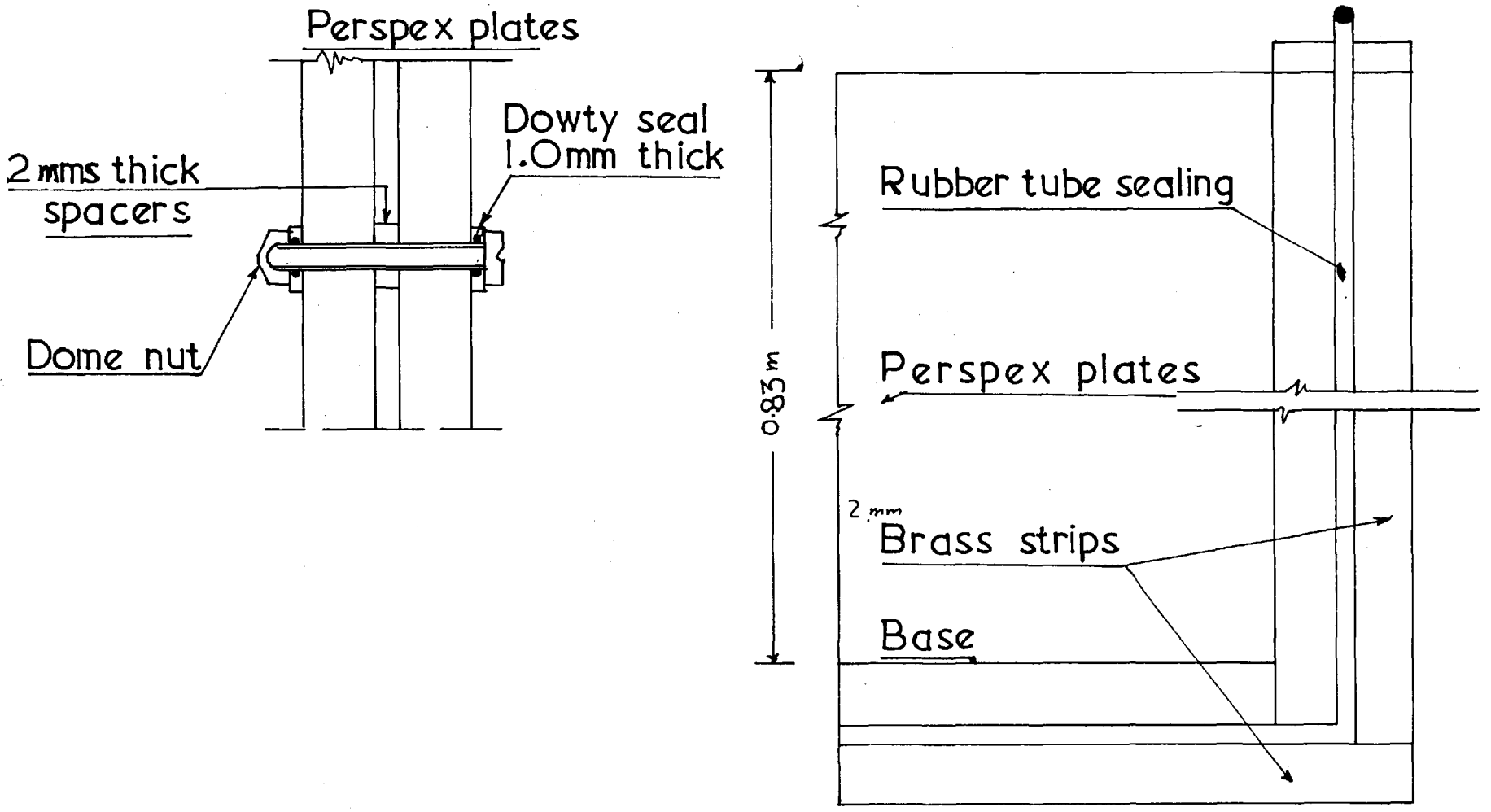


FIG: 5.3 DETAILS OF SPACERS AND BRASS STRIPS

with brass strips and rubber O-ring sealing. Emptying outlets, 2.5 cm above the bottom of the plates, were provided to drain off the oil when the model was not in use.

In order to study the effect of the depth of the impermeable bed, three tile drain rows were provided in the front Perspex plate (Fig. 5.4). The lower row was 22.90 cm , the intermediate 42.90 cm and the top row 57.70 cm above the impermeable bed. A number of extra tile drains were provided to facilitate the study of flow between misaligned drains and drains lying over a sloping impermeable bed.

(b) Rainfall distribution system:

Uniform rates of rainfall were introduced into the interspace from a horizontal distribution pipe C (Fig. 5.5) via 118 hypodermic tubes, 1.5 mm diameter and spaced 2.5 cm apart, screwed into the distribution pipe. The pipe C was 254 cm long and 4 cm in diameter and was fed in turn from pipes A and B; A being supplied from a constant head reservoir. All three pipes were mounted on a common supporting frame. The arrangement of supply pipes A, B and C, and their size relative to the hypodermic tubes (diameter ratio 45) ensured a constant pressure at all the hypodermics and therefore a uniform "rainfall" distribution along the interspace. The oil from the hypodermic tubes fell on a horizontal shelf where it accumulated and then spread uniformly before dripping into the interspace (Fig. 5.6).

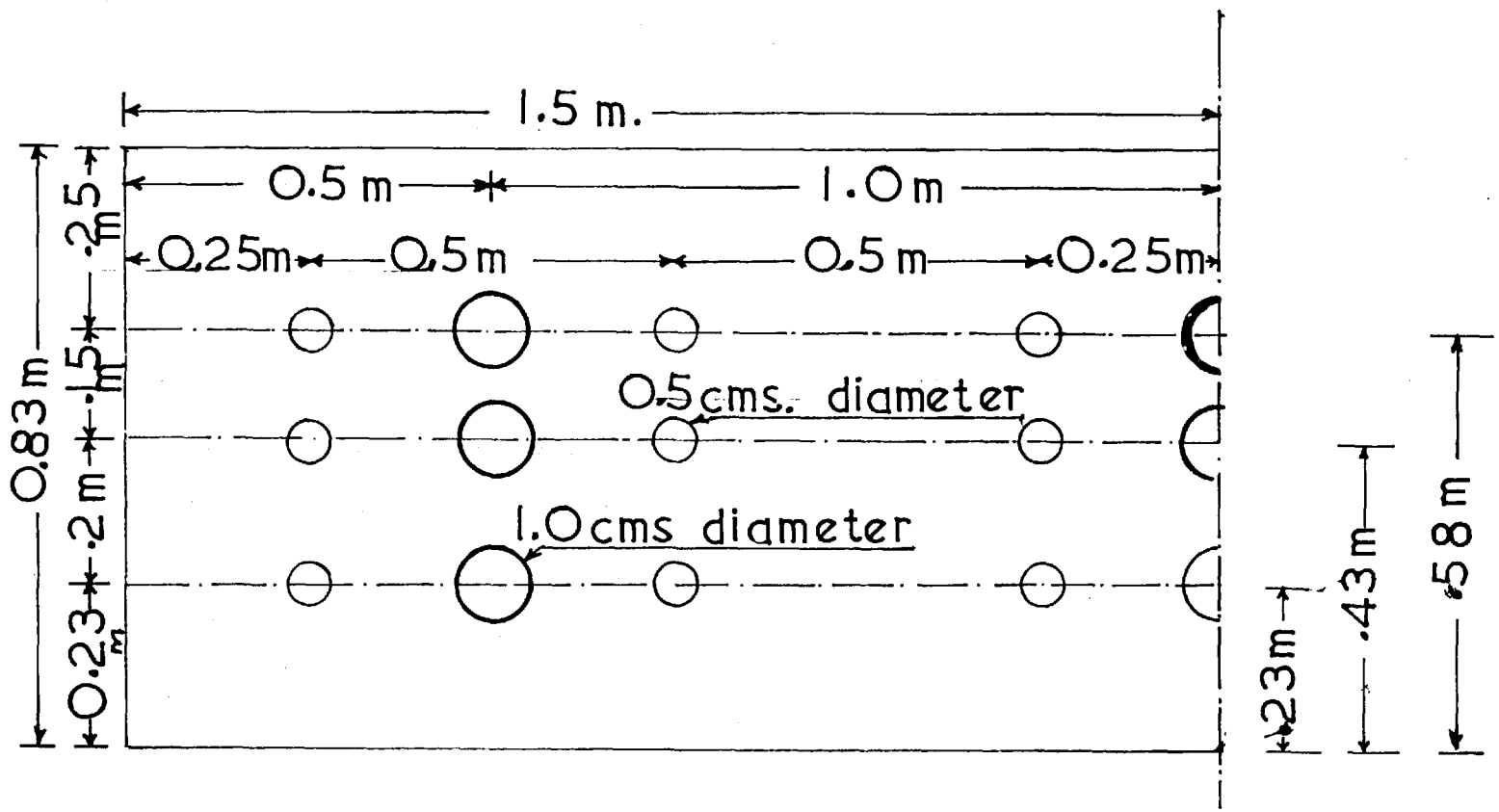


FIG:5.4 ARRANGEMENT OF DRAINS

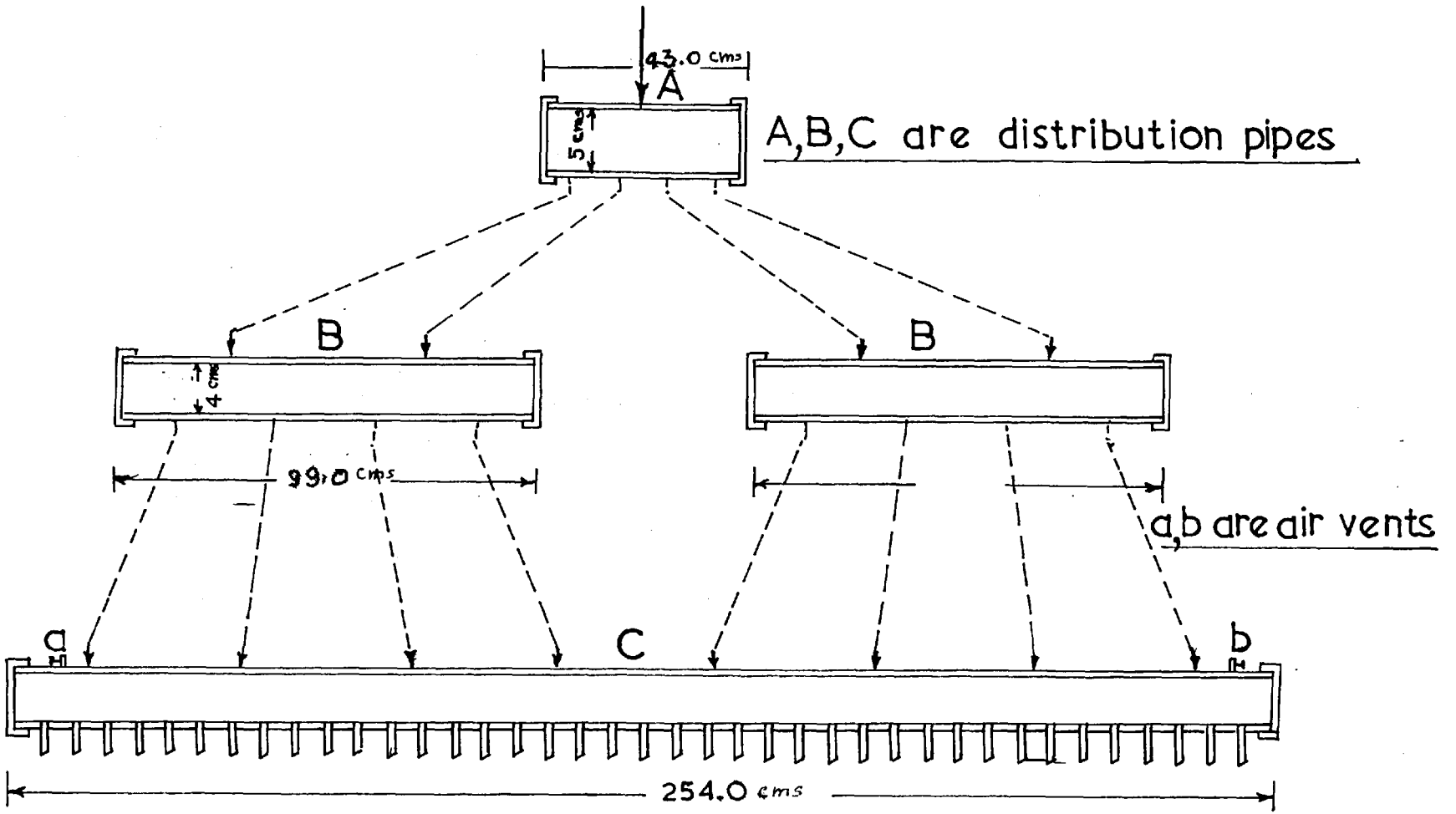
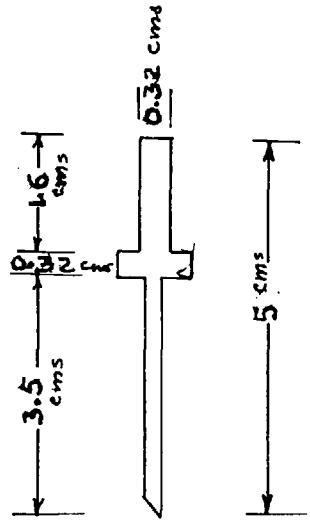
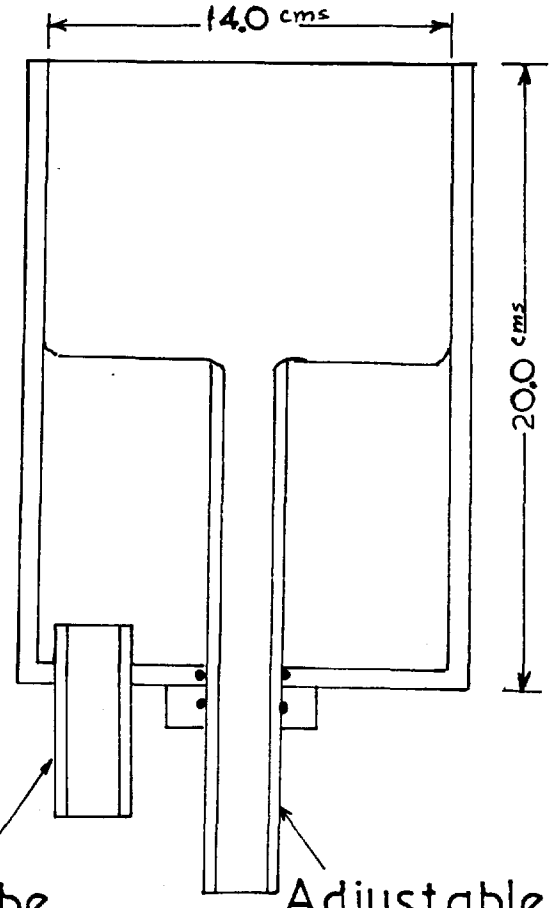


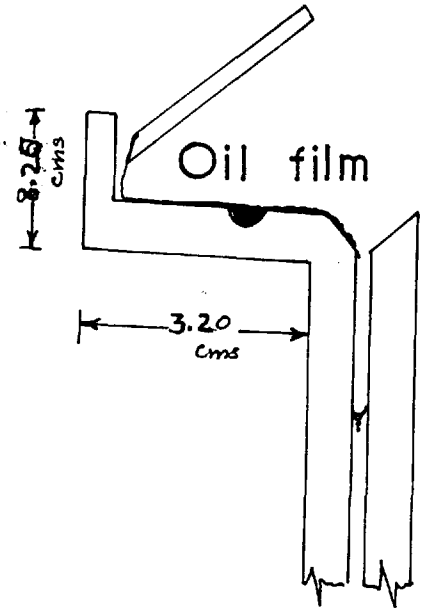
FIG:5.5 RAINFALL DISTRIBUTION SYSTEM



CAPILLARY NEEDLE



CONSTANT HEAD TANK



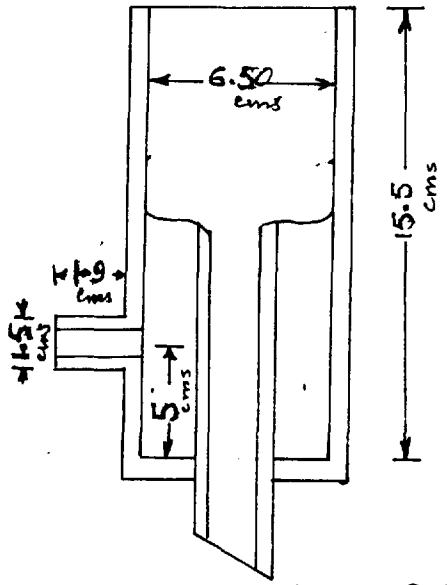


FIG: 5.6

DISCHARGE CONTROL

(c) Rainfall control:

The rainfall was supplied from a constant head reservoir (Fig. 5.6) having an adjustable overflow tube. The rate of rainfall was varied by changing the head difference between the oil level in the constant reservoir and outlet of the hypodermic tubes. Precise control over the rate of rainfall was obtained with valves D and E (Fig. 5.1). Valve D was adjusted to get a desired rate of rainfall and valve E was used for sudden stopping and starting of the oil in the distribution system and hence in the model.

The oil discharged from the model and that received as overflow from the constant head reservoir was collected in a tank from where it was occasionally pumped back into an overhead reservoir. The oil from the overhead reservoir was, in turn, supplied to the constant head reservoir.

(d) Discharge control system:

A discharge control system was provided to study the effect of submergence of a drain outlet on the water table movement. It was used to maintain a constant height of water table above a drain. This height simulated the depth to which a drain was submerged below the water level in an outlet channel. It was also used to create suction in the drain and thus make the drain run "free".

The system consisted of a Perspex cylinder (Fig. 5.6) 15 cm high and 6.5 cm diameter, provided with a 1.5 cm dia. overflow tube and a 1.25 cm diameter tube connected to the drain. The whole system could slide vertically along a stand. The water table height over the drain was controlled by adjusting the oil level in the cylinder by means of a threaded stem provided with a lever at the top. A hook gauge carrying a vernier was used to record the simulated free surface level in the collector channel.

5.4a OBJECTIVES OF THE EXPERIMENTS

The main objective of the experiments on the Hele-Shaw model was to study the water table movement in a symmetrical drainage system and to obtain experimental data to verify some of the existing solutions of unsteady state drainage problems. The study was extended to find the effect of vertical misalignment of one of the drains on the rate of fall of water table.

The second objective was to study the effect of the slope of the impermeable bed on the rate of fall of water table between tile drains. This study will be described in detail in Chapter 6.

5.4 EXPERIMENTAL PROCEDURE FOR A SYMMETRICAL DRAINAGE SYSTEM

Since in a symmetrical drainage system the flow is symmetrical

about a vertical line passing midway between drains, only half of the section between two adjacent drains was considered in the experiments (Section 1.3). Experiments were conducted on a single drain which was 1.0 cm in diameter and was located 150 cm from the two ends of the model. This arrangement represented a model drain spacing of 300 cm. The depth of the drain above the impermeable bed varied from 22.90 cm to 42.90 cm. Oil of viscosity 40 centistokes at 70° F was used in the model.

The experiment was started by allowing oil to flow from the overhead reservoir to the constant head reservoir and then to the rainfall distribution system. The rainfall distribution pipe was made free of air through air vents. From the distribution pipe the oil discharged freely through the hypodermic tubes on to a horizontal shelf (Fig. 5.6) attached to the front Perspex plate, from where it moved down into the interspace in the form of a continuous film of oil. The free surface of the oil in the model continued to build up until the rate of discharge of the drain was equal to the rate of rainfall, i.e. the steady state was reached. This was ascertained by observing the free surface with a Cathetometer. The discharge of the drain was then measured and the flow was adjusted to get any desired rate of rainfall. The rate of rainfall per unit area was calculated by dividing the drain discharge by the product of

the spacing between drains and the interspace.

After the measurement of the steady state discharge, the flow was suddenly stopped by closing the valve E (Fig. 5.1). A stop watch was activated when the water table at the right-hand end (plane of symmetry) of the model started falling. The beginning of a rising water table following a sudden start of rainfall was similarly observed when it started rising above its initial horizontal line passing through the centre of the drain. Readings of the height of water table at the right edge of the model were taken, in each case, at short intervals in the beginning of the run and at gradually increased intervals as the movement became slower.

A 24 mm auto-camera was used to record the profile of the water table at regular intervals of time. Recording was begun when the water table started falling or rising, as the case might be, photographs being taken at a preset time interval. For greater accuracy, the time for each photograph was also recorded by a stop watch. A difference of the order of 3-4 seconds was observed between the interval set on the camera and that at which the photograph was actually taken.

The developed film was projected on to a horizontal screen to approximately half the size of the model and the water table profile was measured to an accuracy of 0.5 mm.

5.5 FLOW CONDITIONS IN THE DRAINS

A detailed description of flow conditions in tile drains is given in Section 1.3. The flow conditions in the drains in the present research were mainly governed by the value of R/K. The drains were running free (Section 1.3(i)) at low R/K and full at high R/K (0.02) with the water table standing at a certain height (Section 1.3(ii)) above the drains due to resistance to flow. This height reduced to zero immediately after the water table started falling.

A drain, in general, could be made to run free by applying suction by means of the discharge control system until the depth of water table above the drain was zero and the drain was running under atmospheric pressure. Similarly, the drain could be submerged below the free surface of an outlet channel by adjusting the oil level in the discharge control cylinder (Section 5.3 d).

5.6 EXPERIMENTAL ACCURACY

5.6.1 Observational errors

Observational errors occur in noting the temperature of the oil, measuring the rate of rainfall and in reading the height of the water table. The temperature was observed to an accuracy of 0.1° F every time the drain discharge was measured. There was no change in temperature during each experimental run. The discharge

was measured to 0.1 cc/min. The height of the water table midway between drains was read directly from the graph paper on the rear Perspex plate. Since the rate of movement of the water table was slow, it was possible to take readings within 0.5 mm. The time was noted with a stop watch to an accuracy of 1/10 th of a second.

5.6.2 Measurement of viscosity

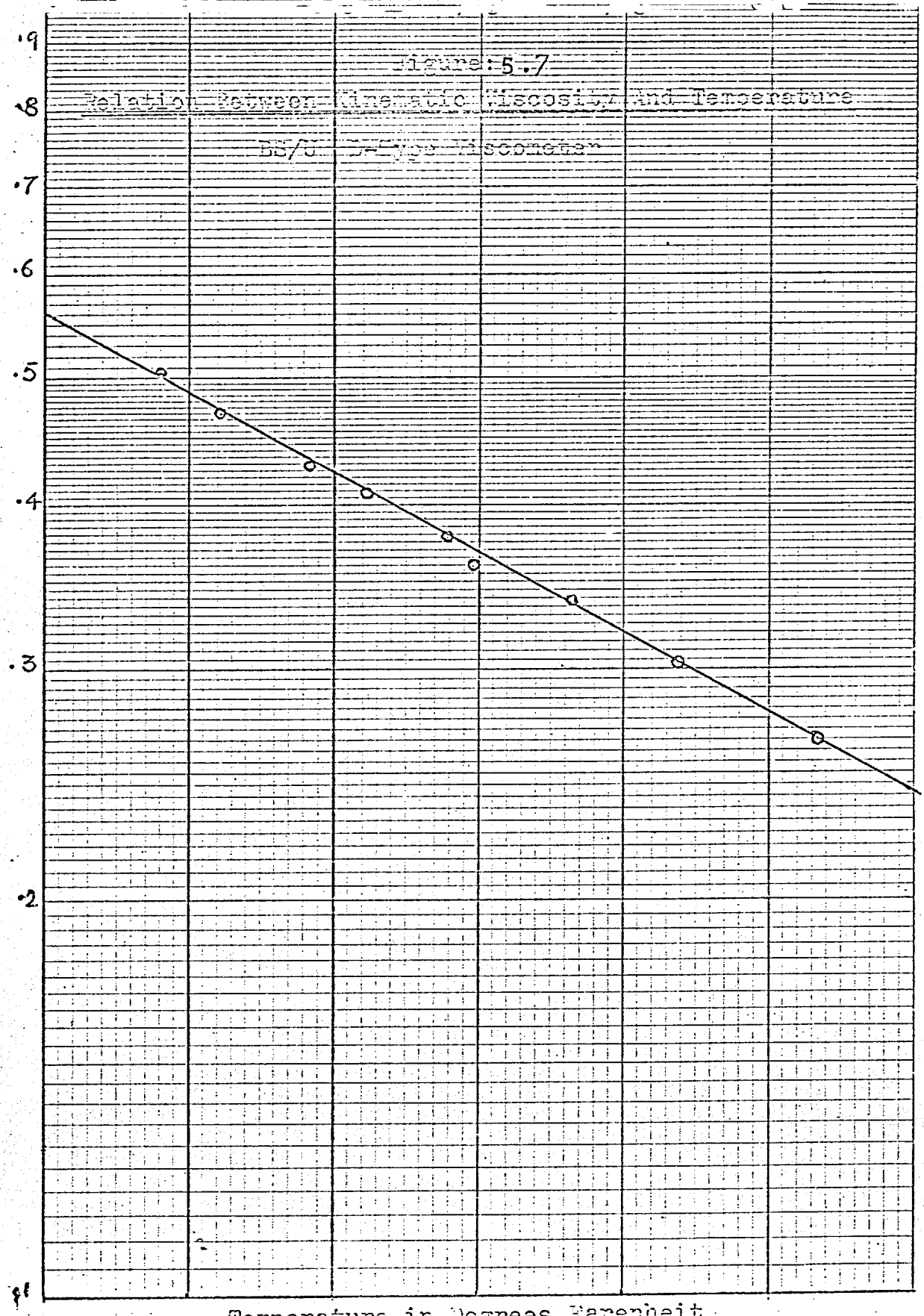
Since the model permeability depends on the viscosity of the oil used in the model, an experiment was conducted to find the effect of temperature on the viscosity. The viscosity was determined by using B.S. U-tube, type D, Viscometer, and by following the standard procedure given in B.S.S No. 188.

The temperature-kinematic viscosity relationship is given in table (5.1) and plotted in Fig. 5.7. The figure shows that there is a small decrease in the viscosity of the oil with a large increase in the temperature. The temperature of the oil in the model varied by $\pm 1^{\circ}$ F in the whole day. The effect of this variation on oil viscosity and hence on the model permeability could therefore be considered insignificant. Fig. 5.8 shows the average model permeability for a temperature range of 55°- 85° F.

Figure: 5.7

Relation Between Kinematic Viscosity And Temperature

BS/U U-Type Viscometer



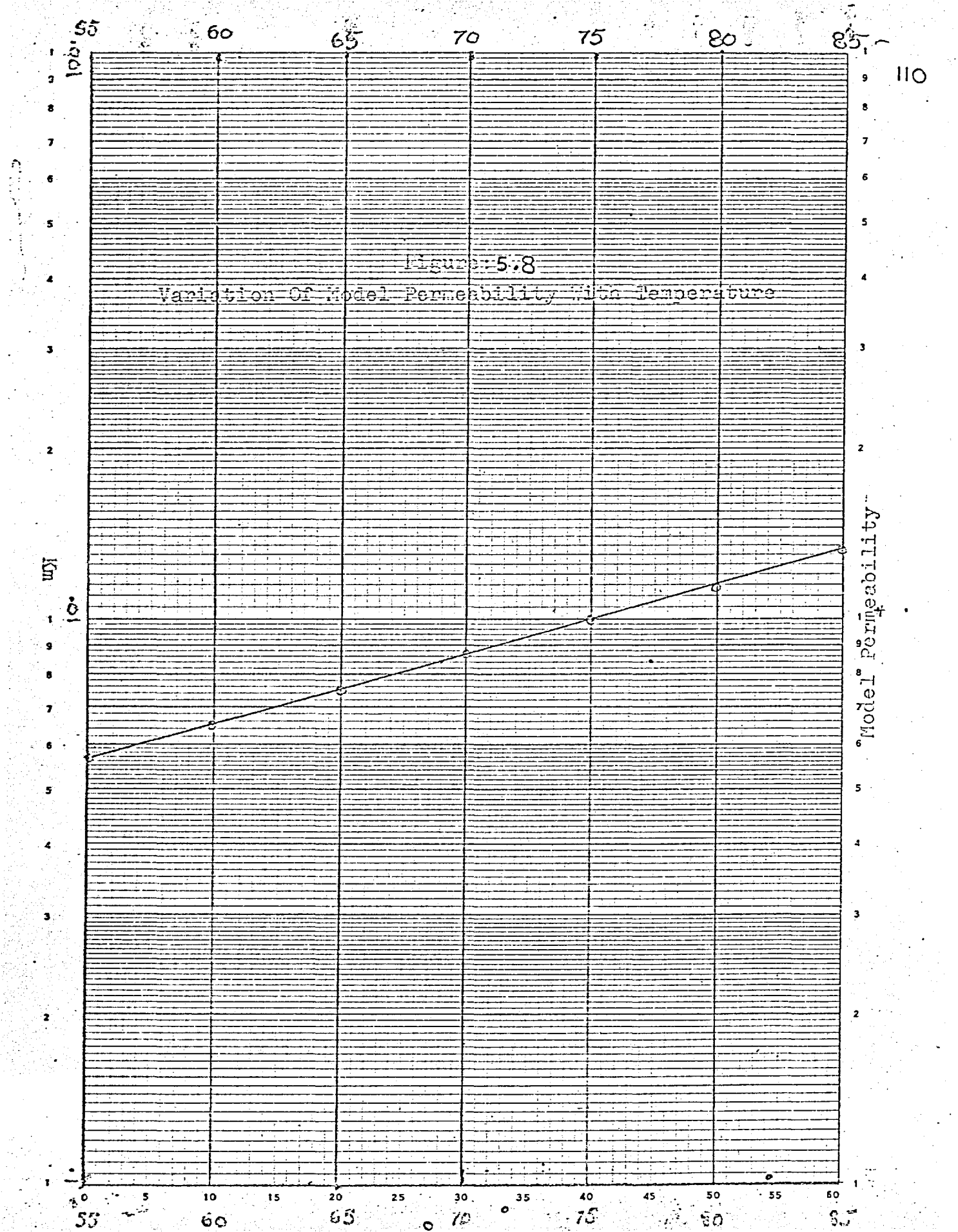


Figure 5.8

Variation Of Model Permeability With Temperature

5.6.3. Uniformity of interspace

The model was checked for uniformity of the interspace as follows.

A measured volume of oil was poured into the interspace and the resulting static levels of oil above the impermeable bed were noted at intervals of 10 cm along the length of the model. This procedure was repeated several times until the model was filled to a depth of 70 cm above the impermeable bed. The interspace was calculated from the relation

$$b = \frac{V}{dL} \quad \ldots\ldots\ldots\ldots\ldots\ldots\ldots\ldots\ldots\ldots \quad (5.17)$$

in which V is the measured volume of oil poured into the interspace each time, d is the corresponding average height of static oil level and L is the length of the model.

Table (5.2) shows values of the interspace at various depths above the impermeable bed. The average value of the interspace was found to be $b = 1.98 \pm 0.03$ mm.

5.6.4 Rainfall distribution

Uniform distribution of rainfall over the whole length of the model was obtained by using 118 hypodermic tubes 1.5 mm in diameter and spaced 2.5 cm apart. The discharge of each tube was measured at a constant head and a variation of the order of 3 % about the mean was observed in some tubes. The effect of this non-uniformity was reduced by allowing the

oil to accumulate over a horizontal shelf before flowing down into the interspace (Fig. 5.6). At the start of each experiment, the tubes were also cleaned to avoid the possibility of any solid matter clogging their openings.

5.6.5 Boundary effect

In the study of the symmetrical drainage system in the model, the plane of symmetry between drains was represented by solid boundaries. Although these boundaries coincide with the vertical midpoint streamline boundary, they introduced additional resistance due to the drag effect along the solid model boundary not present in the prototype.

Since the oil at the solid boundaries has zero velocity relative to the boundary, there is some velocity gradient outwards from the boundary (Fig. 5.9).

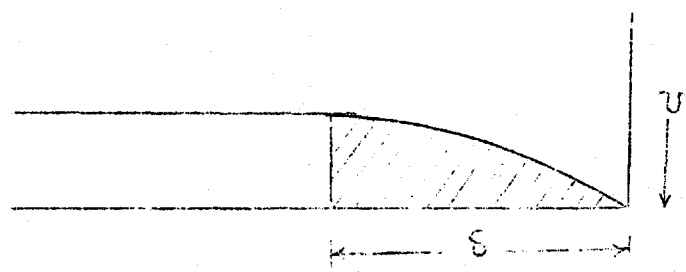


Fig. 5.9

The gradient is limited within the thickness of the boundary layer.

Streeter (63) showed that the thickness of the boundary

layer in a uniform flow is given by:

$$\frac{\delta}{x} = \frac{4.65}{\sqrt{R_e}} \qquad (5.18)$$

in which

$$R_e = \frac{vx}{\nu}$$

and x is the horizontal distance along the boundary from its leading edge, and v is a uniform velocity of flow of the fluid.

In order to make a rough check on the thickness of the boundary layer, the rate of fall of water table along the solid boundary was noted. The average speed (v) of fall of the water table was observed to be 0.125 cms/sec at a distance x = 2.00 cms when the viscosity of the oil was 0.43 stokes. From equation (5.18), the approximate thickness of the boundary layer was found to be 2.65 cms. All observations of the fall of the midpoint water table were, however, taken at a distance 5.0 cms from the boundary. This was necessary because the steady state water table profile was observed to be slightly depressed within 4.0 cms from the edge boundaries. The depression effect might have been caused due to surface tension.

It may be mentioned that the boundary effect can be eliminated by using more than one drain so that no solid boundary exists midway between two adjacent drains. However, since the object of the experiments was to check unsteady state solutions, some of which are based on the Dupuit assumptions requiring

large spacing length (Section 3.1), it was not possible to use more than one drain in the study of the symmetrical drainage system.

5.6.6 Effect of temperature on water table height

Let a loss of head h_1 occur in a length l_1 of the supply system between the oil level in the constant head tank and outlet of the hypodermic tubes. Then the discharge Q of an incompressible fluid of viscosity ν, through 118 hypodermic tubes each of diameter d_c, is given by:

$$Q = 118 \frac{\pi d_c^4}{128 \nu} \cdot \frac{h_1}{l_1} \quad \ldots\ldots\ldots\ldots\ldots\ldots \quad (5.19)$$

$$= \frac{A}{\nu} \cdot \frac{h_1}{l_1} \quad \ldots\ldots\ldots\ldots\ldots\ldots\ldots\ldots \quad (5.19)$$

At the steady state condition, the same discharge through the interspace b of the model is given by:

$$Q = \frac{b^3}{12 \nu} \cdot \frac{dh}{dx} \quad \ldots\ldots\ldots\ldots\ldots\ldots\ldots \quad (5.20)$$

It is presumed that the fluid in the model and in the supply system is subject to the same influence of temperature. A rise in temperature will simultaneously cause an increase of flow in the supply system as well as in the model.

Equation (5.20) can be re-written as

$$\frac{dh}{dx} = \frac{12 \nu}{b^3} \cdot Q = B \nu Q \quad \ldots\ldots\ldots\ldots\ldots \quad (5.21)$$

Substitution of (5.18) into (5.21) yields

$$\frac{dh}{dx} = C \frac{h_1}{l_1} \qquad \text{.....} \qquad (5.22)$$

where C = A.B = constant

Equation (5.22) shows that so long as h_1/l_1 remains constant, the temperature does not affect the water table position.

5.6.7 Capillary effect

The free surface of the oil in the model, exposed to atmospheric pressure, is subject to capillary rise due to surface tension. Because of the capillary effect, the free surface of oil, measured at the bottom of the meniscus, does not represent the actual free surface (p = 0), but the upper surface of the "capillary fringe".

Let the angle of contact (Fig. 5.10) $\theta = 0$. Then for a static equilibrium (i.e. the weight of the fluid held under surface tension be equal to the surface tension force), the basic relation between surface tension and capillary height, for a unit length of the model is approximately given by:

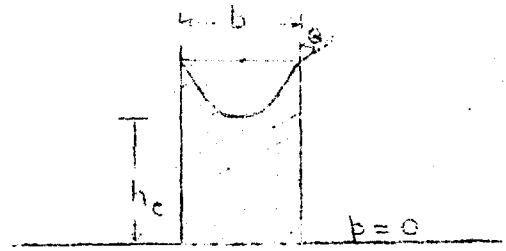


Fig. 5.10

$$2T = \gamma \left[b(h_c + b/2) - \tfrac{1}{2} \pi (b/2)^2 \right]$$

$$h_c = \frac{2T}{\gamma b} - \frac{b}{2}\left[1 - \frac{\pi}{4}\right] \qquad \text{.....} \qquad (5.23)$$

where T is surface tension.

It is obvious from equation (5.23) that the capillary height depends on the width of the interspace and the nature of the fluid. The height can be greatly reduced by increasing the interspace and using oil of high viscosity. It is, of course, presumed that this combination does not disturb the Darcy flow.

Another point worth attention is the restraining effect (delayed oil storage effect) caused by a highly viscous oil (Fig. 5.10a). The delayed oil storage effect occurs during rapid fall of water table because the oil sticks to the walls of the model. An increase in interspace in such a case would augment the rapid fall of water table and thus increase this error. The aim in the experiments was, therefore, to obtain laminar flow without introducing large errors due to the delayed oil storage effect and the capillarity. This was achieved by using an interspace of 2 mms and oil of low viscosity (40 centistokes at 70° F). The capillary rise was determined experimentally and found to be 0.45 cms.

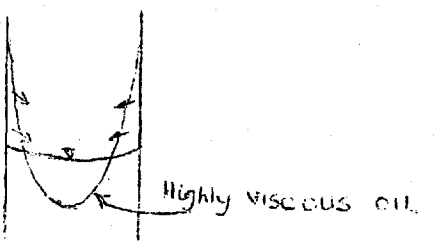


Fig. 5.10a

5.7 EXPERIMENTAL RESULTS FOR THE SYMMETRICAL DRAINAGE SYSTEM

5.7.1 The falling water table

5.7.1.1 Normalised parameters

Considering the falling water table only at the midpoint between drains, the variables in the present problem can be written in a functional relation of the form

$$\frac{Y}{Y_m} = F\left(\frac{Y_m}{d}, \frac{r}{d}, \frac{d}{L}, \sqrt{\frac{Ktd}{fL^2}}\right) \quad \ldots\ldots\ldots\ldots\ldots \quad (5.24)$$

containing only dimensionless (normalised) parameters. These parameters contain only length variables, except the parameter $\sqrt{Ktd/fL^2}$, which may be considered as a dimensionless time parameter. This form of time parameter is preferred over other forms such as Kt/fL and Kt/fd (though these are used in one case later) because it has been used in many analytical solutions, e.g. Glover's, Moody's and Brooks', and it would therefore be easy to compare these solutions with experimental results in the same form.

To verify the similitude between the model and the prototype given by equation (5.24), it is only necessary to demonstrate that, provided the other parameters are constant, Y/Y_m plotted as a function of $\sqrt{Ktd/fL^2}$ is independent of the liquid used. This was checked by repeating the same experiment at different temperatures. No measurable variation of Y/Y_m was observed.

The purpose of normalising the variables is to facilitate ready comparison of curves illustrating either the effect of the individual variables on unsteady state drainage or testing the validity of some analytical solutions. There does not seem to be any hard and fast rule as to the form of the normalised parameters in analytical solutions. The parameters differ from one solution to another, all being some combination of the parameters given in equation (5.24). In some cases in the thesis, therefore, parameters other than those given in equation (5.24) are taken to verify a particular analytical solution, e.g. Y/Y_m, Y_m/L, Kt/fL and d/L in Isherwood's solution (Section 5.7.1.4).

For further convenience in presentation of the experimental results, a term "recession index" is introduced in the thesis. The recession index (R.I) is a measure of the speed of fall of the water table and is defined as the ratio Y/Y_m or h/h_m corresponding to one particular value of the time parameter for all curves. The smaller the value of the recession index, the more rapid will be the rate of fall of the water table, i.e. the lower will be the value of Y/Y_m.

5.7.1.2 Effect of initial steady state water table height Y_m

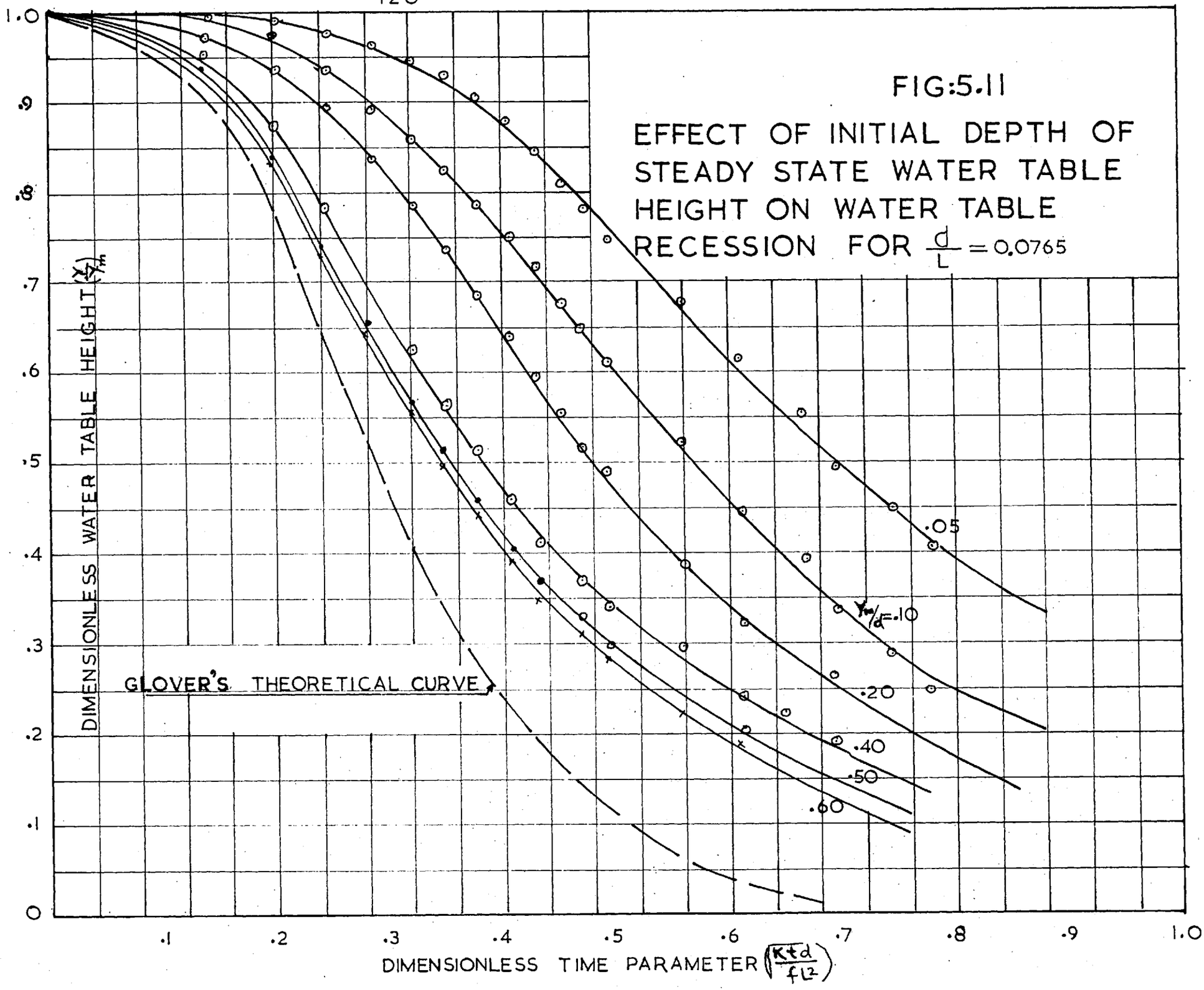
The object of this experiment was to test whether the analytical solutions based on the Dupuit assumptions hold for small values of Y_m/d.

The experiment was conducted by keeping d/L constant at 0.0765. The rate of fall of the midpoint water table was examined for six different values of Y_m/d in the range 0.05 to 0.60. These values were obtained by changing Y_m and keeping d constant.

The results of experimental runs are given in Table 5.3 and plotted in Fig. 5.11. The figure shows that the recession index decreases with Y_m/d (i.e. the water table falls more slowly as Y_m/d decreases). This trend of the experimental results, in general, appears to be in agreement with Isherwood's work (39). Though there are no directly comparable cases, the following parametric values obtained from Isherwood's paper may roughly show that in the Isherwood solution also the midpoint water table falls more slowly as Y_m/d decreases. The time parameter $\sqrt{Ktd/fL^2}$ corresponds to the situation when the midpoint water table is one foot below the ground surface.

Y_m/d	d/L	$\sqrt{Ktd/fL^2}$
0.67	0.12	0.199
0.43	0.14	0.290
0.25	0.16	0.380

The dotted line in Fig. 5.11 represents Glover's solution based on Tapp and Moody's (32) parabolic initial water table profile. Only one such curve is shown because Y/Y_m in Glover's


FIG:5.11
EFFECT OF INITIAL DEPTH OF STEADY STATE WATER TABLE HEIGHT ON WATER TABLE RECESSION FOR $\frac{d}{L} = 0.0765$
DIMENSIONLESS WATER TABLE HEIGHT $(\frac{Y}{Y_m})$
DIMENSIONLESS TIME PARAMETER $(\frac{Kt\,d}{f\,L^2})$
GLOVER'S THEORETICAL CURVE
Y_m/d=.05
.10
.20
.40
.50
.60
0
.1
.2
.3
.4
.5
.6
.7
.8
.9
1.0

solution is independent of Y_m/d. Fig. 5.11 shows that the experimental values of Y/Y_m are everywhere higher than those predicted by Glover's solution. This solution was based on the assumption that $Y_m << d$. With this end in view, the smallest value of Y_m/d used in this study was 0.05. Fig. 5.11 indicates that when Y_m/d is reduced progressively, the difference in recession index between the experimental curves and the Glover curve becomes increasingly greater. In each case Glover's solution predicts smaller value of the recession index. The largest difference occurs when $Y_m/d = 0.05$. The experimental results, thus, contradict the Glover solution and so cast some doubt on the basic assumption with which that solution was obtained.

The smaller value of the recession index in Glover's solution (Fig. 5.11) may be due to the assumption implied in the solution that the whole of the saturated thickness of the medium contributes flow to the drain. Bouwer (64) indicated that for small drain spacing and a deep aquifer (large d/L), little or no flow occurs in the lower part of the aquifer. He called that part of the aquifer a "passive region". It appears that the thickness of the passive region does not depend only on d/L but also on Y_m/d. At small value of Y_m, the flow may be occuring only in a part of the depth d with the result that the thickness of the passive region may be large. As Y_m increases, the thickness of this region decreases and there is a corresponding increase in the

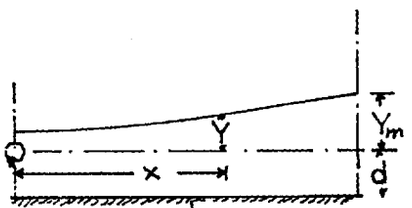
thickness of the active region (the region in which all the flow occurs). Consequently, the flow area between adjacent streamlines in the flow field becomes larger and also the length of the streamlines increases. The increase in the length of the streamlines is associated with an increase in the head loss. The maximum drainage, due to a combination of the effects of the length of flow path and the enlarged flow area, occurs when $Y_m/d = 0.60$. This, in fact, is the case when the flow may be occuring over the full depth d. Any further increase in Y_m may only lead to an increase in the length of flow path which may offset the advantage of an increase in the flow area.

Another point worth attention is that in Glover's equation (equation 4.3), Y/Y_m, at a particular time after the beginning of recession, is constant for fixed values of L, D and K. This conclusion does not hold as can be seen in Fig. 5.12 which shows that at low values of Y_m/d, Y/Y_m decreases very rapidly and becomes essentially constant at $Y_m/d = 0.60$. This indicates that Glover's solution can be expected to hold for $Y_m/d \geq 0.60$.

Finally, the development of Glover's solution was based on the assumption that d/L is small. In the present study, d/L was kept constant at a value of 0.0765. A question may arise as to whether or not this value is sufficiently large to cause the difference in recession index found between the

FIG: 5.12
RELATIONSHIP BETWEEN η AND η_m
FOR VARIOUS VALUES OF τ

$\frac{d}{L} = 0.0765$



$\tau = \sqrt{\frac{K t d}{f L^2}}$

DIMENSIONLESS WATER TABLE HEIGHT $\left(\frac{Y}{Y_m}\right)$

DIMENSIONLESS WATER TABLE HEIGHT $\left(\frac{Y_m}{d}\right)$

1.0 .9 .8 .7 .6 .5 .4 .3 .2 .1 0

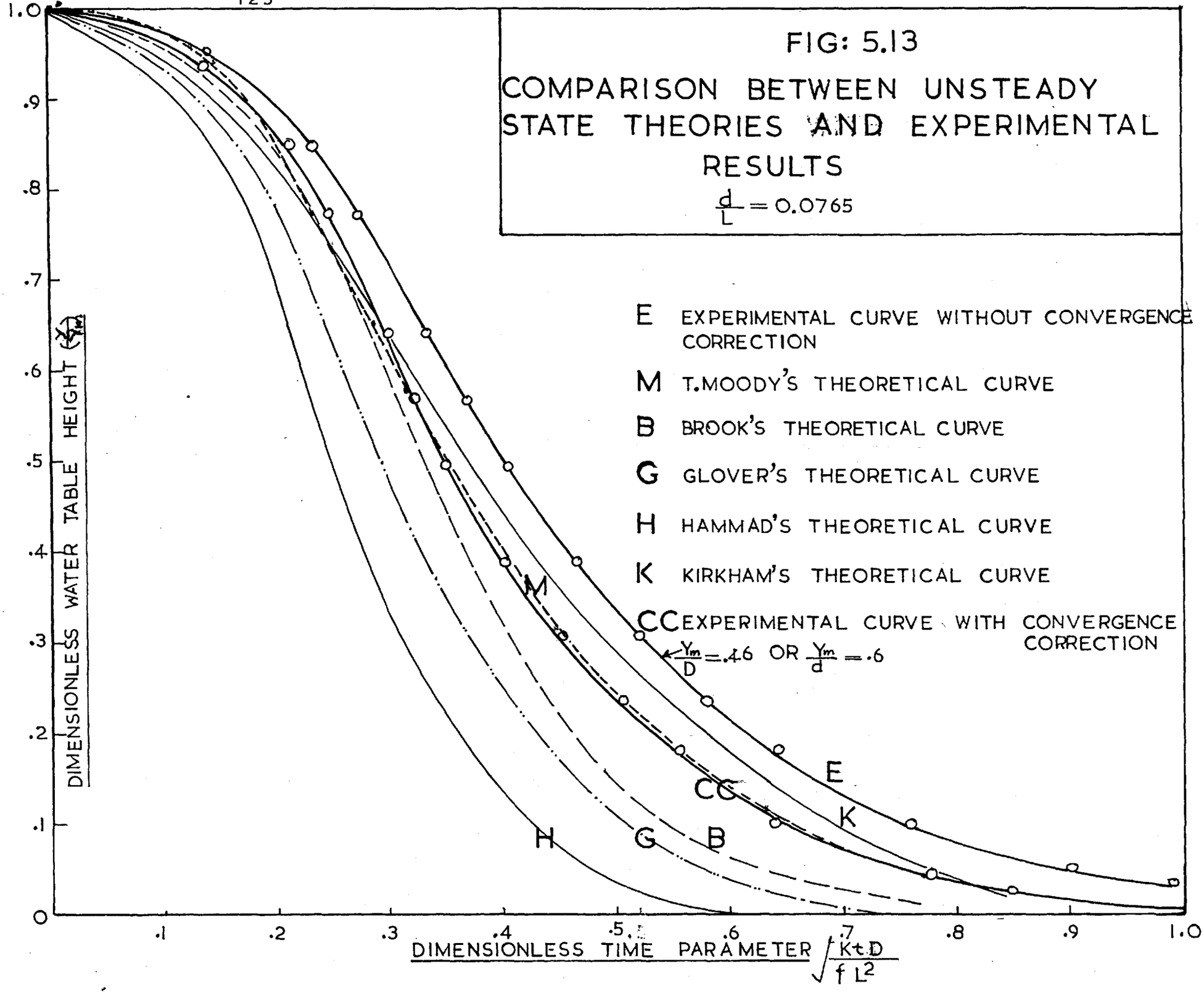
.1 .2 .3 .4 .5 .6

.3 .4 .5 .6

experimental results and the Glover solution. In this connection, reference may be made to Maasland's experimental study (5). The smallest value of D/L used by Maasland was 0.035. Even at this value, he observed that the solution overestimated the (smaller value) recession index. He also noted that the divergence between Glover's solution and his experimental results increased with D/L. Dumm (41) later showed that if Maasland's experimental results were corrected for a convergence effect, all the experimental curves would coincide with Glover's curve. It is therefore apparent that, after the convergence correction (Fig. 5.13), the ratio d/L = 0.0765 used in the present experiments should not contribute appreciably to the difference between the experimental and analytical results.

5.7.1.3 Comparison of experimental results with analytical solutions.

The experimental results for Y_m/d = 0.60 and the results obtained from the solutions by Hammad, Kirkham, Glover, Brook and Isherwood are given in Table 5.4. The data are plotted in Fig. 5.13. The full line with large dots shows the experimental curve without a convergence correction. There is a large difference between Hammad's curve and the experimental curve. Such a difference may be due to the many assumptions (Section 3.3.4) inherent in Hammad's


FIG: 5.13
COMPARISON BETWEEN UNSTEADY STATE THEORIES AND EXPERIMENTAL RESULTS
d/L = 0.0765
E EXPERIMENTAL CURVE WITHOUT CONVERGENCE CORRECTION
M T.MOODY'S THEORETICAL CURVE
B BROOK'S THEORETICAL CURVE
G GLOVER'S THEORETICAL CURVE
H HAMMAD'S THEORETICAL CURVE
K KIRKHAM'S THEORETICAL CURVE
CC EXPERIMENTAL CURVE WITH CONVERGENCE CORRECTION
Ym/D = .46 OR Ym/d = .6
DIMENSIONLESS WATER TABLE HEIGHT (Y/Ym)
DIMENSIONLESS TIME PARAMETER √(K t D / f L²)
1.0
.9
.8
.7
.6
.5
.4
.3
.2
.1
0
.1
.2
.3
.4
.5
.6
.7
.8
.9
1.0

solution, the major source of difference being the assumption that the water table falls uniformly by the same amount everywhere as given by the fall midway between drains. In view of the studies by Childs (4) and Kirkham and Gaskel (43), discussed in Section 4.6.1, the water table, except in the beginning of a recession, falls more rapidly in the middle than elsewhere between the drains. As a result, Hammad's solution would overestimate (predicts lower value) the recession index.

It can be seen from Fig. 5.13 that values of Y/Y_m obtained by Brooks' solution agree reasonably well for small values of $\sqrt{Ktd/fL^2}$ but are too low for high $\sqrt{Ktd/fL^2}$ than the experimental results obtained after correction for convergence. The reason may be that the solution is based on the boundary condition that the water table at the drain drops instantaneously from height Y_m to its theoretical value zero. This requires that the theoretical discharge of the drain should be infinite in the beginning of the recession process. In fact, the drain cannot convey the theoretically infinite discharge; it takes a certain time to establish the above boundary condition. Since the actual rate of flow is considerably less than its theoretical value, the experimental rate of fall of the water table will be slower than predicted by the solution.

Kirkham's curve lies between the experimental curves

obtained with and without a convergence correction. Since Kirkham's solution is not based on the Dupuit assumptions, the curve is compared with the actual experimental curve (without a convergence correction). It appears from the figure that Kirkham's analytical results agree better with the experimental results than those of the Hammad and Glover solution.

It was mentioned in Section 3.3.3 that the Hooghoudt steady state solution agrees very closely ($\pm$ 5%) with Kirkham's steady state solution. Therefore, if the Hooghoudt solution is integrated for the unsteady state (equation 4.16), it would give approximately the same results as those of the Kirkham integrated solution (equation 4.19).

Among the unsteady state solutions, Isherwood's solution is more accurate because it was obtained by solving the Laplace equation. The solution satisfies all the essential boundary conditions of tile drainage problems. It is observed in Fig. 5.14 that Isherwood's theoretical curve, for $d/L \simeq 0.0805$ and $Y_m/d \simeq 0.86$ (36, Fig. 3), fits remarkably well with the experimental curve. It may be noted that d/L in the experiments and the Isherwood solution is 0.0765 and 0.0805 respectively. This small difference between the two ratios may not introduce appreciable error.

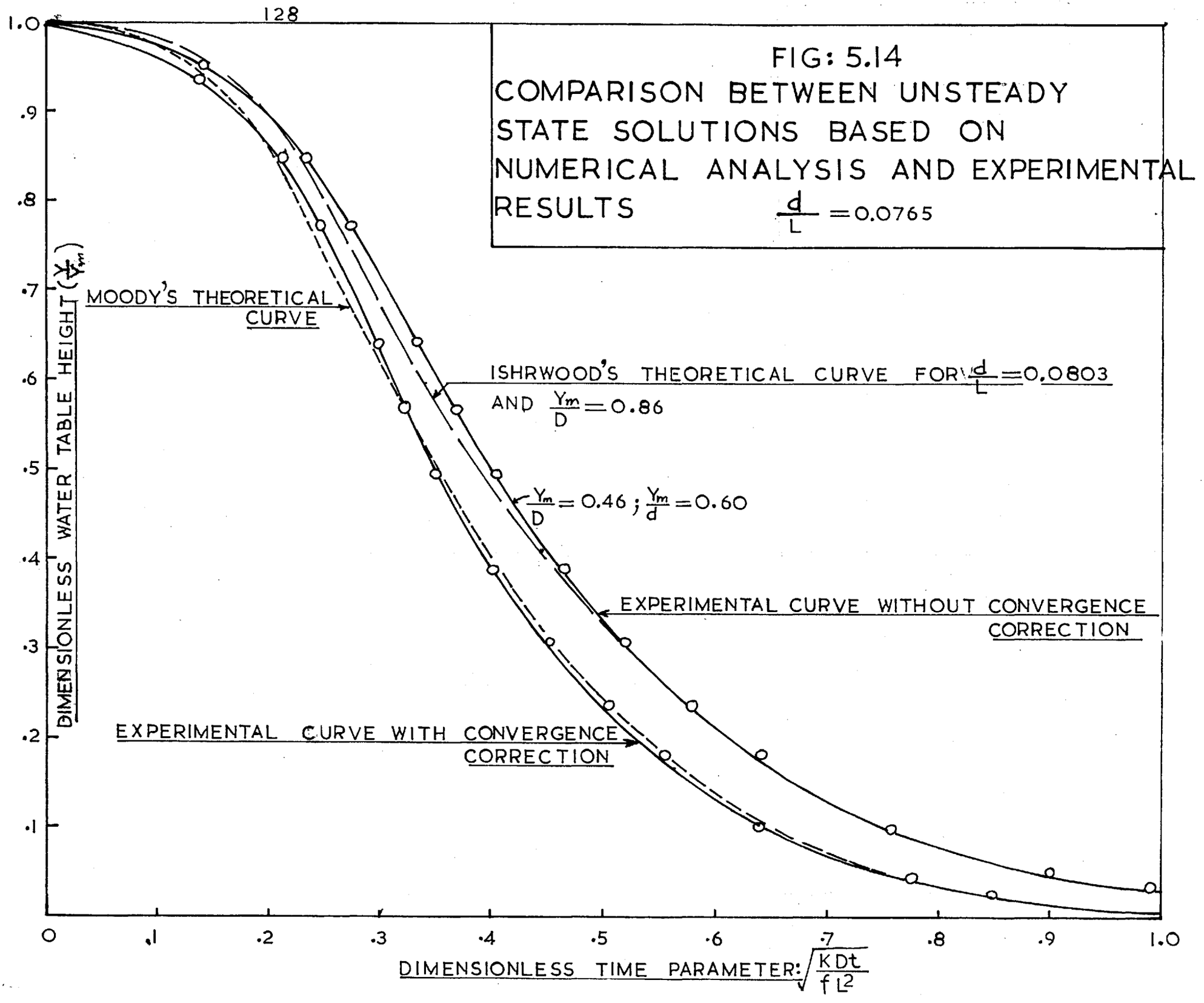


FIG: 5.14
COMPARISON BETWEEN UNSTEADY STATE SOLUTIONS BASED ON NUMERICAL ANALYSIS AND EXPERIMENTAL RESULTS $\frac{d}{L}=0.0765$

A close agreement between Isherwood's theoretical results for $Y_m/D = 0.86$ and experimental results for $Y_m/D = 0.46$ ($Y_m/d = 0.60$) further confirms the conclusion advanced previously in Section 5.7.1.4, namely, that the recession index is unaffected by Y_m/d for $Y_m/d \geq 0.60$.

Moody's theoretical curve in Fig. 5.14 is obtained from Fig. 2 of his paper (15). Since Moody's solution was based on the Dupuit assumptions, the theoretical curve is compared with the experimental curve which is corrected for the convergence effect. The theoretical curve almost coincides with the experimental curve, thus showing a remarkable agreement.

It is interesting to compare the experimental results with Glover's second equation (equation 4.4) because the ratio d/L is very small as required. The experimental and theoretical results are shown in Table 5.5. The theoretical results compare reasonably well with the experimental results. At low values of d/L (≤ 0.0765), it is therefore justified to use Glover's second equation to calculate the rate of fall of water table rather than the first equation (equation 4.3).

5.7.1.4 Effect of depth of impermeable bed

The effect of the depth of the impermeable bed on water table heights for the steady state condition with

TABLE 5.5

COMPARISON OF EXPERIMENTAL RESULTS

WITH GLOVER'S FIRST AND SECOND EQUATION

$Y_m/d = 0.60 \qquad d/L = 0.0765$

Time	Experimental	Glover's I ($d > 0$)	Glover's II ($d=0$)
secs	Y cms	Y cms	Y cms
0	13.70	13.70	13.70
20	11.70	9.38	10.60
40	8.85	5.51	8.70
60	6.80	3.23	7.45
80	5.35	1.89	6.30
100	4.22	1.11	5.58
120	3.42	0.65	4.95
150	2.60	0.34	4.30
180	2.00	0.21	3.80

various rainfall intensities was investigated by Hooghoudt (2), Hammad (13) and Collis-George and Young (29). Hooghoudt observed that the depth has no effect on drainage characteristics for $d/L \geq 0.25$; Hammad for $d/L \geq 0.25$; and Collis-George and Young for $d/L \geq 0.15$.

For the unsteady state condition, Isherwood showed that the impermeable bed deeper than L/8 below the drain axis has little influence on the recession index (Section 4.4). His results were based on the condition that the mid-point water table falls by one foot below the ground surface. He did not present results for the later stages of water table recession. Although Isherwood did not specifically mention the parameters that he kept constant in his analysis, it is noted from Table 2 of his paper that the above conclusion would hold for all values of Y_m/L.

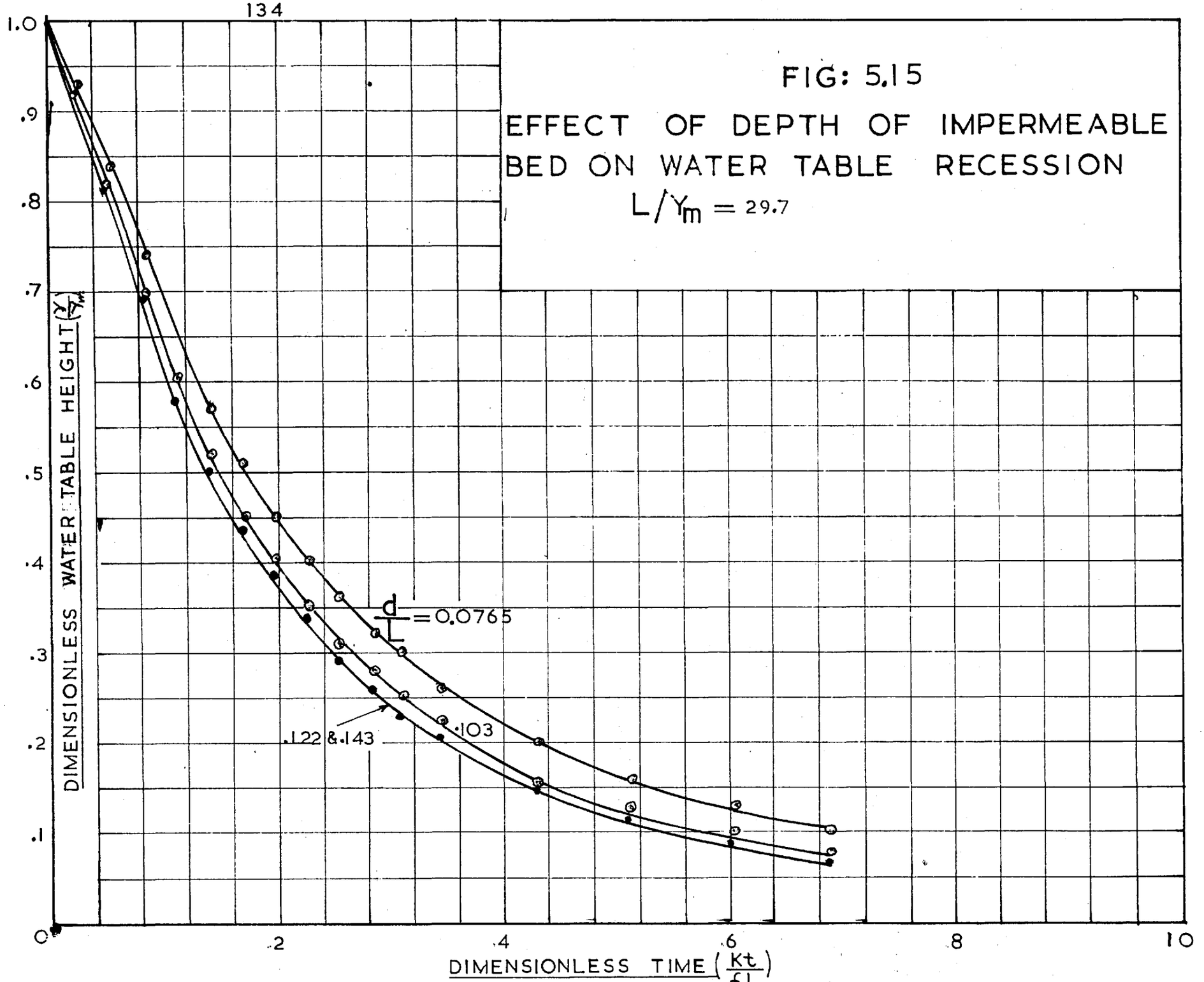
The object of the present experiments was to check Isherwood's conclusion with a curved initial water table (Isherwood assumed a horizontal initial water table) and present a more elaborate treatment of the effect of the depth of the impermeable bed on drainage characteristics. The functional relationship between the variables considered by Isherwood is obtained by transforming equation (5.24) into the form

$$\frac{Y}{Y_m} = F\left(\frac{Y_m}{L}, \frac{d}{L}, \frac{Kt}{fL}\right) \quad \ldots\ldots\ldots\ldots\ldots\ldots \quad (5.25)$$

Experiments were conducted with various depths of the impermeable bed and for a constant ratio $Y_m/L = 0.0337$. Values of $\frac{d}{L}$ used in the experiments were 0.0765, 0.103, 0.123 and 0.143.

The results of the Hele-Shaw model experiments are given in Table 5.6 and plotted in Figs. 5.15 and 5.16. The curves in Fig. 5.16 indicate that the recession index decreases rapidly as the depth of the impermeable bed increases. When d/L approaches 0.123, the recession index becomes constant; that is, the rate of fall of the water table is not affected by the depth of the impermeable bed. It can be seen from Table 5.6 that the recession index is the same for both d/L = 0.123 and d/L = 0.143. This amply substantiates Isherwood's conclusion. In order to check whether this conclusion holds for all values of Y_m/L, additional experimental data, for $Y_m/L = 0.008$, is presented in Table 5.7. The data illustrates that the initial water table height does not affect the relationship between the recession index and the depth of the impermeable bed.

The rapidly decreasing effect of the depth of the impermeable bed on the recession index may be due to the reasons discussed in Section 5.7.1.2. An increase in the depth of the impermeable bed is associated with an increase in the length of the flow path and the flow area between adjacent stream lines. The maximum drainage occurs


FIG: 5.15
EFFECT OF DEPTH OF IMPERMEABLE BED ON WATER TABLE RECESSION
$L/Y_m = 29.7$
DIMENSIONLESS WATER TABLE HEIGHT $(\frac{Y}{Y_m})$
DIMENSIONLESS TIME $(\frac{Kt}{fL})$
$\frac{d}{L} = 0.0765$
.103
.122 & .143
1.0
.9
.8
.7
.6
.5
.4
.3
.2
.1
0
.2
.4
.6
.8
1.0

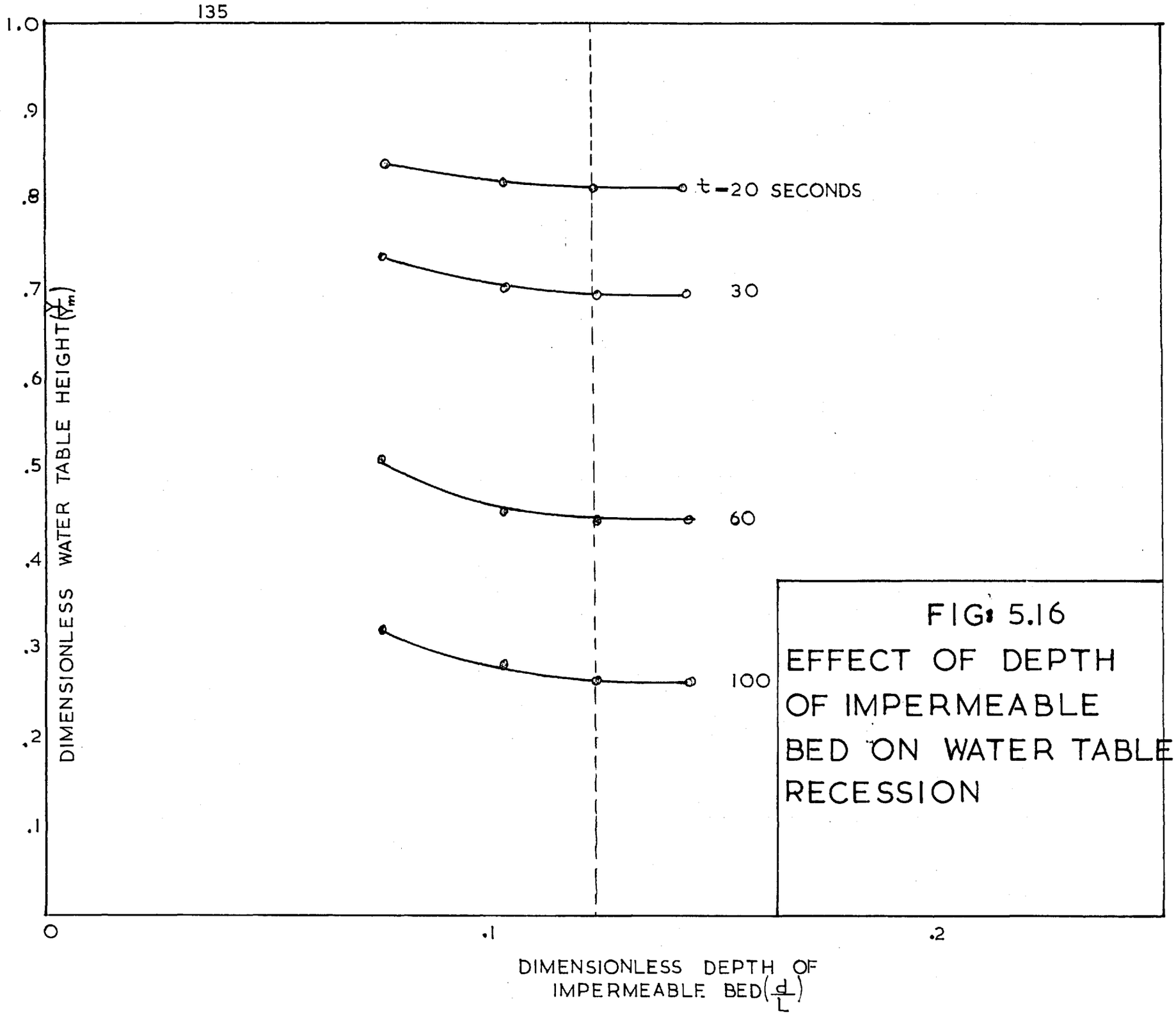


FIG: 5.16
EFFECT OF DEPTH OF IMPERMEABLE BED ON WATER TABLE RECESSION

at d/L = 0.123 when, for a given Y_m/L, a combined effect of the flow resistance and the enlarged flow area has reached a limit after which any further increase in d/L will simply lead to an increased flow resistance which offsets the advantage of the increase in flow area.

5.7.1.5 Effect of drain size

The existing analytical solutions do not give an exact answer to the effect of drain size on the rate of drainage. The assumption of identifying the drain periphery with an equipotential line (Section: 3.3.2) is true only if the drain is running full. As soon as the drain runs partly full, the theoretical shape of the drain equipotential takes the shape of a horse-shoe as against a circular section. It is therefore clear that, in the unsteady state, especially some time after the recession begins, all such solutions lose part of their accuracy.

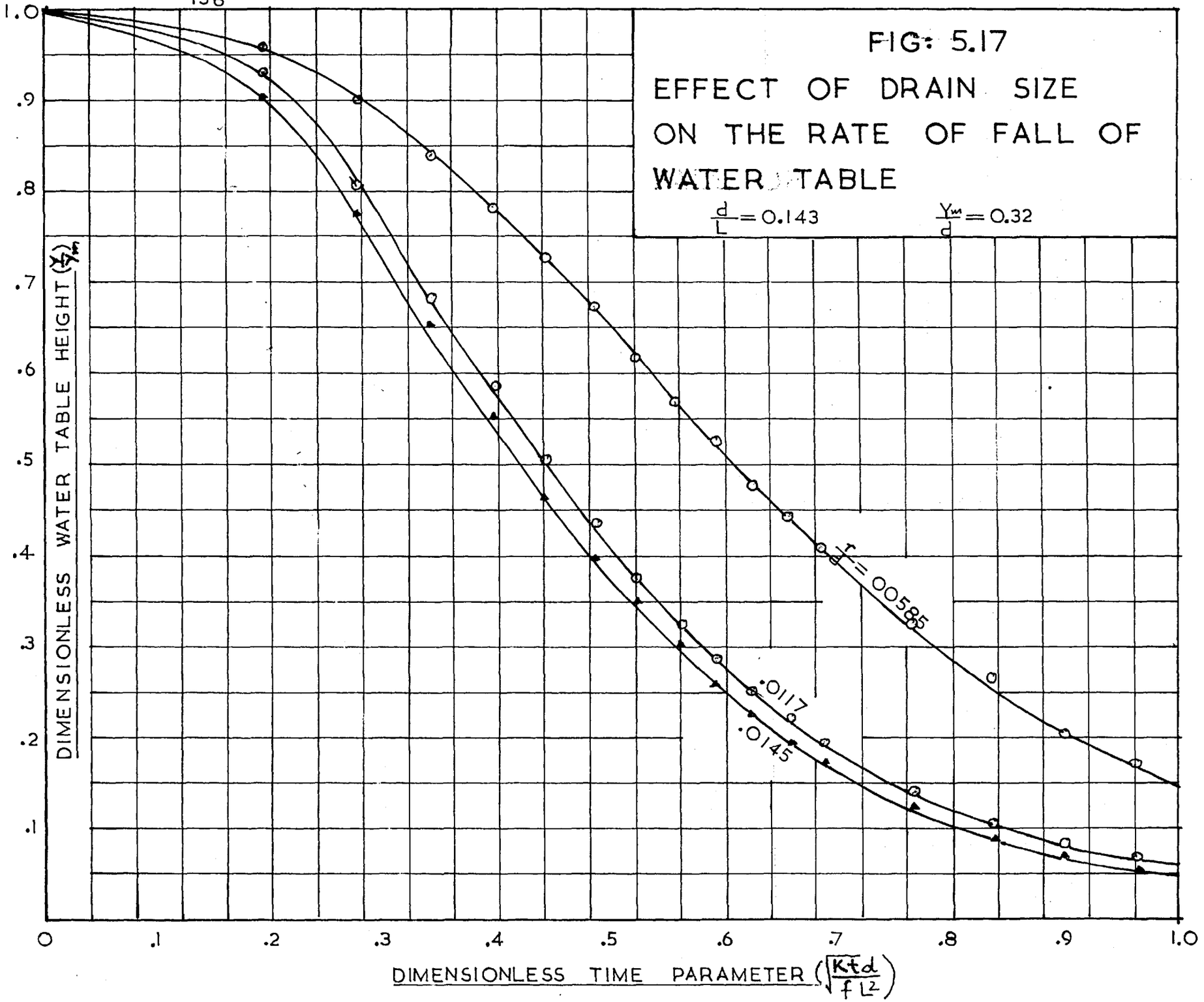
The solutions based on the Dupuit assumptions take the drain as a permeable point sink. This simplification is generally justified by many investigators on the grounds that the drain is very small in comparison to other geometrical drainage parameters.

The object of the present experiment was to study the effect of drain size on the midpoint falling water table.

The steady and unsteady state experimental results are compared with those obtained from the solutions of Hammad and Kirkham with a view to evaluating the discrepancies resulting from the assumptions underlying these solutions.

The functional relationship between the variables involved in the experiment is the same as given by equation (5.24). The initial steady state midpoint water table height was kept constant at 13.70 cms, thus giving $Y_m/d = 0.32$ in equation (5.24). In addition, d/L was equal to 0.143 in all runs. Three drain diameters: 1.25, 1.0 and 0.5 cms were used giving r/d equal to 0.00580, 0.01160, and 0.0145.

The effect of drain size on the rate of fall of the midpoint water table is mainly due to flow resistance near the drain. This resistance is relatively higher for the smaller drains that for the larger ones. It is for this reason that the same initial steady state midpoint water table height can be maintained by introducing a lower rate of rainfall in the case of smaller drains than would be possible in the larger ones. As a result, the recession index would be comparatively high for the smaller drains. This effect is apparent in Fig. 5.17 (Table 5.8). The curves indicate that there is a rapid increase in the recession index when r/d increases from 0.00580 to 0.01160, whereas it is proportionally not as marked in the range $0.01160 < r/d < 0.0145$. This may possibly


FIG: 5.17
EFFECT OF DRAIN SIZE ON THE RATE OF FALL OF WATER TABLE
d/L = 0.143
Ym/d = 0.32
r/d = 00585
.0117
.0145
DIMENSIONLESS WATER TABLE HEIGHT (Y/Ym)
DIMENSIONLESS TIME PARAMETER (√(Ktd/fL²))
0
.1
.2
.3
.4
.5
.6
.7
.8
.9
1.0

be due to a relatively small reduction in resistance to flow near the drain as the drain gets larger.

The experimental data is compared with the theoretical results of Hammad and Kirkham in Fig. 5.18 (Table 5.9). The Kirkham results were calculated from equation (4.19). The experimental and Kirkham results differ considerably for r/d = 0.00585, but agree remarkably well for r/d = 0.01160 and r/d = 0.0145.

It was explained in Section 4.6.1 that the unsteady state solutions based on the integrated form of steady states overestimate the recession index. Since Kirkham's equation (equation 4.19) is based on the same method, it is surprising that such a close agreement between the solution and the experiment as above is obtained. This can, however, be explained by comparing, in Table 5.10, the experimental steady rainfall in the form R/K with that obtained from Kirkham's Solution (equation 3.13). The table shows that for r/d = 0.0116 and r/d = 0.0145 and for a given Y_m, the theoretical R/K is considerably less than its experimental value. A lower theoretical value of steady state R/K will consequently lead to a slow rate of drainage (higher recession index). This may compensate for the higher rate of drainage (lower recession index) obtained when the steady state solution is integrated (Section 4.6.1) to get an unsteady state

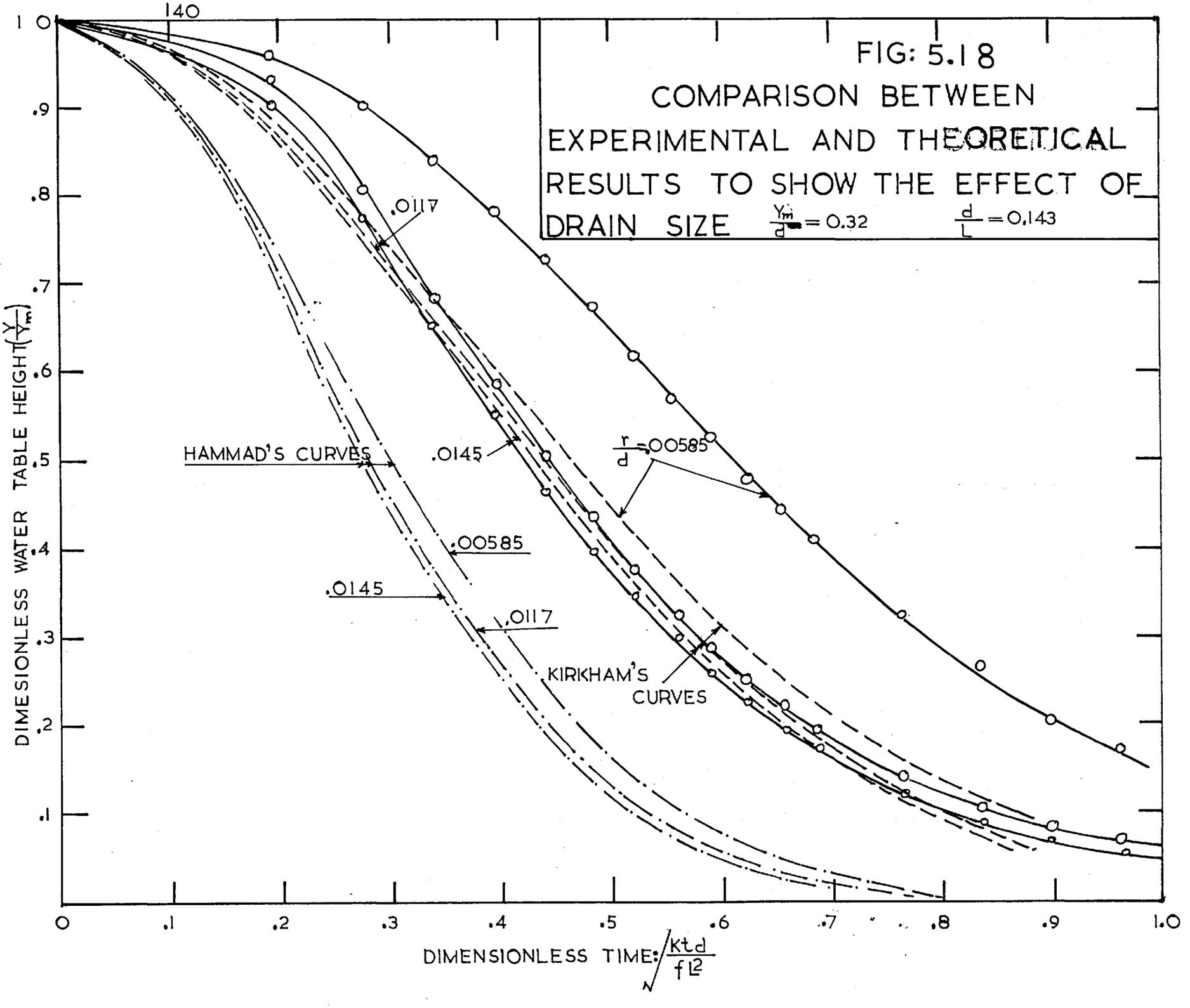

FIG: 5.18
COMPARISON BETWEEN EXPERIMENTAL AND THEORETICAL RESULTS TO SHOW THE EFFECT OF DRAIN SIZE $\frac{Y_m}{d}=0.32$ $\frac{d}{L}=0.143$
DIMESIONLESS WATER TABLE HEIGHT $(\frac{Y}{Y_m})$
DIMENSIONLESS TIME: $\sqrt{\frac{kt\,d}{f\,L^2}}$
1.0
.9
.8
.7
.6
.5
.4
.3
.2
.1
0
.1
.2
.3
.4
.5
.6
.7
.8
.9
1.0
.0117
HAMMAD'S CURVES
.0145
$\frac{r}{d}=.00585$
.00585
.0145
.0117
KIRKHAM'S CURVES

TABLE 5.10

COMPARISON BETWEEN COMPUTED AND EXPERIMENTAL RESULTS

TO SHOW THE EFFECT OF DRAIN SIZE

$d/L = 0.143 \qquad Y_m/d = 0.32$

Experimental		Kirkham		Hammad
Dia: cms.	R/K	$F_1(x,0)$	R/K	R/K
0.50	0.0149	4.292	0.0209	0.0465
1.00	0.0294	3.851	0.0238	0.0525
1.25	0.0340	3.714	0.0242	0.0568

solution. The opposite is, however, true for r/d = 0.00585 because the steady state solution overestimates the value of R/K and hence the rate of drainage.

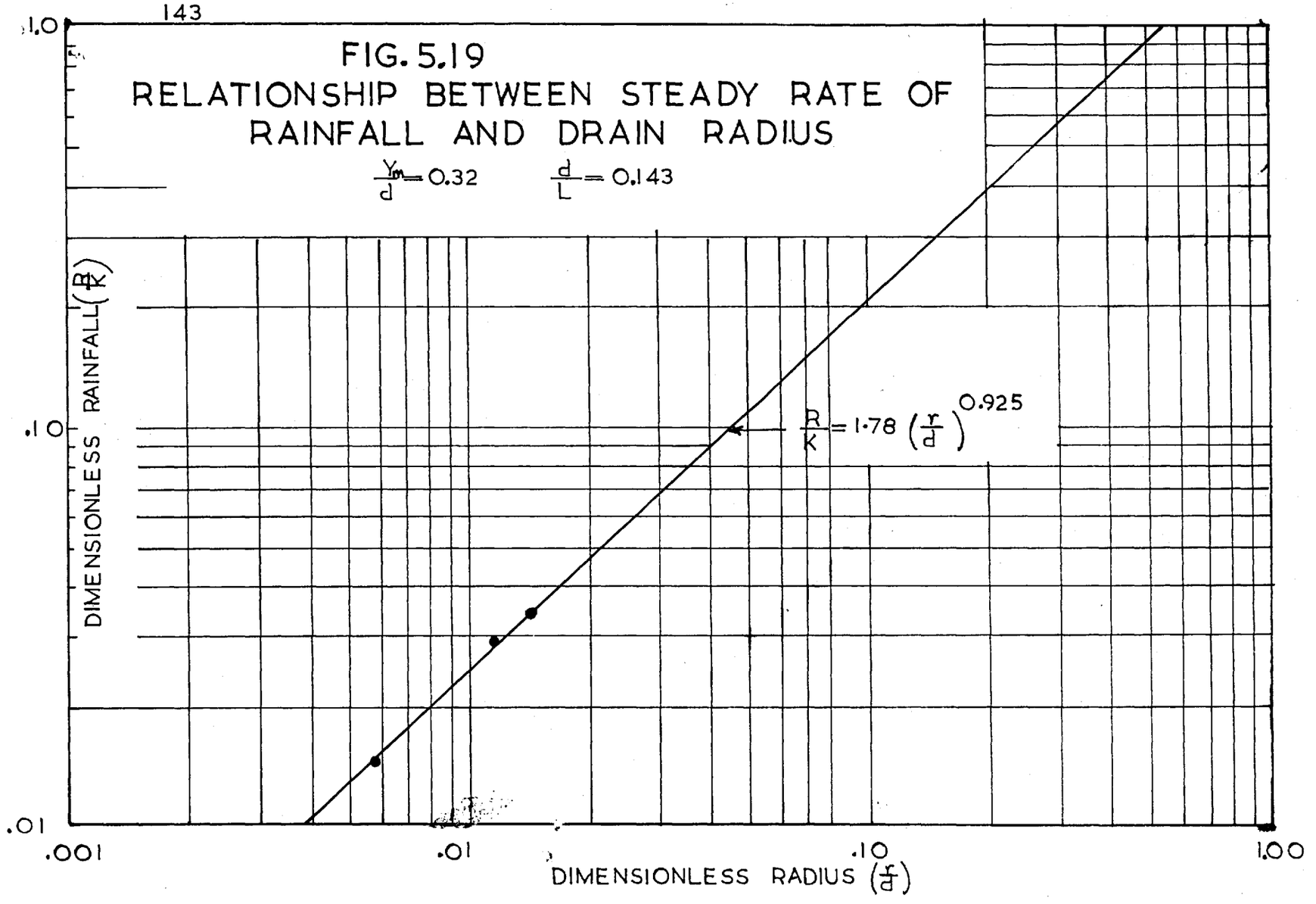
Hammad's theoretical values of R/K in Table 5.10 were obtained by taking Q = RL in equation (3.14) to convert it to the form

$$\frac{K}{R} = \frac{L}{2\pi Y_m} \operatorname{Ln} \frac{Y_m}{r} + \frac{L^2}{2\pi^2 d\, r} \qquad \text{..... (5.26)}$$

K/R in this equation was then calculated by substituting the experimental values of L, d, r and Y_m. The recession index was calculated from equation (4.20). This equation is derived on the same assumptions and is therefore subject to the same drawbacks as those in Kirkham's equation (equation 4.19).

It is clear from Table (5.10) that Hammad's Solution overestimates R/K. Since the theoretical R/K is two to three times higher than its experimental values, the solution predicts a recession index which is considerably lower than the actual one. In fact, there seems to be no resemblance between Hammad's theoretical curves and the corresponding experimental curves in Fig. 5.18.

Finally, it may be of some interest to know the functional relationship between drain size and the rate of steady rainfall required to obtain a given water table height midway between drains. Fig. 5.19 shows a linear logarithmic relationship


FIG. 5.19
RELATIONSHIP BETWEEN STEADY RATE OF RAINFALL AND DRAIN RADIUS
$\frac{Y_m}{d} = 0.32$
$\frac{d}{L} = 0.143$
DIMENSIONLESS RAINFALL $(\frac{R}{K})$
$\frac{R}{K} = 1.78 \left(\frac{r}{d}\right)^{0.925}$
1.0
.10
.01
.001
.01
.10
1.00
DIMENSIONLESS RADIUS $(\frac{r}{d})$

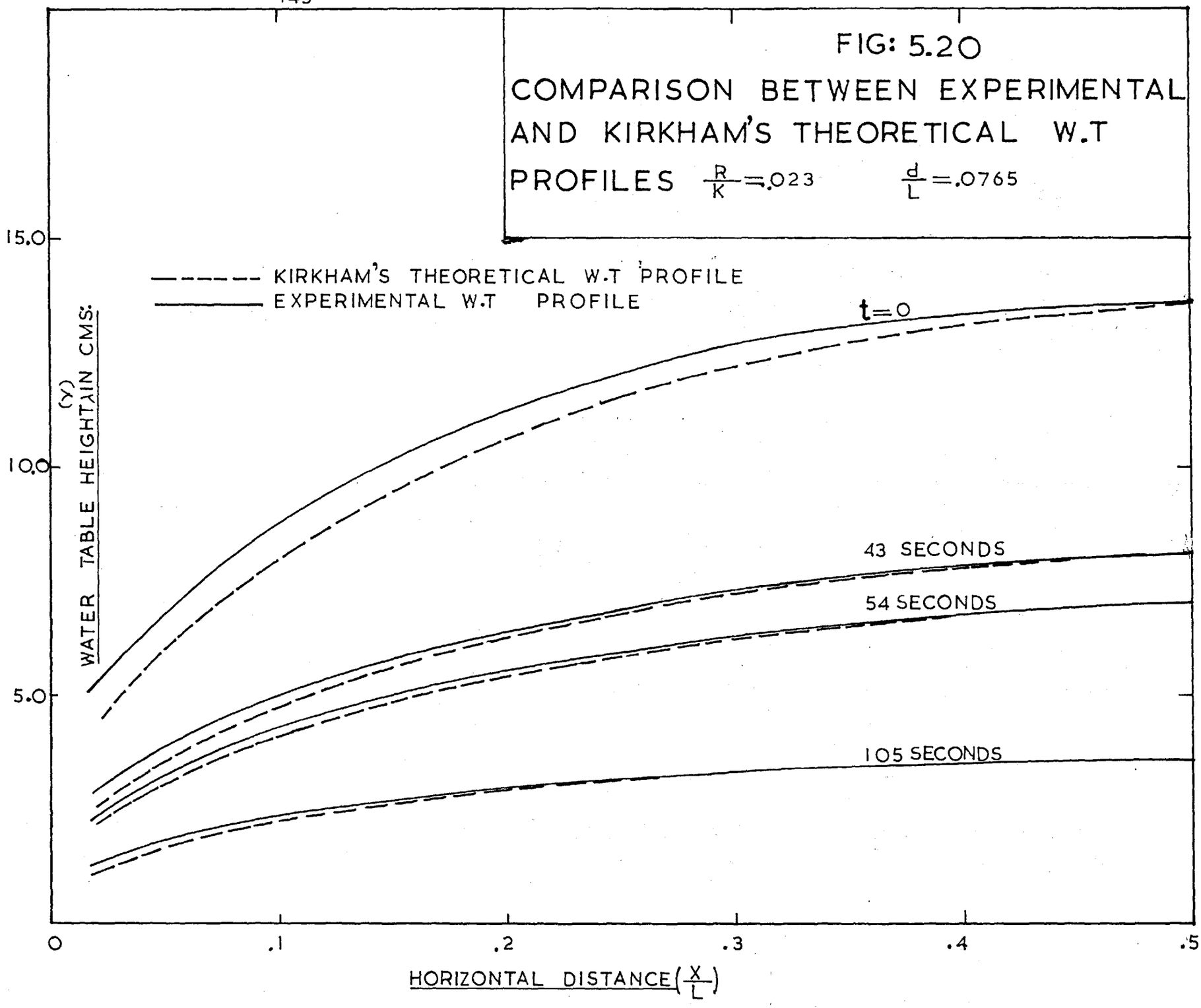
between R/K and r/d. The equation of the straight line is

$$\frac{R}{K} = 1.78 \left(\frac{r}{d}\right)^{0.925} \qquad \text{for } Y_m/d = 0.32, \; d/L = 0.143 \qquad \ldots\ldots\ldots\ldots\ldots\ldots\ldots\ldots \quad (5.27)$$

5.7.1.6 The water table profile

Ligon, Kirkham and Johnson (47) made a comparative study of the rate of drawdown as determined by Kirkham's (21) analytical solution with that observed in a glass bead Glycerol model (47a) of a ditch drainage system. They observed that, except for a short time after the beginning of recession, the experimental and theoretical water table profiles agreed well. The error during the initial stages of recession was found to have occurred near the ditch walls. This was attributed to the neglect of the surface of seepage in the development of the theory.

The present study was carried out to compare the experimental water table profile of a tile drainage system with Kirkham's theoretical water table profile. The experimental and theoretical data are given in Table (5.11) and plotted in Figure 5.20. The theoretical results were computed from equation (3.13) instead of equation (4.19) to see whether the falling water table obtained from the model adjusts itself to the theoretical steady state conditions. The


FIG: 5.20
COMPARISON BETWEEN EXPERIMENTAL AND KIRKHAM'S THEORETICAL W.T PROFILES R/K =.023 d/L =.0765
KIRKHAM'S THEORETICAL W.T PROFILE
EXPERIMENTAL W.T PROFILE
t=0
43 SECONDS
54 SECONDS
105 SECONDS
WATER TABLE HEIGHT IN CMS: (Y)
15.0
10.0
5.0
0
.1
.2
.3
.4
.5
HORIZONTAL DISTANCE (X/L)

theoretical steady state water table profile was obtained by first matching the midpoint water table height at a known time and solving equation (3.13) for R/K for the four curves shown in Fig. 5.20. The values of R/K thus obtained were then used to calculate the water table heights at various horizontal distances from the drain centre.

Except for t = 0, the experimental and theoretical water table profiles agree favourably. A small error in the vicinity of the drain ($2x/L < 0.1$) may be due to the existance of some height of water table over the drain. The results, therefore, indicate that Kirkham's solution can be safely used to find the water table profile between tile drains that are slightly submerged below the water table due to resistance to flow near the drain.

5.7.2 FALLING WATER TABLE BETWEEN SUBMERGED DRAINS

Normally, tile drains project above the outlet channel water level. With such a system one expects a large difference between water table heights midway between and over the drains. This difference turns out to be a disadvantage especially in Peaty soils, as for instance, in Polders in the Nederlands where a rigorous control on water table depth is required. Wesseling (23) reviewed Kirkham's steady state solution and showed that, with the

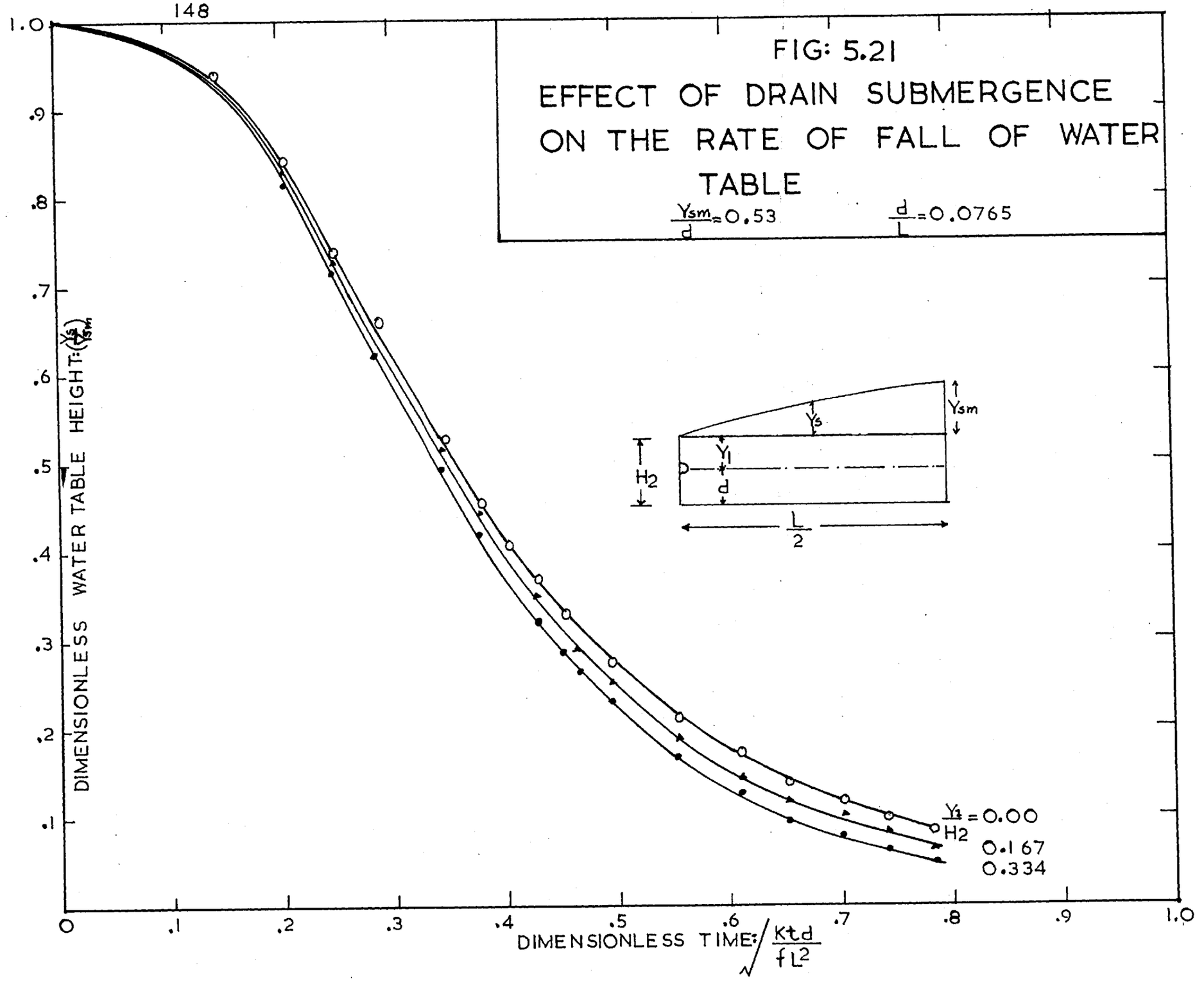
same drain discharge, the above difference can be reduced by laying the drains somewhat deeper and keeping the channel water level above the outlet.

The first experimental study to show the effect of drain submergence on the difference between steady state water table height midway between and over tile drains was carried out by Dujaili (30). He showed that the difference decreased exponentially until it is constant at a submergence ratio equal to 0.70. This implies that for submergence ratio greater than 0.70, the steady state water table rises without change of shape on further increase of the submergence.

The present study was aimed at investigating the effect of drain submergence on the rate of fall of the midpoint water table and to check Kirkham's approximate solution (Section 4.6.2) for unsteady flow between submerged drains. The experiment was conducted by following the procedure described in Sections 5.4 and 5.5. The values of submergence were in the range 0.00 to 0.334.

The model results are illustrated in Fig. 5.21 (Table 5.12). The recession index slightly decreases with drain submergence, although the effect is more pronounced in the latter stages of the recession than in the beginning. Such a small decrease in the recession index does not justify the extra cost involved in laying drains deeper than the normal.

To compare the experimental results with those obtained from


FIG: 5.21
EFFECT OF DRAIN SUBMERGENCE ON THE RATE OF FALL OF WATER TABLE
Ysm/d = 0.53
d/L = 0.0765
DIMENSIONLESS WATER TABLE HEIGHT: Ys/Ysm
DIMENSIONLESS TIME: √(Ktd/fL²)
Ys
Ysm
Y1
H2
d
L/2
Y1/H2 = 0.00
0.167
0.334
1.0
.9
.8
.7
.6
.5
.4
.3
.2
.1
0
.1
.2
.3
.4
.5
.6
.7
.8
.9
1.0

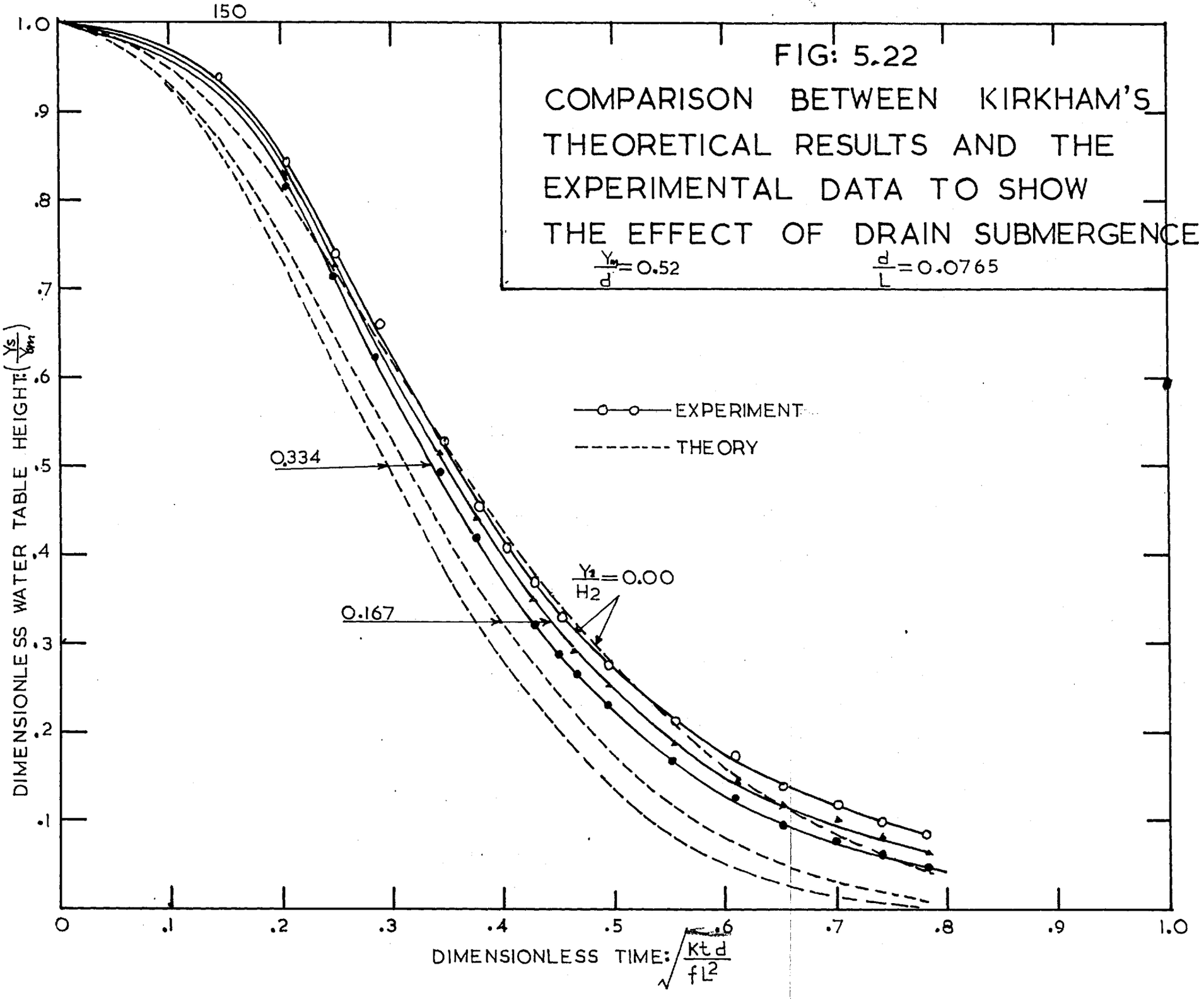
Kirkham's solution (equation 4.19) for submerged drains, the function F(x,0) in equation (4.19) was first determined from equation (3.16) by evaluating the several infinite series involved. This along with the known values of Kt/f, L, Y_m were then substituted in equation (4.19) to get the theoretical heights of the falling water table. The experimental and theoretical results are compared in Fig. 5.22 (Table 5.13).

It is obvious from Fig. 5.22 that there is a considerable difference in recession index between the experimental and theoretical results. This may be due to the ideal assumptions inherent in Kirkham's steady state solution (Section 3.3.3) for submerged drains and in the derivation of equation (4.19). It may be observed that there is a reasonably good agreement between the curves for zero submergence, the reason for which has already been explained in Section 5.7.1.5. A general trend of the effect of submergence on the recession index is indicated by the theoretical curves. They show that the recession index decreases as submergence increases, the rate of decrease diminishing with increasing submergence.

5.7.3 RISING WATER TABLE

5.7.3.1 Effect of rate of rainfall:

This study was conducted for various values of R/K in the

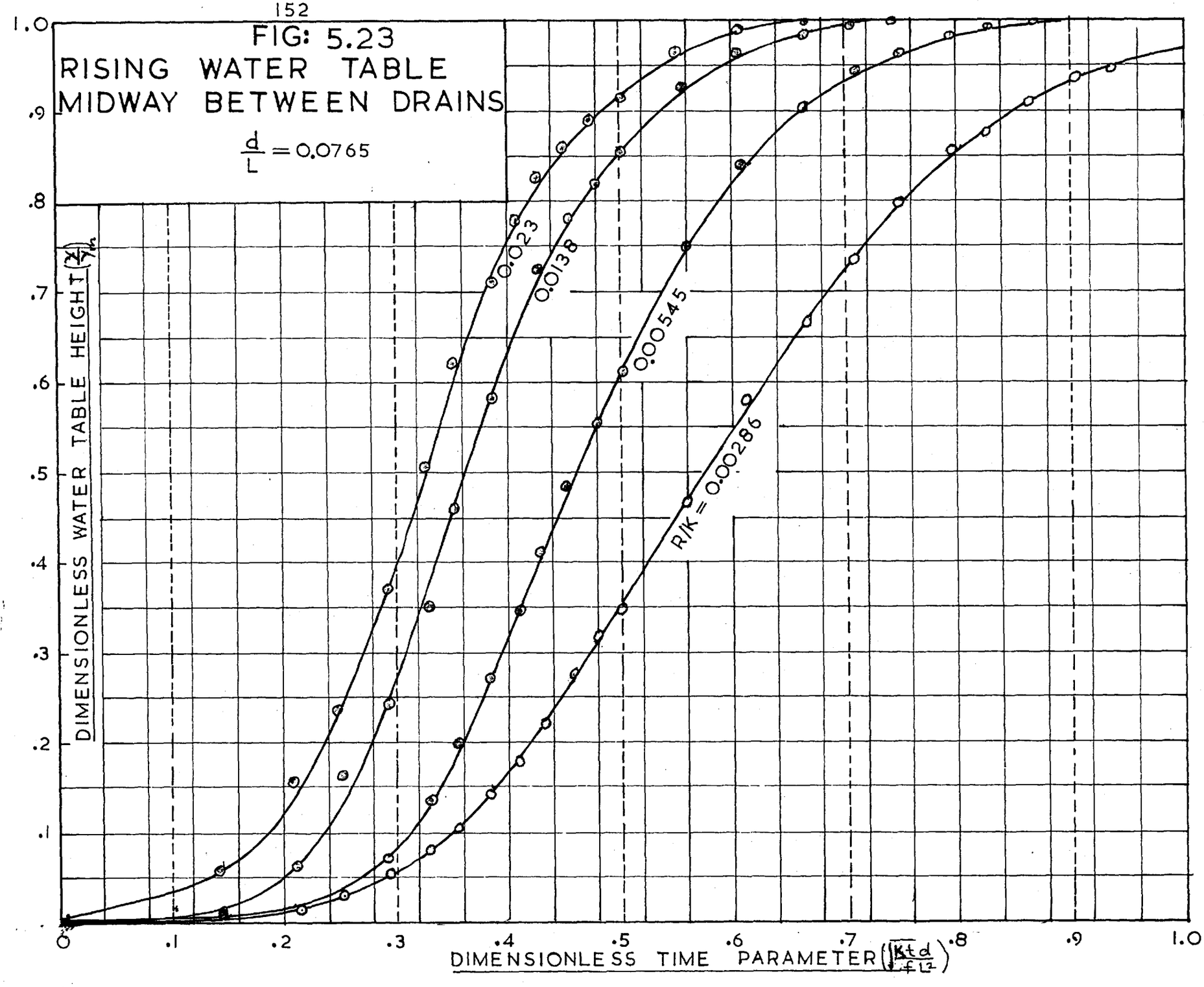

FIG: 5.22
COMPARISON BETWEEN KIRKHAM'S THEORETICAL RESULTS AND THE EXPERIMENTAL DATA TO SHOW THE EFFECT OF DRAIN SUBMERGENCE
$\frac{Y_0}{d}$ = 0.52
$\frac{d}{L}$ = 0.0765
EXPERIMENT
THEORY
0.334
0.167
$\frac{Y_1}{H_2}$ = 0.00
DIMENSIONLESS WATER TABLE HEIGHT: $(\frac{Ys}{Ym})$
DIMENSIONLESS TIME: $\sqrt{\frac{Kt\,d}{fL^2}}$
1.0
.9
.8
.7
.6
.5
.4
.3
.2
.1
0
.1
.2
.3
.4
.5
.6
.7
.8
.9
1.0

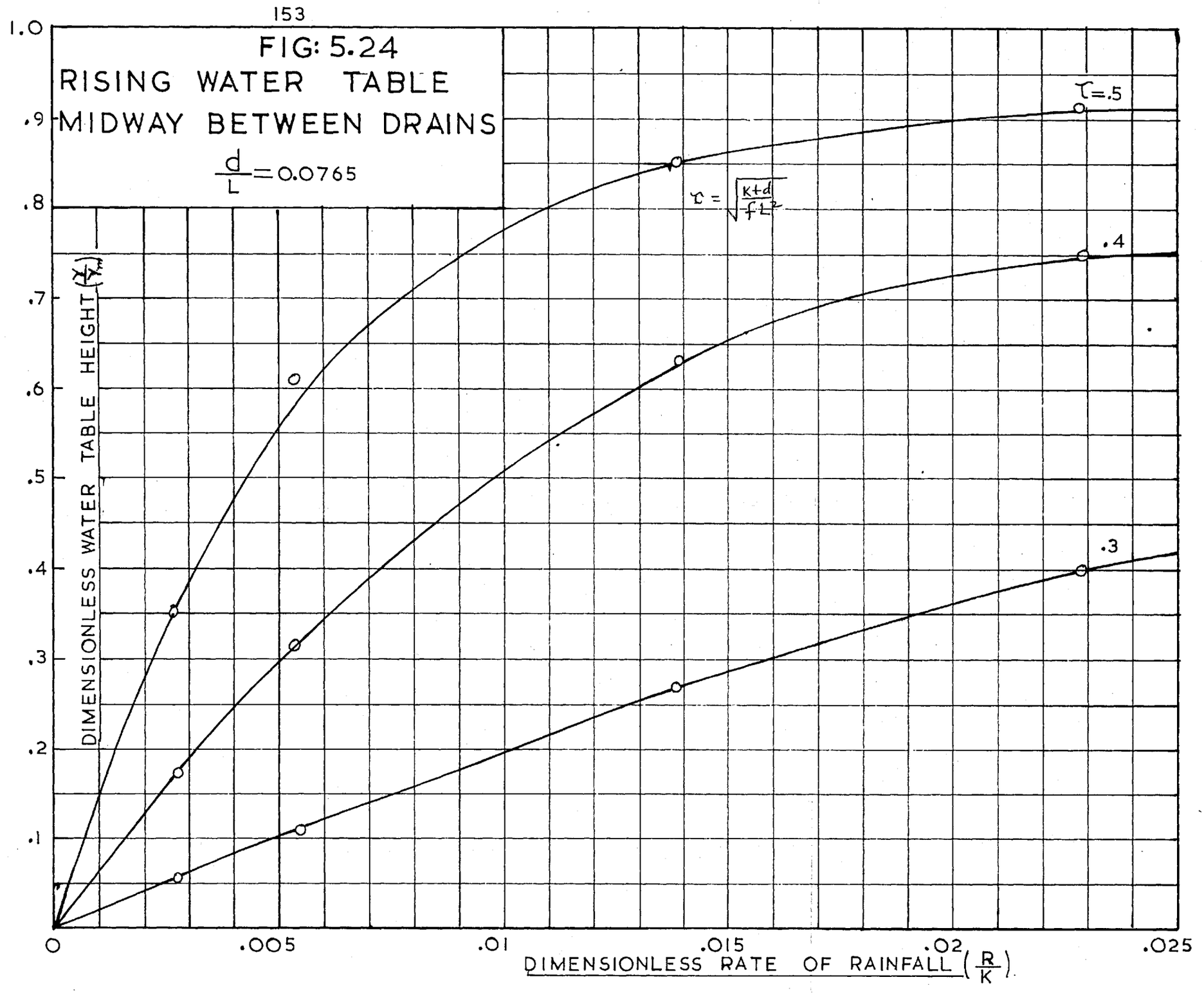
range 0.00286 to 0.023. During the experiment r/d and d/L were kept constant at 0.00136 and 0.0765 respectively. The rise of only the midpoint water table was observed.

The experimental results for various values of R/K are illustrated in Fig. 5.23 (Table 5.14). It is clear in the figure that Y/Y_m, for a fixed value of $\sqrt{Ktd/fL^2}$, increases but at progressively lower rates as R/K increases. This is shown more clearly in Fig. 5.24, which indicates the relationship between the dimensionless rate of rainfall R/K and the dimensionless water table height Y/Y_m at a particular value of the time parameter $\sqrt{Ktd/fL^2}$ after the water table starts rising. The rate of rainfall has appreciable effect on the rising water table when R/K is low (≤ 0.01). This effect, however, gradually diminishes. At $R/K \geq 0.025$, Y/Y_m, for fixed $\sqrt{Ktd/fL^2}$, is practically unaffected by the rate of rainfall, especially for large $\sqrt{Ktd/fL^2}$.

The experimental data for the rising water table and water table drawdown $Y_m - Y$, for the same steady rainfall, are plotted in Fig. 5.25. The dotted lines are the drawdown curves and the full lines represent the rising water table. The curves show that the water table drawdown is quicker for low values of $\sqrt{Ktd/fL^2}$ and slower for higher values of $\sqrt{Ktd/fL^2}$ than for the rising situation.

The model results in Table 5.15 indicate that the rising


FIG: 5.23
RISING WATER TABLE
MIDWAY BETWEEN DRAINS
d/L = 0.0765
R/K = 0.023
0.0138
0.00545
0.00286
DIMENSIONLESS WATER TABLE HEIGHT (Y/Y_m)
DIMENSIONLESS TIME PARAMETER (√(Kt d / f L²))
0
.1
.2
.3
.4
.5
.6
.7
.8
.9
1.0


FIG: 5.24
RISING WATER TABLE
MIDWAY BETWEEN DRAINS
d/L = 0.0765
τ = √((K+d)/(f L²))
τ=.5
.4
.3
DIMENSIONLESS WATER TABLE HEIGHT (Y/Y_m)
DIMENSIONLESS RATE OF RAINFALL (R/K)
1.0
.9
.8
.7
.6
.5
.4
.3
.2
.1
0
.005
.01
.015
.02
.025

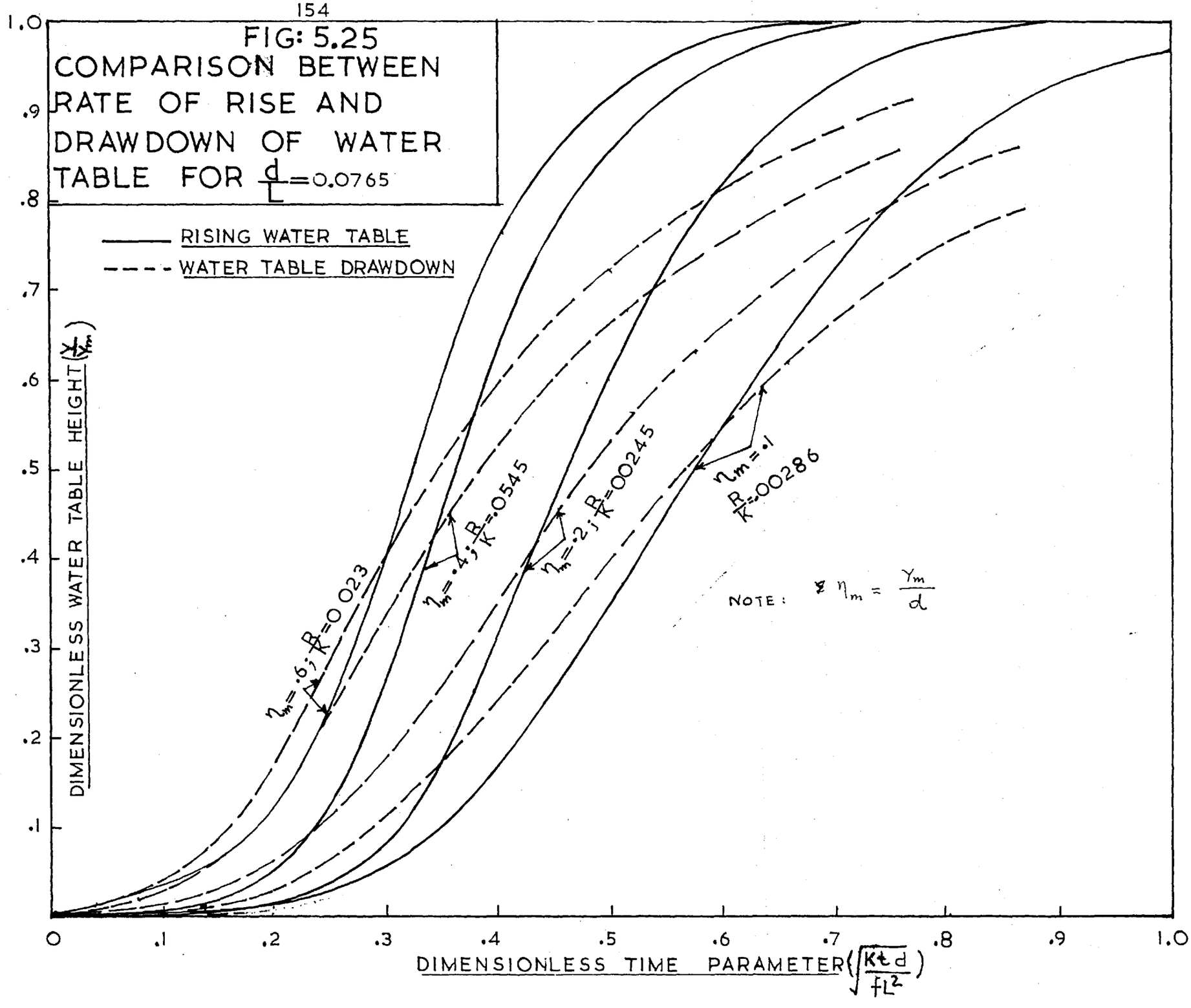

FIG: 5.25
COMPARISON BETWEEN RATE OF RISE AND DRAWDOWN OF WATER TABLE FOR d/L=0.0765
RISING WATER TABLE
WATER TABLE DRAWDOWN
DIMENSIONLESS WATER TABLE HEIGHT (Y/Ym)
DIMENSIONLESS TIME PARAMETER (√(Kt d / fL²))
ηm=.6; R/K=0.023
ηm=.4; R/K=0.0545
ηm=.2; R/K=00245
ηm=.1 R/K=00286
NOTE: ηm = Ym/d
0
.1
.2
.3
.4
.5
.6
.7
.8
.9
1.0

TABLE 5.15

COMPARISON BETWEEN RATE OF RISE AND FALL OF WATER TABLE

$R/K = 0.023$ $d/L = 0.0765$

Time secs	Rising Y(cms)	Drawdown $Y_m - Y$ (cms)
0	0.00	0.00
10	0.85	0.75
20	1.45	2.00
30	3.25	3.60
40	5.00	4.85
50	6.90	5.90
60	8.50	6.90
70	9.70	7.60
80	10.60	8.35
90	11.25	8.95
100	11.85	9.50
110	12.20	9.90
120	12.55	10.28
150	13.20	11.10
180	13.55	11.70
210	13.65	12.15
240	13.70	12.45
270	13.70	12.78

water table takes approximately 90% as much time to reach a steady state condition as the falling water table takes to reach the drain centre. This is in contrast to the common assumption made in drainage design that the water table rises to a steady state condition instantaneously.

5.7.3.2 Effect of depth of impermeable bed:

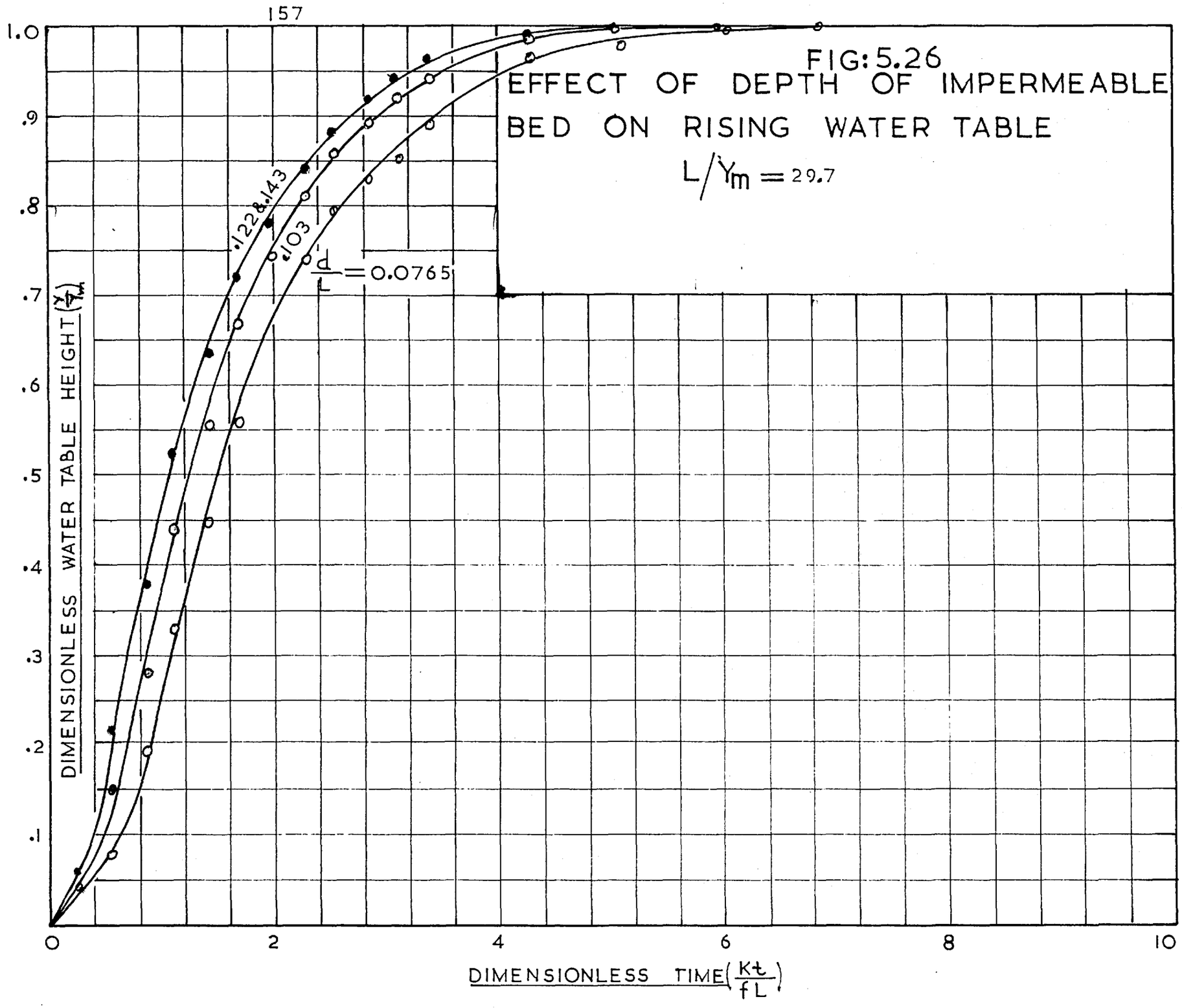
This study was based on the same experimental procedure and the same values of r/d and Y_m/L were used as described in Section 5.7.1.4.

Fig. 5.26 (Table 5.16) shows the effect of the depth of the impermeable bed on the rising water table. It is clear from the figure that the rising water table does not depend on the depth of impermeable bed when $d/L \geq 0.123$. The same conclusion was previously deduced for the falling water table.

5.8 EFFECT OF MISALIGNMENT OF TILE DRAINS ON FALLING WATER TABLE.

5.8.1 Introduction

Analytical tile drainage solutions that have been published so far usually deal with flow through homogeneous isotropic soil between equidistant tile drains lying at the same elevation below the ground surface (symmetrical drainage system). In practice, the depth of drains below the ground surface is governed by the


FIG: 5.26
EFFECT OF DEPTH OF IMPERMEABLE BED ON RISING WATER TABLE
$L/Y_m = 29.7$
.122&.143
.103
$\frac{d}{L} = 0.0765$
DIMENSIONLESS WATER TABLE HEIGHT $(\frac{Y}{Y_m})$
DIMENSIONLESS TIME $(\frac{Kt}{fL})$
1.0
.9
.8
.7
.6
.5
.4
.3
.2
.1
0
2
4
6
8
10

type of crop and the soil conditions. The depth should be such that, after irrigation or rainfall, sufficient water is drained from the root zone to provide storage space for the excess water from the following irrigation or rainfall without exceeding allowable water table heights. The storage space can be maintained evenly distributed in even terrains by laying the drains at the same depth below the ground surface. This requirement, however, can hardly be achieved in rough terrains, where, if the drains are symmetrically aligned, the roots of crops on low ground will remain flooded for most of the time. To guard against such flooding, the drains situated below low grounds are displaced vertically. The amount of displacement is mainly controlled by the requirement of minimum storage space above the displaced drains.

Vertical displacement may also prove useful in arid irrigated areas where a soil condition of high salinity occurs in conjunction with a drainage problem. In these areas, the land is first drained with tile drains to a depth of 2 to 3 metres and then salts are removed from the soil by leaching with large quantities of irrigation water. Kirkham (65) proved analytically that most of the flow of water through the soil to the tile drain occurs above the drains whereas the soil midway between the drains remains unaffected by the leaching process because of very low

horizontal velocity of flow at this point.

Greater leaching can be obtained in the central area between tile drains by displacing vertically downwards, say, one out of every three or four drains in a symmetrical drainage system. The vertical displacement of a drain causes a change in its potential relative to the potential of other drains. There will be an immediate drop of water table over the displaced drain, thus increasing the slope of the water table. This will be associated with an increase in the horizontal velocity of flow and, consequently, a faster rate of fall of water table than in the symmetrical drainage system.

5.8.2 The problem

An experimental study of the effect of misalignment of a tile drain on the steady state flow system was carried out by Dujaili (30). There does not seem to be any published work on the unsteady state. The purpose of the present investigation was, therefore, to observe to what extent the vertical displacement of a tile drain affects the recession index at a critical point. The critical point is defined herein as the highest point on the water table in the misaligned drainage system. This point in the present study was the left-hand edge (the edge far away from the displaced drain) of the model. However, water table recession at the right-hand edge (the edge near to the displaced drain) was

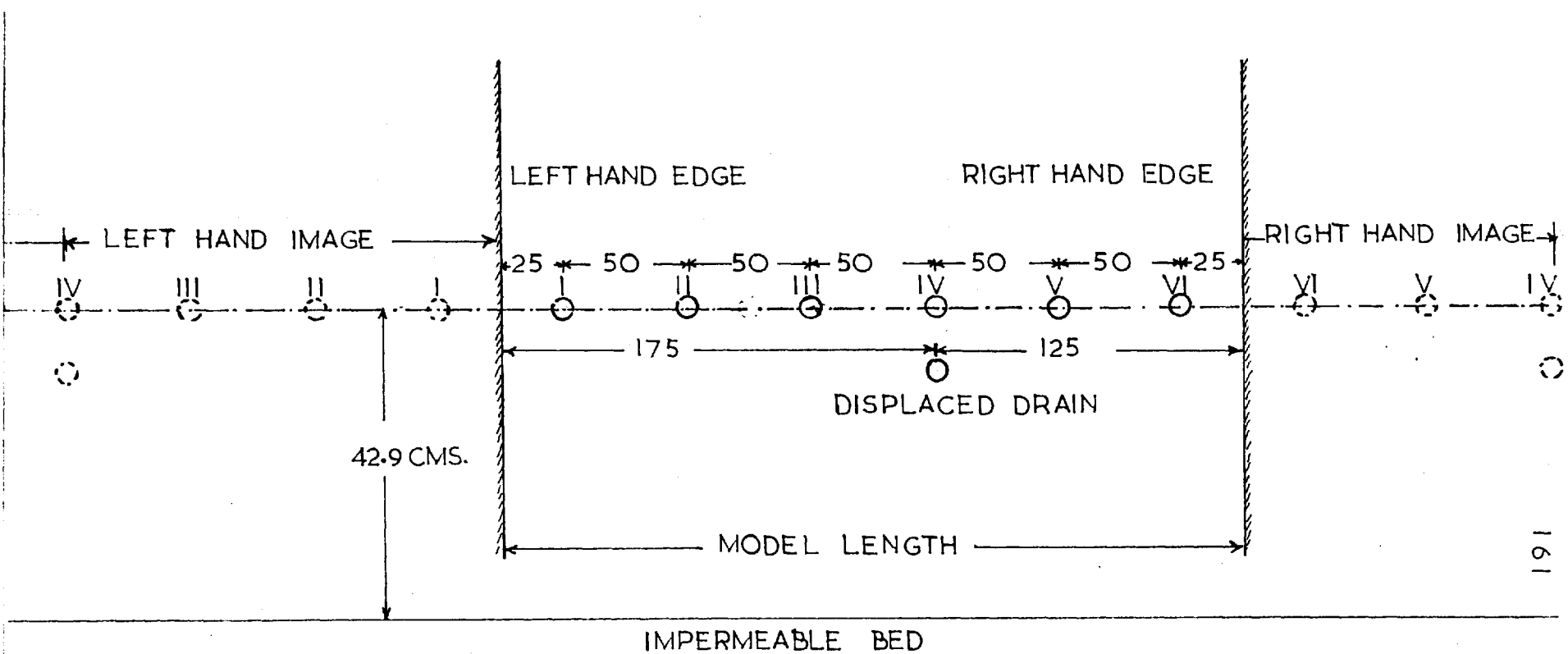
also observed and compared with the fall at the left-hand edge. All water table heights were measured above the impermeable bed.

5.8.3. Experimental procedure

In the present Hele-Shaw model, provision existed for two drain spacing arrangements, either at 0.50 m or at 1.0 m, with 0.5 or 1.0 cms drain diameters. Six drains were required in the first arrangement and three in the second to cover the whole length (300 cms) of the model. The first spacing arrangement was adopted. In this arrangement, the second row of drains (Fig: 5.4) at elevation 42.90 cms. above the impermeable bed was used. The misaligned drainage system is shown in Fig. 5.27 in which drain IV was displaced. The left-hand edge of the model is at a distance of 175 cms from the displaced drain and the right-hand edge at 125 cms.

Since the edge boundaries of the model represent a mirror plane, drains I, II, III and IV in Fig. 5.27 have their images on the other side of the left-hand edge plane. Thus the situation represents seven spacings with eight drains of which the two end drains, drain IV and its image, are displaced downward. The corresponding situation on the right-hand side consists of five spacings with six drains, of which drain IV and its image are displaced. The whole misaligned drainage system thus represents an infinite number of drains of which every 7th and 5th drain are

FIG: 5.27
MISALIGNED DRAINAGE SYSTEM



alternately displaced. Other drains in the system will hereafter be called "symmetrical drains".

The edge boundaries in the model represented planes of symmetry of flow in the misaligned drainage system. The rate of fall of water table at both the edges was recorded.

The general experimental procedure was the same as described in Section 5.4. The experiment was first conducted on a symmetrical drainage system (no displacement) and the initial steady state water table height above the impermeable bed was noted at the left-hand edge of the model. The rainfall was stopped and the rate of fall of water table at the same edge was recorded. Drain IV was then displaced successively by 7, 11.7, 16.4 and 21% of the depth of the impermeable bed below the symmetrical drains ($\Delta Y/d$) and each time the rate of rainfall was adjusted to obtain the same initial steady state water table height. In each case the rate of fall of the water table at the left-hand edge of the model was recorded. Water table recession at the right-hand edge was also observed for displacements of 7% and 21%. The initial steady state water table height above the impermeable bed was 46.60 cms in all runs, thus giving $h_m/d = 1.08$.

5.8.4 Analysis of results: Drain running under some back pressure due to resistance to flow near the drain.

The dimensionless functional relationship between the variables

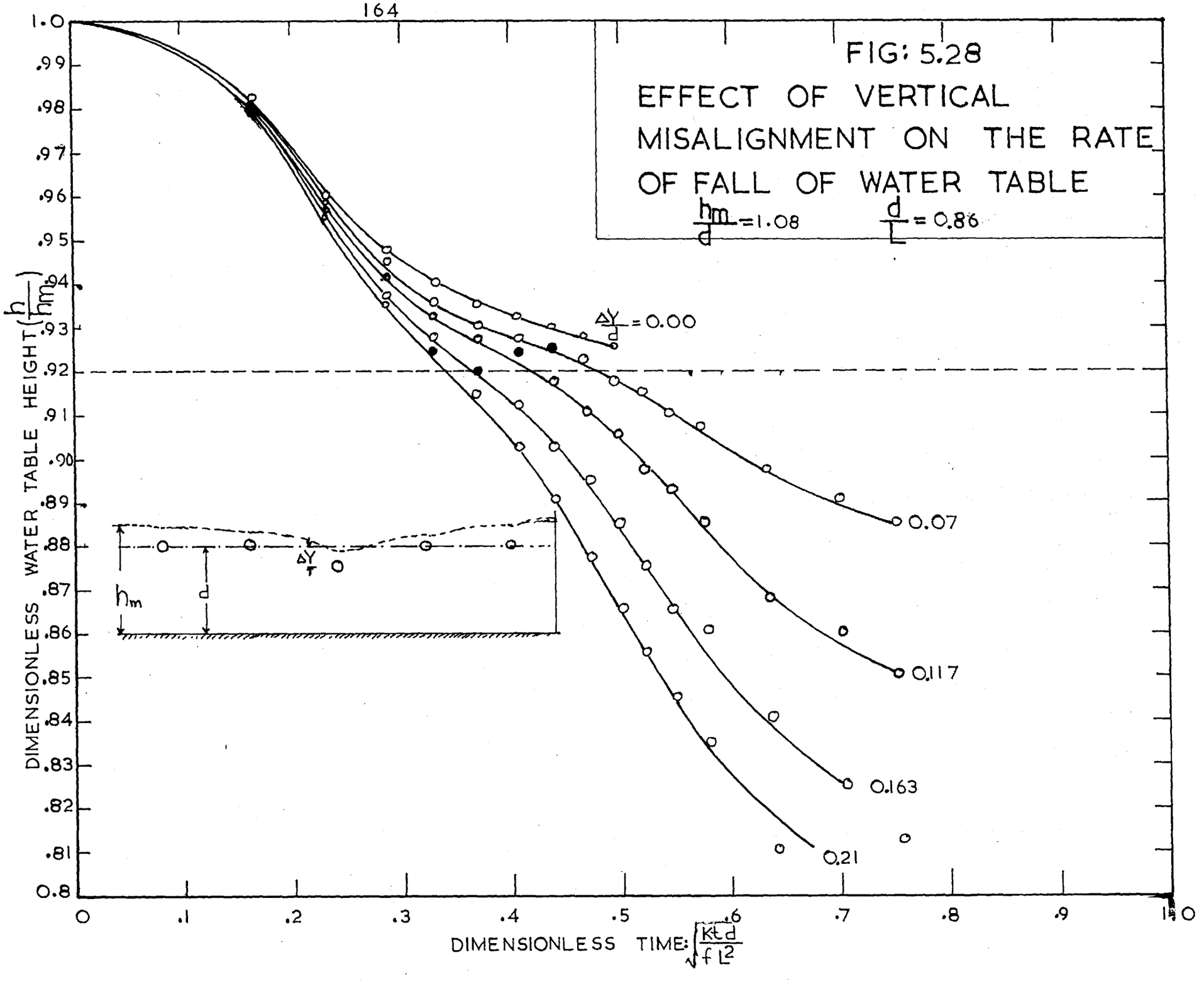
involved can be easily shown to be of the form (Fig. 1.2)

$$\frac{h}{h_m} = F\left(\frac{h_m}{d}, \frac{d}{L}, \frac{\Delta Y}{d}, \sqrt{\frac{Ktd}{fL^2}}\right) \quad \ldots\ldots\ldots\ldots\ldots \quad (5.27)$$

In the experimental programme, h_m/d and d/L were kept constant and a relationship between h/h_m and $\Delta Y/d$, for various values of $\sqrt{Ktd/fL^2}$, was observed.

The model results are shown in Fig. 5.28 (Table 5.17). It is obvious that the recession index (h/h_m) increases with decreasing displacement. It takes a $\sqrt{Ktd/fL^2}$ value of 0.35 for the water table to reach the level of the centre of the symmetrical drains in the case of a 21% displacement as compared with a value of 0.60 for zero displacement. Since the increase in the rate of water table recession is associated with the increase in horizontal velocity of flow, the velocity at the left-hand edge must increase with the amount of displacement. The increased velocity would not only let the water table drop to a desired level in a shorter time, but also increase the leaching process, which otherwise would be slow.

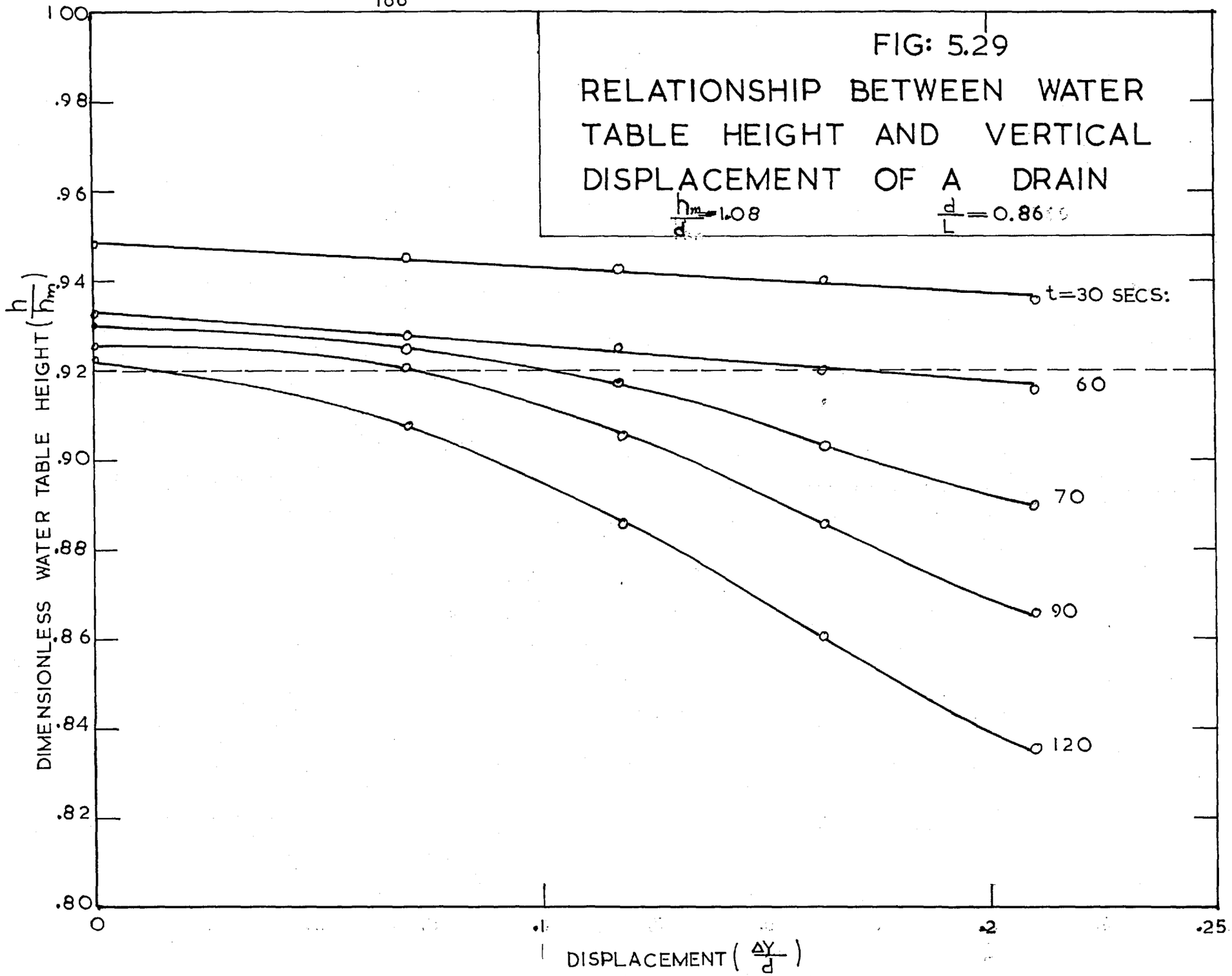
Another noticeable feature in Fig. 5.28 is the change in the recession index as the water table falls below the level of the symmetrical drains (shown by dotted horizontal line). At this stage, the spacing is increased to 350 cms on the left-hand side of the displaced drain and 250 cms on the right. The recession index below the dotted line would therefore, depend on


FIG: 5.28
EFFECT OF VERTICAL MISALIGNMENT ON THE RATE OF FALL OF WATER TABLE
hm/d = 1.08
d/L = 0.86
DIMENSIONLESS WATER TABLE HEIGHT (h/hm)
DIMENSIONLESS TIME: √(Kt d / f L²)
ΔY/d = 0.00
0.07
0.117
0.163
0.21
ΔY
hm
d
1.0
.99
.98
.97
.96
.95
.94
.93
.92
.91
.90
.89
.88
.87
.86
.85
.84
.83
.82
.81
0.8
0
.1
.2
.3
.4
.5
.6
.7
.8
.9
1.0

the combined effect of vertical displacement and the increased spacing. Since the spacing is constant during this stage, the greater the displacement the lower is the recession index (i.e. the higher the drop of water table in a given time).

A relationship between water table height and vertical displacement, for a particular time parameter, is shown in Fig. 5.29. The curves indicate that up to 60 secs ($\sqrt{Ktd/fL^2} = 0.351$) after the beginning of recession, the midpoint water table height is linearly related with the displacement. For times longer than this, however, the water table drop is relatively faster compared with the increase in displacement. Since the curves for t = 30 secs and t = 60 secs are parallel straight lines, the drop in water table height in this interval is constant irrespective of the amount of vertical displacement. This shows that the rate of recession at the left-hand edge is affected by the symmetrical drains for the first 60 secs.

Values of the recession index at the left and right-hand edges of the model are compared in Fig. 5.30 (Table 5.18). Since the right-hand edge is nearer to the displaced drain, the water table falls considerably faster there in comparison with the left-hand edge, thus showing that the leaching process can be accelerated by displacing every 5th drain instead of every 7th drain discussed previously.


FIG: 5.29
RELATIONSHIP BETWEEN WATER TABLE HEIGHT AND VERTICAL DISPLACEMENT OF A DRAIN
$\frac{h_m}{d}$ = 1.08
$\frac{d}{L}$ = 0.86
t=30 SECS:
60
70
90
120
DIMENSIONLESS WATER TABLE HEIGHT $(\frac{h}{h_m})$
DISPLACEMENT $(\frac{\Delta Y}{d})$
1.00
.98
.96
.94
.92
.90
.88
.86
.84
.82
.80
0
.1
.2
.25

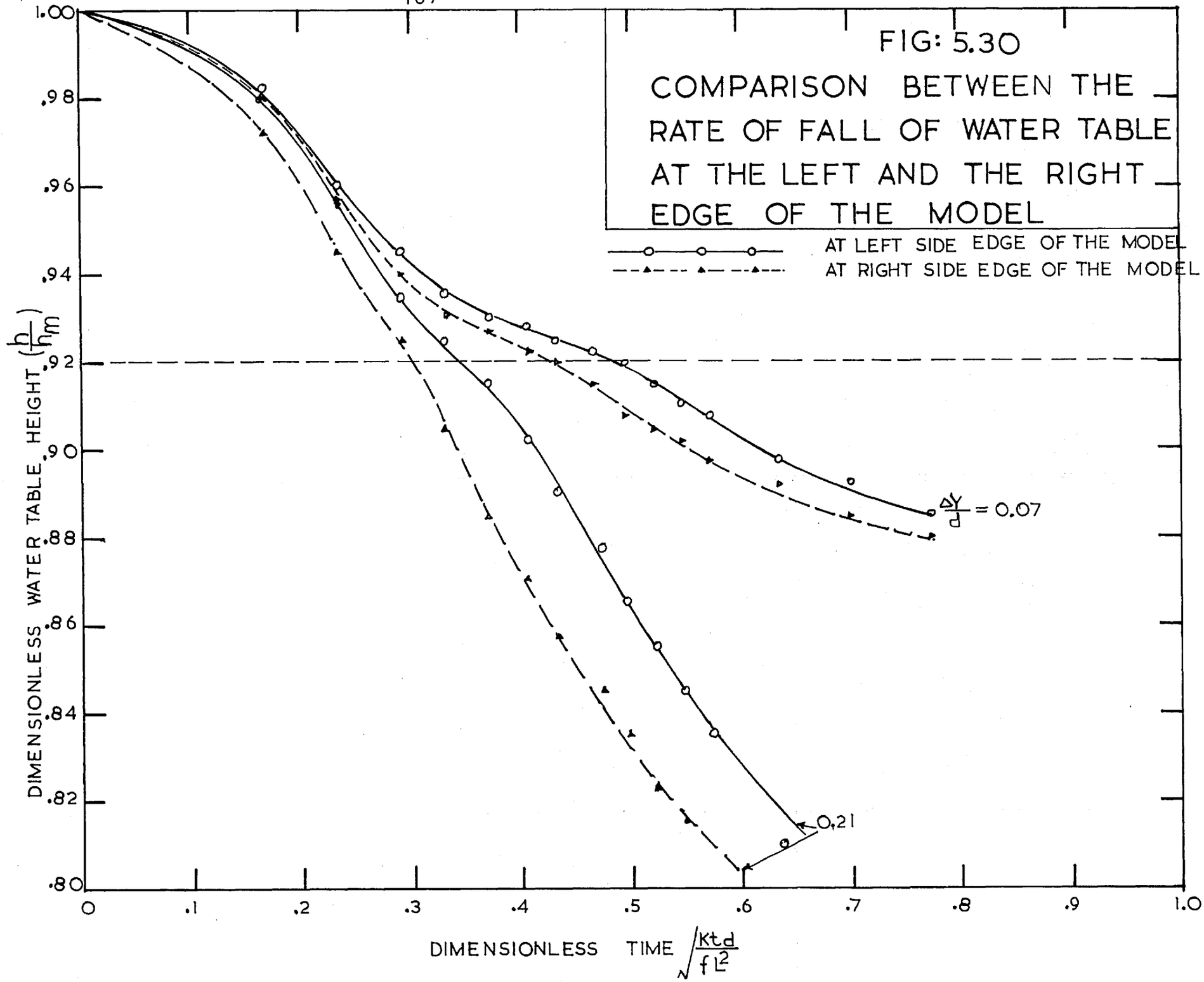


FIG: 5.30

COMPARISON BETWEEN THE RATE OF FALL OF WATER TABLE AT THE LEFT AND THE RIGHT EDGE OF THE MODEL

CHAPTER 6

DRAINAGE OVER A SLOPING IMPERMEABLE BED

This Chapter gives a detailed description of drainage problems over a moderately sloping impermeable bed (slope $\leq$ 10%). Some of the existing experimental and analytical solutions for the steady and unsteady state drainage are first reviewed. A new analytical solution based on the method of Laplace transforms is then obtained for the steady and unsteady drainage of a sloping land with vertical impermeable boundaries at the upstream and downstream sides. The solution is only an approximation to the experimental set up and holds when tile drains lie near the impermeable bed, i.e. for small d/L, a numerical limit of which has not been defined in the literature. In this study, however, a good fit between the experimental and analytical results indicates that $d/L = 0.23$ could be considered to fulfil the assumption made in the solution.

6.1 INTRODUCTION

Chapter 5 discussed drainage problems the solution to which can be grouped into two broad classes: symmetrical drainage systems, where a relatively high water table over flat areas is relieved by a network of equally spaced tile drains, and systems in which one out of a number of equally spaced tile drains is

misaligned vertically.

Many of the drainage problems encountered in practice may not fit into either of the above categories. For example, problems may arise in the drainage of sloping lands along the foothills of a mountain range. Such problems have received comparatively little attention both analytically and experimentally.

A simple problem of drainage of sloping lands is the one in which excess irrigation water from lands at higher elevations or seepage water from irrigation canals may move down the slope along sloping strata to ground at lower elevations. There is no percolation directly over the region of interest. In such cases, the down-slope flowing water is best removed by a system of interceptor tile drains (Fig. 6.1).

A more complex problem of drainage of sloping lands arises due to vertical recharge from rainfall or irrigation at the ground surface directly over the region of interest. In such a case, a continuous saturated condition of the aquifer is prevented by laying a number of symmetrically spaced tile drains (Fig. 6.2). This particular problem of sloping drainage is examined below.

The aquifer may be infinite or it may belong to any one of the following categories:

(a) semi-infinite aquifer with an impermeable boundary at the upstream side;

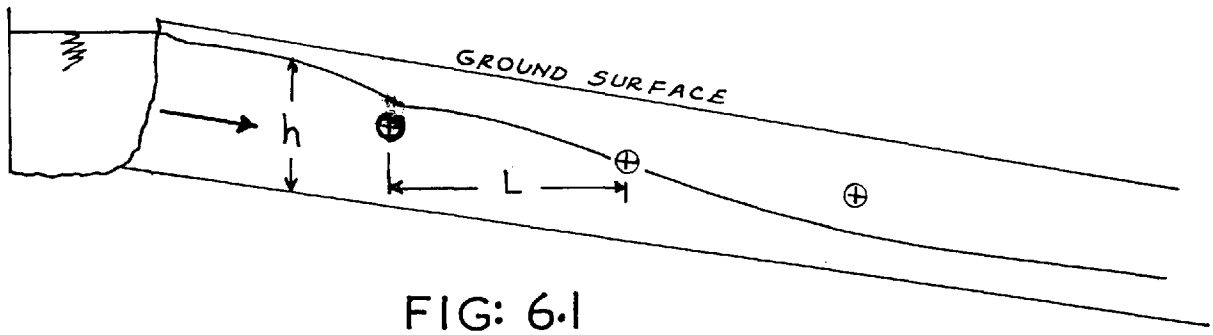


FIG: 6.1

INTERCEPTOR DRAINS
(NO VERTICAL RECHARGE)

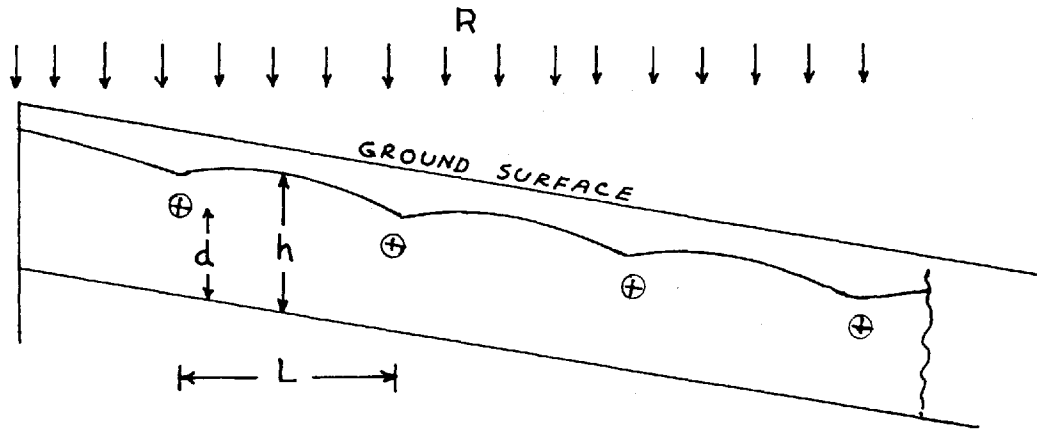


FIG: 6.2

SLOPING DRAINAGE SYSTEM WITH VERTICAL RECHARGE

(b) semi-infinite aquifer with an impermeable boundary at the downstream side;

(c) ~~semi-infinite~~ finite aquifer with vertical impermeable boundaries both at the upstream and downstream sides.

These problems of drainage of sloping lands are more difficult to solve than those of a symmetrical drainage system. Because of unsymmetrical boundary conditions in the former, a separate analysis for the zone between each pair of drains has to be made. For example, in the category C there will be separate analyses for zones adjacent to the impermeable boundaries and for those remote from these boundaries.

6.2 REVIEW

Flow nets for interceptor drains were determined with electric analogue by Childs (1). The investigations showed that, if the drains are placed above the impermeable bed, some water may seep downslope along the impermeable bed under the drains as indicated at the right-hand end of Fig. 6.1. Interceptor drains placed near the impermeable bed were found to be more effective in intercepting the downslope flow than those placed at some distance above it. Childs also carried out an experimental study comparing the efficiency of tile and ditch drains in intercepting downslope flow at different bed slopes. The tile and ditch drains went to the same depths. He observed that the efficiency of either type of

drain depended on the slope of the bed. On a slope of up to 1:30, both types of drains were found to be equally effective. However, when the slope increased to 1:3, the tile drain was observed to be less effective than the ditch drain.

The solutions of the problems arising due to vertical recharge have to be based on a knowledge of the groundwater flow pattern between drains. Gustaffson (66) first presented flow nets for the ponded water condition over equally spaced tile drains in an infinite aquifer overlying a sloping impermeable bed. The drains were considered to discharge freely under atmospheric pressure by applying a certain amount of suction. For such a case, the flow nets showed that the discharge of each drain was equal to R·spacing.

A steady state drainage problem due to vertical recharge was also solved by Schmid and Luthin (67). They developed a mathematical solution for the steady state drainage between equally spaced ditches penetrating to the impermeable bed of an infinite aquifer. In order to simplify the problem, they assumed that the ditches were empty at all times, thus implying that the water was carried off as soon as it seeped into the ditches. Their solution was based on the Boussinesq equation for steady flow over a sloping impermeable bed. The Dupuit assumptions inherent in the solution led to errors which were later checked by an experimental study (68) on a Hele-Shaw model.

The experimental results indicated that the error due to the Dupuit assumptions was small for slopes less than 30%. For slopes greater than this and for higher values of R/K the solution was found to give ditch spacings that were too high. The error was attributed to the omission of the surface of seepage in the analytical treatment of the problem.

The unsteady flow between the open ditches discussed above was first analysed by Luthin and Guitjens (69). They noted the maximum height of the water table with respect to time and showed that the fall of water table in a given time was independent of the bed slope for slopes up to 30%. This indicated that for these slopes any of the unsteady symmetrical drainage solutions could give as good an estimate of the rate of fall of water table over a sloping bed as that for a horizontal bed.

Chauhan, Schwab and Hamdy (70) obtained computer solutions of transient water tables for drainage of sloping land by fully penetrating ditches. Assuming that the water table was initially parallel to the sloping impermeable bed, they analysed the falling water table for zero and time-variable boundary conditions at the ditch drains. Their main conclusion based on comparison between analytical and experimental results was that the time-variable boundary conditions give better solutions than the

zero boundary conditions.

6.3 STATEMENT OF THE PRESENT PROBLEM

The most common drainage problem of a sloping land arising due to vertical recharge is the one in which the land is effectively semi-infinite and is drained either by fully penetrating ditches with the free surface some distance above the bed, or by tile drains located at some distance above the impermeable bed. In each case a solution based on a steady state initial water table profile and on time-variable boundary conditions at the ditches seem closer to natural conditions than those assumed in the solutions reviewed in the previous Section.

Since it is difficult to represent a true semi-infinite system in a finite laboratory model, the present investigation was related to a finite system in which the upstream and downstream boundaries were impermeable (Section 1.5.2). The system (Fig. 6.3a) consisted of three drains located 22.90 cm. above the impermeable bed and spaced 100 cm apart. This sytem was adopted not because it was of great practical significance, but because it allowed a comparison of a technique of analysis (Sections 6.4.2 & 6.4.3) with reasonably accurate experimental data. An approximate analytical solution for the steady and unsteady drainage between fully penetrating ditch drains is obtained. Although this solution is only an approximate representation of the present experimental set up of a tile drainage problem, the analytical and

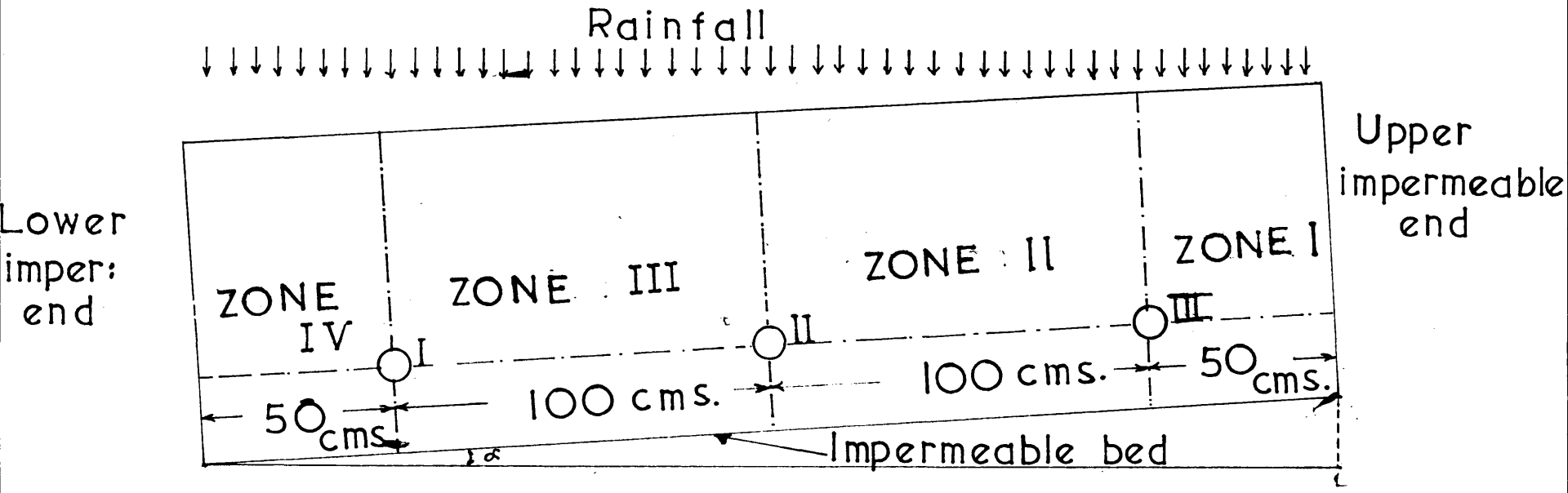


FIG: 6.3a

GENERAL LAYOUT OF INCLINED MODEL

experimental results are compared to find the magnitude of their difference resulting from this approximation.

The study was carried out with two objectives in view. The first objective was to determine analytically the steady state water table profiles over fully penetrating ditches for various values of bed slope and R/K. The second objective was to study the falling water table at the point where the steady state water table height was maximum. In both cases the analytical results are compared with the experimental results for tile drains lying near the impermeable bed.

6.4 MATHEMATICAL ANALYSIS

6.4.1 General

Werner (71) gave a mathematical treatment of some general problems of unconfined groundwater flow over a moderately sloping impermeable bed by solving equation (2.24). He dealt with two cases. The first referred to the flow between two reservoirs penetrating to the bed (Fig. 6.4) and the second to the flow between a water divide and such a reservoir (Fig. 6.5). In the first case, he considered both the downslope flow that would occur from the upper reservoir to the lower one and the vertical recharge from the ground surface.

Werner's Laplace transform technique will be applied

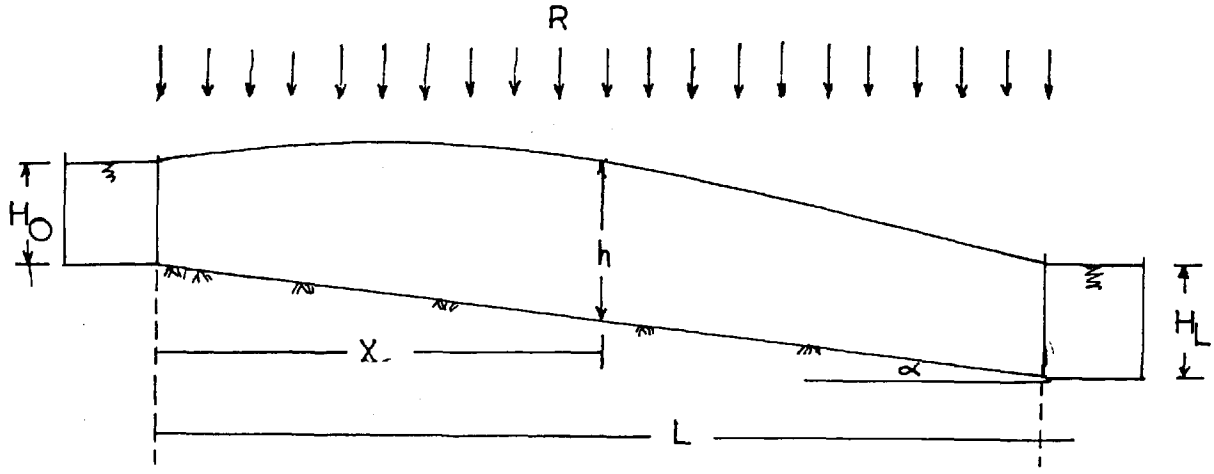


FIG: 6.4

WERNER'S TWO RESERVOIRS SYSTEM

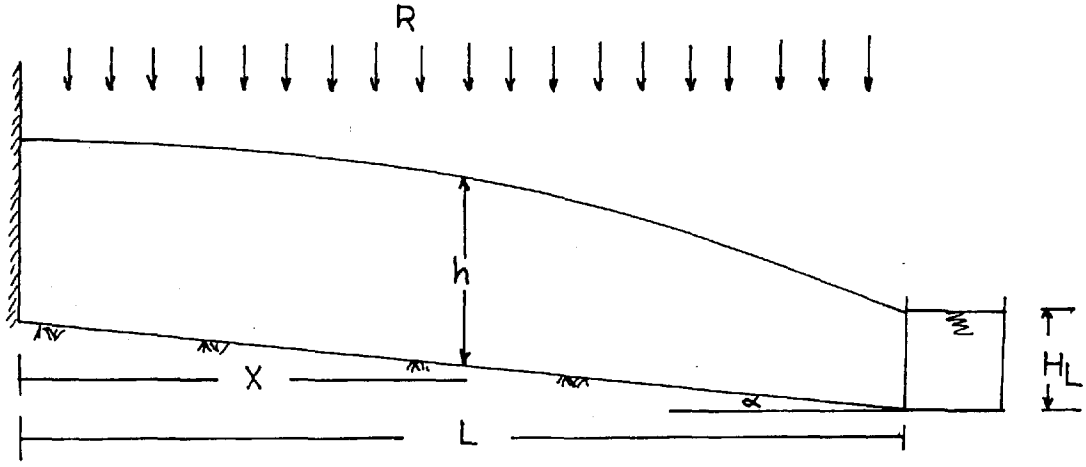


FIG: 6.5

WERNER S SINGLE RESERVOIR SYSTEM

here to derive an analytical solution in the present study. This solution is only an approximation of the experimental set up and is based on the following assumptions:

(1) Werner's reservoir system can be postulated as open ditches which penetrate to the impermeable bed;

(2) the elevation of the free surface of water in the open ditches relative to the impermeable bed is taken equal to the steady state height of water table above the bed at the location of the tile drains in the present study.

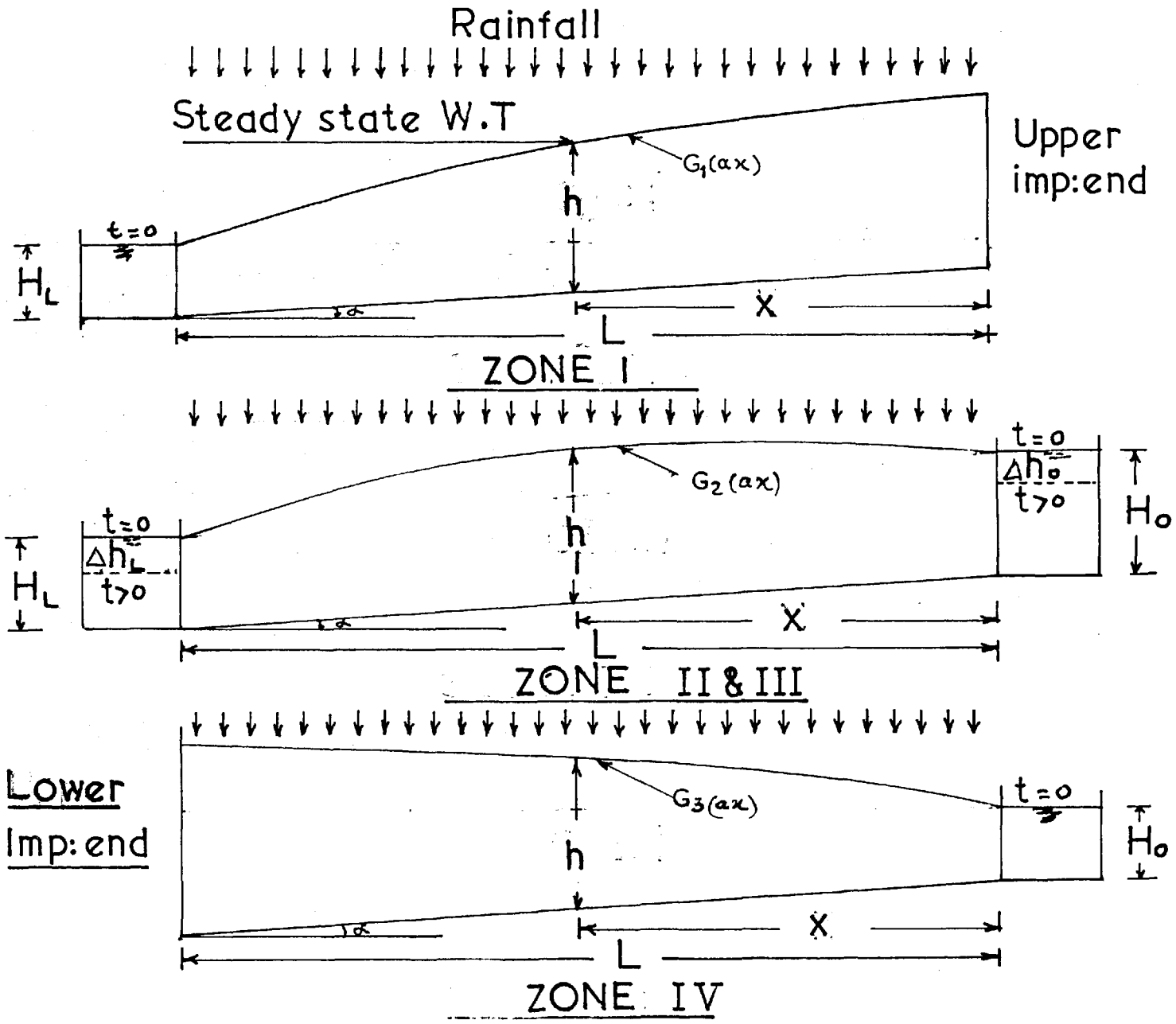
The applicability of a solution based on the concept of fully penetrating ditches to tile drains lying at a certain height above the impermeable bed (second assumption above) may be questioned. In this connection a case reported by Schilfgaarde (2) is relevant. He was of the view that the application of the ellipse equation (equation 3.2) to tile drains rather than open ditches introduces little additional error if the drains are placed near the impermeable bed. He further stated "often the backfilled trenches retain a higher hydraulic conductivity than undisturbed material, so that the tile drains act essentially as open ditches". Under such conditions, therefore, the tile drains would act similarly to open ditches. In the present study, since the water table stood at a certain height above the drains, the ditch water level was taken equal to the steady state height of water

table at the drains (second assumption) rather than the height of drains above the impermeable bed.

Similarly, Hauschild and Kruse (72) derived an approximate solution of unsteady groundwater flow into a surface reservoir. They checked their solution with the data given by Keller and Robinson (73) for interceptor tile drains lying on the impermeable bed. They found a close agreement between the solution and the experimental results, thus further supporting the contention that a solution based on ditch drains can be applied satisfactorily to tile drains lying at or near the bed.

For the present study, it would be rather difficult to derive one mathematical equation which may incorporate all the boundary conditions shown in Fig. 6.5a. The analysis will, therefore, proceed from zone to zone. In Fig. 6.5a, the flow region is divided into four zones. The first zone is the region between the upstream impermeable boundary and drain III. Zones II and III are enclosed between drains II - III and drains I - II respectively. The boundary condition for both the zones are similar. Zone IV is enclosed between the lower impermeable boundary and drain I. The solutions for steady and unsteady state flow in these zones are obtained by solving equations (2.25) and (2.24) for the boundary conditions that are described in Sections (6.4.2) and (6.4.3).

FIG: 6.5a


Rainfall
Steady state W.T
Upper
imp:end
$G_1(\alpha x)$
h
t=0
H_L
X
L
ZONE I
$G_2(\alpha x)$
t=0
Δh_o
t>0
H_o
t=0
Δh_L
t>0
H_L
h
X
L
ZONE II & III
Lower
Imp: end
$G_3(\alpha x)$
t=0
H_o
h
X
L
ZONE IV

6.4.2 Steady State

The steady state condition corresponds to the situation obtained after the vertical recharge from the ground surface has been occurring for a long enough time so that there is no change in the water table position. The solutions for different zones are obtained by solving the equation (Section 2.6)

$$\frac{\partial^2 y}{\partial x^2} - a\frac{\partial y}{\partial x} = -P_o \qquad \text{.....} \qquad (6.1)$$

in which $y = h^2$, $P_o = 2R/K$ and $a = \alpha/D$. This equation was obtained by linearising a non-linear partial differential equation (Section 2.6). In $y = h^2$, the variable h is the vertical distance measured to the water table from the impermeable bed in a direction perpendicular to a horizontal. Other symbols like R, K, α and D are rate of steady recharge, hydraulic conductivity, bed slope and weighted mean depth ($D = \frac{y_m}{2} + d$) of the saturated medium.

(i) Zone I

The boundary conditions are (Fig. 6.5a):

$\frac{\partial h}{\partial x} = \alpha$ at $x = 0$; since the water table is horizontal here.

$h = H_L$ at $x = L$.

It can now be easily verified by substitution (Appendix I) that equation (6.1) and the above boundary conditions yield a solution

$$y = h^2 = G_1(ax) = Z_1 + \frac{P_o}{a} \cdot F_1(ax) \quad \ldots\ldots\ldots\ldots \quad (6.2)$$

in which

$$Z_1 = H_L^2 - 2D^2 \left[e^{aL} - e^{ax} \right] \quad \ldots\ldots\ldots\ldots\ldots\ldots \quad (6.3)$$

and

$$F_1(ax) = x - L + \frac{1}{a} \left[e^{aL} - e^{ax} \right] \quad \ldots\ldots\ldots\ldots\ldots \quad (6.4)$$

(ii) Zones II and III

Fig. 6.5a shows a general layout of zones II and III. The boundary conditions for these zones are:

$h = H_o$ at $x = 0$

$h = H_L$ at $x = L$

For these boundary conditions, the solution of equation (6.1) is as follows: (Appendix I):

$$y = h^2 = G_2(ax) = Z_2 + \frac{P_o}{a} \cdot F_2(ax) \quad \ldots\ldots\ldots\ldots \quad (6.5)$$

in which

$$Z_2 = H_o^2 + (H_L^2 - H_o^2) \cdot \left[\frac{e^{ax} - 1}{e^{aL} - 1} \right] \quad \ldots\ldots\ldots\ldots \quad (6.6)$$

and

$$F_1(ax) = x - L \left[\frac{e^{ax} - 1}{e^{aL} - 1} \right] \quad \ldots\ldots\ldots\ldots\ldots\ldots \quad (6.8)$$

(iii) Zone IV

The boundary conditions are (Fig. 6.5a)

$$\frac{\partial h}{\partial x} = \alpha \qquad \text{at } x = L$$

$$h = H_o \qquad \text{at } x = 0$$

Equation (6.1) and these boundary conditions yield a solution

$$y = h^2 = G_3(ax) = Z_3 + \frac{P_o}{a}\left[x + \frac{1}{a} e^{-aL}(1 - e^{ax})\right] \quad \ldots (6.9)$$

in which

$$Z_3 = H_o^2 - 2D^2 e^{-aL}\left[1 - e^{ax}\right] \quad \ldots\ldots\ldots\ldots\ldots\ldots (6.10)$$

The steady state water table profiles in zones I, II, III and IV will be obtained in Section (6.7.1.2) by substituting measured values of H_o and H_L for various values of a and P_o.

6.4.3 Unsteady state

In order to obtain some approximate solutions for the unsteady state problems whose initial state is shown in Fig. 6.5a, the following equation (Section 2.6) has to be solved in conjunction with the relevant initial and boundary conditions.

$$\frac{\partial^2 y}{\partial x^2} - a\frac{\partial y}{\partial x} = \frac{1}{C}\frac{\partial y}{\partial t} - P \quad \ldots\ldots\ldots\ldots\ldots\ldots\ldots\ldots (6.11)$$

in which

$C = \frac{KD}{f}$, f being the soil porosity.

When the steady state is reached P in equation (6.11) is equal to a certain initial value P_o, $\partial y/\partial t = 0$ and $y = y_1$ so

that

$$\frac{\partial^2 y_1}{\partial x^2} - a\frac{\partial y_1}{\partial x} = -P_o \quad \ldots\ldots\ldots\ldots\ldots\ldots\ldots\ldots \quad (6.1b)$$

With the sudden cessation of rainfall (at time t = 0) P = 0 in equation (6.11) so that, for $t \geq 0$, y is given by

$$\frac{\partial^2 y}{\partial x^2} - a\frac{\partial y}{\partial x} = \frac{1}{C}\frac{\partial y}{\partial t} - 0 \quad \ldots\ldots\ldots\ldots\ldots\ldots\ldots\ldots \quad (6.12)$$

The transformation $y = y_1 - q$ transforms equation (6.12) into the form

$$\left[\frac{\partial^2 y_1}{\partial x^2} - a\frac{\partial y_1}{\partial x}\right] - \left[\frac{\partial^2 q}{\partial x^2} - a\frac{\partial q}{\partial x}\right] = \frac{1}{C}\left(\frac{\partial y_1}{\partial t} - \frac{\partial q}{\partial t}\right)$$

since

$$\partial y_1/\partial t = 0 \text{ and } \frac{\partial^2 y_1}{\partial x^2} - a\frac{\partial y_1}{\partial x} = -P_o \quad \text{(from equation 6.1b)}$$

therefore

$$-P_o - \left[\frac{\partial^2 q}{\partial x^2} - a\frac{\partial q}{\partial x}\right] = -\frac{1}{C}\frac{\partial q}{\partial t}$$

or

$$\frac{\partial^2 q}{\partial x^2} - a\frac{\partial q}{\partial x} + P_o = \frac{1}{C}\frac{\partial q}{\partial t} \quad \ldots\ldots\ldots\ldots\ldots\ldots\ldots\ldots \quad (6.13)$$

Equation (6.13) can be re-written as

$$\frac{\partial^2 p}{\partial x^2} - a\frac{\partial p}{\partial x} = \frac{1}{C}\frac{\partial p}{\partial t} \quad \ldots\ldots\ldots\ldots\ldots\ldots\ldots\ldots \quad (6.14)$$

in which

$$p = q - \frac{P_o}{a} x$$

$$= y_1 - y - \frac{P_o}{a} x \qquad \ldots\ldots\ldots\ldots\ldots\ldots\ldots\ldots \quad (6.15)$$

The main boundary condition considered in the solution of equation (6.14) is the time-variable end condition $H_o(t)$ or $H_L(t)$ or both. It is assumed that, following an instantaneous cessation of recharge, the water level in the ditches falls by a certain distance in a finite time causing a fall of the water table all along the spacing between ditches.

In this analysis H_o and H_L are the steady state heights of free surface in the upper and lower reservoirs, and $H_o(t)$ and $H_L(t)$ the same heights at time t after the beginning of the recession.

(i) Zone I

Assume that the ditch water level (Fig. 6.5a) falls by a certain height $\Delta h_L(t)$ in time t after the cessation of recharge. The numerical value of $\Delta h_L(t)$ would be negative for a falling water table. The initial and boundary conditions are:

$$y(x,0) = y_1 = h^2(x,0) = G_1(ax) \; ; \quad G_1(ax) \text{ is given by equation 6.2}$$

$$\frac{\partial h(0,t)}{\partial x} = \alpha \; ; \quad \text{since water table is horizontal here}$$

$$h(L,t) = H_L - \Delta h_L(t).$$

For the solution of equation (6.14) these initial and boundary conditions will change into

(i) $p(x,0) = -\frac{P_o}{a}x$ (since $y_1 = y$ in equation (6.15)

(ii) $$\frac{\partial p(0,t)}{\partial x} = \frac{\partial q}{\partial x} - \frac{P_o}{a}$$

$$= 2D\frac{\partial h_1}{\partial x} - 2D\frac{\partial h}{\partial x} - \frac{P_o}{a} \qquad \left[\text{using approximation } \frac{\partial}{\partial x}(h^2) \doteq 2D\frac{\partial h}{\partial x}\right]$$

$$= 2D\frac{\partial h_1}{\partial x} - 2D\frac{\partial h}{\partial x} - \frac{P_o}{a}$$

$$= 2D\alpha - 2D\alpha - \frac{P_o}{a}$$

$$= -\frac{P_o}{a}$$

(iii) $$p(L,t) = q - \frac{P_o}{a}L$$

$$= H_L - \left[H_L - \Delta h_L(t)\right]^2 - \frac{P_o}{a}L = \gamma - \frac{P_o}{a}L$$

By Laplace transformation method equation (6.14) will be transformed into

$$\frac{d^2p'}{dx^2} - a\frac{dp'}{dx} = \frac{s}{C}p' + \frac{P_o}{aC}x \qquad \text{..... (6.16)}$$

the solution of which is

$$p' = e^{ax/2}\left[A\sinh(\beta x) + B\cosh(\beta x)\right] - \frac{P_o}{as}x + \frac{P_oC}{s^2}$$

..... (6.17)

in which

$$\beta = \sqrt{\frac{a^2}{4} + \frac{s}{C}}$$

and A, B are arbitrary constants and s is given by

$$\mathcal{L}f(t) = \int_0^{\infty} e^{-st} f(t).dt$$

After satisfying the boundary conditions, the following solution of equation (6.16) is obtained by using the inverse of Laplace transform and the transformation given by equation (6.15) (Appendix II).

$$y(x,t) = G_1(ax) - \lambda\left[1 - 2\,T\,(xt)\right] - 2P_o C\, T_2(x,t) \quad \ldots\ldots \quad (6.18)$$

in which $G_1(ax)$ is given by equation (6.2) and

$$T_1(x,t) = e^{-a(L-x)/2} \sum_{n=0}^{\infty} B_n \cdot \sin\left[r_n(1 - x/L)\right] \cdot e^{-jt}$$

and

$$T_2(x,t) = e^{-a(L-x)/2} \sum_{n=0}^{\infty} B_n \cdot \sin\left[r_n(1-x/L)\right] \left(1 - e^{-jt}\right)$$

$$B_n = \frac{r_n^3}{\sigma\left(\sigma - \frac{aL}{2}\right) \cdot \sin^2(r_n)}$$

and

$$j = \frac{C}{L^2}\left[\left(\frac{aL}{2}\right)^2 + r_n^2\right]$$

$$= \frac{C}{L^2} \cdot \sigma$$

The roots r_n can be taken from available tables (74).

(ii) Zones II and III

Assume that water levels in the upper and lower ditches fall by $\Delta h_o(t)$ and $\Delta h_L(t)$ respectively in time t. Then the initial and boundary conditions are (Fig. 6.5a).

$$y(x,0) = h^2(x,0) = G_2(ax) \qquad \left[\text{where } G_2(ax) \text{ is given by equation (6.5)}\right.$$

$$h(0,t) = H_o - \Delta h_o(t)$$

$$h(L,t) = H_L - \Delta h_L(t)$$

For the solution of equation (6.14) these initial and boundary conditions change into

$$\text{(i)} \quad p(x,0) = -\frac{P_o}{a}x$$

$$\text{(ii)} \quad p(0,t) = H_o^2 - \left[H_o - \Delta h_o(t)\right]^2 - 0 = \lambda$$

$$\text{(iii)} \quad p(L,t) = H_L^2 - \left[H_L - \Delta h_L(t)\right]^2 - \frac{P_o}{a}L = \gamma - \frac{P_o}{a}L$$

These initial and boundary conditions suggest a final solution of the form (Appendix II)

$$y(x,t) = G_2(ax) - e^{ax/2}\left[\left\{\gamma e^{-aL/2} - \lambda\cosh(aL/2)\right\}\cdot\frac{\sinh(ax/2)}{\sinh(aL/2)} + \lambda\cosh(ax/2)\right] - 2T_3(x,t)$$

$$+ e^{ax/2}\cdot P_o C\left[\left\{e^{-aL/2} - \cosh(aL/2)\right\}\frac{\sinh(ax/2)}{\sinh(aL/2)}\cdot t + t\cosh(ax/2)\right] - P_o C 2T_4(x,t) - P_o . Ct$$

..... (6.19)

or

$$y(x,t) = G_2(ax) - \left[(\delta - \lambda) \frac{e^{ax} - 1}{e^{aL} - 1} + \lambda - 2T_3(x,t) \right] - 2P_o C\, T_4(x,t) \quad \ldots\ldots\ldots\ldots (6.20)$$

in which

$$T_3(x,t) = e^{ax/2} \sum_{n=1}^{n=\infty} \left[(-1)^{n+1} \; e^{-aL/2} + \lambda \right] \cdot \frac{n\pi}{r_c} \sin (n\pi x/L)\; e^{-wt}$$

and

$$T_4(x,t) = e^{ax/2} \sum_{n=1}^{n=\infty} \left[(-1)^{n+1} \; e^{-aL/2} + \lambda \right] \cdot \frac{n\pi}{r_c w} \sin (n\pi x/L)\; (1 - e^{-wt})$$

$$w = \frac{C}{L^2} \left[(n\pi)^2 + (aL/2)^2 \right] = \frac{C}{L^2} \cdot r_c$$

(iii) Zone IV

Assume that water level in the upper ditch (Fig. 6.5a) falls by height $\Delta h_o(t)$ in time t after the beginning of the recession. The initial and boundary conditions are:

$y(x,0) = y_1 = G_3(ax)$ [where $G_3(ax)$ is given by equation (6.9)]

$\frac{\partial h(L,t)}{\partial x} = \alpha$

$h(0,t) = H_o - \Delta h_o(t)$

For the solution of equation (6.14) these initial and boundary conditions will change to the form

(i) $p(x,0) = -\frac{P_o}{a} x$

(ii) $\frac{\partial p(L,t)}{\partial x} = -\frac{P_o}{a}$

(iii) $p(0,t) = Ho^2 - \left[H_o^{\,1} - \Delta h_o(t)\right]^2 - 0$

$= \lambda$

Equation (6.14) and these boundary conditions yield a solution (Appendix II)

$$y,(x,t) = G_3(ax) - \left[1 + 2\,T_5(x,t)\right] + 2P_o C\,T_6\,(x,t) \quad \ldots\ldots \quad (6.21)$$

in which $G_3(ax)$ is given by equation (6.9) and

$$T_5(x,t) = e^{ax} \sum_{n=0}^{n=\infty} B_n \sin\,(m_n\,x/L)\left[\sin^2(m_n) - \cos^2(m_n)\right] e^{-\sigma t}$$

$$T_6(x,t) = e^{ax} \sum_{n=0}^{n=\infty} \frac{B_n}{\sigma} \sin(m_n x/L)\left[\sin^2\,(m_n) - \mathrm{Cos}^2(m_n)\right] (1 - e^{-\sigma t})$$

$$B_n = \frac{1}{2\sin^2\,(m_n)\left[1 + \frac{\sigma}{4m_n^{\,2}}\left(\frac{aL}{2} + 1\right)\right] - \frac{\sigma}{m_n}\sin^2(m_n)}$$

in which m_n denote the roots of the equation

$$m_n \cos\,(m_n) = \frac{aL}{2}$$

These roots can be found from available tables (74).

$$\rho = \frac{C}{L^2}\left[m_n^{\,2} + \left(\frac{aL}{2}\right)^2\right] = \frac{C}{L^2}\cdot\sigma \qquad \ldots\ldots \qquad (6.22)$$

Equations (6.18), (6.19) and (6.21) are solved in Section (6.8.1.2) to obtain the falling water table profiles in the four zones. The observed steady state values H_o, H_L and $\Delta h_o(t)$, $\Delta h_L(t)$ at different

times were fed in as data.

6.5 DESCRIPTION OF THE MODEL

The model described in Chapter 5 was used in this study also. However, some essential alterations were made in the manifold holding the rainfall distribution system. The alterations were made with two objectives in view. First of these objectives was that the rainfall distribution system, irrespective of the inclination of the model, should remain horizontal so that there was uniform pressure distribution all along the length of the distribution pipe. The second objective was that the manifold should be movable along its length so that the distribution pipe could come exactly over the model when the inclination of the model was changed. This would prevent oil from falling outside the model.

Plate II shows a general layout of the model. Two galvanised iron pipes were suspended from an 8 in. water supply pipe in the laboratory. The upper ends of the pipes were screwed into two circular clamps around the 8 in. pipe. Their lower ends were screwed into a T-junction (Fig. 6.6). Two 1" x 2" long pieces of flat C.I bar were bolted at each end of the T-junction. The lower ends of the flat bars held two brass pulleys through two C.I. round bar pieces, the ends of which were

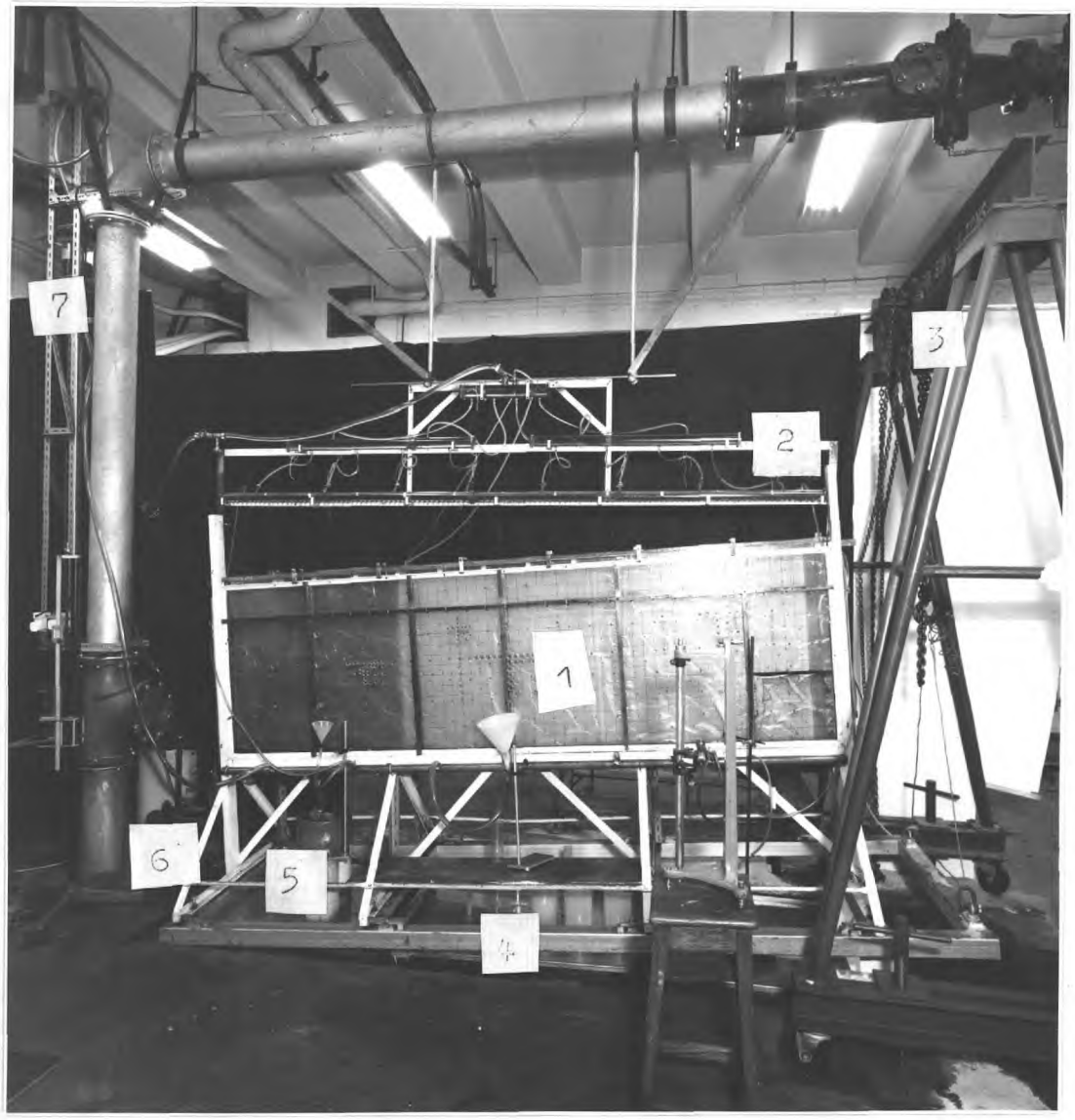


PLATE II

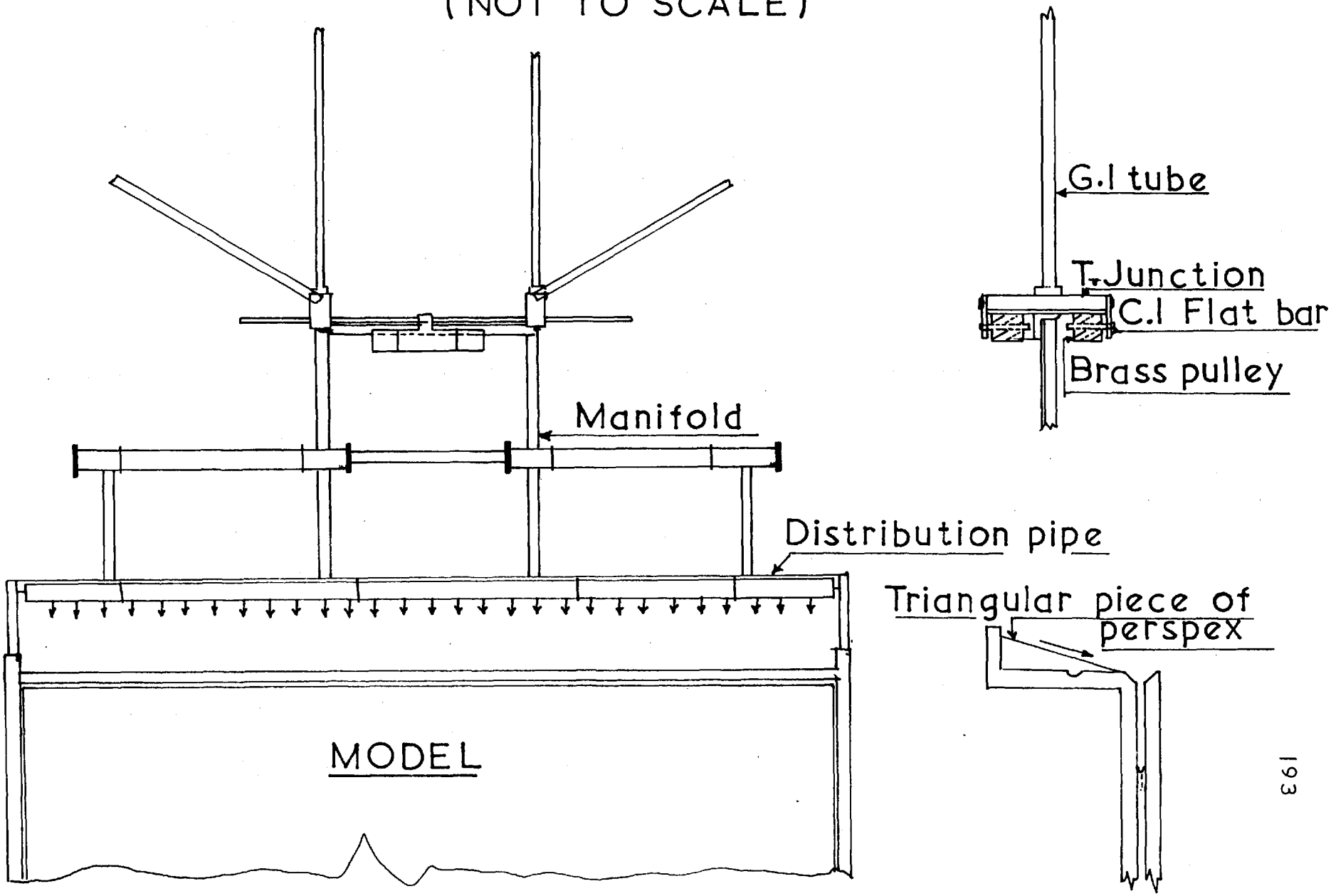
GENERAL LAYOUT OF

MODEL

1. Model
2. Rainfall Distribution System
3. Lifting Crane
4. Base Frame
5. Collecting Tank
6. Pump
7. Constant Level Tank

FIG: 6.6

(NOT TO SCALE)



separated by $\frac{1}{2}$" from each other. A C.I flat bar $1\frac{1}{2}$" x $3\frac{1}{2}$ ft long was fixed on the top angle iron of the manifold supporting the rainfall distribution system. The manifold was then pushed over the pulleys. The whole manifold could thus slide along its length. In order to prevent the distribution system being disturbed while an experiment was in progress, the manifold was temporarily clamped to the model. It was released whenever the slope was changed.

In the symmetrical drainage system, the hypodermic tubes discharged on to a shelf (Fig. 5.6) on the top of one of the Perspex plates on which the oil was allowed to accumulate before flowing down into the interspace. The shelf thus permitted a uniform distribution of oil. This arrangement, however, had a disadvantage for the sloping drainage system. The accumulation of oil on the shelf could cause a downslope flow of oil along the inclined shelf. This eventually would result in a non-uniform flux across the water table. Also, the oil could not be allowed to fall directly into the interspace because of the formation of irregularities on the water table due to entrapped air. To get rid of these irregularities, a triangular piece of Perspex (Fig. 6.6) was fitted into the whole length of the shelf. The slope of the top of the triangle was high enough to permit oil to flow into the interspace immediately after impact.

The model was clamped with a 3" by 3" square C.I base frame (Plate II) to give it a firm support in the inclined position. One side of the frame was held against an angle iron fixed to the ground surface and the other was free. The free side of the frame projected 18 in from one side of the model. The free side of the frame was raised by a one-ton capacity crane through wire rope tied to eye bolts which were screwed into the base frame. To achieve a given slope, wooden supports of the required heights were placed below the free end of the base frame and the model was lowered on to the supports.

6.6 EXPERIMENTAL PROCEDURE

Figure (6.3a) shows an arrangement of drains in the model. Three drains of 0.5 cms dia: and 100 cms spacing were used in the study. More drains could not be used because it was difficult to obtain a reasonable depth (5 to 6 cms) of water table above the centre of the drains even for the maximum amount of rainfall that could be achieved in the model.

Experiments were conducted for moderate slopes ranging from 0-10%. In addition, the effect of the rate of recharge on the steady state water table profile was studied at a slope of 6%. The rate of fall at the highest point on the water table was considered to be an important parameter in the study. The

drains in most experiments were running full with the water table standing at a certain height above them. In addition to this, the steady state water table profile for the maximum rate of recharge was also observed for free discharging drains lying over an impermeable bed having a slope of 6%. Thus the experiments were so conducted that they could show the effect of all the major drainage parameters on the rate of fall of water table.

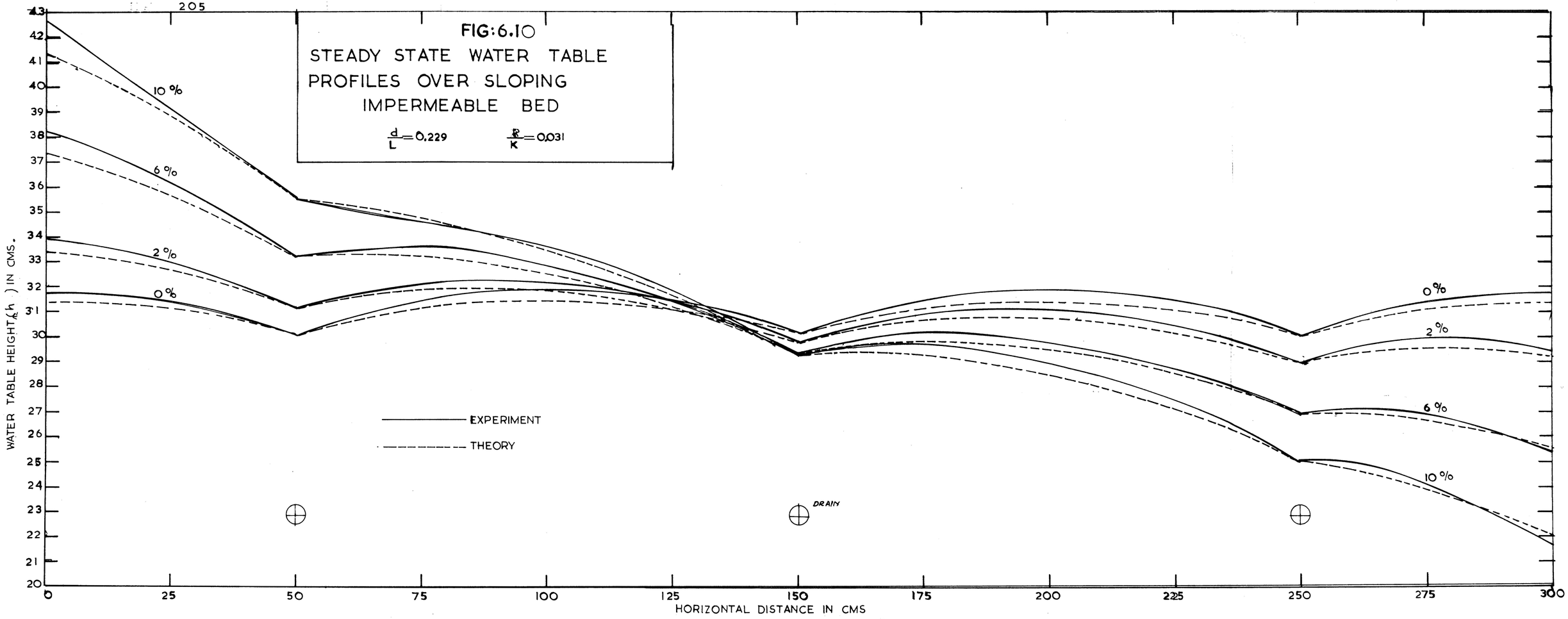
The total steady rate of recharge corresponds to the sum of the measured discharge of each of the three drains. A Piezometer was used to make sure that the steady state existed before the discharge measurements were made. All vertical distances were measured from the inclined bed of the model. It may, however, be pointed out that since the distances were read on a graph paper fixed at the back of the model, all water table heights were measured normal to the sloping impermeable bed. These heights were later converted to heights measured above the impermeable bed with respect to a horizontal plane. Since the slopes were small, there was practically no difference between these measured and computed heights of the water table.

In the experiments, the model was first kept horizontal and a constant rate of rainfall was allowed to drip into it. After the steady state was reached, the rate of discharge of

each drain was measured and the water table profile was noted. The rainfall was then stopped and measurements were made of the falling water table midway between drains lying over a horizontal impermeable bed. After this, the model was inclined at a certain slope.

When the model was in the sloping position, the oil from the rainfall distribution system was allowed to drip into it again. The discharge of each drain was measured to check that the total discharge of all drains remained constant. The steady state water table heights were then noted at 10 cm intervals. The same procedure was repeated at other slopes.

The falling water table observations over the sloping bed were taken at two points. The first was at the downstream impermeable boundary of the model and the second at the highest point in zone II. It was believed that the results obtained for the falling water table at the highest point in this zone would show reasonable similarity to the case when there are an infinite number of drains lying over a sloping bed of an infinite aquifer. The change in water table depth at the highest point in zone II was observed experimentally to be one-tenth of the change at the downstream boundary. The effect of the proximity of the downstream impermeable boundary therefore had negligible effect on the water table profile in zone II.


FIG:6.10
STEADY STATE WATER TABLE PROFILES OVER SLOPING IMPERMEABLE BED
d/L = 0.229
R/K = 0.031
10 %
6 %
2 %
0 %
EXPERIMENT
THEORY
DRAIN
WATER TABLE HEIGHT (h) IN CMS.
HORIZONTAL DISTANCE IN CMS
0
25
50
75
100
125
150
175
200
225
250
275
300
20
21
22
23
24
25
26
27
28
29
30
31
32
33
34
35
36
37
38
39
40
41
42
43

6.7 RESULTS FOR THE STEADY STATE

6.7.1 Submerged flow due to resistance to flow in the drain

6.7.1.1 Experimental results:

Fig. 6.7 (Table 6.1) shows the effect of bed slope on the steady state water table profile at a constant rate of recharge. It is observed from the figure that the steady state water table profile gradually rises on the downstream side ($X < 150$ cms) of the middle drain, whereas it falls on the upstream side ($X > 150$ cms), thereby showing that drain II almost acts as a pivot about which the water table rotates.

Fig. 6.8 (Table 6.2) shows the variation of the discharge with the bed slope. There is a slight decrease in the discharge of the middle drain. The discharge of the lowest drain increases linearly with the bed slope while there is a corresponding decrease in the discharge of the highest drain.

Fig. 6.9 shows that the difference of the squares of the water table heights at the downstream ($X = 0$ cms in Table 6.2) and upstream ($X = 300$ cms in Table 6.2) impermeable boundaries is linearly related with the bed slope. The functional relation can be represented by

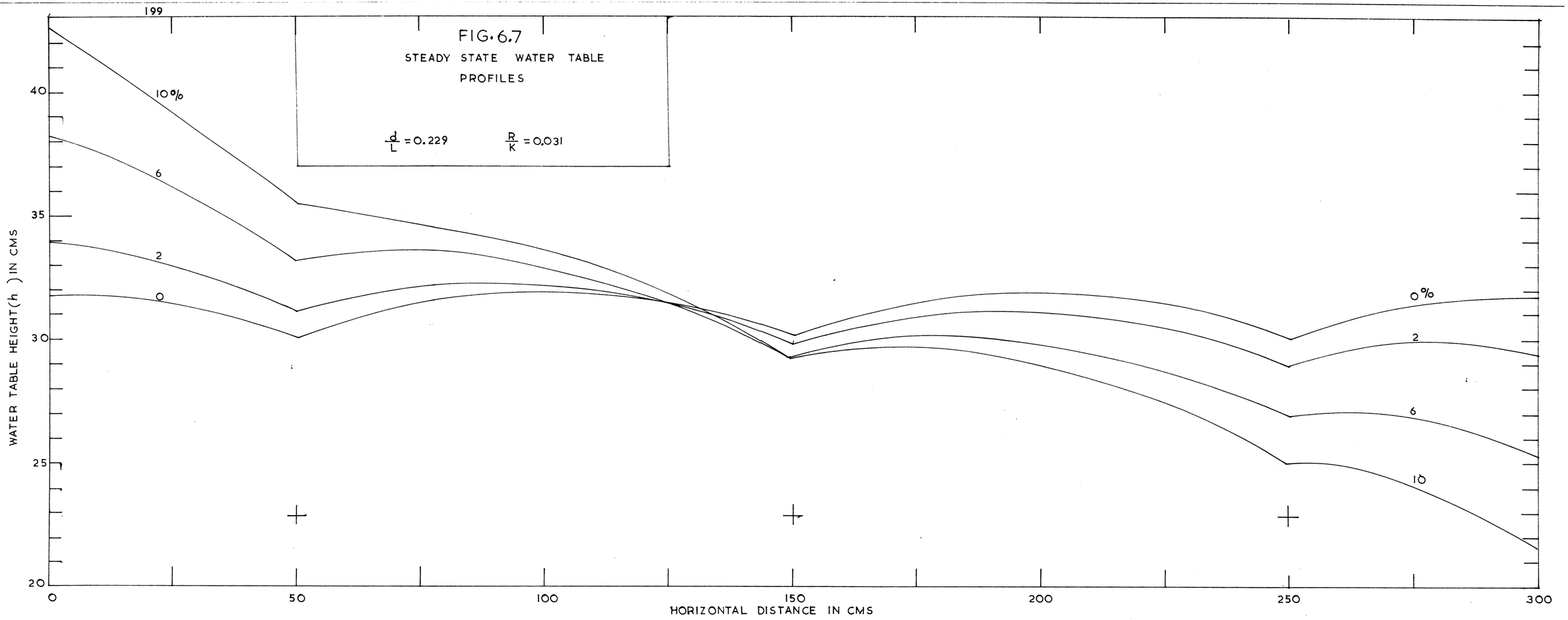
$$h_d^2 - h_u^2 = 1.08 \alpha \quad \ldots\ldots\ldots\ldots\ldots\ldots \quad (6.23)$$

in which h_d is the height of water table at the downstream impermeable boundary and h_u at the upstream boundary, and α is

FIG. 6.7

STEADY STATE WATER TABLE PROFILES

$\frac{d}{L} = 0.229$ $\frac{R}{K} = 0.031$



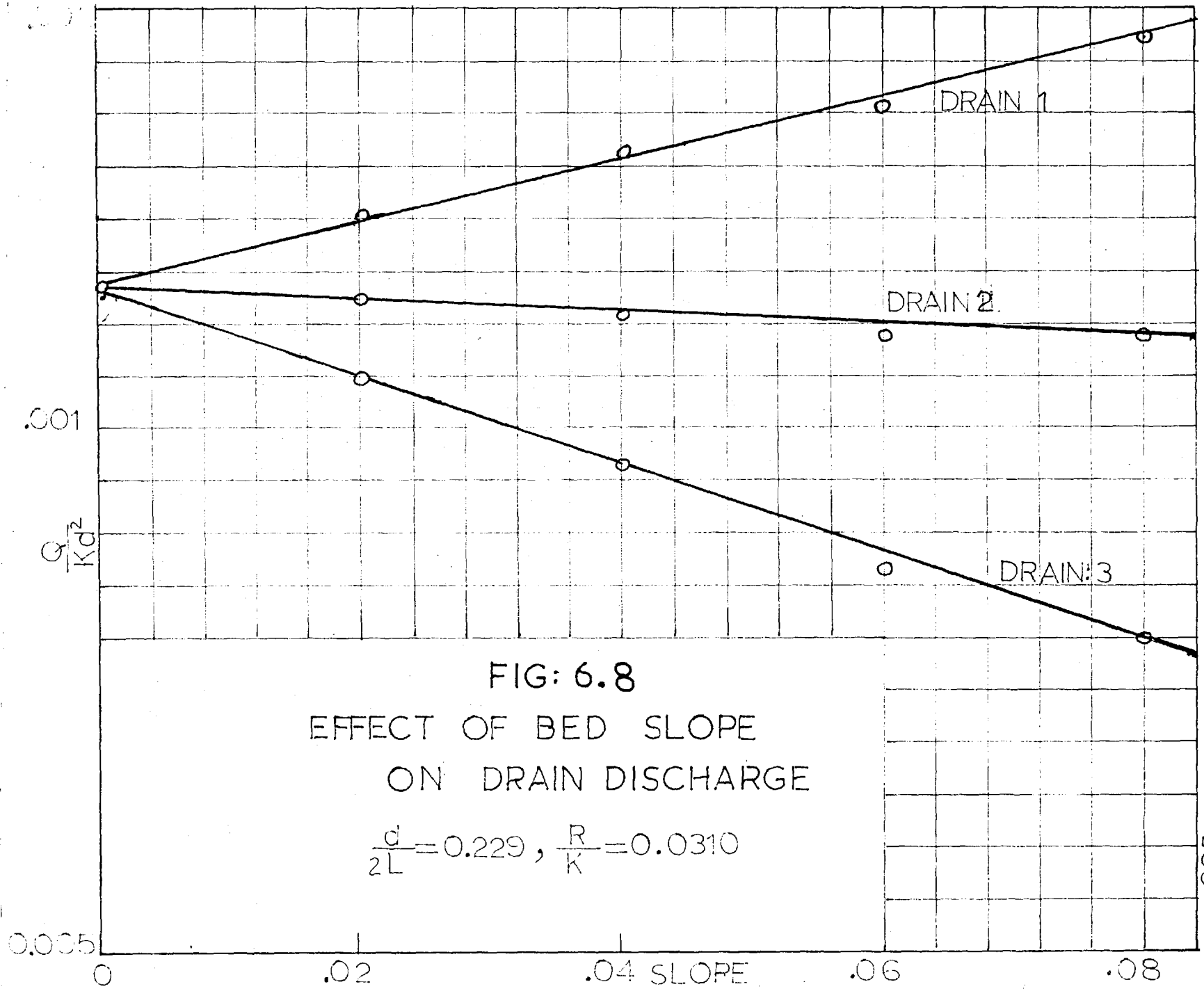
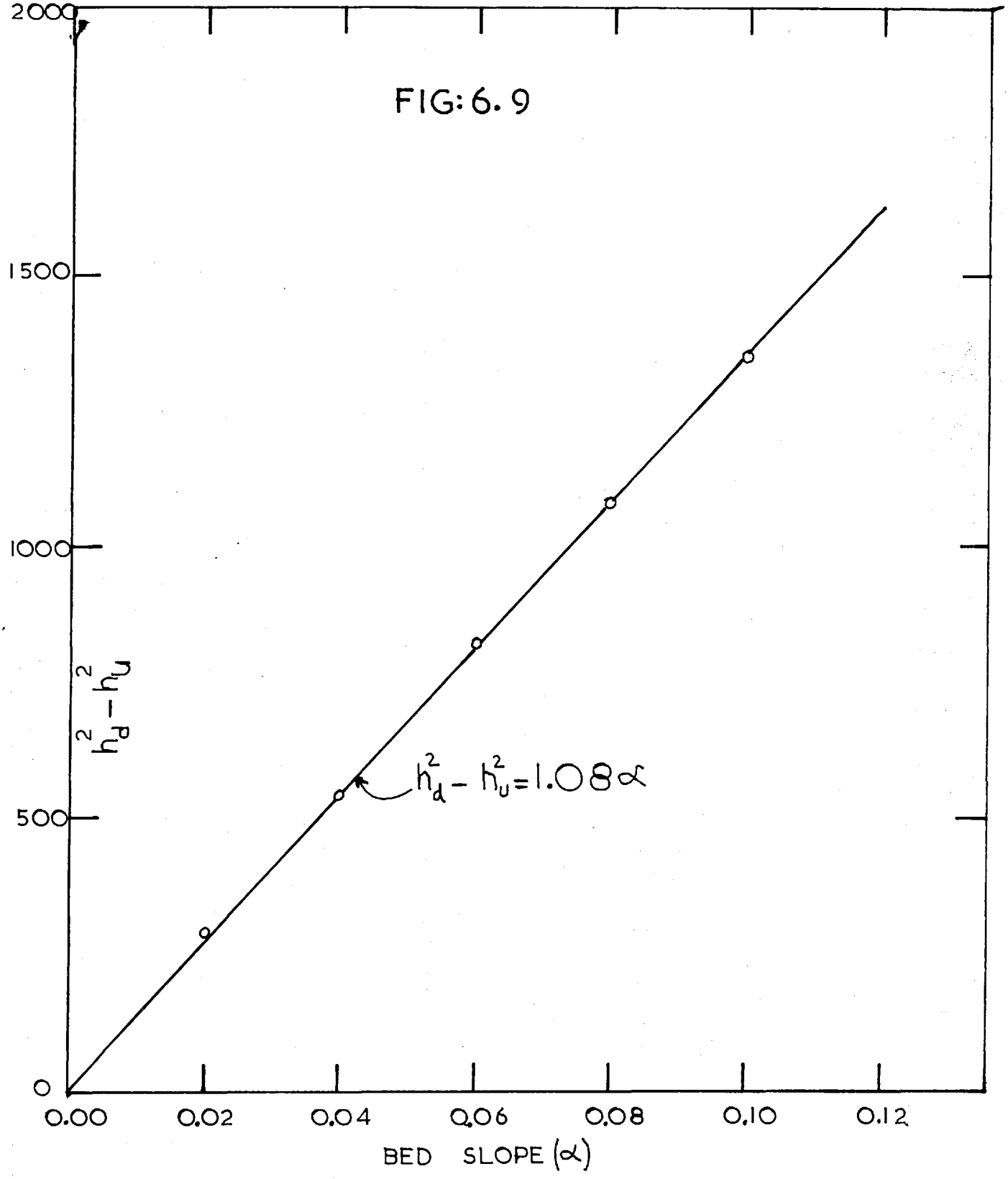


FIG: 6.8

EFFECT OF BED SLOPE ON DRAIN DISCHARGE

$\frac{d}{2L}=0.229$, $\frac{R}{K}=0.0310$

FIG: 6.9


2000
1500
1000
500
0
$h_d^2 - h_u^2$
$h_d^2 - h_u^2 = 1.08\alpha$
0.00
0.02
0.04
0.06
0.08
0.10
0.12
BED SLOPE (α)

the bed slope.

The above functional relationship can also be arrived at analytically, though not exactly for the system examined herein. For a simple analysis, let it be assumed that there is a single drain lying above the sloping impermeable bed. In the steady state, the discharge of this drain would be constant and independent of the bed slope. This would, therefore, represent the middle drain in the present three drain system. Equations (6.2) and (6.9) can be used to find the steady state water table heights at the upstream and downstream impermeable boundaries. By putting $x = 0$ in equation (6.9) and $x = L$ in equation (6.2) we get.

$$h^2 = H_o^2 = H_L^2 \qquad \ldots\ldots\ldots\ldots\ldots\ldots\ldots\ldots \quad (6.24)$$

Thus the height of the water table, at the location of the drain, is independent of the bed slope for the one-drain system. This is also essentially true in Fig. 6.7 for the three-drain system. A slight shift from the middle drain of the point of intersection of the steady state water table profiles may be attributed to experimental errors, probably due to differences of resistance in the three drains.

If we put $x = 0$ in equation (6.2) and $x = L$ in (6.9), we obtain the heights of the steady state water table at the upstream

and downstream boundaries of the single drain system.

$$h_d^2 = H_o^2 - 2D^2 e^{-aL}(1 - e^{aL}) + \frac{P_o}{a}\left[L + \frac{1}{a} e^{-aL}(1 - e^{aL})\right] \quad \ldots\ldots\ldots\ldots\ldots \quad (6.25)$$

and

$$h_u^2 = H_L^2 - 2D^2(e^{aL} - 1) + \frac{P_o}{a}\left[-L + \frac{1}{a}(e^{aL} - 1)\right] \quad \ldots\ldots\ldots\ldots\ldots \quad (6.26)$$

Noting that for the single drain system $H_o^2 = H_L^2$, the difference between (6.25) and (6.26) is given by

$$h_d^2 - h_u^2 = 4D^2 \text{ sin-h}(aL) + \frac{2P_o}{a}\left[L - \frac{1}{a} \text{ sin-h } (aL)\right] \quad \ldots\ldots\ldots\ldots\ldots \quad (6.27)$$

For a symmetrical drainage system, $\alpha = 0$ and therefore from equation (6.27)

$$h_d^2 - h_u^2 = 0$$

As expected, $h_d = h_u$.

For moderate slopes, $\sinh(aL) \simeq aL$ in equation (6.27). Therefore

$$h_d^2 - h_u^2 = 4D^2 aL \quad \ldots\ldots\ldots\ldots\ldots\ldots\ldots\ldots\ldots \quad (6.28)$$

$$= 4D^2 \cdot \frac{\alpha}{D} \cdot L$$

or

$$h_d^2 - h_u^2 \propto D \propto L.$$

This confirms equation (6.23). In equation (6.23) a value of curve slope higher than unity may be due to the experimental errors discussed earlier.

6.7.1.2 Theoretical water table profile

Fig. 6.10 (Table 6.3) shows a comparison between the experimental and theoretical steady state water table profiles at different bed slopes. The theoretical results were computed separately for each Zone discussed in Section 6.4.1. The weighted mean depth D was taken as the mean of the heights of the water table at the two ends of each Zone. In cases where the water table somewhere between the drains was higher than at the lower drain the weighted mean depth was taken as a sum of the water table height at the upper drain and a mean of the difference of the maximum water table height and the height at the lower drain in the Zone concerned. P in equation (6.1) is equal to 2R/K. R was calculated by dividing the sum of the measured discharge of the drains by a product of the length and interspace of the model. H_o and H_L in the steady state equations are the observed heights of water table at the drains.

It may be noted in Fig. 6.10 (Table 6.3) that there is a very close agreement between the experimental and theoretical steady state water table profiles. Maximum error occurs at the downstream impermeable boundary (i.e. X = 0 in Table 6.3) of the system. This may be attributed to a non-uniform distribution of rainfall near the downstream edge of the model. It was observed that at a slope of 0.06 or higher, flow from the first hypodermic tube was running over the lower edge of the model. with the result that some oil from this tube was flowing out of the model and some splashing into it. A small rubber tube was fitted on to the needle to allow the oil to drip just into the inner edge of the model, where oil was also dropping from the second needle. This gave a non-uniform distribution of rainfall in regard to the remaining length of the model.

Table 6.4 shows experimental and theoretical heights of water table at different rates of rainfall in the range 0.0066 to 0.0345 and for a bed slope of 0.06. The maximum percentage difference $[(h_e - h_t)/h_e]$ between the experimental and the theoretical results is of the order of 3 to 4%.

6.7.2 Free flow

Since the steady state water table profile is flatter in the submerged flow case than in free flow, the former conforms

TABLE 6.4

COMPARISON BETWEEN EXPERIMENTAL AND THEORETICAL STEADY STATE WATER TABLE PROFILES

Slope = 0.06 d = 22.90 cms r = 0.25 cms Spacing = 100 cms

R/K		.0345			.0306			.0226	
X cms	h_e cms	h_t cms	% diff:	h_e cms	h_t cms	% diff:	h_e cms	h_t cms	% diff:
0	38.70	37.60	2.60	37.80	36.50	3.45	35.25	34.00	3.55
10	37.65	37.00	1.23	36.85	35.85	2.70	34.35	33.40	2.76
20	36.95	36.20	2.04	36.10	35.40	1.95	33.60	32.80	2.40
30	35.95	35.55	1.10	35.25	34.55	2.00	32.70	32.15	1.70
40	34.80	34.75	0.14	34.15	33.65	1.45	31.85	31.40	1.40
50	33.75	33.75	0.00	32.90	32.90	0.00	30.50	30.50	0.00
60	33.90	33.85	0.14	33.05	32.74	0.91	30.65	30.60	0.00
70	33.80	33.65	0.45	33.10	32.80	0.91	30.80	30.37	1.30
80	33.70	33.55	0.45	32.95	32.75	0.61	30.70	30.40	0.98
90	33.60	33.35	0.74	32.80	32.60	0.61	30.50	30.05	1.48
100	33.50	33.05	1.35	32.70	32.20	1.53	30.40	29.85	1.80
110	33.10	32.70	1.05	32.15	31.80	1.10	30.00	29.55	1.50
120	32.50	32.35	0.46	31.60	31.45	0.47	29.50	29.10	1.35
130	32.05	32.03	0.00	31.00	30.90	0.32	28.90	28.75	0.52
140	30.90	30.95	0.00	30.20	30.40	0.66	28.80	28.80	0.71
150	30.15	30.15	0.00	29.65	29.65	0.00	27.60	27.60	0.00
160	30.65	30.20	1.45	29.95	29.80	0.50	27.85	27.20	2.33
170	30.90	30.40	1.60	30.20	30.00	0.66	27.95	27.30	2.30
180	31.00	30.50	1.60	30.30	29.95	1.15	28.15	28.25	0.36
190	30.80	30.50	0.98	31.20	29.75	1.45	27.90	27.20	2.50
200	30.65	30.25	1.30	29.85	29.45	1.17	27.70	27.00	2.50
210	30.35	30.00	1.15	29.50	29.25	0.85	27.40	26.80	2.20
220	29.85	29.60	0.84	29.15	28.95	0.60	27.00	26.65	1.30
230	29.30	29.10	0.68	28.60	28.30	1.05	26.70	26.35	1.35
240	28.60	28.50	0.35	27.90	27.65	0.90	26.10	25.95	0.96
250	27.70	27.70	0.00	27.00	27.00	0.00	25.25	25.25	0.00
260	27.85	27.65	0.72	27.25	27.00	0.92	25.40	24.75	2.56
280	27.30	27.40	0.37	26.70	26.60	0.38	24.75	24.40	1.42
300	26.30	26.55	0.92	26.65	26.60	0.00	23.60	23.60	0.00

* h_e = Experimental height of water table

h_t = Theoretical height of water table

contd./

TABLE 6.4 (Continued)

R/K		.0173			.0066	
X cms	h_e cms	h_t cms	% diff:	h_e cms	h_t cms	% diff:
0	33.85	33.05	2.36	33.85	33.05	2.36
10	32.90	32.45	1.35	29.50	28.90	2.05
20	32.20	31.40	2.50	28.85	28.20	2.25
30	31.40	30.80	1.90	28.15	27.60	1.95
40	30.50	30.00	1.65	27.35	26.95	1.45
50	29.25	29.25	0.00	26.20	26.20	0.00
60	29.55	29.25	1.02	26.30	26.00	1.14
70	29.45	29.15	1.02	26.35	25.85	1.90
80	29.40	28.90	1.70	26.00	25.75	0.96
90	29.20	28.80	1.37	25.85	25.35	1.15
100	29.00	28.45	1.90	25.60	25.20	1.56
110	28.70	28.20	1.75	25.35	25.05	1.20
120	28.25	27.85	1.42	25.05	24.80	1.00
130	27.75	27.45	1.08	24.70	24.40	1.20
140	27.10	27.00	0.37	24.25	24.20	0.00
150	26.50	26.50	0.00	23.80	23.80	0.00
160	26.80	26.75	0.00	23.75	23.75	0.00
170	26.75	26.60	0.58	23.50	23.60	0.41
180	26.90	26.40	1.85	23.35	23.40	0.21
190	26.65	26.35	1.17	22.85	23.20	1.50
200	26.40	26.20	0.76	22.55	23.05	2.20
210	26.25	26.00	0.95	22.30	22.75	2.00
220	25.85	25.60	0.97	21.90	22.55	3.00
230	25.40	25.20	0.79	21.50	22.20	3.30
240	25.00	24.80	0.80	21.10	21.80	3.30
250	24.30	24.30	0.00	20.70	20.70	0.00
260	24.40	24.20	0.82	20.35	20.90	0.65
280	23.60	23.40	0.85	19.30	20.40	5.20
300	22.45	22.40	0.00	18.20	19.70	8.30

.....

more closely to the Dupuit assumptions implied in the solution than the latter. This is also evident from Tables 6.4 and 6.5. It may be observed that at the downstream impermeable boundary (i.e. at x = 0 in Tables 6.4 and 6.5) the difference between the experimental and theoretical heights of water table is 3.60 cms for the free discharging case (Table 6.5) compared to 1.10 cms for the submerged flow (Table 6.4). The large difference in the former may be due to the curvature of streamlines.

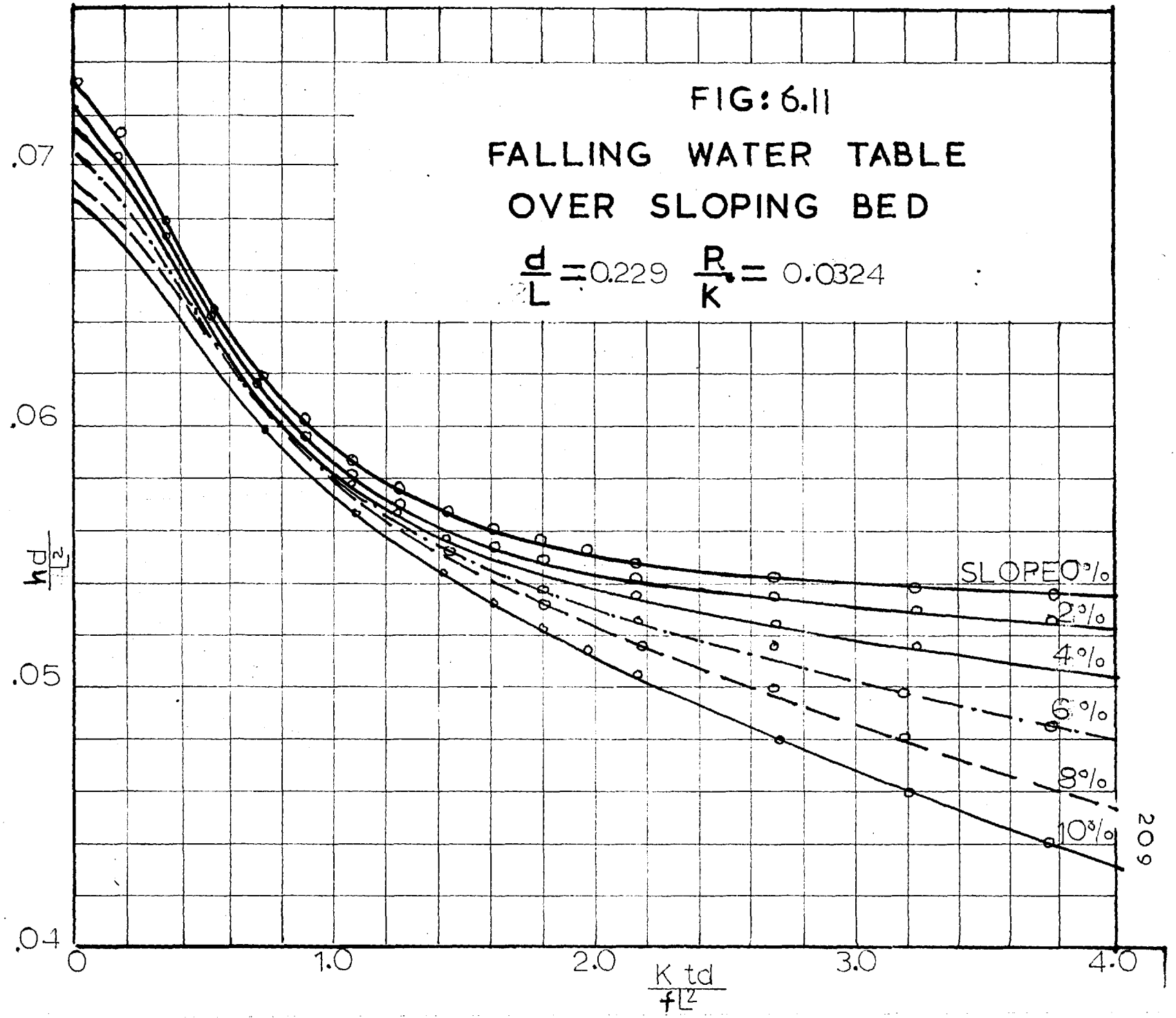
6.8 RESULTS FOR THE UNSTEADY STATE

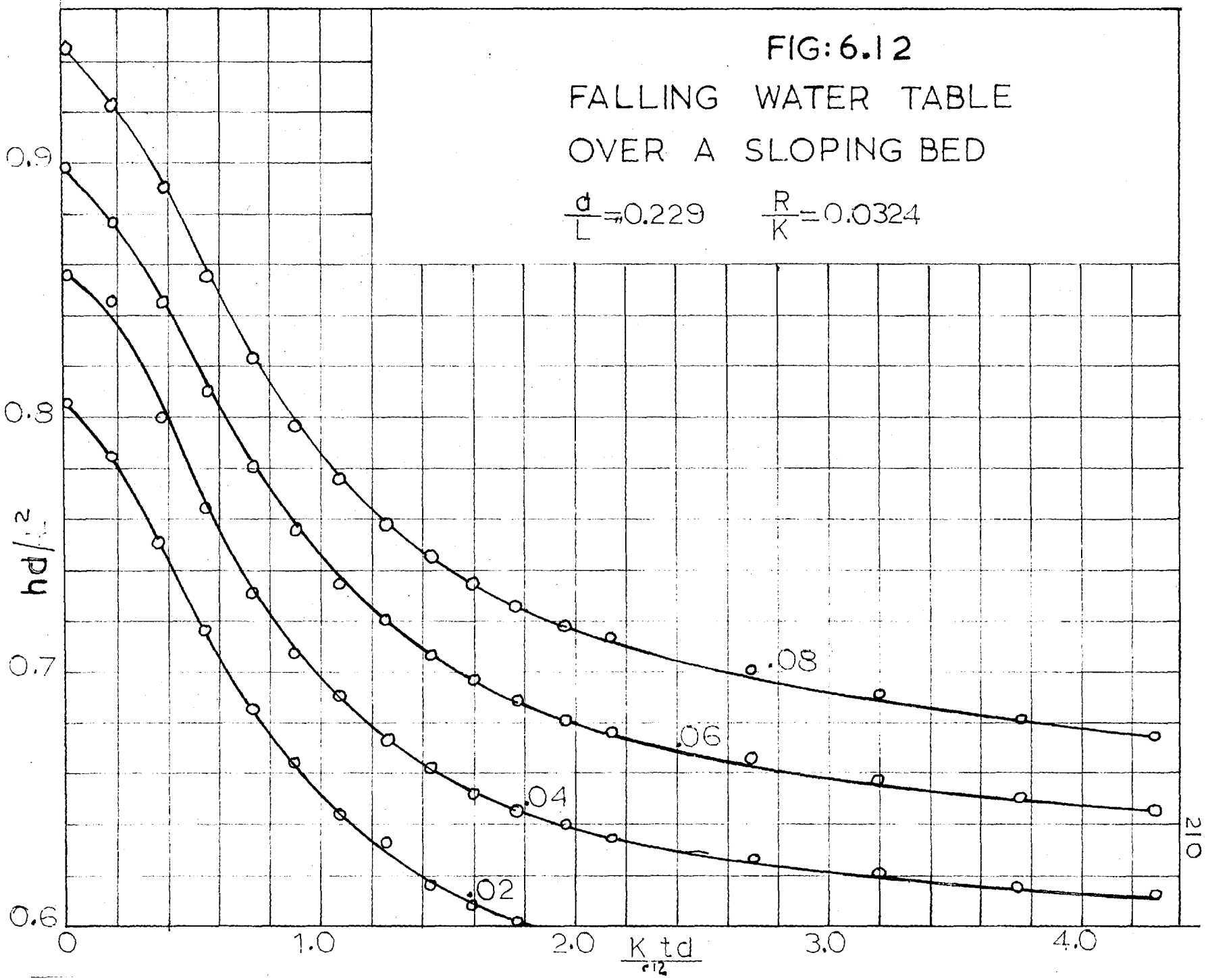
6.8.1 Submerged flow due to resistance to flow in the drains

6.8.1.1 Experimental results:

Fig. 6.11 (Table 6.6) shows a relationship between hd/fL^2 at the highest point on the water table in Zone II and Ktd/fL^2 for various values of bed slope. For a given Ktd/fL^2, hd/L^2 decreases with an increase in bed slope, that is, the water table falls more quickly in Zone II as α increases. A possible explaination for the decrease may be the increased hydraulic gradient due to the increase in bed slope.

Fig. 6.12 (Table 6.7) shows the rate of fall of water table at the downstream impermeable boundary (i.e. at X = 0 in Table 6.7) of the system. It should be noted that owing to the water table being highest at this boundary, it represents the critical point for the system examined herein. For a given Ktd/fL^2, hd/L^2 at


FIG: 6.11
FALLING WATER TABLE
OVER SLOPING BED
$\frac{d}{L}$ = 0.229 $\frac{R}{K}$ = 0.0324
.07
.06
.05
.04
$\frac{hd}{L^2}$
0
1.0
2.0
3.0
4.0
$\frac{K\,td}{fL^2}$
SLOPE 0%
2%
4%
6%
8%
10%
20%


FIG: 6.12
FALLING WATER TABLE
OVER A SLOPING BED
d/L = 0.229
R/K = 0.0324
0.9
0.8
0.7
0.6
hd/L²
0
1.0
2.0
3.0
4.0
K td / r12
.08
.06
.04
.02
210

this critical point also increases with the bed slope (Fig. 6.12).

6.8.1.2 Theoretical water table profile:

The theoretical water table profiles were obtained by programming (Appendix III) the solution derived in Section 6.4.3 for a digital computer. The weighted mean depth D and the heights H_o, H_L and $\Delta h_o(t)$ and $\Delta h_L(t)$ in any Zone, in a given time were fed in as data to obtain the water table profile in the whole Zone.

It may be noted that the drain spacings during the falling water table may not remain constant. For example, some time after the beginning of the recession process, the water table will fall below drain III (Fig. 6.3a) thereby increasing the length of Zone I from 150 cms to 150 cms. In this case, equation (6.18), which was previously applicable to Zone I only, will now apply to Zone I and II combined together. Similarly, equation (6.18) would be extended to Zone III as well, when drain II stops running.

The effect of the increased spacing on the rate of all of water table can be taken into account by measuring $\Delta h_o(t)$ and $\Delta h_L(t)$ with respect to the water table position that was existing at the time when a particular drain stopped running. However, since such experimental values of H_o and H_L could not be obtained precisely, the values immediately preceding those

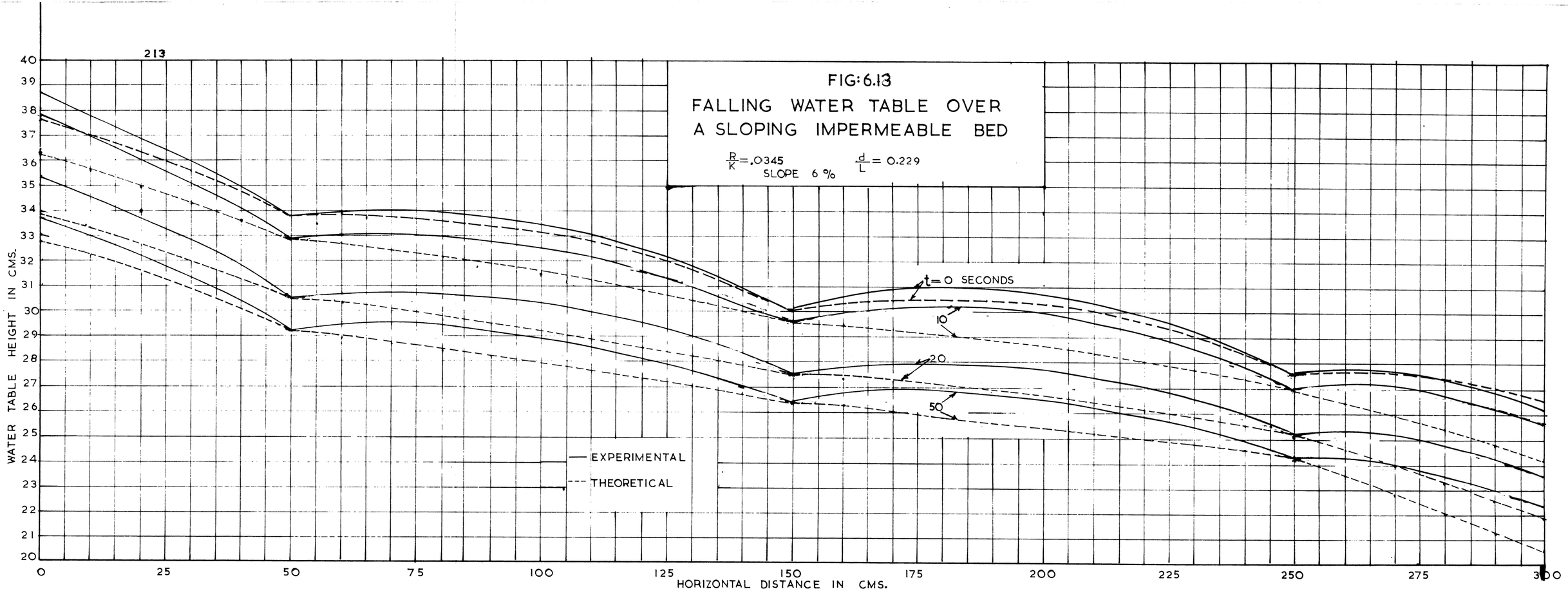
to be computed due to the increased spacing were considered instead. This introduced some error as will be seen later.

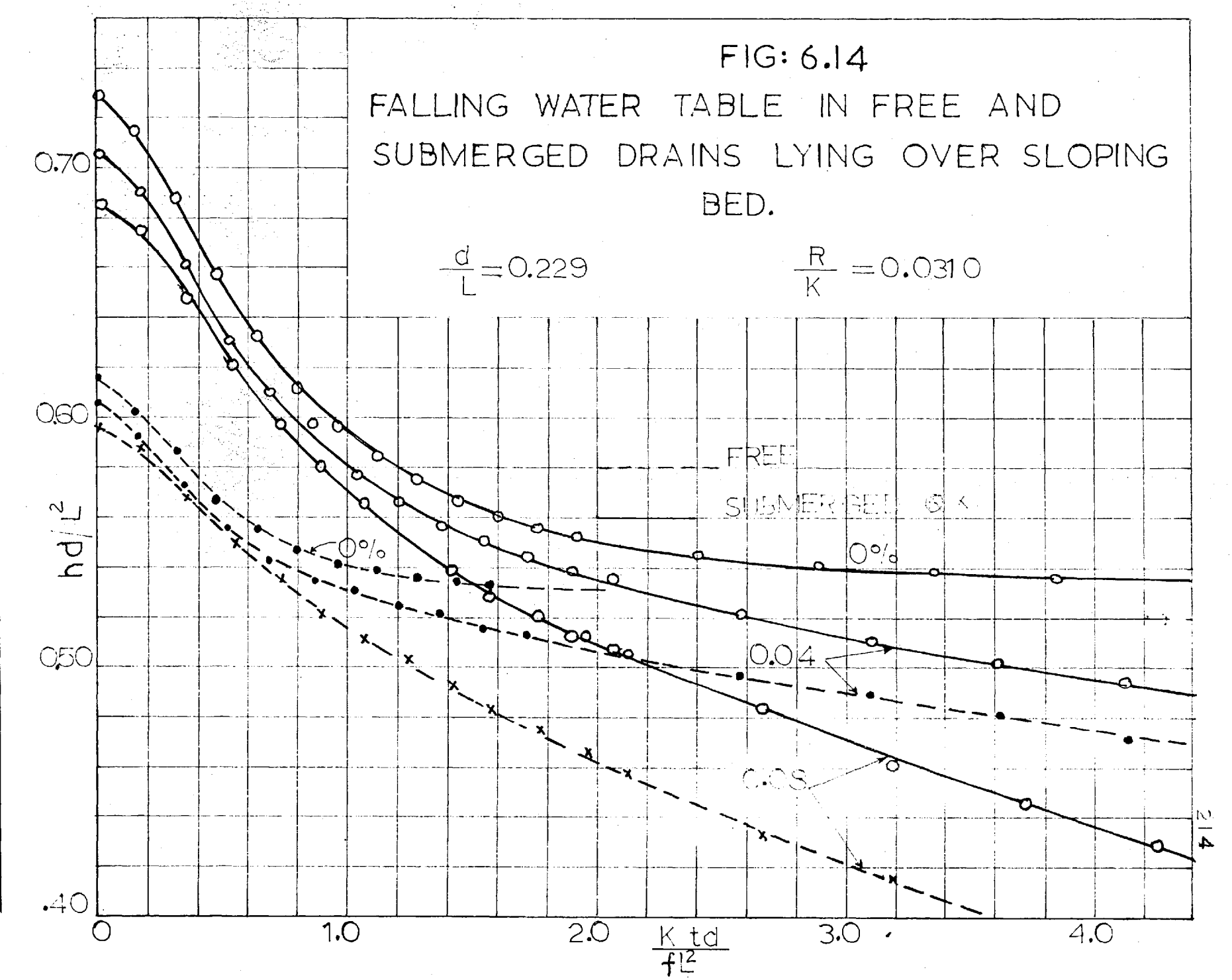
The experimental and theoretical water table profiles at a bed slope of 0.06 are compared in Fig. 6.13 (Table 6.8). Percentage difference between the experimental and theoretical results is of the order of less than 5% of the experimental height of water table, for time less than 80 secs. There is relatively large percentage difference (12%) in the distance 150-300 cms at times 80 and 110 seconds. This is due to the fact that the steady state water table profile considered in the computation was the one when the height of water table was 1.40 cms instead of zero above the bottom of the drain.

6.8.2 Free flow

Fig. 6.14(Table 6.9) shows a comparison of the rate of fall of water table over free discharging and submerged drains (due to resistance to flow in the drains). It is apparent in the figure that, for a given R/K, the initial steady state height of water table is much smaller in the free flow than in the submerged flow case. This is due to the fact that the resistance to flow in the drain is smaller in the former than in the latter case.

It was also observed in the experiment that under free flow condition, the discharge of drain I increased slightly


FIG: 6.13
FALLING WATER TABLE OVER A SLOPING IMPERMEABLE BED
R/K = .0345
SLOPE 6 %
d/L = 0.229
t = 0 SECONDS
10
20
50
EXPERIMENTAL
THEORETICAL
WATER TABLE HEIGHT IN CMS.
HORIZONTAL DISTANCE IN CMS.
40
39
38
37
36
35
34
33
32
31
30
29
28
27
26
25
24
23
22
21
20
0
25
50
75
100
125
150
175
200
225
250
275
300


FIG: 6.14
FALLING WATER TABLE IN FREE AND SUBMERGED DRAINS LYING OVER SLOPING BED.
d/L = 0.229
R/K = 0.0310
0.70
0.60
0.50
.40
hd/L²
FREE
SUBMERGED
0%
0%
0.04
0.08
0
1.0
2.0
3.0
4.0
K td / fL²

above that for the submerged case and there was corresponding decrease in the discharge of drain III. The discharge of the middle drain (drain II), however, remained constant. Table 6.2 shows the discharge of the three drains at different bed slopes.

6.9 CONCLUSIONS

Drainage of moderately sloping land with impermeable boundaries at upstream and downstream sides was investigated for different drain discharge conditions.

The experimental results show that the water table falls more slowly at the downstream impermeable boundary as bed slope increases. Further, the steady discharge of the middle drain in both the free and submerged flow conditions is found to be independent of the bed slope.

A mathematical solution based on evenly spaced ditches that reach to the sloping impermeable bed is proposed. The solution is based on the Boussinesq equation for unsteady flow in unconfined aquifers lying over a sloping impermeable bed. This solution is compared with the experimental data obtained on tile drains lying near the impermeable bed ($d/L = 0.23$).

In comparing the model results with the mathematical solution it is found that the solution based on fully penetrating ditches does not introduce appreciable error when applied to tile drain lying near the impermeable bed.

CHAPTER 7

SUMMARY OF CONCLUSIONS

In this Chapter the summary of conclusions is given in the sequence in which they have been discussed in the thesis (Chapters 5 & 6). The numbers in the brackets at the end of each paragraph refer to the Section in which the respective results have been discussed.

The term 'recession index' in this Chapter refers to the ratio Y/Y_m or h/h_m corresponding to one particular value of the time parameter $\sqrt{Ktd/fL^2}$ or Kt/fL (Section 5.7.1.1).

7.1 SYMMETRICAL DRAINAGE SYSTEM

(i) The recession index decreases at a diminishing rate with increasing steady state midpoint water table height Y_m. The recession index is practically unaffected by Y_m for $Y_m/d \geq 0.60$ or $Y_m/D \geq 0.45$ (5.7.1.1).

(ii) There is a considerable difference between the Glover solution and the experimental results at low Y_m/d. The difference, however, decreases with increasing Y_m/d. The closest fit between Glover's solution and experiment is obtained when $Y_m/d = 0.60$. This contradicts Glover's assumption that $Y_m \ll d$. On the basis

of the experimental results, the Glover solution holds for $Y_m/d \geq 0.60$ (5.7.1.2).

(iii) For $d/L = 0.0765$ and $Y_m/d = 0.60$, Glover's second equation (equation 4.5) fits better with the experimental results than his first equation (equation 4.3) (5.7.1.3).

(iv) At $Y_m/d = 0.60$, there is a close agreement between Kirkham's solution (Section 4.6.2) and the experimental results whereas Hammad's solution (Section 4.6.3), although based on the same assumption, bears no resemblance to the experimental results. Hammad's solution overestimates (predicts lower value of) the recession index (5.7.1.3).

(v) At $Y_m/d = 0.60$, Moody's iterative solution fits remarkably well with the experimental results after the experimental values are corrected for the effect of convergence. This solution has not been checked for other values of Y_m/d. Fig. 1 in Moody's paper (15), however, shows a similar trend for the effect of Y_m/d on the recession index as is stated in Section 7.1(i).(5.7.1.3).

(vi) Comparison has also been made of Isherwood's results for $Y_m/d \simeq 0.86$ with the experimental results for $Y_m/d = 0.60$ ($d/L = 0.0765$ in both cases). A good fit supports the conclusion previously stated in Section 7.1 (ii). (5.7.1.3).

(vii) Further research is needed to show the effect of the

ratio of depth of flow to drain spacing (d/L) on the midpoint water table recession. The main object would be to check Glover's solution by taking $Y_m/d = 0.60$ or $Y_m/D = 0.45$. Maasland (5) carried out such a study using $Y_m/D = 0.25$. In view of the above conclusion, however, it is believed that this value of Y_m/d might have been one of the reasons for not obtaining any good fit between Glover's solution and the experimental results even for such a small value of d/L as 0.035.

(viii) Drainage characteristics are independent of the depth of the impermeable bed below the drain axis once the depth is 0.125 L or more. The same conclusion was reached by Isherwood (Section 4.4) on the basis of the results of computer solutions of the Laplace equation. This conclusion holds for all values of the initial steady state water table height Y_m. (5.7.1.4).

(ix) The effect of drain size on the recession index is studied within the range $0.00585 \leq r/d \leq 0.0145$. The results were compared with the solutions by Hammad (Section 4.6.3) and Kirkham (Section 4.6.2). The experimental results indicate that the recession index is affected considerably in the range $0.00585 \leq r/d \leq 0.01$[illegible]. Kirkham's solution agrees well with the experimental results in the range $0.0116 \leq r/d \leq 0.0145$ whereas Hammad's solution overestimates the recession index.

For a further confirmation of the close agreement between Kirkham's solution and the experimental results, the falling water table profiles were compared with those obtained from Kirkham's solution (Section 4.6.2). Except at t = 0, the experimental and the analytical water table profiles almost coincide, thus suggesting that Kirkham's solution can be used even in those cases where the drains are submerged due to resistance to flow in the drains. (5.7.1.5 & 5.7.1.6)

7.1.2 Falling water table between submerged drains

(i) Kirkham's solution for unsteady flow between submerged drains (Section 4.6.2) is critically examined and checked with the experimental data obtained in the Hele-Shaw model (Section 5.7.2). The results illustrate that the Kirkham solution predicts a lower recession index than the actual. The solution, however, agrees remarkably well with the experimental results for zero submergence ratio. This further confirms the conclusions reached in Section 7.1 (ix). (5.7.2)

(ii) The Kirkham analytical results show that the recession index decreases at a diminishing rate with increasing submergence ratio. (5.7.2)

7.1.3 Rising water table

(i) Y/Y_m, for a fixed value of $\sqrt{Ktd/fL^2}$, increases but

at progressively lower rates as R/K increases.

(ii) The experimental data for the rising water table were compared with the water table drawdown (Y_m - Y). The results indicate that the rising water table takes approximately 90% as much time to reach a steady state condition as the falling water table takes to reach the drain centre. This is in contrast to the common assumption made in drainage design that the water table rises to a steady state condition instantaneously.

(iii) A study of the effect of the depth of the impermeable bed on the midpoint rising water table showed that the conclusions reached for the falling water table (Section 7.2.1 viii) again hold. (5.7.3.2)

7.2 MISALIGNED DRAINAGE SYSTEM: DRAIN RUNNING UNDER BACK PRESSURE DUE TO RESISTANCE TO FLOW IN THE DRAIN.

(i) The misaligned drainage system used represents a symmetrical section out of an infinite number of drains of which every 5th and 7th drain is alternately displaced vertically downwards. It was found that the displacement has a considerable effect on the recession index at a point midway between the displaced drains. (5.8.4)

(ii) By increasing the displacement from zero to 21% of the depth of the impermeable bed, the water table midway between every 7th displaced drain reaches the level of the symmetrical drains in half the time of that it takes in the symmetrical drainage system. (5.8.4)

(iii) There is a change in the recession index as the water table falls below the level of the symmetrical drains . (5.8.4)

7.3 DRAINAGE OVER A MODERATELY SLOPING IMPERMEABLE BED

7.3.1 Steady state

(i) Drainage of moderately sloping land with the impermeable boundaries at the upper and lower ends was investigated. Three drains were used in the study. The drains ran under some back pressure due to resistance to flow in the drains. The experimental results show that with the increase in bed slope, the steady state water table rises at the lower impermeable boundary and falls at the upper impermeable boundary of the system. The bed slope does not affect the water table position at a distance 15% of the spacing downstream from the middle drain. (6.7.1.1.)

(ii) There is a linear relationship between the discharge of the two outer drains and the bed slope within the range tested. The discharge of the lowest drain (Fig. 6.3a) increases linearly with the bed slope whereas there is a corresponding decrease in the discharge of the highest drain. The discharge of the middle drain is almost constant. (6.7.1.1)

(iii) For the boundary conditions examined, there appears to be a linear relationship between the steady state water table heights (for different bed slopes) at the upper and lower impermeable

boundaries. (6.7.1.1)

(iv) Mathematical solutions (both for steady and unsteady states) based on the Boussineq equation for flow in unconfined aquifers lying over a moderately sloping impermeable bed is proposed. The maximum percentage difference between the steady state experimental and the analytical water table heights was of the order of 3 to 4% of the experimental heights. Maximum error occurs at the lower impermeable boundary. (6.7.1.2)

(v) The difference between the experimental and the analytical water table heights is greater in the case when the drains run free than when they are submerged due to resistance to flow in the drains. (6.7.2)

7.3.2 Unsteady state: Drain running under back pressure due to resistance to flow in the drain.

(i) After cessation of recharge, the water table at the lower impermeable boundary of the system falls at a slower rate with increasing bed slope. (6.8.1.1)

(ii) The percentage difference between the experimental and the analytical water table heights during the recession process is of the order of 5 to 12%. (6.8.1.2)

(6.7.2)

Finally, the most important conclusions to be drawn from the research described in this thesis are that the solutions of Hammad, Glover and

Kirkham do not hold for $Y_m < d$ as generally assumed. Accurate results from these solutions can be obtained for $Y_m/d \geq 0.60$.

Boussinesq's equation can be used to study the falling water table over tile drains lying near a moderately sloping impermeable bed ($d/L = 0.23$).

REFERENCES

1. Childs, E.C. (1946) The water table, equipotentials and stream lines in drained land. IV. Drainage of foreign water. Soil Science 62:183-192.

2. Luthin, J.N. (1957) Drainage of Agricultural lands. Amer. Soc. of Agronomy, Madison, Wisconsin. pp. 461-504.

3. Childs, E.C. & O'Donnell, T. (1951) The water table, equipotentials and streamlines in drained land. VI. The rising water table. Soil Science, Vol. 71, No. 3.

4. Childs, E.C. (1947) The water table, equipotentials and stream lines in drained land. V. Soil Science, 63:361-376.

4a. Childs, E.C. (1946) The water table, equipotentials and stream lines in drained land. III. Soil Science, 59:405-415.

5. Maasland, Dirk, E.L. (1967) Falling water table between tile drains. Journal of the Irrigation and Drainage Division: ASCE, June, 1967, pp. 9-.

6. Dumm, Lee. D. (1954) New formula for determining depth and spacing of subsurface drains in irrigated lands. Agricultural Engineer, Vol. 35, pp. 726-730.

7. Muskat, M. (1937) Flow of homogeneous fluids through porous media. McGraw Hill, New York,

8. Rumer, Ralph R., Jr. & Drinker, Philip A. (1966) Resistance to laminar flow through porous media. Journal of Hydraulic Division, ASCE, Vol. 92, No. HY5, Proc. paper 4914, Sept. 1966, pp.156-163.

9. Schilfgaarde, Jan Van (1965) Limitations of Dupuit-Forchheimer Theory in drainage.Transactions ASAE, pp 515-519.

10. Kirkham, Don (1960) An upper limit for the height of water table in drainage design formulae. Trans. Intern. Congress. Soil Science, 7th Congr. Madison 1, pp. 486-492.

11. Guoyon, G. (1964) Consideration Sur l'hydralique des nappes de drainage par canalisations souterrains. Bull. Tech: due Genie Rural 65.

12. Hantush, M. (1963) On the Validity of the Dupuit-Forchheimer well discharge formula. Journal of Geophysical Research, Vol. 68, pp 594-

13. Hammad, H. K. (1957) Drainage of a soil layer of finite thickness by means of a system of covered drains. Proc. 3rd Congress on Theoretical and Applied Mechanics, Indian Soc. of Theoretical & Applied Mech:

14. Hooghoudt, S.B. (1937) Bejdragen tot de Kennis van eenige natuurkundige ..... Versl. Landl. ond. 43: 495. Algemeene Landsdrumkkerij The Hague.

15. Moody, W.T. (1966) Non-linear differential equation of drain spacing. Journal of Irrigation and Drainage Div: ASCE, Vol. 92, June 1966. pp 1-9.

16. Maasland, Dirk, E.L. (1956) The relationship between permeability and discharge, depth and spacing of tile drains. Bulletin No. 1, Groundwater and Drainage Series, Water Conservation and Irrigation Commission, New South Wales.

17. Van Deemter, J.J. (1949) Results of mathematical approach to some flow problems connected with drainage and irrigation. Appl. Sci. Res. AII: 33-53.

18. Wesseling, Jans. (1964) A Comparison of the steady drain spacing formulas of Hooghoudt and Kirkham in connection with design practice. Journal of Hydrology, Vol. 2, pp 25-32.

19. Engelund, F. (1953) Mathematical discussion of drainage problems. Trans. Dan. Acad. Tech. Sci. 3.

20. Watson, K.K. (1960) A study of the determination of drain diameter in drainage theory. Australian Journal of Applied Science, Vol. 11, pp 108-121.

21. Kirkham, Don (1958) Seepage of steady rainfall through soil into drains. Trans. ACU. Vol. 39, pp.892-908.

22. Kirkham, Don (1960) An upper limit for the height of the water table in drainage design formulas. Trans. Intern. Congr. Soil Sci. 7th Congr. Madison 1: 486-492.

23. Wesseling, Jans (1964) The effect of using continuously submerged drains on drain spacings. Journal of Hydrology, Vol. 2, pp. 33-43.

24. Warrick, A.W. (1966) Discussion on Steady State theories for drainage. Journal of the Irrigation and Drainage Div. ASCE, Dec., 1966, pp. 75-83.

25. List (1963) Discussion on depth and spacing of tile drain system. Trans. ASCE, part III, Vol. 128.

26. Schilfgaarde, Van, Kirkham & Frevert (1956) Physical and mathematical theories of tile and ditch drainage and their usefulness in design. Iowa State College Research Bull. 436.

27. Dagan, G. (1964) Spacing of drains by an approximate method. Journal of the Irrigation and Drainage Division, ASCE, Vol. 90.

28. Toksoz, Sadiq & Kirkham, Don (1961) Graphical Solution and interpretation of new drain spacing formula. Journal of Geophysical Research, Vol. 66, pp.509-516.

29. Collis George, N. & Youngs, E.G. (1958) Some factors determining water table heights in drained homogeneous soils. Journal of Soil Science, Vol. 9, pp. 332-338.

30. El-Dujaili, A.M. (1963) The effect of free surface percolation of misalignment of horizontal line sinks. Ph.D. thesis, University of London.

31. Childs, E.C. (1960) The non-steady state of the water table in drained land. J.Geophys.Res. 65: 780-782.

32. Dumm, Lee D. (1964) Transient flow concept in sub-surface drainage. Its validity and use. Trans. ASAE, pp. 142-151.

33. Dumm, Lee D. & Wringer, R.J., Jr. (1964) Designing a subsurface drainage system in an irrigated area through use of the transient-flow concept. Proceedings ASAE, 1964.

34. Bouwer, H. & Schilfgaarde, Jan Van (1963) Simplified method of predicting fall of water table in a drained land. Trans. ASAE, pp. 238-.

35. Dumm, Lee D. (1964) Transient flow concept in subsurface drainage, its validity and use. Trans.ASAE, pp 142-151.

36. Brooks, R.H. (1961) Unsteady flow of ground water into drain tile. Journal of the Irrigation and Drainage Div: ASCE, Vol. 87, June, 1961, pp 27-37.

37. Emile Picards (1890) Memoire sur la theorie des equations aux derives patielles et la methode des approximations successives. Liovilles Journal de Mathematique, Series 4, Vol. 5.

38. Hauschild, W. & Kruse, G. (1960) Unsteady flow of ground water into surface reservoirs. Proceedings ASCE, Vol. 86, July 1960, pp. 13-.

39. Isherwood, J.D.. (1959) Water table recession in tile drained land. Journal of Geophysical Research, Vol. 64, pp 795-804.

40. Schilfgaarde, Jan Van (1963) Design of tile drainage for falling water tables. Journal of the Irrigation and Drainage Division, ASCE, Vol. 89, June, 1963.

41. Dumm, Lee D. (1963) Discussion on design of tile drainage for falling water tables. Journal of Irrigation and Drainage Div: ASCE, Dec. 1963, pp 53-.

42. Brooks, R.H. (1964) Discussion of tile drainage for falling water tables. Journal of Irrigation and Drainage Div: ASCE, March, 1964.

43. Kirkham, Don & Gaskel, R.E. (1951) Falling water table in tile and ditch drainage. Soil Science Soc. Amer. Proc: Vol. 15, pp 37-42.

44. Boumans, J.H. (1953) Het bepalen van de drainafstand met behulp van de boorgaten methode. Land bouwk. Tijdschr., 65, 82-104, 1953.

45. Kraijenhoff, Van de Leur, D.A. (1958) A study of nonsteady groundwater flow with special reference to reservoir coefficient. De Ingeniur, 70 B, pp 87-94.

46. Pollubarinova-Kochina (1962) Theory of groundwater movement. Princeton University Press, Princeton, N.J., p 500.

47. Ligon, J. T., Kirkham, Don & Johnson, H.P. (1964) The falling water table between open ditches. Proc. Soil Science Soc. Amer. Vol, pp 286-293.

47a. Ligon, J. T., Johnson, H.P., Kirkham, D. (1963) Glas bead glycerol model for studying falling water table between open ditch drains. Trans. ASAE, Vol. 6, 1963, pp. 61-64.

48. Hammad, H. K. (1962) Depth and spacing of tile drain system. Proc. ASCE, Vol. 88, No. IR.3, Part I.

49. Werner, P. (1957) Some problems in non-artesian ground-water flow. Trans. AGU, Vol. 38, pp 511-5[illegible]

50. Maasland, M. (1959) Water table fluctuations induced by intermittent recharge. Journal of Geophysical Research, Vol. 64, pp 549-.

51. Schilfgaarde, Jan (1965) Transient design of drainage systems. Journal of Irrigation and Drainage Div: ASCE, Sept. 1966, pp 82-.

52. Donnan, W.W. (1947) Model tests of a tile spacing formula. Soil Sci. Soc. Amer. Proc. 11, 131-136.

53. Childs, E.C. & Youngs, E.C. (1958) The nature of the drains channel as a factor in the design of land drainage system. Journal of Soil Science, Vol. 9, pp 316-331.

54. Luthin, J.N. (1953) An electrical resistance work solving drainage problems. Soil Sci. 75: 259-274.

55. Santing, G. (1957) A horizontal scale model, based on the viscous flow analogy, for studying ground water flow in an aquifer having storage, IASH, pp 105-114, General Assembly Toronto, 1957.

56. Dachler, R. (1936) Grundwasserströmung, Springer, Vienna, pp. 141.

57. Gunther, E. (1940) Lösung von grundwasseraufgaben mit Hilfe der Strömung in dünnen Schichten, Wasserkraft and Wasserwittschaft, Vol. 3, No. 3, pp 49-55.

58. Krul, W.W.J.M. & Liefrinck, F.A. (1946) Recent ground-water investigations in the Netherlands. Amsterdam, Elsevier.

59. Santing, G. (1951) Modele poure l'etude des problemes des l'ecoulement simultane des eaux souterraines douces et salecs, IASH, Vol. 2, pp 184-193.

60. Todd, D.K. (1954) Unsteady flow in porous media by means of a Hele-Shaw viscous fluid model. Trans. Amer. Geophysical Union, Vol. 35, No. 6, p. 905.

61. Marino, M.A.; (1965) Viscous flow model study of the rise and fall of a ground water mound. Water Resources Research, 1965.

62. Luthin, J.N., & Guitjens. (1965) Viscous model study of drain spacing of sloping land and comparison with mathematical solution. Water Resources Research, Vol. 1, pp. 523-530.

63. Streeter, V.L. (1966) Fluid Mechanics, Fourth edition, p.237. McGraw-Hill Book Company, N.Y.

64. Bouwer, H. (1962) Analysing ground water mounds by Resistance Network. ASCE, Journal of Irrigation & Drainage Division, pp 15-36, Sept. 1962.

65. Kirkham, Don (1947) Flow of ponded water into drain tubes in soil overlying an impermeable layer. Trans. AGU pp 369-385, 1947.

66. Gustafsson, Y. (1946) Untersuchungen über die strömungsverhaltnis- in gendrüntem Boden. Acta Agr. Succana 2(1): 1-157 (Stockholm).

67. Schmid, Paul & Luthin, James (1964) The drainage of sloping lands. J.G.R., 69(8), 1525-1529.

68. Guitjens, J. & Luthin, J.N. (1965) Viscous model study of drain spacing of sloping land and comparison with mathematical solution. Water Resources Research, Vol. 1, pp 523-530.

69. Luthin, J.N. & Guitjens, J.G. (1967) Transient solutions for drainage of sloping land. Journal of the Irrigation & Drainag. Div., ASCE, Vol. 93, Sept. 1967, pp 43-51.

70. Chauhan, H.S., Schwal, G.O. & Hamdy, M.Y. (1968) Analytical and Computer Solutions of transient water tables for drainage of sloping land, pp 573-.

71. Werner, D.W. (1957) Some problems in non-artesian ground water flow. Trans. AGU, Vol. 38, pp 511-518.

72. Hauschild, W. & Kruse, G. (1960) Unsteady flow of ground water into a surface reservoir. ASCE, Journal of the Hydraulics Division, July, 1960, pp 13-20.

73. Keller, Jack & Robinson, A.R. (1959) Model study of Interceptor drains. Proc: ASCE, HYD(Div.), Sept., 1959, pp 25-.

74. Carslaw, H.S. & Jaeger, J.C. Conduction of heat in solids, Oxford Univ. Press, London, 1948.

T A B L E S

TABLE 5.1

VARIATION OF VISCOSITY WITH TEMPERATURE

BS/U D-Type Viscometer

Coeffecient as per BSS/188 =0.1

Temperature ^{o}F	Average time secs	Kinematic visc: Centi-Stokes
54.0	503.5	50.35
61.2	475.2	47.52
64.4	429.5	42.95
66.2	405.0	40.50
68.0	386.1	38.61
69.9	362.5	36.25
73.4	339.8	33.98
77.0	305.0	30.50
81.9	268.0	26.80

.....

TABLE 5.2

COMPUTATION OF INTERSPACE

BY STATIC METHOD

Horiz:dist:cms	0	100	200	300		
Volume in ccs.	Static water level in cms.					
Initial	4.30	4.40	4.40	4.30	Mean diff: cms	b mms
250	8.55	8.60	8.60	8.55	4.20	1.98
250	12.90	12.85	12.85	12.85	4.30	1.95
250	17.20	17.20	17.15	17.20	4.35	1.93
250	21.40	21.40	21.40	21.40	4.20	1.98
250	25.60	25.70	25.70	25.70	4.30	1.95
250	29.95	30.00	29.95	29.95	4.25	1.97
250	34.20	34.20	34.15	34.15	4.20	1.98
250	38.45	38.45	38.40	38.40	4.15	1.99
250	42.65	42.60	42.60	42.60	4.20	1.98
250	46.80	46.80	46.75	46.75	4.20	1.98
250	50.95	51.00	50.95	50.95	4.20	1.98
250	55.00	55.10	55.05	55.05	4.15	1.99
250	59.10	59.10	59.10	59.10	4.05	2.04
250	63.25	63.25	63.25	63.25	4.15	1.99

Mean = 1.98 mms

.....

TABLE 5.3

EFFECT OF INITIAL DEPTH OF WATER TABLE ON THE RATE OF RECESSION

$d/L = 0.0765$

Y_m/d	0.05	0.10	0.20	0.40	0.50	0.60
Time	Y	Y	Y	Y	Y	Y
secs.	cms	cms	cms	cms	cms	cms
0	1.14	2.30	4.53	9.12	11.45	13.70
10	1.135	2.28	4.38	8.70	10.85	12.95
20	1.13	2.24	4.23	8.00	9.55	11.70
30	1.11	2.15	4.05	7.10	8.45	10.10
40	1.10	2.05	3.78	-	7.50	8.85
50	1.08	1.98	3.56	5.70	-	7.80
60	1.06	1.90	3.32	5.15	5.90	6.80
70	1.03	1.81	3.10	4.65	5.25	6.10
80	1.00	1.72	2.90	4.20	4.65	5.35
90	0.96	1.65	2.70	3.75	4.20	4.75
100	0.92	1.55	2.50	3.40	3.75	4.22
110	0.89	1.50	2.33	3.10	3.40	3.80
120	0.85	1.40	2.21	2.75	3.10	3.42
150	0.77	1.20	1.75	2.22	2.30	2.60
180	0.70	1.02	1.44	1.73	1.90	2.00
210	0.63	0.90	1.21	1.40	1.45	1.55
240	0.56	0.77	1.00	1.15	1.20	1.25
270	0.51	0.66	0.84	0.95	0.97	0.92
300	0.46	0.57	0.73	0.83	0.82	0.80

.....

TABLE 5.4

COMPARISON OF EXPERIMENTAL RESULTS WITH UNSTEADY STATE SOLUTIONS

$Y_m/d = 0.60$, $d/L = 0.0765$

Time secs.	Expt: Y cms	Hammad Y cms	Kirkham Y cms	Glover Y cms	Brooks Y cms
0	13.70	13.70	13.70	13.70	13.70
20	11.70	7.35	10.50	9.38	10.80
40	8.85	3.93	7.95	5.51	6.90
60	6.80	2.11	6.10	3.23	5.30
80	5.35	1.13	4.60	1.89	3.80
100	4.22	0.607	3.56	1.11	2.60
120	3.42	0.326	2.74	0.65	1.81
150	2.60	0.175	1.92	0.34	0.61
180	2.00	0.094	1.37	0.21	0.34
210	1.55	0.050	0.80	-	-
240	1.25	0.027	-	-	-
270	0.92	0.014	-	-	-
300	0.80	0.008	-	-	-

.....

TABLE 5.4 (Continued)

	Expt:	Moody	Isherwood $Y_m/d = 6/8$ $d/L = 0.080$
Time secs	Y cms	Y cms	Y cms
0	13.70	13.70	13.70
20	11.70	10.60	11.50
40	8.85	7.55	8.75
60	6.80	5.60	6.65
80	5.35	4.10	5.06
100	4.22	2.81	
120	3.42	2.26	
150	2.60	1.51	
180	2.00	1.10	
210	1.55	0.685	
240	1.25	0.480	
270	0.92	0.342	
300	0.80	0.206	

.....

TABLE 5.6

EFFECT OF THE DEPTH OF IMPERMEABLE BED ON WATER TABLE RECESSION

$Y_m/L = 0.0337$

d/L	0.0765	0.103	0.123	0.143
Time	Y	Y	Y	Y
secs	cms	cms	cms	cms
0	10.05	10.10	10.10	10.10
10	9.35	9.35	9.40	9.45
20	8.40	8.25	8.25	8.25
30	7.45	7.10	7.00	7.00
40	-	6.10	5.85	5.90
50	5.75	5.25	5.10	5.15
60	5.10	4.55	4.45	4.45
70	4.55	4.10	3.95	3.90
80	4.00	3.55	3.45	3.40
90	3.53	3.10	2.95	2.95
100	3.25	2.80	2.60	2.55
110	2.95	2.50	2.30	2.30
120	2.60	2.25	2.10	2.05
150	2.02	1.65	1.55	1.57
180	1.62	1.30	1.20	1.15
210	1.30	1.05	0.90	0.90
240	1.07	0.83	0.75	0.73
270	0.90	0.70	0.64	0.63
300	0.80	0.62	0.57	0.53

.....

TABLE 5.7

EFFECT OF DEPTH OF IMPERMEABLE BED ON WATER TABLE RECESSION

$Y_m/L = 0.008$

d/L	0.073	0.103	0.123	0.143
Time	Y	Y	Y	Y
secs.	cms	cms	cms	cms
0	2.38	2.42	2.42	2.42
10	2.35	2.38	2.35	2.35
20	2.31	2.28	2.25	2.25
30	2.26	2.20	2.10	2.10
40	2.18	2.00	2.00	2.00
50	2.11	1.90	1.85	1.83
60	2.00	1.80	1.73	1.70
70	1.91	1.70	1.62	1.60
80	1.80	1.62	1.50	1.47
90	1.72	1.52	1.40	1.37
100	1.64	1.42	1.30	1.30
110	1.57	1.33	1.22	1.21
120	1.50	1.25	1.15	1.12
150	1.28	1.03	0.92	0.90
180	1.10	0.90	0.75	0.77
210	0.96	0.80	0.65	0.60
240	0.83	0.65	0.56	0.58
270	0.72	0.56	0.50	0.52
300	0.64	0.48	0.45	0.45

.....

TABLE 5.8

EFFECT OF DRAIN SIZE ON WATER TABLE RECESSION

$d/L = 0.143$ $Y_m/d = 0.32$

r/d	0.00585	0.0116	0.0145
Time	Y	Y	Y
secs.	cms	cms	cms
0	13.70	13.70	13.70
10	13.15	12.70	12.40
20	12.35	11.00	10.65
30	11.50	9.30	9.00
40	10.65	8.00	7.55
50	9.90	6.90	6.40
60	9.15	5.95	5.50
70	8.45	5.15	4.80
80	7.75	4.45	4.15
90	7.10	3.90	3.55
100	6.50	3.40	3.10
110	6.05	3.00	2.70
120	5.55	2.70	2.40
150	4.40	1.90	1.70
180	3.60	1.45	1.25
210	2.80	1.15	0.95
240	2.30	0.95	0.75
270	1.90	0.75	0.60
300	1.60	0.65	0.50

.....

TABLE 5.9

COMPARISON BETWEEN COMPUTED AND EXPERIMENTAL RESULTS

TO SHOW THE EFFECT OF DRAIN SIZE

$d/L = 0.143$ $\quad Y_m/d = 0.32$

r/d		0.00585			0.0116			0.0145	
Time	Y_e*	Y_h*	Y_k*	Y_e	Y_h	Y_k	Y_e	Y_h	Y_k
sec.	cms	cms	cms	cms	cms	cms	cms	cms	cms
0	13.70	13.70	13.70	13.70	13.70	13.70	13.70	13.70	13.70
20	12.35	7.82	10.70	11.00	7.27	10.45	10.65	7.08	10.30
40	10.65	4.46	8.30	8.00	3.86	7.90	7.55	3.66	7.70
60	9.15	2.55	6.50	5.95	2.05	6.00	5.50	1.90	5.80
80	7.75	1.45	5.10	4.45	1.10	4.50	4.15	0.98	4.35
100	6.50	0.83	3.90	3.40	0.58	3.35	3.10	0.51	3.30
120	5.55	0.47	3.10	2.70	0.31	2.60	2.40	0.26	2.45
140	4.80	0.27	2.35	2.20	0.16	1.95	1.92	0.14	1.85
160	4.10	0.15	1.90	1.71	0.09	1.50	1.50	0.07	1.35
180	3.60	0.90	1.50	1.45	0.05	1.10	1.25	0.04	1.00
200	3.02	0.05	1.10	1.17	0.03	0.85	0.99	0.02	0.72
220	2.60	0.03	0.85	1.03	0.02	0.62	0.82	0.01	0.60
240	2.30	0.02	0.70	0.95	0.01	0.50	0.75	0.00	0.42

* Y_e = Experimental water table height.
Y_h = Hammad's theoretical water table height.
Y_k = Kirkham's theoretical water table height.

.....

TABLE 5.11

COMPARISON BETWEEN EXPERIMENTAL AND THEORETICAL WATER TABLE PROFILE

R/K = 0.023 d/L = 0.0765

Y_c = Computed value

Y_e = Experimental value

x/L	0.500		0.300		0.267	
$F_1(x,0)$	4.978		4.458		4.271	
Time secs.	Y_e cms	Y_c cms	Y_e cms	Y_e cms	Y_e cms	Y_c cms
0	13.70	13.70	12.65	12.31	12.20	11.79
43	8.20	8.20	7.37	7.35	7.15	7.05
54	7.15	7.15	6.35	6.50	6.15	6.10
64	6.10	6.10	5.57	5.56	5.33	5.20
74	5.45	5.45	4.85	4.85	4.70	4.65
85	4.85	4.85	4.25	4.35	4.10	4.17
95	4.18	4.18	3.80	3.76	3.65	3.60
105	3.80	3.80	3.35	3.42	3.25	3.27
115	3.45	3.45	3.00	3.10	2.85	2.97
126	3.12	3.12	2.70	2.73	2.55	2.67

.....

TABLE 5.11 (Continued)

x/L	0.234		0.200		0.167	
$F_1(x,0)$	4.055					
Time secs.	Y_e cms	Y_c cms	Y_e cms	Y_c cms	Y_e cms	Y_c cms
0	11.75	11.20	11.10	10.05	10.45	9.75
43	6.70	6.70	6.35	6.27	5.96	5.83
54	5.85	5.78	5.55	5.44	5.15	5.02
64	5.10	4.94	4.80	4.62	4.40	4.29
74	4.45	4.40	4.17	4.13	3.95	3.84
85	3.90	3.96	3.75	3.71	3.40	3.45
95	3.40	3.42	3.25	3.20	3.13	2.97
105	3.05	3.10	2.85	2.90	2.75	2.70
115	2.75	2.82	2.55	2.64	2.45	2.45
126	2.25	2.54	-	2.38	2.16	2.21

TABLE 5.11 (Continued)

x/L	0.150		0.133		0.117	
$F_1(x,0)$	3.375		3.214		3.055	
Time secs.	Y_e	Y_c	Y_e	Y_c	Y_e	Y_c
0	10.05	9.32	9.65	8.88	9.30	8.43
43	5.70	5.56	5.47	5.30	5.20	5.04
54	4.95	4.80	4.80	4.56	4.55	4.35
64	4.29	4.11	4.15	3.90	4.00	3.71
74	3.80	3.68	3.67	3.50	3.45	3.32
85	3.30	3.29	3.20	3.14	3.05	2.98
95	3.00	2.84	2.85	2.70	2.70	2.57
105	2.65	2.58	2.50	2.46	2.40	2.33
115	2.35	2.34	2.25	2.24	2.15	2.12
126	2.13	2.11	2.07	2.01	2.00	1.91

TABLE 5.11 (Continued)

x/L	0.100		0.0835		0.0668	
$F_1(x,0)$	2.875		2.638		2.481	
Time secs.	Y_e cms	Y_c cms	Y_e cms	Y_e cms	Y_e cms	Y_c cms
0	8.65	7.94	8.05	7.40	7.45	6.82
43	4.85	4.74	4.70	4.45	4.25	4.10
54	4.25	4.10	4.10	3.84	3.70	3.54
64	3.75	3.50	3.50	3.27	3.20	3.02
74	3.25	3.13	3.05	2.92	2.85	2.70
85	2.90	2.87	2.70	2.62	2.45	2.42
95	2.55	2.42	2.40	2.27	2.20	2.09
105	2.25	2.20	2.10	2.05	2.00	1.87
115	2.00	1.99	1.80	1.85	1.75	1.72
126	1.85	1.80	1.75	1.61	1.65	1.55

TABLE 5.12

EFFECT OF DRAIN SUBMERGENCE ON WATER TABLE RECESSION

$d/L = 0.0765$ $Y_m/d = 0.52$

Y_1/H_2	0.00	0.167	0.268	0.334
Time	Y	Y	Y	Y
secs.	cms	cms	cms	cms
0	12.10	12.10	12.10	12.10
10	11.35	11.35	11.25	11.25
20	10.10	10.00	9.90	9.85
30	8.90	8.80	8.70	8.70
40	7.90	7.80	7.60	7.50
50	-	-	-	-
60	6.35	6.25	6.15	5.95
70	5.50	5.40	5.20	5.05
80	4.90	-	-	-
90	4.45	4.20	4.02	3.90
100	3.95	3.75	3.60	3.45
110	3.70	3.45	3.35	3.20
120	3.30	3.05	2.90	2.80
150	2.55	2.30	2.15	2.05
180	2.05	1.75	1.65	1.55
210	1.65	1.40	1.30	1.15
240	1.40	1.25	1.05	0.95
270	1.20	1.00	0.90	0.80
300	0.95	0.75	0.70	0.65

.....

TABLE 5.13

COMPARISON OF COMPUTED AND EXPERIMENTAL RESULTS TO SHOW THE EFFECT OF DRAIN SUBMERGENCE

$d/L = 0.0765$ $Y_m/d = 0.52$

Y_1/H_2	0.00		0.167		0.334	
Time secs.	Y_e cms	Y_k cms	Y_e cms	Y_k cms	Y_e cms	Y_k cms
0	12.10	12.10	12.10	12.10	12.10	12.10
20	10.10	9.75	10.00	9.10	9.85	8.70
40	7.90	7.90	7.80	6.80	7.55	6.30
60	6.35	6.30	6.25	5.10	5.95	4.50
80	4.90	5.10	-	3.80	-	3.30
100	3.95	4.10	3.75	2.85	3.45	2.35
120	3.30	3.30	3.05	2.10	2.80	1.70
140	2.78	2.70	2.54	1.60	2.23	1.20
160	2.37	2.15	2.06	1.20	1.82	0.90
180	2.05	1.75	1.75	0.90	1.55	0.63
200	1.80	1.40	1.55	0.60	1.25	0.45
220	1.57	1.15	1.35	0.50	1.05	0.35
240	1.40	0.90	1.25	0.35	0.95	-

.....

Y_e = Experimental height of water table

Y_k = Kirkham's theoretical water table height

TABLE 5.14

EFFECT OF RATE OF RAINFALL ON RISING WATER TABLE

$d/L = 0.0765$

R/K	0.00286	0.00545	0.0138	0.179	0.023
Y_m/d	0.10	0.20	0.40	0.50	0.60
Time	Y	Y	Y	Y	Y
secs.	cms	cms	cms	cms	cms
0	0.00	0.00	0.00	0.00	0.00
10	0.02	0.02	0.12	0.15	0.85
20	0.04	0.04	0.55	0.85	1.45
30	0.07	0.12	1.50	2.10	3.25
40	0.12	0.32	2.25	3.45	5.00
50	0.18	0.60	3.20	4.70	6.90
60	0.23	0.95	4.20	5.90	8.50
70	0.32	1.22	5.30	6.90	9.70
80	0.40	1.57	-	7.90	10.60
90	0.50	1.85	6.60	8.55	11.25
100	0.61	2.20	7.10	9.10	11.80
110	0.71	2.48	7.45	9.60	12.20
120	0.78	2.75	7.80	9.95	12.55
150	1.05	3.40	8.46	10.50	13.20
180	1.30	3.81	8.80	10.95	13.55
210	1.50	4.10	8.95	11.12	13.65
240	1.67	4.28	9.08	11.25	13.70
270	1.80	4.38	9.12	-	-
360	2.04	4.52	-	-	-
600	2.25	-	-	-	-

.....

TABLE 5.16

EFFECT OF DEPTH OF IMPERMEABLE BED ON RISING WATER TABLE

d/L	0.0765	0.103	0.123	0.143
Time	Y	Y	Y	Y
secs.	cms	cms	cms	cms
0	0.00	0.00	0.00	0.00
10	..	0.40	0.60	0.45
20	0.85	0.60	2.25	1.75
30	1.95	2.85	3.85	3.20
40	3.35	4.45	5.30	4.80
50	4.50	5.65	6.40	6.00
60	5.60	6.70	7.30	7.10
70	-	7.50	7.90	7.80
80	7.40	8.20	8.45	8.40
90	7.95	8.70	8.85	8.80
100	8.30	9.10	9.20	9.20
110	8.65	9.35	9.45	9.40
120	8.95	9.55	9.60	9.60
150	9.50	10.00	9.90	9.90
180	9.80	10.12	10.02	10.02
210	9.97	10.17	10.10	10.10
240	10.04	-	-	-

.....

TABLE 5.17

EFFECT OF VERTICAL DISPLACEMENT OF TILE DRAIN ON FALLING WATER TABLE

$d/L = 0.86$ $\quad h_m/d = 1.08$

dY	0.00	0.07	0.117	0.163	0.21
Time secs.	h cms	h cms	h cms	h cms	h cms
0	46.60	46.60	46.60	46.60	46.60
10	45.80	45.80	45.70	45.70	45.70
20	44.85	44.80	44.75	44.65	44.60
30	44.25	44.10	44.00	43.85	43.70
40	43.75	43.60	43.50	43.40	43.20
50	43.60	43.40	43.25	43.00	42.75
60	43.50	43.25	43.05	42.55	42.10
70	43.40	43.15	42.75	42.15	41.55
80	43.32	43.00	42.45	41.75	41.00
90	43.25	42.85	42.15	41.25	40.30
100	43.20	42.65	41.85	40.85	39.90
110	43.15	42.50	41.55	40.45	39.40
120	43.10	42.35	41.30	40.10	39.00
150		41.90	40.40	39.20	37.80
180		41.55	40.05	38.50	36.95
210		41.30	39.60	37.05	36.35
240		-	-	-	-

.....

TABLE 5.18

EFFECT OF VERTICAL DISPLACEMENT OF TILE DRAIN ON THE FALLING WATER TABLE AT THE LEFT AND RIGHT HAND EDGES

$d/L = 0.86$ $\quad h_m/d = 1.08$

$\Delta Y/d$	0.07		0.21	
Time	Left	Right	Left	Right
secs.	h(cms)	h(cms)	h(cms)	h(cms)
0	46.60	46.60	46.60	46.60
10	45.80	45.80	45.70	45.40
20	44.80	44.70	44.60	44.10
30	44.10	43.90	43.70	43.10
40	43.60	43.45	43.20	42.20
50	43.40	43.20	42.75	41.40
60	43.25	43.00	42.10	40.60
70	43.15	42.80	41.55	40.00
80	43.00	42.60	41.00	39.40
90	42.85	42.40	40.30	38.90
100	42.65	42.20	39.90	38.40
110	42.50	42.10	39.40	38.00
120	42.35	41.90	39.00	37.65
150	41.90	41.55	37.80	36.80
180	41.55	41.30	36.95	36.20
210	41.30	41.05	36.35	35.70

.....

TABLE 6.1

EFFECT OF BED SLOPE ON THE STEADY STATE WATER TABLE PROFILES

d = 22.90 cms r = 0.25 cms

Bed slope	0.00	0.02	0.04	0.06	0.08	0.10
X cms	Water table height in cms					
0	31.80	34.00	36.00	38.30	40.40	42.70
10	31.65	33.50	35.20	37.35	38.90	41.10
20	31,45	33.15	34.70	36.50	38.00	39.65
30	31.30	32.70	33.95	35.60	36.95	38.60
40	30.60	32.00	33.20	34.45	35.55	36.95
50	30.10	31.20	32.00	33.25	34.40	35.50
60	30.65	31.55	32.35	33.25	34.10	35.00
70	31.25	32.00	32.60	33.70	34.15	34.80
80	31.45	32.30	32.75	33.65	33.90	34.45
90	31.[illegible]	32.15	32.50	33.10	33.50	34.05
100	31.80	32.15	32.35	32.70	33.15	33.70
120	31.45	31.50	31.55	31.90	32.05	32.30
140	30.60	30.30	30.20	30.20	30.20	30.40
150	30.10	29.80	29.60	29.40	29.30	29.30
160	30.60	30.20	29.95	29.80	29.60	29.55
180	31.45	31.00	30,40	30.20	29.80	29.60
200	31.80	31.00	30.25	29.70	29.20	28.80
220	31.45	30.60	29.60	28.95	28.25	27.80
240	30.60	29.65	28.60	27.80	26.65	26.35
250	30.10	29.00	27.85	27.00	25.85	25.10
260	30.60	29.50	28.25	27.20	25.95	25.00
280	31.45	30.00	28.10	26.70	25.00	23.65
300	31.80	29.50	27.35	25.50	23.45	21.70

.....

TABLE 6.2

VARIATION OF DRAIN DISCHARGE WITH BED SLOPE

d/L = 0.229 r = 0.25 cm.

Description	Slope 0.00	0.02	0.04	0.06	0.08	0.10
	Drain discharge in cc/min					
Drain I						
Submerged	285.0	315.0	348.0	382.0	415.0	453.0
Q/Kd^2	0.00127	0.0014	0.00152	0.00161	0.00174	0.00191
Free	285.0	320.0	365.0	408.0	463.0	505.0
Drain II						
Submerged	280.0	280.0	277.0	277.0	277.0	277.0
Q/Kd^2	0.00127	0.00124	0.00121	0.00117	0.00117	0.00117
Free	285.0	285.0	285.0	285.0	280.0	280.0
Drain III						
Submerged	280.0	245.0	213.0	172.0	141.0	105.0
Q/Kd^2	0.00127	0.00109	0.00093	0.000725	0.000595	.0044
Free	285.0	240.0	190.0	150.0	106.0	68.0

.....

TABLE 6.3

COMPARISON BETWEEN EXPERIMENTAL AND THEORETICAL STEADY STATE WATER TABLE PROFILES AT VARIOUS BED SLOPES

R/K = 0.031 d/L = 0.229

Slope	0.00		0.02		0.04	
X	h_e	h_t	h_e	h_t	h_e	h_t
cms	cms	cms	cms	cms	cms	cms
0	31.80	31.40	34.00	33.37	36.00	35.10
10	31.65	31.30	33.50	33.63	35.20	34.70
20	31.45	31.20	33.15	32.80	34.70	34.15
30	31.30	30.95	32.70	32.37	33.95	33.53
40	30.60	30.60	32.00	31.84	33.20	32.81
50	30.10	30.10	31.20	31.20	32.00	32.00
60	30.60	30.60	31.55	31.51	32.35	32.20
70	31.30	30.95	32.00	31.72	32.60	32.30
80	31.45	31.20	32.30	31.82	32.75	32.30
90	31.65	31.30	32.00	31.83	32.50	32.20
100	31.80	31.40	32.15	31.75	32.35	32.02
120	31.45	31.20	31.50	31.27	31.55	31.35
140	30.60	30.60	30.30	30.40	30.20	30.30
150	30.10	30.10	29.80	29.80	29.60	29.60
160			30.20	30.20	29.95	29.90
180			31.00	30.64	30.40	30.17
200			31.00	30.68	30.25	30.03
230			30.20	29.99	29.25	29.05
250			29.00	29.00	27.85	27.85
300			29.50	29.36	27.35	27.34

h_e = Experimental water table heights

h_t = Analytical water table heights

TABLE 6.3 (continued)

Slope	0.06		0.08		0.10	
X cms	h_e cms	h_t cms	h_e cms	h_t cms	h_e cms	h_t cms
0	38.30	37.28	40.40	39.36	42.70	41.41
10	37.35	36.65	38.90	38.54	41.10	40.40
20	36.50	35.95	38.00	37.65	39.65	39.30
30	35.60	35.15	36.95	36.65	38.60	38.15
40	34.45	34.25	35.55	35.57	36.95	36.86
50	33.25	33.25	34.40	34.40	35.50	35.50
60	33.25	32.30	34.10	34.30	35.00	35.26
70	33.70	33.23	34.15	34.09	34.80	34.94
80	33.65	33.08	33.90	33.81	34.45	34.54
90	33.10	32.85	33.50	33.45	34.05	34.05
100	32.70	32.05	33.15	32.98	33.70	33.48
120	31.90	31.56	32.05	31.80	32.30	32.10
140	30.20	30.23	30.20	30.24	30.40	30.33
150	29.40	29.40	29.30	29.30	29.30	29.30
160	29.80	29.64	29.60	29.42	29.55	29.35
180	30.20	29.78	29.80	29.35	29.60	29.11
200	29.70	29.50	29.20	28.88	28.80	28.48
220	28.95	28.83	28.25	27.99	27.80	27.50
230	28.50	28.32	27.65	27.39	27.10	26.77
240	27.80	27.72	26.65	26.68	26.35	25.99
250	27.00	27.00	25.85	25.85	25.10	25.10
260	27.20	26.95	25.95	25.64	25.00	24.73
280	26.70	26.51	25.00	24.88	23.65	23.64
300	25.50	25.62	23.45	23.65	21.70	22.07

.....

TABLE 6.5

COMPARISON OF STEADY STATE WATER TABLE PROFILES

UNDER FREE FLOW CONDITION

bed Slope=0.06 , R/K = 0.0348 , L/d=0.229

r=0.25 cm.

Water table height in cms.

X	h_e	h_t	$\frac{h_e - h_t}{h_e} 100$
cms	cms	cms	%
0	31.50	27.90	11.30
10	30.60	27.20	11.10
20	29.65	26.40	10.90
30	28.70	25.40	11.50
40	27.20	24.40	10.30
50	23.15	23.15	0.00
60	26.50	24.00	9.40
70	27.15	24.72	9.00
80	27.20	24.83	8.80
90	27.55	24.80	10.40
100	27.45	25.00	8.90
120	26.70	24.60	7.90
140	25.40	23.62	7.10
150	23.15	23.15	0.00
160	25.45	23.80	6.50
180	26.25	24.70	5.90
200	26.25	25.00	4.80
220	25.70	24.60	4.30
230	25.30	24.25	4.15
250	23.15	23.15	0.00
260	24.30	23.40	3.70
280	23.85	23.20	2.70
300	22.80	22.30	2.20

h_e = Experimental height of the water table.

h_t = Theoretical height of the water table.

TABLE 6.6

EFFECT OF BED SLOPE ON THE RATE OF FALL OF WATER TABLE

AT THE HIGHEST POINT IN ZONE II

R/K = 0.310 L/d = 0.229 r = 0.25 cm.

Slope						
Time	Water table height (h) in cms.					
Secs.						
0	31.70	31.55	31.10	30.65	30.10	29.85
10	31.10	30.75	30.40	30.00	29.65	29.15
20	29.60	29.35	29.05	28.65	28.35	28.00
30	28.15	27.90	27.50	27.40	27.20	26.80
40	27.00	26.80	26.15	26.40	26.25	25.85
50	26.25	25.95	-	25.65	25.50	25.15
60	25.60	25.35	25.20	25.05	24.85	24.45
70	25.10	24.85	24.75	24.65	24.35	23.95
80	24.70	24.40	24.30	24.20	23.85	23.40
90	24.40	24.15	24.00	23.80	23.40	23.00
100	24.20	23.95	23.75	23.40	23.00	22.65
110	24.00	23.75	23.50	23.15	22.70	22.30
120	23.85	23.65	23.30	22.90	22.40	21.95
150	23.65	23.30	22.80	22.25	21.65	20.85
180	23.45	23.05	22.40	21.70	20.80	19.90
210	23.35	22.85	22.10	21.15	20.10	19.05
240	23.30	22.65	21.75	20.70	19.45	18.30
270	23.25	22.55	21.45	20.25	18.85	17.65
300	23.20	22.45	21.20	19.85	18.40	17.10

.....

TABLE 6.7

EFFECT OF BED SLOPE ON THE RATE OF FALL OF WATER TABLE AT THE DOWNSTREAM IMPERMEABLE BOUNDARY

R/K = 0.031 d/L = 0.229 r = 0.25 cm

Slope	0.02	0.04	0.06	0.08	0.10
Time	Water table height in cms.				
secs					
0	35.25	37.45	39.20	41.20	41.90
10	34.25	36.45	38.25	40.30	41.20
20	32.75	34.85	36.85	38.80	39.70
30	31.30	33.30	33.35	37.30	38.20
40	29.95	31.95	34.05	35.95	36.80
50	29.00	30.90	32.95	34.80	35.60
60	28.15	30.05	32.15	33.85	34.75
70	27.50	29.35	31.45	33.15	34.00
80	26.95	28.90	30.85	32.50	33.45
90	26.55	28.45	30.45	32.05	32.90
100	26.30	28.15	30.05	31.65	32.50
110	26.10	27.90	29.75	31.35	32.25
120	25.90	27.70	29.55	31.10	31.95
150	25.55	27.35	29.05	30.50	31.25
180	25.35	27.10	28.70	30.15	30.80
210	25.20	26.85	28.40	29.75	30.45
240	25.10	26.70	28.15	29.40	30.05
270	25.00	26.55	27.90	29.15	29.75
300	24.95	26.40	27.70	28.90	29.45

.....

TABLE 6.8

COMPARISON BETWEEN EXPERIMENTAL AND THEORETICAL UNSTEADY STATE WATER TABLE PROFILES

R/K= 0.0345 Slope=0.06 d/L=0.229 r = 0.25 cms

Time secs.	0		10		20		30	
X cms.	h_e cms	h_t cms	h_e cms	h_t cms	h_e cms	h_t cms	h_e cms	h_t cms
0	38.70	37.85	37.85	36.18	35.25	33.89	34.90	33.58
10	37.65	37.26	36.85	35.57	34.35	33.24	33.95	32.97
20	36.95	36.52	36.10	34.96	33.60	32.58	33.20	32.27
30	35.95	35.70	35.25	34.26	32.70	31.89	32.35	31.58
40	34.80	34.79	34.15	33.60	31.85	31.20	31.40	30.89
50	33.75	33.75	32.90	32.90	30.50	30.50	30.20	30.20
60	33.90	33.85	33.05	32.64	30.65	30.23	30.30	29.90
70	33.80	33.85	33.10	32.38	30.80	29,95	30.35	29.60
80	33.70	33.75	32.95	32.10	30.70	29.68	30.40	29.32
90	33.60	33.54	32.80	31.81	30.50	29.40	30.15	29.03
100	33.50	33.24	32.70	31.46	30.40	29.07	29.95	28.69
120	32.50	32.33	31.60	30.81	29.50	28.52	29.20	28.16
140	30.90	30.99	30.20	30.05	28.20	27.91	27.85	27.59
150	30.15	30.15	29.65	29.65	27.60	27.60	27.30	27.30
160	30.65	30.42	29.95	29.47	27.85	27.39	27.50	27.05
180	31.00	30.60	30.30	29.10	28.15	26.97	27.30	26.55
200	30.65	30.34	29.85	28.61	27.70	26.52	27.35	26.10
220	29.85	29.64	29.15	28.02	27.00	26.03	26.75	25.58
240	28.60	28.47	27.90	27.35	26.10	25.51	25.70	25.10
250	27.70	27.70	27.00	27.00	25.25	25.25	24.85	24.85
260	27.85	27.70	27.25	26.46	25.40	24.58	25.15	24.17
280	27.30	27.16	26.70	25.40	24.75	23.27	24.40	22.70
300	26.30	26.20	25.65	24.14	23.60	21.85	23.45	21.21

h_e = Experimental water table height

h_t = Theoretical water table height

TABLE 6.8 (continued)

Time secs	50		80		110	
X cms	h_e cms	h_t cms	h_e cms	h_t cms	h_e cms	h_t cms
0	33.85	33.92	31.10	30.64	30.25	30.03
10	32.90	32.05	30.20	29.92	29.50	29.29
20	32.20	31.37	29.05	29.20	28.85	28.54
30	31.40	30.67	28.95	28.44	28.15	27.77
40	30.50	29.97	28.10	27.68	27.35	26.99
50	29.25	29.25	26.90	26.90	26.20	26.20
60	29.55	28.96	27.05	26.64	26.30	25.95
70	29.45	28.70	27.15	26.39	26.35	25.70
80	29.40	28.40	26.85	26.13	26.00	25.46
90	29.20	28.12	26.70	25.90	25.85	25.22
100	29.00	27.80	26.40	25.58	25.60	24.93
120	28.25	27.30	25.90	25.14	25.05	24.51
140	27.10	26.76	25.05	24.64	24.25	24.01
150	26.50	26.50	24.40	24.40	23.80	23.80
160	26.80	26.27	24.55	23.85	23.75	23.20
180	26.90	25.81	24.35	22.81	23.35	22.05
200	26.40	25.37	23.75	21.90	22.55	21.03
220	25.85	24.93	23.20	21.05	21.90	20.10
240	25.00	24.51	22.60	20.30	21.10	19.24
250	24.30	24.30	22.35	19.95	20.70	18.85
260	24.40	23.54	22.00	18.94	20.35	17.75
280	23.60	22.05	20.90	16.96	19.30	15.60
300	22.45	20.51	--	14.88	18.20	13.30

.....

TABLE 6.9

EFFECT OF BED SLOPE ON THE RATE OF FALL OF THE WATER TABLE BETWEEN FREE DISCHARGING AND SUBMERGED DRAINS

R/K = 0.0324 d/L = 0.229 r=0.25 cm.

Slope	0.00		0.02		0.04	
Time secs.	Water table height (h) in cms.					
0	31.80	26.90	31.40	26.70	30.80	26.40
10	31.20	26.35	30.80	26.05	30.10	25.85
20	30.05	25.60	29.60	25.10	28.80	25.00
30	28.70	24.75	28.40	24.35	27.50	24.20
40	27.60	24.20	27.25	23.90	26.45	23.65
50	26.65	23.85	26.30	23.60	25.75	23.35
60	26.00	23.60	25.70	23.40	25.20	23.15
70	25.50	23.50	25.20	23.25	24.70	22.95
80	25.10	23.40	24.75	23.15	24.30	22.75
90	24.75	23.25	24.40	23.05	24.00	22.55
100	24.45	23.30	24.05	22.95	23.70	22.40
110	24.45	23.30	24.05	22.95	23.70	22.40
120	24.10	23.20	23.80	22.80	23.35	22.15
150	23.80	23.15	23.40	22.60	22.65	21.65
180	23.65	23.13	23.20	22.50	22.25	21.30
210	23.50	-	22.90	22.35	21.85	20.90
240	23.40	-	22.65	22.20	21.50	20.55
270	23.35	-	22.55	22.05	21.20	20.25
300	23.30	-	22.45	21.95	20.90	20.00

.....

TABLE 6.9 (continued)

Slope	0.06		0.08		0.10	
Time secs.	Water table height(h) in cms.					
0	30.30	26.30	29.90	26.05	29.90	26.05
10	29.80	25.75	29.50	25.70	29.30	25.60
20	28.40	24.85	28.35	24.85	28.00	24.50
30	27.30	24.05	27.10	24.00	26.85	23.70
40	26.30	23.55	26.05	23.30	25.80	23.00
50	25.30	23.15	25.30	22.75	25.00	22.40
60	24.90	22.85	24.65	22.30	24.25	21.95
70	24.35	22.50	24.05	21.90	23.60	21.50
80	23.95	22.25	23.50	21.50	23.05	20.95
90	23.55	22.00	23.05	21.10	22.50	20.50
100	23.20	21.75	22.70	20.70	22.15	20.00
110	22.90	21.50	22.35	20.30	21.70	19.50
120	22.60	21.25	22.00	20.00	21.35	19.10
150	21.85	20.50	21.10	18.85	20.20	17.95
180	21.25	19.85	20.15	18.05	19.15	16.95
210	20.70	19.30	19.45	17.35	18.35	16.15
240	20.20	18.85	18.75	16.75	17.50	15.50
270	19.65	18.45	18.20	16.25	16.75	14.85
300	19.20	18.10	17.65	15.80	16.20	14.35

.....

A P P E N D I C E S

APPENDIX I

SOLUTION OF THE DIFFERENTIAL EQUATION

$$\frac{\partial^2 y}{\partial x^2} - a\frac{\partial y}{\partial x} = -P_o \quad \ldots\ldots\ldots\ldots (1)$$

This can be made homogeneous in the form

$$\frac{\partial^2 Y}{\partial x^2} - a\frac{\partial Y}{\partial x} = 0 \quad \ldots\ldots\ldots (2)$$

in which $Y = y - \frac{P_o}{a}x$

Differentiating this equation with respect to x

$$\frac{\partial Y}{\partial x} = \frac{\partial y}{\partial x} - \frac{P_o}{a}$$

But

$$\frac{\partial y}{\partial x} = 2\sqrt{y}\,\frac{\partial h}{\partial x} \quad \text{(refer Section 2.6)}$$

As in Section 2.6 we take $\sqrt{y} \doteqdot D$

so

$$\frac{\partial y}{\partial x} \doteqdot 2D\frac{\partial h}{\partial x} \quad \ldots\ldots\ldots\ldots (3)$$

(i) Zone I

The boundary conditions (Section 6.4.2(i)) for the transformed equation (2) will be

$$\frac{\partial Y}{\partial x} = \frac{\partial y}{\partial x} - \frac{P_o}{a}$$

From equation (3)

$$\frac{\partial Y}{\partial x} = 2D\frac{\partial h}{\partial x} - \frac{P_o}{a}$$

Since $\frac{\partial h}{\partial x} = \infty$ (refer Section 6.4.2(i))

therefore

$$\frac{\partial Y}{\partial x} = 2D\alpha - \frac{P_o}{a} \qquad \text{at} \qquad x = 0$$

and

$$Y = H_L^2 - \frac{P_o}{a} L \qquad \text{at} \qquad x = L$$

Integrating differential equation (2) twice, we will get

$$Y = -\frac{B}{a} + C\, e^{ax} \qquad \ldots\ldots\ldots\ldots\ldots\ldots \quad (4)$$

where B and C are arbitrary constants. For the first boundary condition

$$\frac{\partial Y}{\partial x} = 2\alpha D - \frac{P_o}{a} C = Ca$$

or

$$C = \frac{2\alpha D}{a} - \frac{P_o}{a^2}$$

Substituting this in equation (4), will yield

$$Y = -\frac{B}{a} + \left(\frac{2\alpha D}{a} - \frac{P_o}{a^2} \right) e^{ax} \qquad \ldots\ldots \quad (5)$$

For the second boundary condition

$$-\frac{B}{a} = H_L^2 - \left(\frac{2\alpha D}{a} - \frac{P_o}{a^2} \right) e^{aL} - \frac{P_o}{a} L \ldots \quad (6)$$

Substitution of equation (6) in equation (5) will, after some simplification, yield

$$y = H_L^2 - 2D^2(e^{aL} - e^{ax}) + \frac{P_o}{a^2}(e^{aL} - e^{ax}) + \frac{P_o}{a}(x-L)$$

$$\ldots\ldots\ldots (7)$$

or

$$y = G_1(ax) = Z_1 + \frac{P_o}{a^2}(e^{aL} - e^{ax}) + \frac{P_o}{a}(x - L) \quad .... \quad (8)$$

where $Z_1 = H_L^2 - 2D^2(e^{aL} - e^{ax})$

(ii) Zones II and III

The transformed boundary conditions (Section 6.4.2 (ii)) are:

$$Y = H_o^2 \qquad \text{at} \qquad x = 0$$

$$Y = H_L^2 - \frac{P_o}{a} L \quad \text{at} \qquad x = L$$

Substituting these boundary conditions in equation (4) and simplifying, we will get

$$Y = y - \frac{P_o}{a}x = H_o^2 + \frac{H_L^2 - \frac{P_o}{a}L - H_o^2}{e^{aL} - 1}(e^{ax} - 1)...($$

which after further simplification, becomes

$$y = G_2(ax) = H_o^2 + (H_L^2 - H_o^2).f(ax) + \frac{P_o}{a}(x - L.f(ax))..(10)$$

in which

$$f(ax) = \frac{e^{ax} - 1}{e^{aL} - 1}$$

(iii) Zone IV

The transformed boundary conditions are (Section 6.4.2(iii)).

$$\frac{\partial Y}{\partial x} = 2\alpha D - \frac{P_o}{a} \qquad \text{at} \quad x = L$$

$$Y = H_o^2 \qquad \text{at} \quad x = 0$$

After substituting these boundary conditions in equation(4), we will get

$$Y = y - \frac{P_o}{a} = H_o^2 - \frac{\frac{2\times D}{a} - \frac{P_o}{a}}{e^{aL}} + \frac{\frac{2\times D}{a} - \frac{P_o}{a^2}}{e^{aL}} e^{ax}$$

or

$$y = H_o^2 - 2D^2 e^{-aL} (1 - e^{ax}) + \frac{P_o}{a}(x + \frac{1}{a}e^{-aL}(1-e^{ax})$$

or

$$y = G_3(ax) = Z_3 + \frac{P_o}{a}\left[x + \frac{1}{a} e^{-aL}(1 - e^{ax})\right] \quad \ldots\ldots (11)$$

$$\ldots\ldots (12)$$

in which

$$Z_3 = H_o^2 - 2D^2 e^{-aL} (1 - e^{ax})$$

.....

APPENDIX II

SOLUTION OF THE DIFFERENTIAL EQUATION

(refer Section 6.4.3)

$$\frac{d^2p'}{dx^2} - a\frac{dp'}{dx} - \frac{s}{C}p' = \frac{P_o}{aC}x \quad \ldots\ldots\ldots \quad (1)$$

in which

$$p'(s) = \int_0^\infty e^{-st}\, p(t)\, dt$$

The general solution of equation (1) has the form

$$p' = e^{ax/2}\left[A\sinh(\beta x) + B\cosh(\beta x)\right] - \frac{P_c}{as}x + \frac{P_o C}{s^2}$$

$\ldots\ldots\ldots$ (2)

in which A and B are arbitrary constants and

$$\beta = \sqrt{\frac{a^2}{4} + \frac{s}{C}} \quad \ldots\ldots\ldots\ldots\ldots\ldots \quad (3)$$

(i) Zone I

The boundary conditions for the transformed equation (1) are (the initial condition is already incorporated in this equation).

(i) $p'(L,t) = \left(\lambda - \frac{P_o}{a}L\right)\frac{1}{s}$

(ii) $\frac{\partial p'(0,t)}{\partial x} = -\frac{P_o}{as}$

Substituting the above boundary conditions in equation(2), we obtain

$$p' = \left(\frac{\lambda}{s} - \frac{P_o C}{s^2}\right) e^{-a(L-x)/2} \left[\frac{\frac{a}{2}\sinh(\beta x) - \beta\cosh(\beta x)}{\frac{a}{2}\sinh(\beta L) - \beta\cosh(\beta L)}\right] - \frac{P_o}{as}x + \frac{P_o C}{s^2} \quad \ldots\ldots\ldots \quad (4)$$

The inverse Laplace transform of equation (4) will be (71)

$$p = \left[\lambda e^{-a(L-x)/2} \oint \frac{R(x)\, e^{st}}{ds}\, ds\right] - \left[P_o C\, e^{-a(L-x)/2} \oint \frac{R(x) e^{st}}{s^2} ds\right] - \frac{P_o}{as} + \frac{P_o C}{1} \quad \ldots\ldots \quad (5)$$

where

$$R(x) = \frac{\frac{a}{2}\sinh(\beta x) - \beta\cosh(\beta x)}{\frac{a}{2}\sinh(\quad) - \beta\cosh(\beta L)}$$

The poles are determined by equating the denominator of equation (5) to zero. Thus for the terms in the first square bracket of equation (5)

$$s\left[\frac{a}{2}\sinh(\beta L) - \beta\cosh(\beta L)\right] = 0$$

i.e. either $s = 0$ or $\frac{a}{2}\sinh(\beta L) - \beta\cosh(\beta L) = 0$

For $\frac{a}{2}\sinh(\beta L) - \beta\cosh(\beta L) = 0$, let $\beta L = i\, r_n$, then

$$r_n \cot(r_n) = \frac{aL}{2} \qquad \ldots\ldots\ldots\ldots\ldots\ldots (6)$$

Now, by using

$$s = \beta^2 - \frac{a^2}{4} \qquad \ldots\ldots\ldots\ldots\ldots\ldots (7)$$

the poles of the integrand in equation (5) are

For $s = 0$ $\beta = a/2$

and $s = -j$ $\beta = i\, r_n/L$

then from equation (7)

$$j = \frac{c}{L^2}\left[r_n^2 + (aL/2)^2\right] = \frac{c}{L^2}\,r^2 \ldots\ldots (8)$$

By Cauchy's theorem (71), the residues of the integrand in the first square bracket of equation (5) may be written as

$$\frac{\frac{a}{2}\sinh(\beta x) - \beta\cosh(\beta x)\cdot e^{st}}{\left[\frac{a}{2}\sinh(\beta L) - \beta\cosh(\beta L)\right] + \left[s\,\frac{a}{2}L\cosh(\beta L)\frac{\partial\beta}{\partial s} - \beta L\sinh(\beta L)\frac{\partial\beta}{\partial s} - \cosh(\beta L)\frac{\partial\beta}{\partial s}\right]} \ldots (9)$$

For $s = 0$, $\beta = a/2$, therefore,

$$\text{Residues} = \frac{a/2\,\sinh(ax/2) - a/2\,\cosh(ax/2)}{a/2\,\sinh(aL/2) - a/2\,\cosh(aL/2)}$$

Converting the hyperbolic sine and cosine in exponential form and simplifying, we will get

$$\text{Residues} = e^{a(L-x)/2}$$

For $s = -j$, $\beta = i\, r_n/L$

Now, from equation (7)

$$\frac{\partial \beta}{\partial s} = \frac{1}{2C\beta} = \frac{1}{2C\, i\, r_n/L} \qquad \ldots\ldots\ldots\ldots \quad (10)$$

Substituting these values in equation (9) and using equations (6) and (8) , we will get the residues equal to

$$- \frac{2 r_n^3}{\tau(\tau - aL/2)\sin^2(r_n)} \sin(r_n(1-x/L))e^{-jt}$$

$$\ldots\ldots \quad (11)$$

Therefore the inverse transformation of the terms in the first square bracket of equation (5) are

$$\lambda\left[1 - 2\, T_1(x,t)\right] \qquad \ldots\ldots\ldots\ldots\ldots\ldots \quad (12)$$

in which

$$T_1(x,t) = e^{-a(L-x)/2} \sum_{n=0}^{\infty} B_n \sin(r_n(1-x/L))e^{-jt}$$

and

$$B_n = \frac{r_n^3}{\tau(\tau - aL/2)\sin^2(r_n)} \qquad \ldots \quad (13)$$

Since 1/s corresponds to integration over t between limits from zero to t, the inverse transform of the terms in the second square bracket of equation (5) will be

$$P_o C \left[t - T_2(x,t)\right] \quad \ldots\ldots\ldots\ldots\ldots \quad (14)$$

in which

$$T_2(x,t) = e^{-a(L-x)/2} \sum_{n=0}^{\infty} B_n \sin\left(r_n(1-x/L)\right)(\ldots jt)$$

in which B_n is given by equation (13)

Collecting expressions (12) and (14), we obtain, taking account of equation (5)

$$p = y_1 - y - \frac{P_o}{a} x = \lambda\left[1 - 2\,T_1(x,t)\right] - P_o C \left[t - 2T_2(x,t)\right] - \frac{P_o}{a} x + \frac{P_o C\, t}{1}$$

or

$$y(x,t) = G_1(ax) - \lambda\left[1 - 2\,T_1(x,t)\right] + 2P_o C\, T_2(x,t) \quad \ldots \quad (15)$$

(ii) Zones II and III

Boundary conditions for the transformed equation (1) are (refer Section 6.4.3).

(i) $p'(0,t) = \frac{\lambda}{s}$

(ii) $p'(L,t) = \left(\gamma - \frac{P_o}{a} L\right) \frac{1}{s}$

Substituting these boundary conditions in equation (2), we

will obtain

$$p' = e^{ax/2}\left[\left\{\left(\frac{\gamma}{s} - \frac{P_o C}{s^2}\right)e^{-La/2} - \left(\frac{\lambda}{s} - \frac{P_o C}{s^2}\right)\cosh(\beta L)\right\}\frac{\sinh(\beta x)}{\sinh(\beta L)} + \left\{\left(\frac{\lambda}{s} - \frac{P_o C}{s^2}\right)\cosh(\beta x)\right\}\right] + P_o Ct - \frac{P_o}{a}x \quad \ldots\ (16)$$

or

$$p' = e^{ax/2}\left[\left\{\left(\gamma e^{-aL/2} - \lambda\cosh(\beta L)\right\}\frac{\sinh(\beta x)}{s.\sinh(\beta L)}\right] + \left\{\frac{\lambda}{s}\cosh(\beta x)\right.$$
$$- e^{ax/2}\left[\left\{P_o C\, e^{-aL/2} - P_o C\cosh(\beta L)\right\}\frac{\sinh(\beta x)}{s^2\sinh(\beta L)}\right.$$
$$\left.\left. + \left\{\frac{P_o C}{s^2}\cosh(\beta x)\right\}\right] + \frac{P_o Ct}{1} - \frac{P_o}{a}x \quad \ldots\ldots \quad (17)$$

Cosider the integrands in the first square bracket of equation (17). The poles of the first integrand are

$s = 0$ and $\sinh(\beta L) = 0$, in which β is given by equation (7). Now, when

$s = 0$, $\beta = a/2$ and when $\sinh(\beta L) = 0$, $\beta = in\pi/L$

also, when $s = -w$, $w = C/L^2\left[n^2\pi^2 + (aL/2)^2\right] = \frac{C}{L^2} r_c$ .. (18)

By Cauchy's theorem, residues of the first integrand in equation (17) are

$$\frac{\left[\gamma e^{-aL/2} - \lambda\cosh(\beta L)\right]\sinh(\beta x)}{\sinh(\beta L) + L.s.\cosh(\beta L)}\, e^{st}$$

When $s = 0$, $\beta = a/2$, therefore the residues are

$$= \frac{\left[\gamma e^{-aL/2} - \lambda\cosh(aL/2)\right]\sinh(ax/2)}{\sinh(aL/2)} \quad \ldots\ldots (19)$$

For $s = -w$, $\beta = in\pi/L$, therefore the residues are

$$= \frac{\left[\gamma e^{-aL/2} - \lambda\cosh(in\pi)\right]\cdot\sinh(in\pi x/L)}{+ L(-w)(-1)^n \frac{L}{2Cin\pi}} e^{-wt}$$

$$= -2\sum_{n=1}^{\infty}\left[(-1)^{n+1}\gamma e^{-aL/2} + \lambda\right] n\pi/r_c \cdot \sin(n\pi x/L)\, e^{-wt} \quad \ldots\ldots\ldots (20)$$

The pole of the second integrand in the first square bracket of equation (17) is only $s = 0$ and the residues will be

$$\lambda\cosh(\beta x)\, e^{st}$$

when $s = 0$, $\beta = a/2$, therefore residues are

$$\lambda\cosh(ax/2) \quad \ldots\ldots\ldots\ldots\ldots\ldots (21)$$

Therefore the transformation of the T terms in the first square bracket of equation (17) are obtained by adding equations (19), (20) and (21) i.e.

$$e^{ax/2}\left[\left\{\gamma e^{-aL/2} - \lambda\cosh(aL/2)\right\} \frac{\sinh(ax/2)}{\sinh(aL/2)} + \lambda\cosh(ax/2)\right] - 2\,T_3(x,t) \ldots (22)$$

in which

$$T_3(x,t) = e^{ax/2}\sum_{n=1}^{\infty}(-1)^{n+1}\gamma e^{-aL/2} + \lambda\Big] \frac{n\pi}{r_c} \sin(n\pi x/L) e^{-wt}$$

Since $1/s$ corresponds to integration over t between limits from zero to t, the inverse Laplace transformation of the terms in the second square bracket of equation (17) will be

$$e^{ax/2}\, P_o C \left[\left\{ e^{-aL/2} - \cosh(aL/2) \right\} \frac{\sinh(ax/2)}{\sinh(aL/2)} \cdot t + t \cosh(ax/2) \right] - 2 \frac{P_o C}{\lambda} T_4(x,t) + P_o C t - \frac{P_o}{a} x \qquad \ldots\ldots\ldots (23)$$

in which

$$T_4(x,t) = e^{ax/2} \sum_{n=1}^{n=\infty} \left[(-1)^{n+1}\, e^{-aL/2} + 1 \right] \frac{n\pi}{wr_c} \sin(n\pi x/L). \; (1-e^{-wt})$$

Collecting expressions (22) and (23), we obtain, taking account of equation (17)

$$p = y_1 - y - \frac{P_o}{a} x = e^{ax/2} \left[\left\{ \gamma e^{-aL/2} - \lambda \cosh(aL/2) \right\} \frac{\sinh(ax/2)}{\sinh(aL/2)} + \lambda \cosh(ax/2) \right] - 2T_3(x,t) - e^{ax/2}\, P_o C \left[\left\{ e^{-aL/2} - \cosh(aL/2) \right\} \frac{\sinh(ax/2)}{\sinh(aL/2)} t + t \cosh(ax/2) \right] - P_o C 2T_4(x,t) + P_o C t - \frac{P_o}{a} x$$

or

$$y(x,t) = G_2(ax) + \left[(\gamma - \lambda).f(ax) + \lambda - 2T_3(x,t) \right] + \\ - 2\,P_o C\,T_4(x,t) \qquad \ldots\ldots\ldots\ldots (24)$$

in which

$$f(ax) = \frac{e^{ax} - 1}{e^{aL} - 1}$$

and $G_2(ax)$ is given by equation (10) in Appendix I.

(iii) Zone IV

Boundary conditions for the transformed equation(1) are (refer Section 6.4.3).

$$(i)\ \frac{\partial p'(L,t)}{\partial x} = -\frac{P_o}{as}$$

$$(ii)\ p'(0,t) = \frac{\lambda}{s}$$

By substituting these boundary conditions in equation(2),we obtain

$$p' = e^{ax/2}\left(\frac{\lambda}{s} - \frac{P_o C}{s^2} \right) \left[- \frac{\beta \sinh(\beta L) + a/2 \cosh(\beta L)}{\beta \cosh(\beta L) + a/2 \sinh(\beta L)} \sinh(\beta x) \right. \\ \left. + \cosh(\beta x) \right] - \frac{P_o}{as} x + \frac{P_o C}{s^2} \qquad \ldots\ldots\ldots (25)$$

The inverse Laplace transform of equation (25) will be given by

$$p' = e^{ax/2}\left[\oint \frac{R(x)\, e^{st}}{s}\, ds + \oint \frac{\cosh(\beta x)\, e^{st}}{s}\, ds\right]$$

$$- e^{ax/2} P_o C\left[\oint \frac{R(x)\, e^{st}}{s^2}\, ds + \oint \frac{\cosh(\beta x)\, e^{st}}{s^2}\, ds\right]$$

$$- \frac{P_o}{a} x + P_o C t \quad \ldots\ldots\ldots\ldots\ldots\ldots\ldots \quad (26)$$

in which

$$R(x) = - \sinh(\beta x) \frac{\beta \sinh(\beta L) + a/2 \cosh(\beta L)}{\beta \cosh(\beta L) + a/2 \sinh(\beta L)}$$

The poles of the first integrand within the first square bracket of equation (26) are

$$s = 0 \quad \text{or} \quad a/2 \sinh(\beta L) = - \beta \cosh(\beta L)$$

Let $\beta L = i\, m_n$, then

$$a/2\, i \sin(m_n) = -\beta \cos(m_n)$$

or $$m_n \cot(m_n) = - aL/2 \quad \ldots\ldots\ldots\ldots\ldots\ldots (27)$$

Now, from equation (7)

when $s = 0$, $\beta = a/2$

and when $s = -\rho$, $\beta = i\, m_n/L$

where

$$\rho = \frac{C}{L^2}\left[m_n^2 + (aL/2)^2\right] = \frac{C}{L^2}\tau \quad (28)$$

By Cauchy's theorem, residues of the integrand can be written as

$$\frac{-\sinh(\beta x)\left[\beta\sinh(\beta L) + a/2\cosh(\beta L)\right] e^{st}ds}{\beta\cosh(\beta L) + a/2\sinh(\beta L) + s\left[\frac{\partial\beta}{\partial s}(aL/2+1)\cosh(\beta L)\right.}$$

$$\left.\beta L\sinh(\beta L)\right]$$

Now, for $s = 0$, $\beta = a/2$, therefore residues are equal to

$$-\sinh(ax/2) \quad \ldots\ldots\ldots\ldots\ldots (29)$$

For $s = -\rho$, $\beta = i\,m_n/L$, therefore, residues are equal to

$$\frac{2\sin(m_n x/L)\left[\sin^2(m_n) - \cos^2(m_n)\right] e^{-\rho t}}{2\sin(2m_n)\left[1 + \frac{\rho}{4m_n^2}(aL/2+1)\right] - \frac{\rho}{m_n}\sin^2 m_n}$$

$$= 2\sum_{n=0}^{\infty} B_n \sin m_n x/L\left[\sin^2(m_n) - \cos^2(m_n)\right] e^{-\rho t}$$

$\ldots\ldots\ldots\ldots\ldots\ldots (30)$

in which

$$B_n = \frac{1}{2\sin(2m_n)\left[1 + \frac{\rho}{4m_n^2}(aL/2+1)\right] - \frac{\rho}{m_n}\sin^2 m_n}$$

The pole of the second integrand in the first square bracket of equation (26) is only $s = 0$, therefore the residues will be

$$\cosh(ax/2) \quad \ldots\ldots\ldots\ldots\ldots (31)$$

Therefore the transformation of the terms in the first square bracket of equation (26) are obtained by adding equations (29),(30) and (31) viz.

$$e^{ax/2}\,\lambda\left[\left(-\sinh(ax/2)+\cosh(ax/2)\right)+2\,T_5(x,t)\right]$$

or

$$=\lambda\left[1+2\,T_5(x,t)\right] \quad \ldots\ldots\ldots\ldots\ldots\ldots \quad (32)$$

in which

$$T_5(x,t) = e^{ax/2}\sum_{n=0}^{\infty} B_n \sin m_n x/L \left[\sin^2(m_n)-\cos^2(m_n)\right] .e^{-\rho t}$$

Since $1/s$ corresponds to integration over t between limits from zero to t, the inverse Laplace transformation of the terms in the second square bracket of equation(26) will be

$$= P_o C\,(t + 2\,T_6(x,t) \quad \ldots\ldots\ldots\ldots\ldots\ldots \quad (33)$$

Collecting expressions (32) and (33) , we obtain, taking account of equation (26)

$$p = y_1 - y - \frac{P_o}{a}x = \lambda\left[1 + 2\,T_5(x,t)\right] - P_o C\left[t + 2T_6(x,t)\right] + P_o C\,t - \frac{P_o}{a}x$$

or

$$y(x,t) = G_3(a\,x) - \lambda\left[1 + 2\,T_5(x,t)\right] + 2\,P_o C\,T_6(x,t)$$

$$\ldots\ldots\ldots\ldots \quad (34)$$

in which $G_3(ax)$ is given by equation(12) in Appendix I.

and

$$T_6(x,t) = e^{ax/2} \sum_{n=0}^{\infty} B_n / (\quad \sin(m_n x/L) \left[\sin^2(m_n) - \cos^2(m_n) \right].$$

$$(1 - e^{-\varphi t})$$

(iv) Checking the solutions

By substitution it is easily found that equation(2) satisfies equation(1). Equations (15),(24) and (34) are obtained by substituting the appropriate boundary conditions in equation(2). It is shown below that these equations satisfy the boundary conditions.

(i) equation (15)

(a) When $t = 0$, $T_2(x,t) = 0$

$= 0$

therefore, $y(x,0) = G_1(ax)$

(b) when $x = L$, $\sin r_n(1-x/L) = 0$

so $T_1(0,t) = T_2(0,t) = 0$

therefore,

$$y(L,t) = \left[H_L - \Delta h_L \right]^2$$

Similarly, $y(0,t) = 2D\alpha$

(ii) equation (24)

(a) when $t = 0$, $\gamma = \lambda = 0$

therefore $T_3(0,t) = 0$

Similarly, $T_4(0,t) = 0$

in which $G_3(ax)$ is given by equation(12) in Appendix I.

and

$$T_6(x,t) = e^{ax/2} \sum_{n=0}^{\infty} B_n / \left(\sin(m_n x/L) \left[\sin^2(m_n) - \cos^2(m_n) \right] \cdot \left(1 - e^{-\theta t} \right) \right)$$

(iv) Checking the solutions

By substitution it is easily found that equation(2) satisfies equation(1). Equations (15),(24) and (34) are obtained by substituting the appropriate boundary conditions in equation(2). It is shown below that these equations satisfy the boundary conditions.

(i) equation (15)

(a) When $t = 0$, $T_2(x,t) = 0$

$= 0$

therefore, $y(x,0) = G_1(ax)$

(b) when $x = L$, $\sin r_n(1-x/L) = 0$

so $T_1(0,t) = T_2(0,t) = 0$

therefore,

$y(L,t) = \left[H_L - \Delta h_L \right]^2$

Similarly, $y(0,t) = 2D\alpha$

(ii) equation (24)

(a) when $t = 0$, $\gamma = \lambda = 0$

therefore $T_3(0,t) = 0$

Similarly, $T_4(0,t) = 0$

therefore, $y(x,0) = G_2(ax)$

(b) when $x = 0$, $\sin(n\pi x/L) = 0$

therefore, $T_3(0,t) = T_4(0,t) = 0$

also $f(a0) = 0$

and $y(0,t) = G_2(a0) - \lambda$

$= \left[H_o - \Delta h_o(t)\right]^2$

(b) when $x = L$, $\sin(n\pi x/L) = \sin(n\pi) = 0$

therefore $T_3(L,t) = T_4(L,t) = 0$

$f(aL) = 1$

and $y(L,t) = G_2(La) - \delta$

$= \left[H_L - \Delta h_L(t)\right]^2$

(iii) equation (34)

(a) when $t = 0$, $\lambda = 0$

and $T_6(x,0) = 0$

therefore $y(x,0) = G_3(ax)$

(b) when $x = 0$, $\sin(m_n x/L) = 0$

therefore $T_5(0,t) = T_6(0,t) = 0$

and $y(0,t) = \left[H_o - \Delta h_o(t)\right]^2 = G_3(a0) - \lambda$

Similarly, for $x = L$ it can be proved that

$y(L,t) = 2D\infty$

.....

APPENDIX III

COMPUTER PROGRAME

```
C          MOVING WATER TABLE OVER A SLOPING BED
      DIMENSION D1(30),D2(30),D3(30),D4(30),H1(30),H2(30),
      PN1(100),RN4(100),RN(100),SG1(30),SG2(30),SG3(30),
      SG4(30),Z1(30),Z2(30),Z3(30),Z4(30),AK(30),T(30),X(30),
      B(100)
C
      COMMON D1,D2,D3,D4,H01,H02,H03,HL1,HL2,HL3,H1,H2,H3,
      RN1,RN2,RN4,SG1,SG2,SG3,SG4,Z1,Z2,Z3,Z4,AL1,AL2,ALPHA,
      A1,A2,A3,A4,I,J,AK,T,X,PM
C
C     READ THE DATA
      READ(5,1) AL1,AL2,ALPHA,F,PM
    1 FORMAT(5X,2(F6.2,5X),3(F7.4,5X))
C
      READ(5,2)(AK(K),I=1,7)
    2 FORMAT(5X,7(F6.3,4X))
C
C     WEIGHTED MEAN DEPTHS
      READ(5,3)(D1(J),D2(J),D3(J),D4(J),J=1,7)
    3 FORMAT(4(5X,F7.3))
C     WATER TABLE DEPTHS OVER U/S DRAINS
      READ(5,4) H01,H02,H03
    4 FORMAT(3(5X,F7.3))
C
C     WATER TABLE DEPTHS OVER D/S DRAIN
      READ(5,5) HL1,HL2,HL3
    5 FORMAT(3(5X,F7.3))
C
C     FALL OF WATER TABLE OVER THE DRAINS
      READ(5,6)(H1(M),H2(M),H3(M),M=1,7)
    6 FORMAT(3(5X,F7.3))
```

```
C     READ THE ROOTS OF THE EQUATION R COT(R)= C
C     AND R COT(R) = - C .
      READ(5,7) (RN1(N),N=1,6)
    7 FORMAT(5X,6(F9.4,2X))
C
      READ(5,8) (RN4(NN),NN=1,6)
    8 FORMAT(5x,6(F9.4,2X))
C
C     READ THE TIME INTERVAL
      READ(5,50) (T(J),J=1,7)
   50 FORMAT(5X,7(F5.1,5X))
C
C     VALUES OF RN1 WHEN THE THIRD DRAIN IS NOT RUNNING
      READ(5,42) (RN2(JK),JK=1,6)
   42 FORMAT(5X,6(F9.4,2X))
C
      CALL OUTPUT(1)
C
C     DO LOOP FOR THE TIME INTERVAL
      DO 9 I = 1,7
C
C     DO LOOP FOR THE HORIZONTAL DISTANCE
      IF(I.GE.6) GO TO 40
      DO 10 MJ= 1,11
      J = MJ
      X(J)= (J-1)*10
      IF(J.EQ.1) X(J)=0.0
      IF(J.GT.6) GO TO 11
      CALL SECT1
C
      CALL SECT4
C
   11 CALL SECT2
      CALL SECT3
   10 CONTINUE
```

```
      CALL OUTPUT(2)
      GO TO 9
C
 40   DO 43 J=1,16
      X(J) = (J-1)*10
      IF(J.EQ.1) X(J)= 0.0
      IF(J.GT.11) GO TO 45
C
      CALL SECT4
C
      CALL SECT2
C
      CALL SECT3
C
   45 CALL SECT1
   43 CONTINUE
      CALL OUTPUT(2)
    9 CONTINUE
      STOP
      END

      SUBROUTINE SECT1
      DIMENSION ....
C
      COMMON  ......
C
C     COMPUTATION OF WATER TABLE PROFILE BETWEEN U/S
C     IMPERMEABLE BOUNDARY AND DRAIN III
C     STEADY STATE PART OF THE SOLUTION
      F = 1.00
      IF(I.GE.6) AL1 = 150.0
      IF(I.GE.6) GO TO 80
      AI = ALPHA/D1(1)
      A1 = ALPHA/D1(I)
```

```
      F2AX = X(J)-AL1 + (*.)/AI)*(EXP(AI*AL1)-EXP(AI*X(J)))
      ZS1 = HL1**2 -2.0*D1(1)**2*(EXP(AI*AL1)-EXP(AI*X(J)))
C
      RG1 = ZS1+(PM/AI)*F2AX
      SG1(J) = RG1**0.5
      GO TO 81
C
   80 RG1 = SG1(J)**2
C
C     TRANSIENT PART OF THE SOLUTION
   81 TERM1 = EXP(-A1*(AL1-X(J))/2.0)
      SUM8 = 0.0
      SUM  = 0.0
C     DO LOOP FOR THE SOLUTION OF INFINITE SERIES
      DO 32 K = 1,6
      IF(I.EQ.6) RN1(K)=RN2(K)
      EQ1K = ((A1*AL1)/2.0)**2 + RN1(K)**2
      Z1K = AK(I)*D1(I)/F
      W = W*T(I)
      IF(WT.GT.80.0) WT=80.0
      DENOM = (EQ1K-A1*AL1/2.0)*0.5*(1.0-COS(2.0*RN1(K)))
      B(K) = (RN1(K)**3)/(EQ1K*DENOM)
C
      TERM2 =B(K)*SIN(RN1(K)*(1.0-X(J)/AL1))*EXP(-WT)
      SUM = SUM+TERM2
      TERM8= B(K)/W*SIN(RN1(K)*(1.0-X(J)/AL1))*(1.0-EXP( /T))
      SUM8 = SUM8+TERM8
      IF(T(I).EQ.0.0) GO TO 83
      IF((ABS(TERM2).LE.1.E-4).AND.(ABS(TERM8).LE.1.E-4)) GO
      TO 12
C
   32 CONTINUE
      WRITE(6,13) TERM2,TERM8
   13 FORMAT(50X,6HTERM2=F10.6,10X,6HTERM8=F10.6)
```

```
   12 T1XT = TERM1*SUM
      T2XT = TERM1*SUM8
      IF(I.GE.6) GO TO 82
      Z1(J) = RG1 +(H1(I)**2-2.0*HL1*H1(I))*(1.0-2.0*T1XT)
      -2.0*PM*Z1K*T2XT
      WRITE(6,104) SUM,SUM8
  104 FORMAT(30X,1H1,10X,F10.6,5X,F10.6)
      Z1(J) = Z1(J)**0.5
      IF(I.EQ.5) SG1(J) = Z1(J)
      GO TO 83
C
   82 FRACT=H2(I)-H2(I-1)
      H2L=HL2 - H2(I-1)
C
      IF(I.EQ.7) FRACT = H2(I) - H2(I-2)
      IF(I.EQ.7) H2L = HL2 - H2(I-2)
C
      PM1 = 0.0132
      Z1(J) = RG1 + (FRACT**2 - 2.0*H2L*FRACT)*(1.0-T1XT)-
      2.0*PM1*Z1K*T2XT
      Z1(J) = Z1(J0**0.5
   83 RETURN
      END

      SUBROUTINE SECT2
      DIMENSION .....
C
      COMMON  ......
C
C     COMPUTATION OF WATER TABLE PROFILE BETWEEN DRAIN II
C     AND DRAIN III
C
C     STEADY STATE PART OF THE SOLUTION
```

```
      F = 1.00
      IF(J.GT.11) GO TO 29
      IF(I.GE.6) GO TO 29
      AI=ALPHA/D2(1)
      A2=ALPHA/D2(I)
      FAX= (EXP(AI*X(J))-1.0)/(EXP(AI*AL2)-1.0)
      F1AX= X(J) - AL2*FAX
      ZS2 = H01**2+(HL2** - H01**2)*FAX
      RG2=ZS2+(PM/AI)*F1AX
      SG2(J) =RG2**0.5
C
C     TRANSIENT PART OF THE SOLUTION
C     POLES OF THE INTEGRANDS
      Z2K=AK(I)*D2(I)/F
      P2 = (A2*X(J))/2.0
      Q2 = (A2*AL2)/2.0
      ALAMB=2.0*H01*H1(I)-H1(I)**2
      GAMMA=2.0*HL2*H2(I)-H2(I)**2
      TERM3=(GAMMA*EXP(-Q2)-ALAMB*COSH(Q2))*(SINH(P2)/SINH(Q2))
      TERMF=T(I)*PM*Z2K*(EXP(-Q2) -COSH(Q2))*(SINH(P2)/SINH(Q2
      ))
C
C     DO LOOP FOR THE SOLUTION OF INFINITE SERIES
      SUM7=0.0
      SUM = 0.0
      CJ=1.0
      DO 33 KK = 1,500
      BK=KK
      EQ2K=(A2*AL2/2.0)**2.0+(BK*3.141)**2.0
      P = (EQ2K/AL2**2)*Z2K
      PT = P*T(I)
      IF(PT.GT.80.0) PT=80.0
C
      C2=BK*3.141*X(J)/AL2
      C3=BK*3.141/EQ2K
```

```
      TERM4=(GAMMA*EXP(-Q2)*CJ+ALAMB)*C3*SIN(C2)*EXP(-PT)
      SUM=SUM+TERM4
      TERM9=(EXP(-Q2)*CJ +1.0)*C3/P*SIN(C2)*(1.0-EXP(-PT))
      SUM7=SUM7+TERM9
C
      IF(T(I).EQ.0.0) GO TO 29
      IF((ABS(TERM4).LE.1.E-6).AND.(ABS(TERM9).LE.1.E-6)) GO
      TO 14
      CJ= - 1.0*CJ
   33 CONTINUE
      WRITE(6,13) TERM4,TERM9
   13 FORMAT(50X,6HTERM4=F10.6,10X,6HTERM9=F10.6)
   14 TERM5 = ALAMB*COSH(P2) - 2.0*SUM
      TERM6= PM*Z2K*(COSH(P2)*T(I)-2.0*SUM7)
C
      Z2(J) = RG2 - EXP(P2)*(TERM3+TERM5)+EXP(P2)*(TERM4+
      TERM6)-PM*Z2K*T(I)
      Z2(J) = Z2(J)**0.5
      WRITE(6,103) SUM,SUM7
  103 FORMAT(30X,1H2,10X,F10.6,5X,F10.6,
      IF(I.EQ.5) SG1(J+5) = Z2(J)
   29 RETURN
      END


      SUBROUTINE SECT3
      DIMENSION ..........
C
      COMMON .......
C
C     COMPUTATION OF WATER TABLE PROFILE BETWEEN DRAIN I AND
C     DRAIN II
C     STEADY STATE PART OF THE SOLUTION
      F = 1.00
```

```
      IF(J.GT.11) GO TO 30
      AI = ALPHA/D3(1)
      A3 = ALPHA/D3(I)
      FAX= (EXP(AI*X(J))-1.0)/(EXP(AI*AL2)-1.0)
      F1AX= X(J) - AL2*FAX
      ZS2 = H02**2 + (HL3**2 - H02**2)*FAX
      RG3 = ZS2 + (PM/AI)*F1AX
      SG3(J) = RG3**0.5
C
C     TRANSIENT PART OF THE SOLUTION
      Z3K = AK(I)*D3(I)/F
      P3 = (A3*X(J))/2.0
      ALAMB=2.0*H02*H2(I) - H2(I)**2
      GAMMA = 2.0*HL3*H3(I)-H3(I)**2
      Q3=(A3*AL2)/2.0
C
      TERM7 = T(I)*PM*Z3K*(EXP(-Q3) - COSH(Q3))*(SINH(P3)/
      SINH(Q3))
      TERM3 = (GAMMA*EXP(-Q3)-ALAMB*COSH(Q3))*(SINH(P3)/
      SINH(Q3))
C
      DO LOOP FOR THE SOLUTION OF INFINITE SERIES
      SUM7 = 0.0
      SUM = 0.0
      CJ=1.0
      DO 15 JJ=1,500
      BJ= JJ
      EQ3K = (A3*AL2/2.0)**2 + (BJ*3.141)**2
      P = (EQ3K/AL2**2)*Z3K
      PT = P*T(I)
      IF(PT.GT.80.0) PT=80.0
C
      B2 = BJ*3.141*X(J)/AL2
      B3 = BJ*3.141/EQ3K
```

```
      TERM4 =(GAMMA*EXP(-Q3)*CJ+ALAMB)*(B3)*SIN(B2)*EXP(-PT)
C
      SUM = SUM + TERM4
      TERM9 = (EXP(-Q3)*CJ+1.0)*(B3)/P*SIN(B2)*(1.0-EXP(-PT))
      SUM7 = SUM7 + TERM9
C
      IF(T(I).EQ.0.0) GO TO 30
      IF(ABS(TERM4).LE.1.E-4).AND.(ABS(TERM9).LE.1.E-4)) GO
      TO 17
      CJ = -- 1.0*CJ
   15 CONTINUE
      WRITE(6,16) TERM4,TERM9
   16 FORMAT(50X,6HTERM4=F10.6,10X,6HTERM9=F10.6)
   17 TERM5 = ALAMB *COSH(P3) - 2.0*SUM
      TERME = PM*Z3K*(COSH(P3)*T(I) - 2.0*SUM7)
C
      Z3(J) = RG3 - EXP(P3)*(TERM3+TERM5) +EXP(P3)*
      (TERM7 + TERME) - PM*Z3K*T(I)
      Z3(J) = Z3(J)**0.5
      WRITE(6,102) SUM,SUM7
  102 FORMAT(30X,1H3,10X,F10.6,3x,F10.6)
      RETURN
      END

      SUBROUTINE SECT4
      DIMENSION ........
      COMMON .............
C
C     COMPUTATION OF WATER TABLE PROFILE BETWEEN D/S
C     IMPERMEABLE BOUNDARY AND DRAIN I
C
C     STEADY STATE PART OF THE SOLUTION
      F = 1.00
      IF(J.GT.6) GO TO 31
```

```
      IF(I.GE.6) AL1 =  50.0
      AI = ALPHA/D4(1)
      A4 = ALPHA/D4(I)
      ZS3 = H03**2-2.0*D4(1)**2*EXP(-AI*AL1)*91.0-EXP(AI*X(J)))
      RG4 = ZS3+(PI/AI)*(X(J)+(1.0/AI)*EXP(-AI*AL1)*(1.0-EXP(
     1AI*X(J)))
      SG4(J) = RG4**0.5
C
      TRANSIENT PART OF THE SOLUTION
      Z4K = AK(I)*D4(I)/F
      P4 = (A4*X(J))/2.0
      TERM4 = H3(I)**2 - 2.0*H03*H3(I)
C
C     DO LOOP FOR THE SOLUTION OF INFINITE SERIES
      SUM = 0.0
      SUM8 = 0.0
      DO 18 IJ=1, 6
      SIGMA=RN4(IJ)**2 + Q4**2
      P=(SIGMA/AL1**2)*Z4K
      PT =P*T(I)
      IF(PT,GT.80.0) PT = 80.0
C
      BRACK = 1.0+(SIGMA/(4.0*RN4(IJ)**2))*(Q4+1.0)
      TERM2 =(SIGMA/RN4(IJ))*0.5*(1.0-COS(2.0*RN4(IJ)))
      DENOM = 2.0*SIN(2.0*RN4(IJOO*BRACK - TERM2
      B(IJ) = 1.0/DENOM
C
      TERM7 = B(IJ)*SIN(RN4(IJ)*X(J)/AL1)*((SIN(RN4(IJ)))**2-
     1(COS(RN4(IJ)))**2)*EXP(-PT)
      SUM = SUM +TERM7
      TERM8 = B(IJ)/2*SIN(RN4(IJ)*X(J)/AL1)*((SIN(RN4(IJ)))**
     1)*91.0-EXP(-PT))
      SUM8 = SUM8+TERM8
      IF(T(I).EQ.0.0) GO TO 31
```

```
      IF((ABS(TERM7).LE.1.E-4).AND.(ABS(TERM8).LE.1.E-4) GO
      TO 20
   18 CONTINUE
      WRITE(6,19) TERM7,TERM8
   19 FORMAT(50X,6HTERM7=F10.6,10X,6HTERM8=F10.6)
   20 Z4(J) =RG4+TERM4*(1.0+2.0*EXP(P4)*SUM)+2.0*PM*Z4K*SUM8*
      EXP(P4)
      WRITE(6,101) SUM,SUM8
  101 FORMAT(30X,1H4,10X,F10.6,5X,F10.6)
C
      Z4(J) = Z4(J)**0.5
   31 RETURN
      END


      SUBROUTINE OUTPUT(JM)
      DIMENSION ..........
C
      COMMON ..............
      GO TO (21,22),JM
C     WRITE THE TITLE
   21 WRITE(6,23)
   23 FORMAT(47X,38HFALLING WATER TABLE OVER A SLOPING BED,//)
C     WRITE(6,24) ALPHA,PM
   24 FORMAT(53X,6HSLOPE=F5.3,6X,14HREPLENISHMENT=F5.4,/)
C
      WRITE(6,25)
   25 FORMAT(5X,4HTIME,7X,1HX,11X,3HSG1,7X,2HZ1,11X,3HSG2,8X,
      2HZ2,11X,3HSG3,7X,2HZ3,11X,3HSG4,8X,2HZ4,/)
      GO TO 27
C     OUTPUT(2)
   22 WRITE(6,26) T(I),X(I),SG1(1),Z1(1),SG2(1),Z2(1),SG3(1),
      Z3(1),SG4(1),Z4(1)
   26 FORMAT(6X,F5.1,4X,F5.1,8X,F7.3,2X,F7.3,7X,F7.3,3X,F7.3,
      6X,F7.3,4X,F7.3,6X,F7.3,4X,F7.3)
```

```
      IF(I.GE.6) GO TO 70
      WRITE(6,28)(X(J),SG1(J),Z1(J),SG2(J),Z2(J),SG3(J),Z3(J),
     SG4(J),Z4(J),J=2,11)
   28 FORMAT(15X,F5.1,8X,F7.3,2X,F7.3,7X,F7.3,3X,F7.3,6X,F7.3,
     4X,F7.3,6X,F7.3,4X,F7.3)
      GO TO 75
C
   70 WRITE(6,71)(X(J),SG1(J),Z1(J),SG2(J),Z2(J),SG3(J),Z3(J),
     SG4(J),Z4(J),J=2,16)
   71 FORMAT(15X,F5.1,8X,F7.3,2X,F7.3,7X,F7.3,3X,F7.3,6X,F7.3,
     4X,F7.3,6X,F7.3,4X,F7.3)

C     WRITE(6,38)
   38 FORMAT(////)
   27 RETURN
      END

      FUNCTION COSH(Z)
      A=EXP(Z)
      B=1.0/A
      COSH=(A+B)*0.5
      RETURN
      END
C
      FUNCTION SINH(Z)
      A=EXP(Z)
      B=1.0/A
      SINH=(A-B)*0.5
      RETURN
      END
```